An investigation of the roles of TRPV1, TRPA1 and Hydrogen Sulfide in thermoregulation

Fernandes, Maria Antionetta

Awarding institution:
King's College London

An investigation of the roles of TRPV1, TRPA1 and Hydrogen Sulfide in thermoregulation

Thesis submitted for the degree of

Doctor of Philosophy

King's College London

Maria A Fernandes BSc (Hons), MRes

Institute of Pharmaceutical Sciences

King's College London

Franklin-Wilkins Building

Waterloo Campus

London, SE1 9NH

Abstract

The Transient Receptor Potential Vanilloid 1 (TRPV1) ion channel is an integrator of noxious stimuli, including noxious heat (>43°C), low pH (<6) and capsaicin (the pungent component of chilli peppers). Transient Receptor Potential Ankyrin 1 (TRPA1) is a closely related channel, activated by reactive oxygen species, hydrogen sulfide (H_2S) and mustard oil. Their expression on primary sensory neurons is well characterised. Recent studies show that they are also expressed in non-neuronal tissue. Whilst TRPV1 and TRPA1 antagonism is a promising analgesic and anti-inflammatory strategy, early generation TRPV1 antagonists produced a poorly understood cross-species side effect of hyperthermia. H_2S is a vasodilator and TRPA1 activator. Inhalation of H_2S can suspend animation, a state that includes a decreased body temperature. The role of TRPA1 and H_2S in TRPV1-mediated hyperthermia was investigated using TRPV1 and TRPA1 antagonists, knockout mice, H_2S donors and modulators of endogenous H_2S producing enzymes.

The effects of TRPV1 antagonists SB366791 and JNJ17203212 and TRPA1 antagonists HC030031 and TCS5861528 on thermal and mechanical nociceptive thresholds of naïve mice were determined using the Hargreaves and automated Von Frey techniques, respectively. Antagonist-induced changes in core body temperature of conscious, ambulatory mice were determined using radiotelemetry. Only JNJ17203212 produced a significant increase in core body temperature.

The effects of the same antagonists on capsaicin- and mustard oil- induced blood flow changes in the pinna and knee were investigated, using full-field laser Doppler perfusion. The capsaicin-induced increase in pinna blood flow demonstrated a neuronal response; in the knee decreased flux demonstrated non-neuronal TRPV1 activation. Mustard oil similarly increased flux in the pinna and knee: TRPA1 does not exhibit any vasoconstrictor activity in this model. JNJ17203212 significantly attenuated capsaicin-induced blood flow changes in the pinna and knee. No inhibition was observed with SB366791. HC030031 significantly reduced mustard oil-induced blood flow increases in the pinna and knee whilst TCS5861528 had no effect.

Finally, the involvement of TRPA1 blockade and H_2S in JNJ17203212-mediated hyperthermia was determined, using HC030031 and GYY4137, respectively. Whilst TRPA1 was not directly involved in our model, GYY4137 attenuated the hyperthermia elicited by JNJ17203212, suggesting H_2S may have a role in TRPV1 antagonist-mediated hyperthermia.

Acknowledgements

First and foremost, I have to thank Julie, my supervisor. Through thick and thin, tears and triumphs, you've been my biggest cheerleader, and enabled me to follow my passions. I would also like to thank my second supervisor, Dr David Mountford who gave advice whenever I came knocking, and Professors Sue Brain and Stuart Bevan who inspired me to pursue this journey in the final year of my undergraduate degree. I am grateful for the funding from the Centre for Integrative Biomedicine, which made this project possible.

Thank you to those who provided genetically modified animals for this project: to Khadija Alawi who maintained the TRPV1 colony and to Aisah Aubdool of the Brain group for providing TRPA1 wild type and knockout mice. Thanks must go to Patrick Fox and the FWB BSU team, I am grateful for their help teaching me to administer drugs orally and for taking such good care of our mice. Special thanks go to my colleagues in the lab. To Khadija: you've been a great sounding board and co-worker and, most of all, a great friend. I'd also like to thank the Keeble group and Brain group past and present for being a pleasure to work with – particularly Rabea and Beth for their advice with the FLPI. I'm grateful for Anna Starr's help with blinded treatments. Fiona – you've been an inspiration since we first met and your help at the eleventh hour will be repaid with many hours at the Mayflower. Thank you to Claire and Ross: "You guys keep me young!" – you know the rest. I'm grateful for the moral support of my colleagues at the Society for General Microbiology over the past few months – they've made working two demanding jobs at the same time that much easier!

I'm grateful for the example set by Dr Wallage at St Bernard's, for showing me that it's good to be inquisitive. I'll be eternally grateful to Peter Finn; and to Julie, Marlene, Sonal, and the rest of the team at Guys and St Thomas': without them I would not be where I am today. I greatly appreciate the support from Jude Hall and Dom Spina during difficult times.

Speaking of which, 'thank you' is not enough to show my gratitude to my parents (but I'll say it anyway). Thank you for all the opportunities you have given me, and for your unconditional support. And finally: Tom. Thank you for being there throughout all of this. Your support and understanding is not underestimated.

Table of Contents

Abstract 1

Acknowledgements 3

Table of Contents 4

List of Figures 10

List of Tables 14

Chapter 1 Introduction 19

1.1 The Transient Receptor Potential Vanilloid 1 (TRPV1) and Ankyrin 1 (TRPA1) channels 19

1.1.1 ThermoTRP channels 20

1.1.2 The discovery of TRPV1 and TRPA1, promising targets for novel analgesics 22

1.1.3 Structure and Expression 22

1.1.4 Agonists, antagonists and endogenous control 25

1.2 TRPV1 and TRPA1 in pain and inflammation 32

1.3 Non-neuronal TRPV1 and TRPA1 36

1.3.1 TRPV1 and TRPA1 in vasculature 40

1.4 TRPV1 and TRPA1 in thermoregulation 42

1.4.1 Thermoregulation 42

1.4.2 TRPV1 activation and antagonism results in thermoregulatory dysfunction 42

1.4.3 TRPA1 and thermoregulation 45

1.5 The physiological roles of Hydrogen Sulfide 46

1.5.1 Endogenous H_2S production and metabolism 46

1.5.2 Pharmacological tools 48

1.5.3 H_2S interactions *in vivo* 50

1.5.4 H_2S actions in pain 51

1.5.5 H_2S actions in vasculature 51

1.5.6 H_2S actions in inflammation 52

1.5.7 H_2S actions in metabolism and thermoregulation 53

1.6 Summary 54

1.7 Aims 55

Chapter 2 Materials and Methods 56

2.1 Animals 56

2.1.1 Generation of TRPV1 WT and KO mice 56

2.1.2 Genotyping TRPA1 wild type and knock out mice 59

2.2 Preparation and administration of experimental compounds 62

2.3 Measuring mechanical and thermal nociceptive thresholds 65

2.3.1 TRPV1 and TRPA1 antagonists in thermal nociceptive threshold testing 65

2.3.2 TRPV1 and TRPA1 antagonists in mechanical nociceptive threshold testing 65

2.4 Measuring changes in core body temperature using radiotelemetry 68

2.4.1 Implantation of telemetry probes. 68

2.4.2 Recording core body temperature of conscious ambulatory mice. 68

2.5 Measuring peripheral blood flow using speckle contrast imaging 69

2.5.1 Measuring blood flow in the ear in response to various agonists 69

2.5.2 The effect of antagonists on agonist-induced changes in blood flow 71

2.6 Measurement of dorsal skin plasma extravasation 72

2.6.1 Dorsal skin injections and collection of samples 72

2.6.2 Evans Blue extraction and quantification 72

2.7 *In vitro* methods 74

2.7.1 Tissue collection 74

2.7.2 Measurement of gene expression using Real Time Polymerase Chain Reaction 74

2.7.3 Protein Quantification 79

2.8 Statistical analysis 84

Chapter 3 Characterisation of TRPV1 and TRPA1 antagonists in Pain and Thermoregulation 85

3.1 Introduction 85

3.2 Hypothesis and Aims 87

3.3 Results 88

3.3.1 The effects of TRPV1 antagonists on nociceptive thresholds 88

3.3.2 The effects of TRPA1 antagonists on nociceptive thresholds. 91

3.3.3 The effects of TRPV1 antagonists on core body temperature of conscious mice 94

3.3.4 The effects of TRPA1 antagonists on core body temperature 99

3.4 Discussion 102

3.4.1 Key findings 102

3.4.2 The effect of TRPV1 antagonists on pain 102

3.4.3 The effect of TRPA1 antagonists on pain 103

3.4.4 The effect of TRPV1 antagonists on core body temperature 103

3.4.5 The effect of TRPA1 antagonists on core body temperature 104

3.4.6 Conclusions 104

Chapter 4 Characterisation of the roles of TRPV1 and TRPA1 in blood flow 106

4.1 Introduction 106

4.2 Hypothesis and Aims 107

4.3 Results 108

4.3.1 Characterisation of the effects of capsaicin on blood flow in the ear and exposed synovial membrane 108

4.3.2 Characterisation of the effects of mustard oil on blood flow in the ear and exposed synovial membrane 108

4.3.3 The effects of TRPV1 antagonists on capsaicin-induced blood flow changes in the ear and exposed synovial membrane 111

4.3.4 The effects of TRPA1 antagonists on mustard oil-induced changes in blood flow in the ear and exposed synovial membrane 115

4.4 Discussion 119

4.4.1 Key findings 119

4.4.2 The effect of capsaicin on the vasculature in different tissues 119

4.4.3 The ability of TRPV1 antagonists to block capsaicin-induced blood flow responses 120

4.4.4 The effect of mustard oil on the vasculature in different body tissues 121

4.4.5 The ability of TRPA1 antagonists to block mustard oil-induced blood flow responses 122

4.4.6 Conclusions 122

Chapter 5 Investigation of the role of TRPA1 in TRPV1 antagonist-induced hyperthermia 123

5.1 Introduction 123

5.2 Hypothesis and Aims 124

5.3 Results 125

5.3.1 Basal core body temperature of TRPV1 WT and KO mice 125

5.3.2 The effect of a TRPA1 antagonist on the core body temperature of TRPV1 WT and KO mice 127

5.3.3 The effect of treatment with HC030031 on JNJ17203212-induced hyperthermia 129

5.3.4 The effect of JNJ17203212 on the core body temperature of TRPA1 WT and KO mice 129

5.4 Discussion 132

5.4.1 Key findings 132

5.4.2 Absence of TRPV1 has no effect on core body temperature. 132

5.4.3 TRPA1 antagonism results in hypothermia in the absence of TRPV1. 132

5.4.4 The effect of JNJ17203212 on the core body temperature of TRPA1 KO mice 134

5.4.5 Conclusions 134

Chapter 6 The effect of H_2S on TRPV1 antagonist-induced hyperthermia 135

6.1 Introduction 135

6.2 Hypothesis and Aims 137

6.3 Results 138

6.3.1 Investigation of H_2S producing enzymes in TRPV1 WT and KO mice 138

6.3.2 The effect of manipulating H_2S levels on core body temperature of naïve CD1 mice 141

6.3.3 The effects of H_2S donors on blood flow 145

6.3.4 The effect of H_2S on plasma extravasation 147

6.3.5 The effect of TRPV1 deletion on H_2S - induced plasma extravasation 150

6.3.6 The effects of blocking endogenous H_2S production on L-cysteine donor – induced plasma extravasation 152

6.3.7 The effect of GYY4137 on JNJ17203212-induced hyperthermia 154

6.4 Discussion 157

6.4.1 Key findings 157

6.4.2 Investigation of H_2S producing enzymes in TRPV1 WT and KO mice 157

6.4.3 The effects of H_2S donors on blood flow and plasma extravasation 158

6.4.4 The effect of manipulating H_2S levels on core body temperature 160

6.4.5 The effect of GYY4137 on JNJ17203212-induced hyperthermia 161

6.4.6 Conclusions 162

Chapter 7 General Discussion 164

7.1 Summary of Results 164

7.2 The hyperthermic TRPV1 antagonist JNJ17203212 inhibits changes in flow in the microvasculature 165

7.3 TRPA1 in thermoregulation 166

7.4 H_2S and TRPV1 167

7.5 Study limitations and further work 168

7.6 Final conclusions..... 170

References..... 171

List of Figures

Chapter One

Figure 1.1 The temperature dependency of the firing rate of different TRP channels (Berne and Levy, 2010).....21

Figure 1.2 The structure of the TRPV1 channel.....23

Figure 1.3 Schematic of the structure of the TRPA1 channel.....24

Figure 1.4 Activation of neuronal TRPV1 and TRPA1 leads to release of inflammatory neuropeptides CGRP and Substance P.....33

Figure 1.5 Schematic of the vasodilatory response to TRP channel activation.....39

Figure 1.6 Schematic of the purported vasoconstriction response to TRPV1 channel activation directly on smooth muscle cells.....39

Figure 1.7 Enzymatic production and metabolism of H_2S.....47

Chapter Two

Figure 2.1 Gel electrophoresis image demonstrating TRPV1 WT (188bp) and KO (neomycin, 700bp) genomic DNA.....60

Figure 2.2 Gel electrophoresis image demonstrating TRPA1 WT (310bp) and KO (200bp) genomic DNA....61

Figure 2.3 Experimental set up for thermal nociceptive threshold testing.....67

Figure 2.4 Experimental set up for mechanical nociceptive threshold testing.....67

Figure 2.5 FLPI set up to investigate the effects of topical agonists on microvasculature regions on interest.....70

Figure 2.6 Demarcation of i.d. injection sites on a female CD1 mouse injected with Evans Blue dye.....73

Chapter Three

Figure 3.1 The effects of 5 mg kg-1 SB366791 i.p. on paw withdrawal thresholds in the dynamic plantar aesthesiometer test of mechanical nociception, and paw withdrawal latency in the Hargreaves test of thermal nociception in male CD1 mice.....89

Figure 3.2 The effects of 30 mg/kg JNJ17203212on paw withdrawal thresholds in the dynamic plantar aesthesiometer test of mechanical nociception, and paw withdrawal latency in the Hargreaves test of thermal nociception in male CD1 mice.....90

Figure 3.3 The effects of 100 mg/kg HC030031 on paw withdrawal thresholds in the dynamic plantar aesthesiometer test of mechanical nociception, and paw withdrawal latency in the Hargreaves test of thermal nociception in male CD1 mice.....92

Figure 3.4 The effects of 10 mg/kg TCS5861528 on paw withdrawal thresholds in the dynamic plantar aesthesiometer test of mechanical nociception, and paw withdrawal latency in the Hargreaves test of thermal nociception in male CD1 mice.....93

Figure 3.5 The core body temperature and activity levels of naïve, telemetered, male CD1 mice over 24 hours.....95

Figure 3.6 The effects of 5 mg/kg SB366791 i.p. on core body temperature and activity levels of male CD1 mice.....96

Figure 3.7 The effects of 30 mg/kg JNJ17203212 i.p. on core body temperature and activity levels of male CD1 mice.....97

Figure 3.8 Hyperthermic effects of JNJ17203212 are TRPV1-dependent.....98

Figure 3.9 The effects of 100 mg/kg HC030031 p.o. on core body temperature and activity levels of male CD1 mice.....100

Figure 3.10 The effects of 10 mg/kg TCS5861528 p.o. on core body temperature and activity levels of male CD1 mice.....101

Chapter Four

Figure 4.1 Characterisation of the effects of capsaicin on the ear and exposed synovium of anaesthetised male CD1 mice.....109

Figure 4.2 Application of mustard oil to the ear and the exposed synovial membrane of anaesthetised male CD1 mice.....110

Figure 4.3 SB366791 (5 mg/kg) does not inhibit capsaicin-induced increases in flux in the ear, or capsaicin-induced decreases in flux in the exposed synovial membrane of anaesthetised male CD1 mice.....113

Figure 4.4 The TRPV1 antagonist JNJ17203212 (30 mg/kg) significantly inhibited capsaicin-induced changes in blood flow in the ear and exposed synovial membrane of anaesthetised male CD1 mice.....114

Figure 4.5 The effect of 100 mg/kg HC030031 on mustard oil-induced changes in blood flow in the ear and exposed synovial membrane.....117

Figure 4.6 The effect of 10 mg/kg TCS5861528 p.o. on mustard oil-induced changes in blood flow in the ear and exposed synovial membrane.....118

Chapter Five

Figure 5.1 The core body temperature and activity of telemetered naive male TRPV1 WT and KO mice..126

Figure 5.2 Administration of 100 mg/kg HC030031 in telemetered male TRPV1 WT and KO mice after a one-hour baseline period.....128

Figure 5.3 The effect of oral administration of the TRPA1 antagonist HC030031 30 minutes before administration of JNJ17203212 on core body temperature.....130

Figure 5.4 The core body temperature and activity of TRPA1 WT and KO mice after i.p. injection of 30 mg/kg JNJ17203212.....131

Chapter Six

Figure 6.1 RNA expression analysis of Cystathionine Beta Synthase and Cystathionine Gamma Lyase by qRT-PCR in naive TRPV1 WT and KO mice.....139

Figure 6.2 Protein expression analysis of Cystathionine Beta Synthase and Cystathionine Gamma Lyase by Western blot in naive TRPV1 WT and KO mice.....140

Figure 6.3 Administration of 5.6 mg/kg NaSH i.p. in telemetered male CD1 mice.....142

Figure 6.4 Administration of 50 mg/kg GYY4137 in telemetered male CD1 mice.....143

Figure 6.5 The effect of i.p. administration of 11 mg/kg D,L-propargylglycine in telemetered male CD1 mice.....144

Figure 6.6 Application of Sodium Nitroprusside, Sodium Hydrosulfide, and GYY4137, to the exposed synovial membrane of anaesthetised male CD1 mice.....146

Figure 6.7 The effects of H2S on plasma extravasation in the dorsal skin of male and female CD1 mice...148

Figure 6.8 The effect of NaSH and GYY4137 on Substance P -mediated plasma extravasation in the dorsal skin of male and female CD1 mice.....149

Figure 6.9 The effect of TRPV1 deletion on i.d. Substance P and H2S donor coadministration in the dorsal skin of female mice.....151

Figure 6.10 The effects of D,L-Propargylglycine on i.d. Substance P and H2S donor L-cysteine coadministration in the dorsal skin of female TRPV1 wild type mice.....153

Figure 6.11 The effect of pre-treatment with GYY4137 on JNJ17203212-mediated hyperthermia in male CD1 mice.....155

Figure 6.12 Pre-treatment with 50 mg/kg decomposed GYY4137 reduces JNJ17203212-induced hyperthermia in male CD1 mice.....156

List of Tables

Chapter 1

Table 1.1 Common Agonists and Endogenous Modulators of TRPV1 and TRPA1 26

Table 1.2 Antagonists and agonists of TRPV1 and TRPA1 used in the studies in this thesis 31

Table 1.3 Non-neuronal expression of TRPV1 37

Table 1.4 Non-neuronal expression TRPA1 38

Chapter 2

Table 2.1 Primers used in TRPV1 and TRPA1 genotyping experiments 57

Table 2.2 PCR reaction mix for genotyping TRPV1 mice 58

Table 2.3 Compounds used in *in vivo* experiments. 64

Table 2.4 Sequence of PCR primers used in this project 76

Table 2.5 Relative components of the final RT-qPCR mastermix 77

Table 2.6 Components of Resolving and Stacking gels for SDS-PAGE 81

Table 2.7 Antibodies used in Western blotting experiments 83

Abbreviations

12-(S)-HPETE	12-(S)-hydroperoxyeicosatetraenoic acid
15-(S)-HETE	15-(S)-hydroxyeicosatetraenoic acid
3-MST	3-mercaptopyruvate sulfurtransferase
ADP	adenosine diphosphate
AMP	adenosine monophosphate
AOAA	aminooxyacetic acid
ATP	adenosine triphosphate
ATP	adenosine triphosphate
BAT	brown adipose tissue
BBB	blood brain barrier
BSA	bovine serum albumin
CaMKII	calcium calmodulin dependent kinase II
cAMP	cyclic adenosine mono-phosphate
Caps	capsaicin
CBS	Cystathionine β Synthase
CFA	complete Freund's adjuvant
CGRP	calictonin gene-related peptide
CNS	central nervous system
CO	Carbon Monoxide
COX	cyclooxygenase
CSE	Cystathionine γ Lyase
DAG	diacylglycerol
DRG	dorsal root ganglia
ECL	enhanced chemiluminescence
FLPI	full field laser Doppler perfusion imager
GPCR	g protein-coupled receptor
GYY4137	morpholin-4-ium 4 methoxyphenyl(morpholino) phosphinodithioate
H_2S	hydrogen sulfide

HPRT	hypoxanthine guanine phosphoribosyl transferase
HRP	horseradish peroxidase
i.d.	intradermal
i.p.	intra-peritoneal
i.v.	intra-venous
IL	interleukin
K_{ATP}	ATP-sensitive K+ channels
kDa	kilo Dalton
KO	knock out
MIA	monoiodoacetate
MO	mustard oil
MSU	monosodium urate
NA	noradrenaline
NADA	N-arachidonoyl-dopamine
NK	neurokinin
NO	Nitric Oxide
NPY	neuropeptide Y
OA	osteoarthritis
p.o.	*per os* (oral)
PAG	D,L- propargylglycine
PAR	protease activated receptor
PCR	polymerase chain reaction
PIP2	phophatidylinositol-4,5-bisphosphate 2
PKA	protein kinase A
PKC	protein kinase C
PKG	cGMP-dependent protein kinase or protein kinase G
PLA_2	phospholipase A_2
PLC	phospholipase C
qRT-PCR	quantitative reverse-transcription PCR
RA	rheumatoid arthritis

ROS	reactive oxygen species
RTX	resiniferatoxin
s.c.	subcutaneous
SAM	S-adenosylmethionine
S.E.M.	standard error of the mean
SDS-PAGE	sodium-dodecyl sulphate polyacrylamide gel electrophoresis
SERCA	sarco/endoplasmic reticulum Ca2+-ATPase
SP	Substance P
TNFα	tumor necrosis factor α
TRP	Transient Receptor Potential
TRPA1	Transient Receptor Potential Ankyrin Family member 1
TRPM8	Transient Receptor Potential Melastatin Family member 8
TRPV	transient receptor potential vanilloid
TRPV1	Transient Receptor Potential Vanilloid Family member 1
UCP	uncoupling protein
WT	wild type

List of Publications and Presented Abstracts

PUBLICATIONS

Fernandes ES, **Fernandes MA** & Keeble JE (2012). The functions of TRPA1 and TRPV1: moving away from sensory nerves. *Brit J Pharmacol 166(2):510-21.* ***(top ten most cited British Journal of Pharmacology articles in 2014)***

CONFERENCE ABSTRACTS

Fernandes MA, Whiteman M, Keeble JE (2013) The hydrogen sulfide donor GYY4137 attenuates transient receptor potential vanilloid 1 (TRPV1) antagonist-mediated hyperthermia. Oral Presentation. *Second European Conference on the Biology of Hydrogen Sulfide. Exeter, UK.*

Fernandes MA, Gaffen Z, Pitcher A, Gadd M, Keeble J (2012). Daphnia in Pharmacology Outreach to School-Age Children. Oral Presentation. *BPS Winter meeting, London, UK.*

Fernandes MA, Keeble JE (2012). The differing effects of various TRPV1 and TRPA1 antagonists on capsaicin and mustard oil- induced changes in blood flow in mice. Poster Presentation. *BPS Winter meeting, London, UK.*

Fernandes MA, Keeble JE (2011). The Effects Of The TRPA1 Antagonists TCS5861528 And HC030031 On Core Body Temperature And Activity Of Conscious Mice. Poster Presentation. *BPS Winter meeting, London, UK.*

Ng O, **Fernandes MA**, Keeble JE (2011) Modelling burrowing behaviour: studies using TRPV1 wild type and knockout mice. Poster Presentation. *BPS Winter meeting, London, UK.*

Fernandes MA, Keeble JE (2011). The effect of the TRPV1 antagonist, SB366791, on thermal nociceptive thresholds and capsaicin-induced vascular responses in mice. Poster Presentation. *International Congress on Inflammation, Paris, UK.*

Chapter 1 Introduction

1.1 The Transient Receptor Potential Vanilloid 1 (TRPV1) and Ankyrin 1 (TRPA1) channels

The transient receptor potential (TRP) superfamily of non-selective cation channels is formed of several related families with widespread functions in both human physiology and pathophysiology (Pedersen et al., 2005). The first member of the family was described in Drosophila as a channel mediating an unusually transient response to light (Cosens and Manning, 1969). In the years following this discovery, the families comprising this group of cation channels were classed as TRPC (canonical), TRPP (polycystin), TRPM (melastatin), TRPML (mucolipin), TRPN (NOMPC; no mechanoreceptor potential channel), TRPA (ankyrin) and TRPV (vanilloid), each of which in turn (except for TRPA which has only one member) contain several members (Pedersen et al., 2005). All TRP channels are tetramers formed of subunits with six trans-membrane domains and cation-selective pores, which frequently show high calcium permeability (Latorre et al., 2009). The physiological roles of this superfamily are diverse – from visual and auditory sensation and pain signal transduction, to cell survival and smooth muscle contraction (Pedersen et al., 2005).

The mammalian vanilloid family consists of 6 members – TRPV1 - 6. TRPV1-TRPV4 can be activated by heat (Clapham, 2003), as well as being polymodal chemoreceptors, with the four receptors being activated by a wide array of exogenous and endogenous ligands (Nilius and Voets, 2004). The roles of TRPV1 and TRPA1 have shown the highest levels of interaction, especially with regard to pain and inflammation. Indeed, recent evidence shows that agonists of each channel have the ability to heterologously desensitise both; an indicator, perhaps, of the close association that these two proteins have (Simons et al., 2003; Akopian et al., 2007; 2008; Ruparel et al., 2008). TRPV1 and TRPA1 in particular of all the TRP channels, act as integrators of many stimuli. For instance, they both have roles in thermosensation and chemosensation amongst others that will be described in more detail to follow.

1.1.1 ThermoTRP channels

TRPV1, TRPA1 and another related TRP channel, TRPM8 (a member of the melastatin subfamily) are collectively known as the 'thermoTRP' channels due to their purported roles in temperature sensation. Indeed, these and other members of the TRPV subfamily are activated by varying temperature (Figure 1.1). It is important to also note that although TRPV1 is involved in both thermoregulation (discussed later) and thermosensation, there is currently no evidence that the two functions are related. TRPV1 is activated by temperatures exceeding >42°C – i.e. it senses noxious heat. TRPM8 is known to be activated by cold temperatures and compounds associated with cooling temperatures (Peier et al., 2002), whilst TRPA1 is proposed to be activated at temperatures <17°C (Story et al., 2003). The role of these latter two channels in thermoregulation rather than thermosensation is not well understood, with a far less established role than TRPV1.

A role for TRPV1 as a peripheral thermosensor is well established (Szolcsanyi et al., 1971). Unlike TRPV1 knockout mice, which displayed impaired thermal nociception (Caterina et al., 2000), an examination of the phenotype of TRPA1 knockouts regarding a role for this receptor in noxious temperature sensation has proved controversial. Two independent colonies of TRPA1 knockout animals have been generated (Bautista et al., 2006; Kwan et al., 2006). Both groups knocked out the portion of the gene coding for the pore-forming loop of the protein (the fifth and sixth transmembrane domains). However, Bautista and colleagues reported normal responses to cold temperatures both *in vivo* and *in vitro* in TRPA1 knockout mice (Bautista et al., 2006). Conversely, knockouts in the Kwan study displayed a clear functional deficit to cold stimulation (Kwan et al., 2006). Despite abundant research into the role of TRPA1 in cold sensation over the past five years, its role in thermosensation is still unclear, although we can be certain that it does have some part to play in this process.

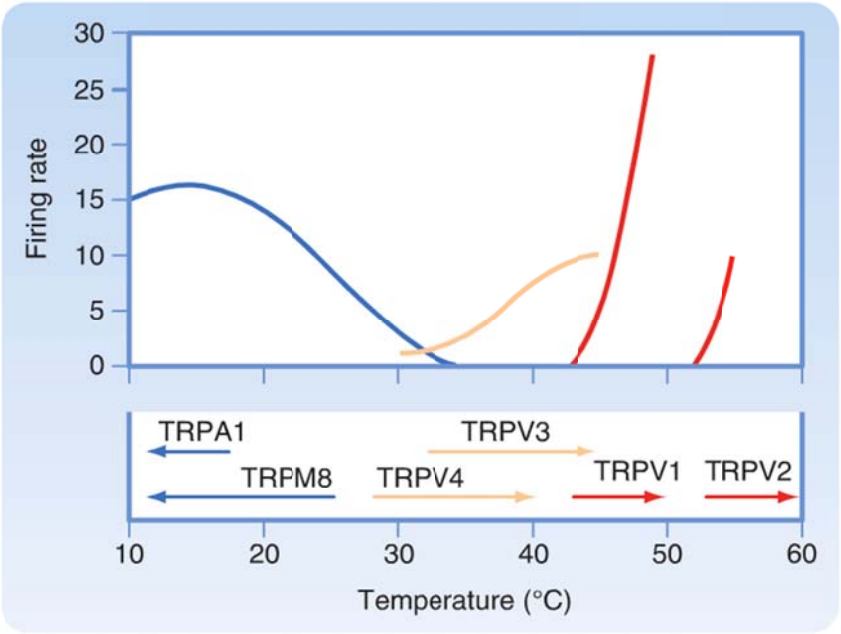

Figure 1.1 The temperature dependency of the firing rate of different TRP channels (Berne and Levy, 2010). Each so-called thermoTRP channel has different temperature sensitivity. The TRPA1 channel is activated by temperatures up to 17°C and the TRPV1 channel temperatures over 42°C.

1.1.2 The discovery of TRPV1 and TRPA1, promising targets for novel analgesics

Despite the knowledge that capsaicin was able to selectively activate sensory nerve fibres since 1967 (Jancsó et al., 1967), the existence of a receptor for the hot pepper-derived compound capsaicin was not shown for years after (Szolcsanyi and Jancso-Gabor, 1975). TRPV1 was finally cloned in 1997 as the vanilloid receptor (VR-1) (Caterina et al., 1997). When its homology with the TRPC channel was confirmed, VR-1 was renamed as TRPV1. In 2000, Hayes and colleagues cloned and identified TRPV1 in humans (Hayes et al., 2000) followed in 2002 by Savidge et al.; who identified TRPV1 in guinea pigs (Savidge et al., 2002).

TRPA1 was cloned in 1999 (Jaquemar et al., 1999), the effects of some of its agonists also being elucidated much earlier. However, its location on sensory nerves was only more recently discovered in 2003 (Story et al., 2003). Indeed, the effects of mustard oil (allyl isothiocyanate (AITC)), the classic TRPA1 agonist, were identified much earlier than the receptor itself – AITC induces neurogenic inflammation in a similar manner to capsaicin (Koltzenburg and McMahon, 1986; Bandell et al., 2004). TRPA1 was initially named ANKTM1 and renamed after the discovery of its homology with other TRP channels. As will be discussed later, TRPA1 is primarily an integrator of irritant noxious stimuli, akin to TRPV1's integration of painful stimuli.

1.1.3 Structure and Expression

TRPV1 and TRPA1, like other TRP channels, are tetrameric cation channels, formed of subunits containing six transmembrane domains. Figure 1.2 shows a schematic of the structure of TRPV1, and Figure 1.3 is a schematic of TRPA1. The cytoplasmic N- and C- termini of both channels are where the channels differ significantly. Whilst both proteins possess ankyrin binding repeats, TRPA1 has a distinctive domain present on the N-terminus containing 14-18 ankyrin binding repeats, a structural motif considered important in the proposed mechanosensation/mechanotransduction role for this channel (Brierley et al., 2009; Kwan et al., 2009). The crystal structure of TRPV1 was discovered in 2008 (Moiseenkova-Bell et al., 2008), and the structure of TRPA1 more recently in 2011 (Cvetkov et al., 2011). These structures can better inform future drug development of target specific compounds.

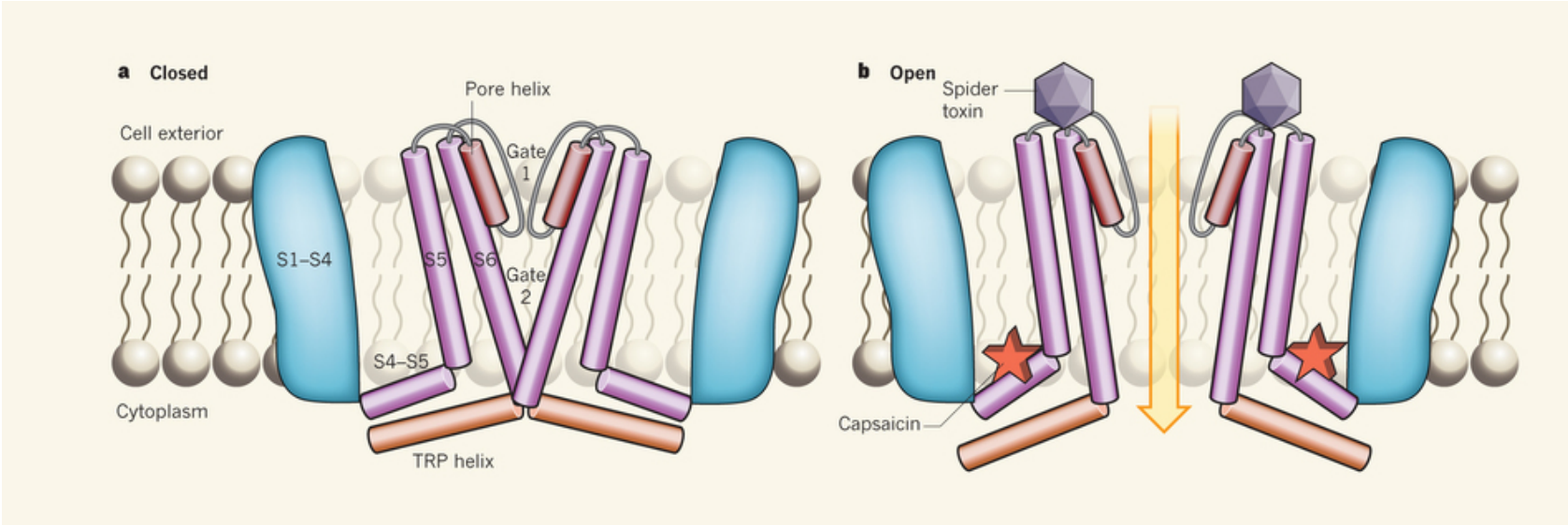

Figure 1.2 The structure of the TRPV1 channel in a) the closed and b) open states. Each channel is formed of 4 subunits, each of which is a 6 transmembrane domain protein. Capsaicin binds on the intracellular side to open the channel and allow influx of cations. Figure from (Henderson, 2013).

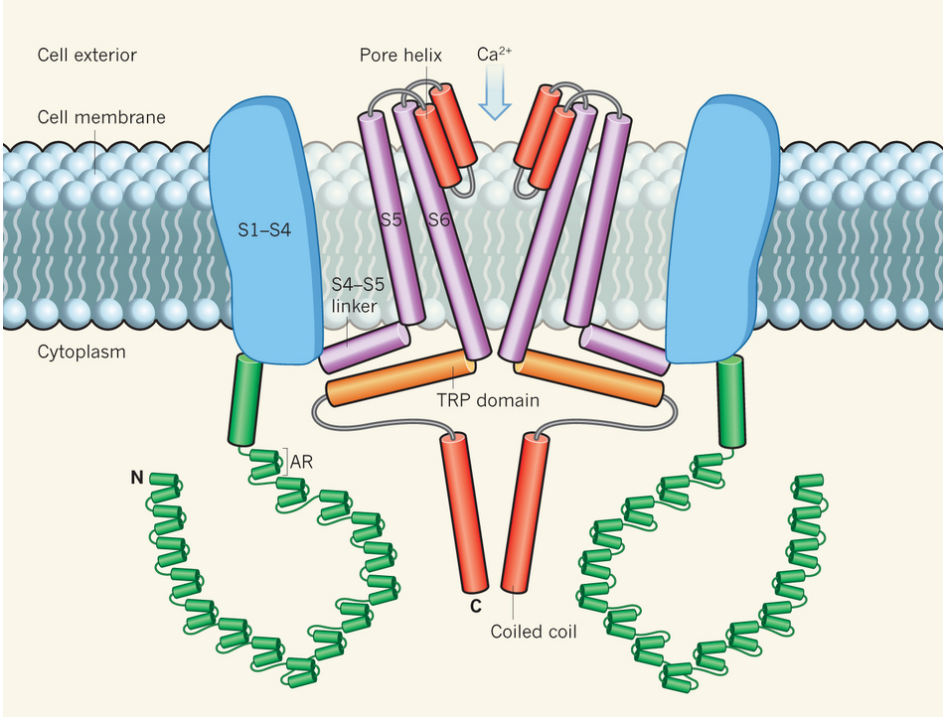

Figure 1.3 Schematic of the structure of the TRPA1 channel. Each channel is formed of 4 subunits, each subunit has 6 transmembrane domains. The intracellular domain has a high number of ankyrin repeats (AR), which is characteristic of this channel. Image from (Clapham, 2015).

Several binding sites for intracellular signalling molecules have been found on the termini of TRPV1, including binding sites for kinases, PIP_2 and calmodulin (CaM). These binding sites further the case for TRPV1 as an important integrator of stimuli and an instrumental component of intracellular signalling cascades. Further research will reveal the intracellular structure of TRPA1, however indications that it too has binding sites for signalling molecules like kinases have been made – bradykinin (BK) has the ability to sensitise this TRP channel via PLC and PKA activation (Wang et al., 2007).

Whilst the structure of these channels is intrinsically linked to their function, their distribution also gives many indications about their roles in physiology, and indeed pathophysiology. TRPV1 was initially discovered on sensory nerves, more specifically Aδ and C pain-conducting fibres (Caterina et al., 1997), sparking interest in its function in pain and neurogenic inflammation. TRPA1 was also initially located on sensory nerves, with 97% of TRPA1-expressing neurons also expressing TRPV1, and 30% of TRPV1-expressing neurons also expressing TRPA1 (Story et al., 2003). It is rare to find TRPA1 expressed without TRPV1, again highlighting the seemingly important relationship between the two receptors. Recently, non-neuronal locations for these channels have been found – this has been reviewed extensively (Fernandes et al., 2012) and will be covered later in this chapter.

1.1.4 Agonists, antagonists and endogenous control

Table 1.1 outlines exogenous and endogenous modulators of TRPV1 and TRPA1. Capsaicin was the original activator of TRPV1 (Caterina et al., 1997). TRPV1 is additionally activated by low pH (<6) and high temperatures (>43°C) – conversely, TRPA1 is purported to be activated by temperatures below 17°C, a finding that has as many studies advocating this role (Story et al., 2003; Bandell et al., 2004; Sawada et al., 2007; Karashima et al., 2009) as disputing it (Jordt et al., 2004; Nagata et al., 2005). More recently, Aubdool and colleagues showed that TRPA1 plays a crucial role as a vascular cold sensor, thus preventing tissue damage in cold environments (Aubdool et al., 2014).

Exogenous agonists of TRPV1 include the vanilloids olvanil and resiniferatoxin (Szallasi et al., 1999), and the non-pungent capsinoid capsiate (Ohnuki et al., 2001). Similarly, TRPA1 is activated by pungent plant-

	TRPV1	TRPA1
Exogenous Agonists	Capsaicin (Caterina et al., 1997)	Allyl Isothiocyanate (Bandell et al., 2004)
	Vanilloids (e.g. Olvanil, Resiniferatoxin) (Szallasi & Blumberg, 1989)	Environmental pollutants, e.g. acrolein (Bautista et al., 2006) Irritants (e.g. Formalin) (McNamara et al., 2007)
	Capsinoids (e.g. Capsiate) (Ohnuki et al., 2001)	Glibenclamide (Babes et al., 2013)
	Noxious high temperature (>43°C) (Caterina et al., 1997)	Cold temperatures (<17°C) (Karashima et al., 2009; Kwan et al., 2006)
	Low pH (<6.0) (Caterina et al., 1997)	Allicin (Macpherson et al., 2005)
	Camphor (Xu et al., 2005)	Icilin (Story et al., 2003)
		Cinnamaldehyde (Macpherson et al., 2006)
		Tetrahydrocannabinol (Jordt et al., 2004)
		NaSH (Streng et al., 2008)
Endogenous Agonists	Anandamide (Zygmunt et al., 1999)	Oxidative stress products (Bessac et al., 2008) e.g. 4-hydroxynonenal (Trevisani et al., 2007).
	Lipoxygenase products (e.g. LTB4) (Huang et al., 2002; Hwang et al., 2000)	Lipid peroxidation products (Taylor-Clark et al., 2008)
	N-acyldopamines (Huang et al., 2002; Chu et al., 2003)	Zinc, copper and cadmium (Gu & Lin, 2010; Hu et al., 2009)
Endogenous Modulators (via activation of intracellular pathways)	Bradykinin (Chuang et al., 2001)	Bradykinin (Bandell et al., 2004; Wang et al., 2007)
	PAR-2 agonists (Amadesi et al., 2004)	PAR-2 agonists (Dai et al., 2007)
	NGF (Chuang et al., 2001)	
	ATP (Chuang et al., 2001)	

Table 1.1 Common Agonists and Endogenous Modulators of TRPV1 and TRPA1 (Fernandes et al., 2012)

derived compounds: AITC (present in horseradish and wasabi) (Bandell et al., 2004), allicin (Macpherson et al., 2005), and cinnamaldehyde (Macpherson et al., 2006). In addition to these plant-derived compounds, TRPA1 is stimulated by environmental pollutants such as acrolein (Bautista et al., 2006) and irritant substances e.g. formalin (Macpherson et al., 2007). Tobacco smoke also activates TRPA1 (Andrè et al., 2008), and more recently TRPA1 has been shown to be activated by hydrogen sulfide (H_2S) via the use of sulfide salts such as NaSH (Streng et al., 2008). Hinman and colleagues showed that covalent activation of TRPA1 is by thiol reactive electrophiles that bind to cysteine and lysine residues within the cytoplasmic domain of the channel – a finding that was backed by Macpherson and colleagues (Hinman et al., 2006; Macpherson et al., 2007). Whilst TRPV1 is activated by capsaicin, a compound associated with an acute burning sensation, TRPA1 is activated by cooling-associated compounds icilin and menthol (Story et al., 2003; Karashima et al., 2007; Rawls et al., 2007; Andersson et al., 2009) and cooling temperatures (Aubdool et al., 2014) and is associated with the 'slow burn' type pain experienced when ingesting wasabi and mustard- both foodstuffs containing AITC. This adds to the enigma of TRPA1 and its role in temperature sensation and control. Endogenously, TRPV1 is activated by eicosanoids such as 12-S-HPETE (Sexton et al., 2007) and the endocannabinoid anandamide (Zygmunt et al., 1999) – similarly, there has been evidence that TRPA1 is activated by another cannabinoid (albeit not endogenous): THC (Jordt et al., 2004). TRPA1 is well-characterised as a sensor of oxidative damage, being activated by products of this process (Bessac et al., 2008), and is known to be a sensor of metals such as cadmium, zinc and copper (Hu et al., 2009; Gu and Lin, 2010). Compounds that raise intracellular concentrations of such metals activated TRPA1 in studies including Ca^{2+} fluorimetry (Rosenbaum et al., 2003; Andersson et al., 2009). So, whilst endogenous lipoxygenase products activate TRPV1, endogenous oxidation products activate TRPA1. TRPV1 has a defined (albeit non-specific as its original target is the CB1 receptor) endogenous activator in the form of anandamide (Zygmunt et al., 1999); however, products of inflammation aside, an endogenous agonist of TRPA1 has yet to be specified. H_2S seems to be a good candidate for this role, as H_2S donated by NaSH has effects selective to TRPA1 (Streng et al., 2008; Andersson et al., 2012; Pozsgai et al., 2012) and endogenous H_2S producing enzymes are colocalised with TRPA1 (Eberhardt et al., 2014).

Evidence of endogenous control of TRPV1 is provided by Chuang and colleagues who showed that whilst TRPV1 can be blocked by phosphatidylinositol 4,5-bisphosphate (PIP_2), Bradykinin (BK) application results

in phospholipase C (PLC) activation and subsequent hydrolysis of PIP_2, leading to removal of this block (Chuang et al., 2001). Sensitisation of the channel can occur, i.e. reducing the temperature activation of TRPV1 from 43°C. BK was the first mediator found to reduce the temperature threshold for TRPV1 channels to ~24°C in sensory neurons (Sugiura et al., 2002). This sensitisation is mediated by BK B_2 receptors; stimulation of these GCPRs can result in downstream phosphorylation of TRPV1 channels by protein kinase C (PKC) (Sugiura et al., 2002; Numazaki et al., 2003; Rosenbaum et al., 2003). Similarly, PAR-2 activation by proteases can sensitise TRPV1 and reduce temperature gating to ~24°C in sensory neurons, another PKC-dependent mechanism (Dai et al., 2004). Other endogenous modulators of TRPV1 are 5HT, prostaglandins, nerve growth factor (NGF) and ATP (Woolf et al., 1994; Chuang et al., 2001; Ji et al., 2002) (Table 1.1).

Like many ion channel receptors, TRPV1 can be desensitised both acutely and chronically (i.e. tachyphylaxis) (Koplas et al., 1997) by stimulation with capsaicin or protons. This may be due to increases in intracellular calcium and the subsequent effects of CaM (Numazaki et al., 2003; Rosenbaum et al., 2003). There are intracellular binding sites for CaM on the TRPV1 protein; it has been shown that CaM can interact with peptides from the N-terminal region in a Ca2+-dependent manner *in vitro* (Rosenbaum et al., 2003), and the C-terminal region in a Ca^{2+}-independent manner (Numazaki et al., 2003). Sanz-Salvador and colleagues used primary cultures of sensory nerves alongside recombinant cells to show that chronically exposing sensory nerve-associated TRPV1 to capsaicin redistributes TRPV1 to intracellular reservoirs from the plasma membrane; following which process TRPV1 channels undergo lysosomal degradation. This process is independent of usual clathrin and dynamin endocytic routes and dependent on PKA (Sanz-Salvador et al., 2012).

Desensitisation of TRPA1 is a more complex process; whilst it can also be modulated by PIP_2 (Karashima et al., 2008), it is becoming apparent that as well as being desensitised by high concentrations of agonists (Dai et al., 2007) TRPA1 can also be cross-desensitised by activation of TRPV1. As previously discussed, TRPA1 is often colocalised with TRPV1, with both channels being present on 20-40% of sensory neurons (Caterina et al., 2000; Bautista et al., 2005). The activation of TRPV1 has been shown to be dependent on TRPA1 to an extent. Akopian and colleagues showed two methods of desensitisation – calcium-dependent

by capsaicin –induced PIP_2 depletion; or calcium-independent by MO-directed inhibition of TRPA1. TRPV1 co-expression also had an effect on the extent of TRPA1 desensitisation (Akopian et al., 2007). There is also evidence that TRPA1 can be desensitised by TRPV1-selective cannabinoids (Andre et al., 2009; da Costa et al., 2009) and activation of TRPA1 with cannabinoids can cross desensitise TRPV1 (Akopian et al., 2008).

It is clear that both TRPV1 and TRPA1 channels can act as integrators of noxious painful and inflammatory stimuli and have close relation to each other. Therefore it follows that antagonists of each channel were initially targeted as anti-inflammatory, analgesic compounds.

Several antagonists have been developed as pharmacological tools to explore the roles of TRPV1 and TRPA1. The first TRPV1 antagonist was capsazepine (Bevan et al., 1992), a competitive antagonist which provided evidence for blockade of TRPV1 as a viable analgesic (Bevan et al., 1992). Other antagonists followed, with SB366791 (Gunthorpe et al., 2004), AMG9810 (Gavva et al., 2005), JNJ17203212 (Swanson et al., 2005) and other so-called first generation antagonists demonstrating much higher selectivity for TRPV1, with the ability to block all three modes of activation of TRPV1 (i.e. heat, pH and capsaicin). Most of these antagonists showed efficacy in *in vivo* pain models, including (amongst others) capsaicin-induced eye-wiping and Complete Freund's Adjuvant (CFA)- induced hyperalgesia (Gunthorpe et al., 2004; Gavva et al., 2005; Swanson et al., 2005). According to studies by Gavva and colleagues, the majority of published TRPV1 antagonists will have their usefulness limited to use as pharmacological tools, as most lack optimal properties for clinical development e.g. selectivity, solubility and, importantly, oral bioavailability (Gavva et al., 2007a).

TRPA1 antagonists are limited, with only a handful available for exploration of the physiological and pathophysiological roles of TRPA1. AP-18 is a compound that is useful for *in vitro* and local *in vivo* studies, but cannot be administered systemically. It was originally used to demonstrate that TRPA1 has an important role in mechanical hyperalgesia (Petrus et al., 2007). Another antagonist, HC030031 has been more extensively characterised and is the antagonist of choice for many studies of TRPA1 function (Eid et al., 2008) and has been used to confirm the function of TRPA1 in health and disease (Andre et al., 2009; da

Costa et al., 2009; Earley et al., 2009; Bodkin et al., 2014) as well as the efficacy of TRPA1 agonists such as cinnamaldehyde (Silva et al., 2011) and purported agonist glibenclamide, the K_{ATP} channel blocker (Babes et al., 2013). Finally and most recently, the Abbott antagonist A-967079 has also been shown to block TRPA1 and has particular importance for pain studies (McGaraughty et al., 2010; Chen et al., 2011).

The agonists and antagonists used in this thesis are outlined in Table 1.2. Capsaicin and mustard oil have been used as agonists of TRPV1 and TRPA1, respectively, and the ability of selected antagonists to inhibit their responses was investigated.

	TRPV1	TRPA1
Agonists	a 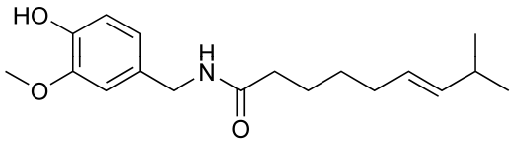	d 
Antagonists	b 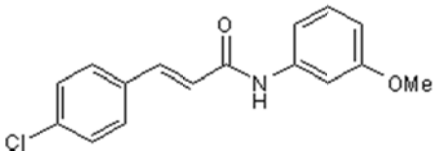 c 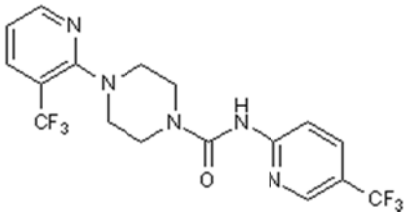	e 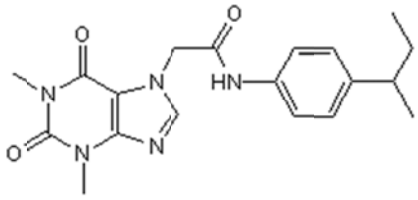 f 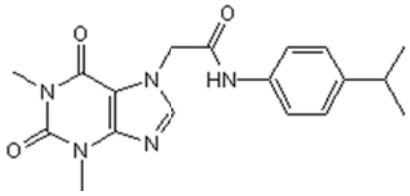

Table 1.2 Antagonists and agonists of TRPV1 and TRPA1 used in the studies in this thesis:

a) Capsaicin is the most commonly used TRPV1 agonist used in pharmacological studies, and d) mustard oil, or allyl isothiocyanate is commonly used as a TRPA1 agonist. Antagonists of the TRPV1 channel include b) SB366791 and c) JNJ17203212. Antagonists of the TRPA1 channel include e) TCS5861528 and f) HC030031. Structures obtained from the manufacturer (Tocris ltd).

1.2 TRPV1 and TRPA1 in pain and inflammation

Historically, the focus of research on both TRPV1 and TRPA1 has been on their roles in pain. As previously mentioned, both channels integrate a large range of noxious stimuli, including stimuli of different modalities. This sensory role, together with their neuronal location, is linked with the importance of TRPV1 (and increasingly, TRPA1) in pain sensation and transduction. An important component of the pain transduction role of these channels is neurogenic inflammation.

Both TRPV1 and TRPA1 are expressed on C and A δ nerve fibres in the dorsal root ganglia of the spinal cord (Caterina et al., 1997; Story et al., 2003). TRPV1 is also expressed in the cervical ganglia and TRPA1 in the trigeminal ganglia (Diogenes et al., 2007). Activation of the channels leads to an influx of calcium ions into the neuron and subsequent release of neuropeptide transmitters, including substance P (SP) and calcitonin gene-related peptide (CGRP) (Figure 1.4). These neuropeptide transmitters are pro-inflammatory and are responsible for the phenomenon known as neurogenic inflammation (defined as the oedema formation, increase blood flow and inflammatory cell recruitment after release of neuropeptides on sensory nerve activation (Holzer, 1998). SP is well known to cause plasma extravasation (Lembeck and Holzer, 1979) and CGRP causes inflammation-associated increases in blood flow (Brain et al., 1985). In addition to these roles, CGRP and SP affect leukocyte accumulation (Cao et al., 2000; Costa et al., 2006).

Most of the initial studies of TRPV1 concerned its role in pain as capsaicin causes pain. This was bolstered by its positioning on pain-signalling nerves. Deletion of the TRPV1 ion channel gene in mice increased the pain threshold in response to noxious heat and mechanic stimuli in studies, compared to wild type controls (Caterina et al., 2000). Mice genetically modified to lack the TRPV1 receptor have been shown to have an increased threshold to noxious heat accompanied by decreased tissue swelling in a model of murine joint inflammation (Caterina et al., 2000; Keeble et al., 2005). The actions of TRPV1 antagonists in both mice and rats further solidify the role of TRPV1 in pain sensation and signalling as they are able to attenuate pain and/or nociceptive signalling (Gavva et al., 2005; Kanai et al., 2005; Varga et al., 2005).

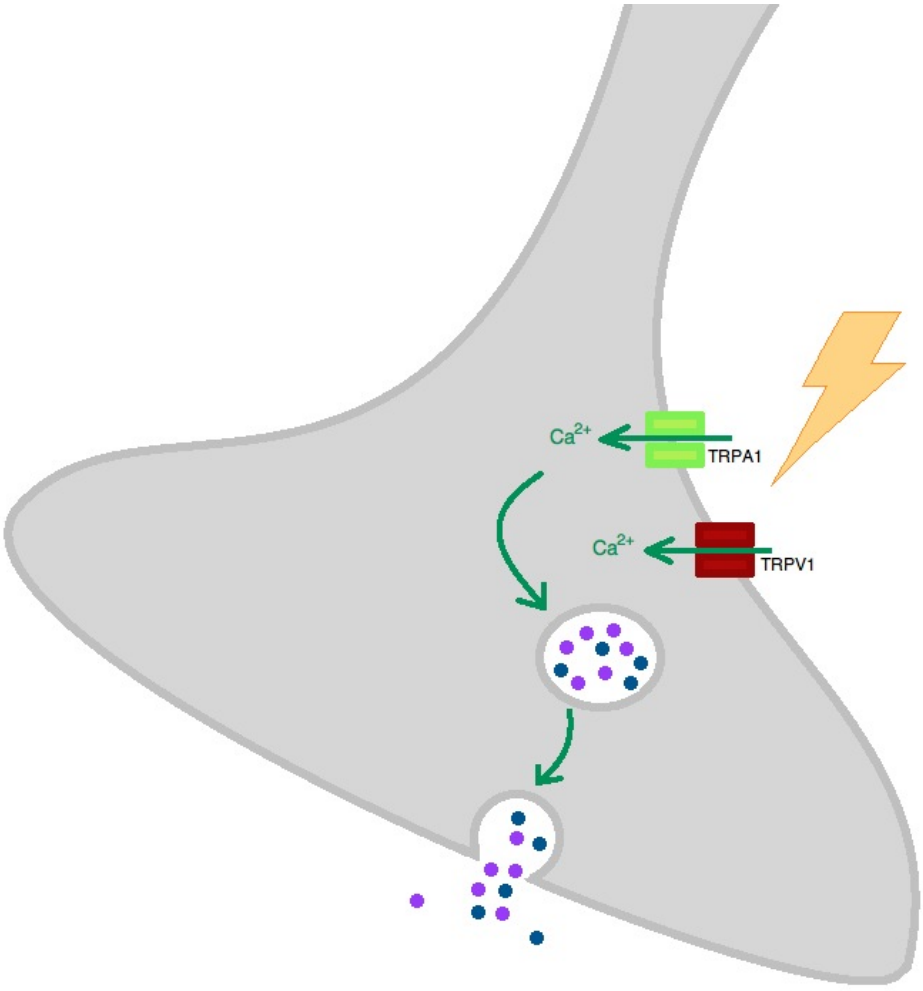

Figure 1.4 Activation of neuronal TRPV1 and TRPA1 leads to release of inflammatory neuropeptides CGRP and Substance P. Activation of the TRP channels on neuronal terminals results in influx of Ca^{2+} and subsequent exocytosis of neuropeptide-containing vesicles. The release of these neuropeptides results in neurogenic inflammation.

TRPA1 is also emerging as an important player in pain signalling. As discussed in section 1.1, TRPA1 is the molecular sensor of irritant chemicals such as AITC and allicin, which provoke a painful sensation when activating TRPA1 (as most people who have tasted mustard or wasabi can attest). Cinnamaldehyde, another TRPA1 agonist caused a dose dependent increase in nociceptive behaviour in TRPV1 WT and KO mice (Bandell et al., 2004). TRPA1 is also suggested to mediated the pro-nociceptive role of the gasotransmitter H_2S (Andersson et al., 2012).

Trevisani and colleagues have provided evidence of TRPA1's role in pain and neurogenic inflammation, showing TRPA1 activation by 4-hydroxynonenal, a product of lipid peroxidation by reactive oxygen species (Trevisani et al., 2007). Both TRPV1 and TRPA1 cause SP and CGRP release from neurons, and this together with the aforementioned colocalisation of the two channels suggests that they are involved in similar processes. Indeed, TRPA1 knockout mice show similar reduction in nociceptive responses to noxious thermal and mechanical stimuli: AITC induced pain behaviours are blocked by HC030031 (Eid et al., 2008). Incidentally, in the same paper HC030031 attenuated pain behaviours in response to complete Freund's adjuvant (CFA) and spinal ligation but did not alter thermal sensitivity. Similarly, AP-18, a structurally unrelated TRPA1 antagonist, almost completely removed CFA-induced mechanical hyperalgesia but not thermal hyperalgesia. AP-18 did not reduce CFA-induced mechanical hyperalgesia in TRPA1 knock out mice. The mice did develop hyperalgesia despite being deficient in TRPA1, which the authors suggested was due to compensatory mechanisms, considering the channel's purported importance in mechanosensation (Petrus et al., 2007).

Arthritis is a prime example of a condition involving both pain and inflammation, and is a condition in which both TRPV1 and TRPA1 seem to play an important role. Both channels have long been investigated in this therapeutic area due to the intrinsic involvement of sensory nerves in the inflammation associated with arthritic conditions; the synovial joint is rich in sensory nerves (Iwasaki et al., 1995), and increases in neuropeptide levels are seen in adjuvant-associated joint inflammation (Bulling et al., 2001). Keeble and colleagues used TRPV1 knockout mice to demonstrate that wild type mice had greater CFA-induced joint swelling than their knock out littermates (Keeble et al., 2005). The same study also showed that TRPV1 is necessary for the action of TNF α, a critical component of the pathology of rheumatoid arthritis. TRPA1

also has a central role in arthritis; recent studies by Fernandes and colleagues used pharmacological tools and genetically modified mice to demonstrate a pivotal role for TRPA1 in mechanical hyperalgesia following intraplantar TNFα administration, and also CFA-induced arthritis (Fernandes et al., 2011).

The role of TRPA1 in CFA-induced arthritis has been echoed in studies of aged mice (Garrison and Stucky, 2014), and in studies by McGaraughty and colleagues (2010). The latter group used two models of induced osteoarthritis (OA) – monoiodoacetate (MIA) and CFA- induced OA – and demonstrated that TRPA1 was important for firing of wide dynamic range (WDR) and non-specific (NS) neuronal firing in response to mechanical stimuli (Von Frey and mechanical pinch stimuli) (McGaraughty et al., 2010). The TRPA1 antagonist A-967079 blocked increases in neuronal signals in response to mechanical stimulation in both naïve and OA mice (McGaraughty et al., 2010). Finally, TRPA1 has been shown to play a key role in monosodium urate (MSU)- induced inflammation, which is a model of gout, a painful joint condition (Trevisan et al., 2013; Moilanen et al., 2015). Trevisan and colleagues showed that MSU-induced joint inflammation had a large oxidative stress component, shown to be mediated by TRPA1 as it could be blocked by HC030031 and knock out of TRPA1 in mice (Trevisan et al., 2013). Moilanen and colleagues used TRPA1 WT and KO mice alongside HC030031 to comprehensively show that TRPA1 is central to MSU-induced inflammation in three different models: air pouch inflammation, spontaneous weight bearing test and paw oedema (Moilanen et al., 2015).

1.3 Non-neuronal TRPV1 and TRPA1

Recent studies suggest that TRPV1 and TRPA1 are not, as traditionally assumed, solely present in the nervous system as integrators of noxious stimuli. Rather, they are also present in many other tissues (see Table 1.3 and Table 1.4 for an extensive list of non-neuronal expression sites and possible functions of both receptors). TRPV1, for example has been found in the smooth muscle cells of the vasculature, where activation causes vasoconstriction (Kark et al., 2008); adipocytes, leading to adipogenesis (Zhang et al., 2007c); the urothelial cells of the bladder causing contraction (Birder et al., 2002; Lazzeri et al., 2004), and lymphocytes, (Saunders et al., 2007) to name just a few (Table 1.3). Its roles in these different organs range from physiological to pathophysiological, supplemented by new evidence suggesting a protective effect of TRPV1 in dermatitis (Banvolgyi et al., 2005).

One of the most important studies highlighting the many expression sites (both centrally and throughout the body) of TRPV1 came with the generation of a TRPV1 reporter mouse (Cavanaugh et al., 2011). This showed functional expression of TRPV1 in vascular smooth muscle cells within thermoregulatory tissues using many studies including calcium fluorimetry and in-situ hybridisation. TRPA1 is also located in non-neuronal tissues (Table 1.3). Whilst expression studies concerning TRPA1 have tended to present TRPA1 on sensory nerves associated with many organs, TRPA1 is expressed on the vascular endothelium (Yang et al., 2010) and the urothelium of the bladder (Streng et al., 2008) to name two of the emerging novel sites of expression. In this case, as well as that of some non-neuronally expressed TRPV1, it is thought that TRPA1 may function directly on the tissue as a cation ion channel, much the same as other calcium channels (e.g. in the vasculature; see Figure 1.6). In this case, the TRP channel would lead to a contraction of the tissue, as shown by Kark and colleagues in a study concerning TRPV1 and vascular smooth muscle (Kark et al., 2008). This is contrary to the classic action of TRPV1 agonists (and indeed TRPA1 agonists on TRPA1) on the vasculature, which usually cause a relaxation of blood vessels (see Figure 1.5) where TRPV1 activation resulted in release of vasodilatory peptides such as CGRP.

	Expression Site	Immuno (-staining/ -fluorescence)	RT-PCR	Western Blot	$[Ca^{2+}]$ functionality	Possible role/effects on activation
MOUSE	Arteriolar smooth muscle cells	▪	✓	▪	✓	Vasoconstriction (Cavanaugh et al., 2011)
	Mesenteric arteries and endothelial cells	✓	✓	▪	✓	Vasorelaxation (Yang et al., 2010)
	Laryngeal Epithelium	✓	▪	▪	▪	laryngeal nociceptors (Hamamoto et al., 2008)
	Preadipocytes and Adipose tissue	✓	✓	▪	✓	Adipogenesis (Zhang et al., 2007c)
	Urothelium	▪	✓	▪	▪	stretch-evoked ATP release (Birder et al., 2002)
RAT	Vascular Smooth Muscle	✓	✓	▪	▪	Vasoconstriction (Kark et al., 2008)
	Pulmonary Artery Smooth Muscle	▪	✓	✓	▪	Vasoconstriction (Yang et al., 2006)
	Pancreatic B cells	▪	✓	✓	▪	increased insulin secretion (Akiba et al., 2004)
HUMAN	Corneal Epithelium	▪	▪	✓	✓	inflammatory mediator secretion (Zhang et al., 2007a)
	Corneal Endothelium	▪	✓	✓	▪	temperature sensation (Mergler et al., 2010)
	Cerebromicrovascular Endothelium	✓	✓	▪	✓	regulation of BBB permeability (Golech et al., 2004)
	Blood	✓	▪	▪	▪	nociception; inflammatory processes? (Saunders et al., 2001)
	Mononuclear cells	▪	✓	▪	▪	
	Epidermal Keratinocytes	✓	✓	▪	✓	noxious chemical sensor (Inoue et al., 2002)
	Preadipocytes and Adipose tissue	✓	✓	▪	✓	Adipogenesis (Zhang et al., 2007c)
	Synoviocytes	▪	✓	▪	✓	adaptive/pathological changes in arthritic inflammation (Kochukov, 2006)
	Nasal Vasc. Endothelium and Submucosal Glands	✓	✓	▪	▪	stimulate epithelial secretions (Seki et al., 2006)

Table 1.3 Non-neuronal expression of TRPV1

	Expression Site	Immuno (-staining/ -fluorescence)	RT-PCR	Western Blot	$[Ca^{2+}]$ functionality	Possible role/effects on activation
MOUSE	Auditory hair cell; Organ of Corti; Utricle, Saccule and Crista Ampullaris	✓	▪	✓	✓	Mechanosensor? (Nagata et al., 2005)
	Enterochromaffin cells	▪	✓	▪	✓	regulates gastrointestinal motility via 5HT release (Nozawa et al., 2009)
	Hair follicle keratinocytes	✓	✓	▪	▪	modulation of cutaneous nerve firing (Kwan et al., 2009)
RAT	Cerebral and cerebellar artery endothelium	✓	✓	▪	✓	Vasodilation (Earley et al., 2009)
	Urothelium	✓	✓	▪	▪	detrusor overactivity (Streng et al., 2008)
	Enterochromaffin cells	▪	✓	▪	✓	regulates gastrointestinal motility via 5HT release (Nozawa et al., 2009)
HUMAN	Undifferentiated keratinocytes	▪	▪	▪	✓	thermosensation? (Tsutsumi et al., 2010)
	Skin basal keratinocytes	✓	▪	▪	▪	? (Anand et al., 2008)
	Keratinocytes in Epidermis and Dermis of Hair follicle	▪	✓	✓	▪	keratinocyte differentiation; inflammation; mechano- and thermosensor (Atoyan et al., 2009)
	Melanocytes	▪	✓	✓	▪	
	Fibroblasts	▪	✓	✓	▪	
	Synoviocytes	▪	✓	▪	✓	adaptive/pathological changes in arthritic inflammation (Kochukov, 2006)
	Enterochromaffin cells	▪	✓	▪	✓	regulates gastrointestinal motility via 5HT release (Nozawa et al., 2009)
	Dog brain and cerebellum	▪	✓	▪	▪	? (Doihara et al., 2009)

Table 1.4 Non-neuronal expression TRPA1

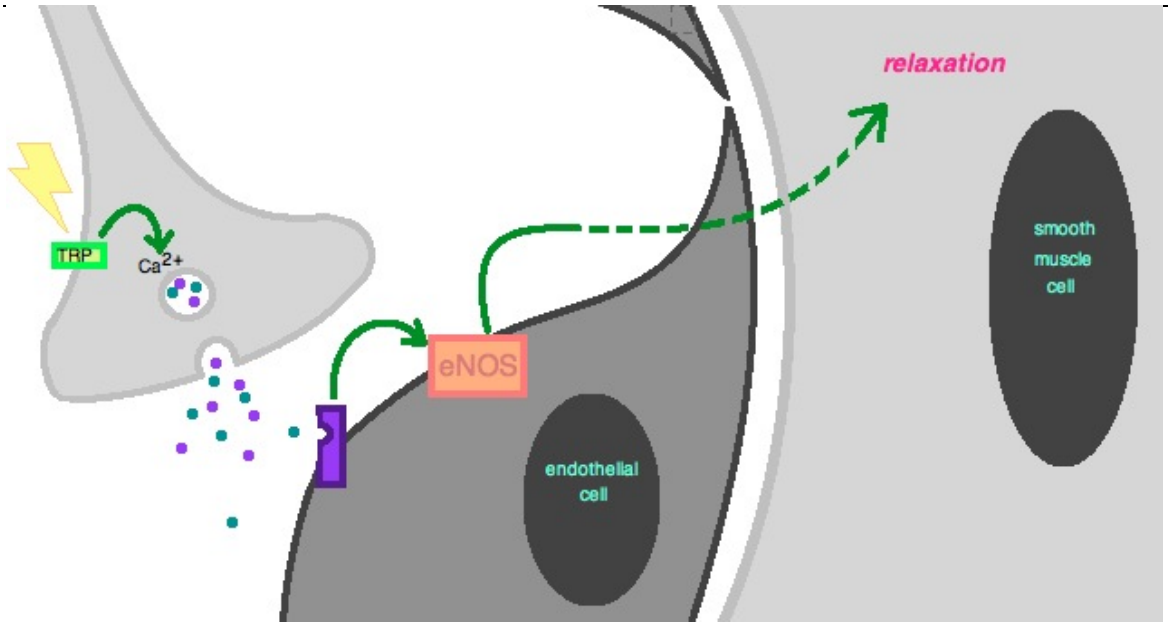

Figure 1.5 Schematic of the vasodilatory response to TRP channel activation. Activation of TRPA1 or TRPV1 on nerve terminals leads to an increase in $[Ca^{2+}]_i$, causing subsequent release of neuropeptides such as Substance P and CGRP. One method of vasodilation is caused by the neuropeptides activating receptors on endothelial cells, causing downstream activation of endothelial nitric oxide synthase (eNOS). eNOS produces NO, which diffuses to smooth muscle cells and causes vasorelaxation.

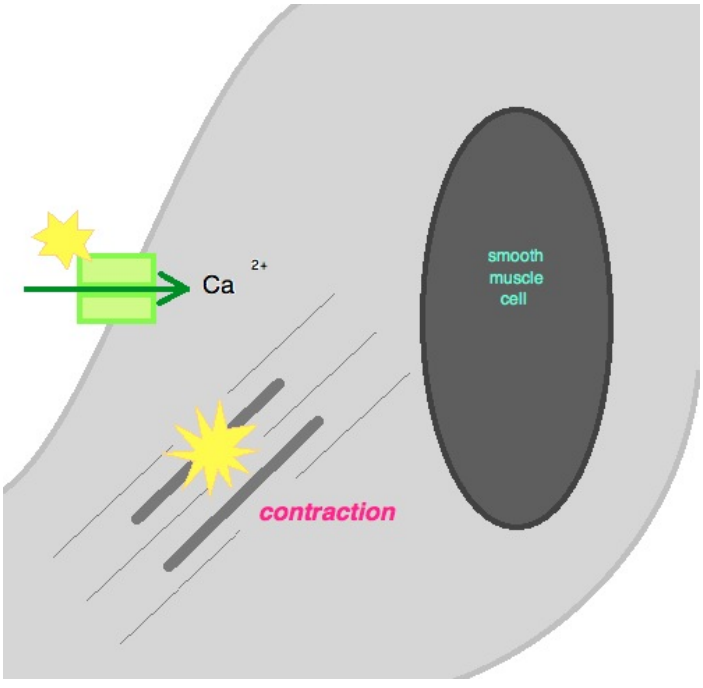

Figure 1.6 Schematic of the purported vasoconstriction response to TRPV1 channel activation directly on smooth muscle cells. TRPV1 directly located on the plasma membrane of smooth muscle cells results in an increase in $[Ca^{2+}]_i$, which results in downstream activation of the contraction cascade (via myosin light chain kinase).

In any case, the role of non-neuronal TRPV1 and TRPA1 channels is still being investigated. It is clear that understanding these roles will clarify the mechanisms involved in TRPV1-mediated hyperthermia; however this is not the only factor that should be considered. As previously mentioned, Garami and colleagues suggested that different modes of activation of TRPV1 contribute to hyperthermia, another important factor to take into account, considering the multitude of stimuli activating the channel (Garami et al., 2010). TRPA1 in particular is an enigma in the world of temperature sensation and regulation. Whilst contradictory evidence has been presented concerning its role in cold temperature sensation, we know that icilin causes hyperthermia in rodents (Ding et al., 2008). This interesting finding suggests that TRPA1 may have a role in thermoregulation, should icilin be acting via TRPA1. It may be that icilin is acting on TRPM8 or indeed on a pathway downstream of TRPA1 activation that is the same as that involved in TRPV1-mediated hyperthermia.

1.3.1 TRPV1 and TRPA1 in vasculature

The roles of TRPA1 and TRPV1 in the vasculature have been the focus of increasing investigation. Capsaicin has long been known to be vasoactive, an effect that has been attributed to activation of TRPV1 on sensory neurons, release of inflammatory neuropeptides and subsequent neurogenic inflammation (Brain and Grant, 2004). The release of inflammatory neuropeptides is also characteristic of TRPA1 activation. This local neurogenic inflammation comprises vasodilation and plasma extravasation, including vascular changes in the smooth muscle layer. The vasodilatory effects are complex and are mediated by CGRP, a potent vasodilator (Brain et al., 1985). CGRP acts on CGRP receptors which are usually formed by the coexpression of the calcitonin receptor-like receptor (CRLR) and receptor-accessory-modifying protein 1 (RAMP1; (McLatchie et al., 1998; Juaneda et al., 2000). The mechanisms for CGRP-induced vasodilation include nitric oxide (NO) (Figure 1.5), which is endothelium-dependent and mediated by increased levels of cGMP via guanylyl cyclase (Brain and Grant 2004; Hay et al., 2004). However, CGRP can still cause vasodilation in the absence of the endothelium; CGRP can act directly on smooth muscle cells to increase cAMP via adenylyl cyclase. This has been shown by Edvinsson and colleagues, with endothelium denuded arteries in cat brain vessels (Edvinsson et al., 1985) and human intracranial arteries (Edvinsson et al., 1998). The increase in cAMP leads to increased phosphorylation (and therefore activation) of K_{ATP} channels by protein kinase A (PKA). Substance P (SP) is responsible for the plasma extravasation

component of neurogenic inflammation. The effects of SP are mediated by neurokinin 1 (NK1) receptors, which are located on post-capillary endothelial cells. SP can also have vascular permeability effects via non-receptor-dependent mast cell-dependent mechanisms (Holzer, 1998).

More recently, expression of TRPV1 has been shown in vascular smooth muscle cells, where activation causes influx of calcium ions and, in turn, contraction (see Figure 1.6) in certain tissues: arterioles (Czikora et al., 2012), skeletal muscle (Kark et al., 2008), and the synovial membrane (Keeble and Brain, 2006). Therefore the role of TRPV1 in the vasculature is a complex one, which seems to be expression dependent. TRPA1 has also been investigated in the vasculature, as activation of this channel also releases vasoactive mediators (Earley et al., 2009). Some of the vascular responses to H_2S have been attributed to its ability to activate TRPA1 (Streng et al., 2008; Pozsgai et al., 2012). It is not yet known if activation of TRPA1 has differing effects in different microvascular beds, like TRPV1.

Further to the initial focus of research on the roles of TRPV1 and TRPA1 in pain and inflammation, the expression of these channels in other tissues has highlighted the need to understand their function in different tissues, in order to understand the important issue of on-target side effects, an issue raised in the development of TRPV1 antagonists. Whilst these compounds are a great prospect for pain treatment, TRPV1 antagonists caused hyperthermia in rodents, dogs and humans. The mechanism of this characteristic is poorly understood, and could be mediated by the same receptors involving pain, or entirely differently located receptors. In order to overcome the obstacle of hyperthermia, we first need to understand the role of TRP channels in thermoregulation.

1.4 TRPV1 and TRPA1 in thermoregulation

1.4.1 Thermoregulation

The body temperature of mammals must be kept stable, and this occurs via a homeostatic mechanism coordinated by the central nervous system (CNS). The CNS coordinates the fine balance of core body temperature to ensure essential processes are not affected by temperature fluctuations and that executive function is maintained (Morrison and Nakamura, 2011). As reviewed by Romanovsky et al., several physiological and behavioural thermoeffectors work together with peripheral thermosensors to maintain core body temperature (Romanovsky et al., 2009).

Lesion and stimulation studies of the preoptic region and anterior part of the hypothalamus show that these areas act as the temperature control centre of the brain (Boulant, 2000). Increases in sympathetic neural activity and subsequent changes in thyroid and brown adipose tissue activity act to increase temperature whilst piloerection (in non-human mammals) and cutaneous vasoconstriction (Morrison and Nakamura, 2011) maintain set temperature by reducing heat loss. Heat loss mechanisms when the body temperature is too high include cutaneous vasodilation (Morrison and Nakamura, 2011), sweating and panting; in humans, the somatic nervous system can coordinate behaviours such as clothing removal to facilitate heat loss. In smaller animals, this behaviour can present as heat avoidance and shade seeking (Almeida et al., 2006). The sympathetic nervous system is involved in temperature induced vascular responses with involvement of noradrenaline and α_2-adrenoceptors (Freedman et al., 1992; Chotani et al., 2000; Honda et al., 2007). TRP channels not only play a role in detection of peripheral temperature, they may also play a role in the physiological response to temperature changes.

1.4.2 TRPV1 activation and antagonism results in thermoregulatory dysfunction

The development of TRPV1 antagonists as novel analgesic and anti-inflammatory compounds was halted by their hyperthermic side effects. Over the past two decades the ability of TRPV1 antagonists has been investigated, with many groups showing the ability of these compounds to cause hyperthermia (Gavva et al., 2005 Gavva et al., 2007a; 2007b; 2008; Honore et al., 2009). Despite this, TRPV1 antagonist-induced hyperthermia is still a poorly understood phenomenon. Evidence has emerged of the role of TRPV1 in body temperature regulation, and it is thought that this is linked to the changes in body temperature that

have been seen in clinical and preclinical trials. Despite a wide range of structures and properties, most TRPV1 antagonists cause hyperthermia. Interestingly, this can occur in the absence of an agonist (Steiner et al., 2007; Gavva et al., 2007b) suggesting that the TRPV1 channel is constitutively active.

Like all homeostatic mechanisms, thermoregulation relies on maintaining a balance between heat loss and heat production (Romanovsky et al., 2009). Heat loss occurs predominantly via cutaneous vasodilation – for example, in humans from skin, and rodents from the tail skin. In mammals, heat production occurs in thermogenic organs, which are usually under central control (Lowell and Spiegelman, 2000). In adult humans, this is usually skeletal muscle, through exercise-induced thermogenesis. Heat is also produced as a by-product of respiration. In rodents (and human babies) heat production occurs primarily in brown adipose tissue (BAT), where uncoupling protein 1 (UCP1; thermogenin) – the most potent mammalian thermogenic protein (Kozak and Harper, 2000) is expressed. BAT was thought to be solely located in animals and human infants, however it has been shown in adult humans (Nedergaard et al., 2007). UCP1 is instrumental in adaptive non-shivering thermogenesis in a cold environment, demonstrated by studies in mice with the gene deleted (Golozoubova et al., 2001). Interestingly, homologues of UCP1: UCP2 and UCP3 (Fleury et al., 1997; Boss et al., 1997a; 1997b) are expressed in other tissues, such as skeletal muscle (another site of thermogenesis). However, they have not been linked with thermoregulation (UCP3 having been indicated as having a role in lipid metabolism and obesity (van Abeelen et al., 2008).

Early studies by Jancso-Gabor et al., showed that large doses of capsaicin led to permanent, irreversible desensitisation of animals to the compound's hypothermic effects (Jancsó et al., 1967). The animals were subsequently unable to regulate their body temperature in warm environments resulting in hyperthermia. A similar recent study (Lutaif et al., 2008) showed a fast, significant increase in rectal temperature in response to chronic systemic capsaicin administration. Intriguingly, this was coupled with an increase in levels of UCP-1, a protein important in thermogenesis, indicating that UCP1 may possibly be linked to TRPV1-mediated hyperthermia.

Several studies in both animals and humans have reported a rise in body temperature to fever ranges after administration of TRPV1 antagonists (Gavva et al., 2005; 2007a; 2007b; 2008; Honore et al., 2009), a

phenomenon not observed in TRPV1 knockout mice (Steiner et al., 2007). Whilst investigations with peripherally restricted antagonists have shown that this is a peripherally mediated effect (Tamayo et al., 2008), the exact mechanism remains to be elucidated. The hyperthermia caused by TRPV1 antagonists does however decrease on repeated administration (Gavva et al., 2007a), in a manner distinct from agonist-induced desensitisation of TRPV1. Other studies show that acetaminophen also decreases the antagonist – associated hyperthermia (Bertolini et al., 2006) - another mechanism that remains to be elucidated. Interestingly, TRPV1 antagonist-induced hyperthermia is proposed to originate from the abdominal cavity (Steiner et al., 2007), which is not necessarily associated with BAT deposits, conversely this is the site of white adipose tissue deposits.

Recently, Garami and colleagues suggested that different modes of activation of TRPV1 play a role in hyperthermia - as some antagonists do not cause hyperthermia – drawing correlations between modes of activation and antagonists settling on the hypothesis that antagonists blocking proton-activation of TRPV1 do not cause hyperthermia (Garami et al., 2010).

We propose that TRPV1 antagonist-mediated hyperthermia may be caused by activation of non-neuronal TRPV1 (i.e. activation other than the intended, sensory neuronal site of expression). As discussed, activation of TRPV1 on sensory nerves leads to SP and CGRP release. This has been demonstrated in skin, where application of capsaicin leads to neuropeptide-mediated vasodilation and a subsequent increase in blood flow (Grant et al., 2002). However, concomitant activation of TRPV1 directly on vascular smooth muscle cells, for example would cause a vasoconstriction. Subsequent decreases in cutaneous blood flow, accompanied by an increase in central blood flow would result in a rise in core body temperature – as we know, cutaneous blood flow is necessary for heat dissipation in mammals. TRPV1 activation resulting in vasoconstriction has been shown by Kark and colleagues, where skeletal muscle arterioles constricted on TRPV1 activation (Kark et al., 2008). In addition, Keeble and Brain have shown that capsaicin applied directly to the exposed wild type murine synovial membrane results in vasoconstriction, a phenomenon not seen in TRPV1 knockout mice (Keeble and Brain, 2006).

1.4.3 TRPA1 and thermoregulation

The TRPA1/TRPM8 agonist icilin induces hyperthermia that is dependent on nitric oxide production and NMDA receptor activation (Ding et al., 2008). If this is a TRPA1 effect, it is an intriguing one; agonists at TRPA1 cause hyperthermia whilst those at TRPV1 cause hypothermia. However it is unclear as to whether icilin-induced hyperthermia is an effect mediated by TRPA1 or TRPM8, or even TRPV1. Further investigation of TRPA1 and temperature, including the development of more specific TRPA1 pharmacological tools will help to determine whether TRPA1 is in fact more than simply a thermosensor. This may be a little optimistic as although TRPV1 and TRPA1 have similar roles e.g. release of neuropeptides, the case for the involvement of TRPA1 in thermosensation is far from strong.

The purported mechanisms of TRPV1-mediated hyperthermia rely in some part on TRPV1 expression in locations other than sensory nerves, such as the vasculature and thermogenic organs (e.g. brown adipose tissue and skeletal muscle). Indeed, TRPV1 and TRPA1 are expressed widely throughout the body, and investigation of their functions in tissues, especially those critical in temperature control, can shed some light on the mechanisms of TRPV1 antagonist mediated hyperthermia. At the same time, investigation of TRPA1 in similar locations throughout the body can aid our understanding of the interaction between TRPV1 and TRPA1. This can enable ascertainment of the usefulness of TRPA1 as an alternative or indeed simultaneous target for a pain therapeutic with a thermoneutral profile.

1.5 The physiological roles of Hydrogen Sulfide

Hydrogen Sulfide (H_2S) is a noxious, colourless gas; its most characteristic trait is the smell of rotten eggs. The foul smell can be detected by humans at concentrations as low as 0.5 ppb and the LC_{50} for 5 minutes exposure is 800 ppm (Wang, 2012). Therefore it came as some surprise in 1996 when Abe and Kimura used NaSH to show that endogenous H_2S may function as a neurotransmitter – similar to nitric oxide (NO) and carbon monoxide (CO) (Abe and Kimura, 1996). This was followed with studies showing H_2S activity in the vasculature (Hosoki et al., 1997).

H_2S is a small molecule, with a weight of 34.08 kDa. It can exist endogenously as H_2S, HS^- and theoretically as S^{2-} (the latter only possibly existing endogenously at very high pH levels). As a gas, it does not need a specific transporter or facilitator to enter cells, as it can diffuse directly across cell membranes (Mathai et al., 2009). There are many endogenous sources of sulfide and hydrogen sulfide, as it is produced endogenously during the metabolism of sulfur-containing amino acids, particularly the transsulfuration pathway (Wang, 2002). H_2S can also be produced non-enzymatically, to a much lesser degree than the enzyme-mediated pathways. This occurs in erythrocytes, where inorganic and organic polysulfides can be reduced by products of the oxidation of glucose and is thiol- and glutathione- dependent (Weisiger et al., 1980; Searcy and Lee, 1998).

1.5.1 Endogenous H_2S production and metabolism

Figure 1.7 details the endogenous enzymatic production and metabolism of H_2S. H_2S can be synthesised endogenously by a number of enzymes: cystathionine β-synthase (CBS) and cystathionine γ-lyase (CSE) as well as 3-mercaptopyruvate sulfurtransferase (3-MST) and cysteine aminotransferase (CAT). These enzymes can be found both in the cytosol and mitochondria – the latter being the case with 3-MST and CAT in particular. The majority of endogenous H_2S production is via CBS and CSE, which are both pyridoxal 5'-phosphate-dependent enzymes. CBS and CSE catalyse the breakdown of certain sulfur-containing amino acids and cystathionine. Expression of these enzymes differs: the majority of reports suggest that CBS is centrally located whilst CSE is restricted to the periphery, however this has more recently been disputed, as CBS has been found in the periphery and CSE in the CNS (Whiteman et al., 2011).

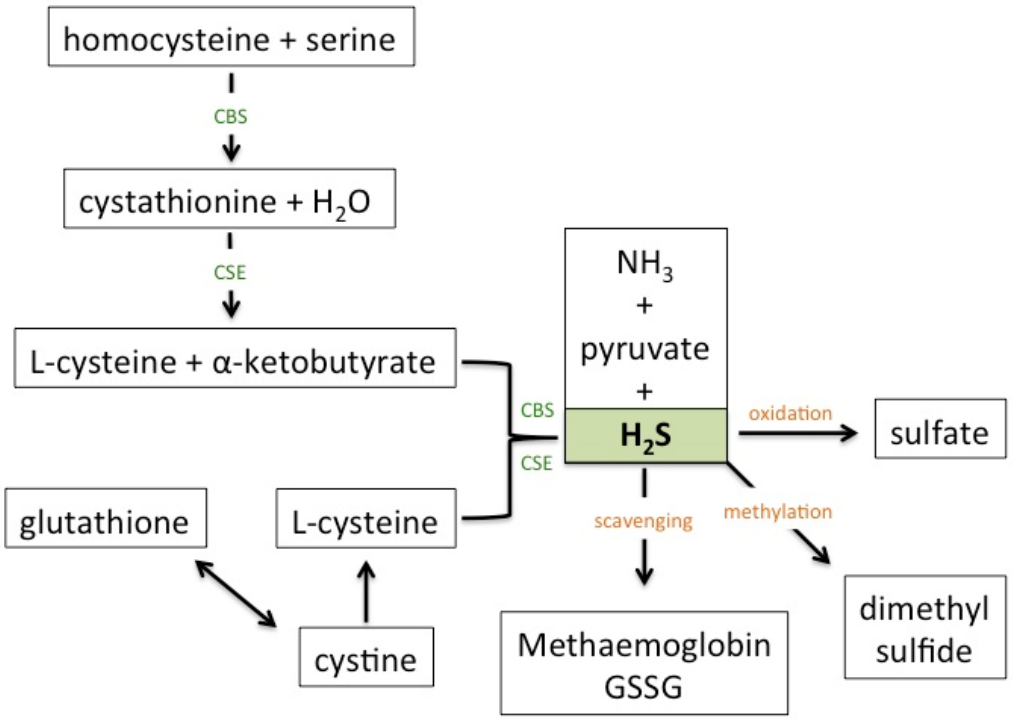

Figure 1.7 Enzymatic production and metabolism of H_2S (adapted from (Wang, 2002; Sun et al., 2008).

GSSG= Glutathione disulfide; CBS= cystathionine β-synthase; CSE= cystathionine γ-lyase

CBS was first isolated in 1969 (Braunstein et al., 1969). Human CBS is a homotetramer with intracellular binding sites for PLP on the N-terminus (Banerjee and Zou, 2005) and S-adenosylmethionine (SAM) on the C terminus (Kery et al., 1998). CBS is suggested to be the predominant source of H_2S in the nervous system, it is highly expressed in the brain (Robert et al., 2003; Enokido et al., 2005), however this has more recently been disputed, as CBS is expressed in the periphery and CSE in the CNS (Whiteman et al., 2011).

CSE was initially cloned from rat liver in 1990 (Erickson et al., 1990), however its role in H_2S physiology was elucidated later when Zhao and colleagues cloned it from rat vascular cells (Zhao et al., 2001). This study showed the importance of NO in the activity of CSE, and the subsequent importance of H_2S in vasorelaxation, as it increases the activity of cGMP-dependent protein kinases, in turn stimulating CSE (Zhao et al., 2001).

The importance of both enzymes has mostly been determined using pharmacological tools such as inhibitors and modulators (see section 1.5.2). The scientific community studying H_2S have attempted to produce CBS and CSE KO mice, however homozygous CBS KO mice had severe stunted growth and died within 5 weeks – heterozygotes have instead been used to determine the effects of CBS *in vivo* (Watanabe et al., 1995). CSE KO mice have been more successful: Yang and colleagues bred a CSE KO mouse and showed that the enzyme is important in the vasculature (Yang et al., 2008). CSE KO mice had hypertension that was rescued by treatment with exogenous H_2S in the form of NaSH – showing that lack of endogenous H_2S was the cause of the hypertension (Yang et al., 2008).

H_2S is predominantly cleared by methylation in the cytosol (Weisiger et al., 1980); oxidation to sulfate in mitochondria (Furne et al., 2001; Lagoutte et al., 2010); or being scavenged by methaemoglobin or glutathione (Smith and Abbanat, 1966; Beauchamp et al., 1984).

1.5.2 Pharmacological tools

In the absence of reliable homozygous enzyme KO mice, the investigation of physiological and pathophysiological roles of H_2S has been conducted with the use of sulfide donors and endogenous enzyme inhibitors. The most important thing to consider in all studies published thus far is the extremely

high dose of donors, salts and other H_2S generating compounds needed to elicit a response, both *in vivo* and *in vitro*. The most often-used "donor" has been the sulfide salt NaSH, a sulfide salt, similar to Na_2S and CaS, which dissociates rapidly in aqueous solution. NaSH was used in the first study showing H_2S is involved in neurotransmission (Abe and Kimura, 1996). These salts enabled many roles of H_2S to be elucidated in early functional investigation; however the biggest disadvantage of these compounds is that they generate H_2S immediately on contact with solvent, therefore are not particularly physiologically relevant. More recently, slower H_2S releasing donors have been developed. These compounds allow a more physiologically relevant investigation of the effects of H_2S than the fast burst release of the sodium sulfide salts. The most widely used of these slower release compounds is morpholin-4-ium 4 methoxyphenyl(morpholino) phosphinodithioate, or GYY4137; a donor based on Lawesson's reagent, another sulfide donor which releases sulfide in organic solvents (Li et al., 2009). Li and colleagues showed that GYY4137 was able to relax rat aortic rings (via K_{ATP}) and caused hypotension *in vivo*, whilst avoiding cytotoxic damage (Li et al., 2009).

There are other donors and sulfide-releasing compounds available, including organic compounds such as allicin, the TRPA1 agonist (Benavides et al., 2007), and sulfide-releasing-NSAIDs and other chimeras (Chattopadhyay et al., 2012). Cysteine analogues such as N-acetyl cysteine (NAC) and S-allyl cysteine have also been used as a method of increasing intracellular H_2S (Wang et al., 2010).

Other pharmacological tools include those used to study the function of endogenous enzymatic production of H_2S. Hydroxylamine is a PLP-dependent enzyme inhibitor, therefore is not widely used due to its lack of specificity – it is also an NO donor. The most commonly used CBS inhibitor is the PLP-dependent enzyme inhibitor, Aminooxyacetate (AOAA), however its specificity for CBS is controversial – in fact it blocks CSE more potently than CBS (Papapetropoulos et al., 2015). S-adenosyl-L-methionine (SAM) can also bind to CBS allosterically, allowing it to be activated more easily (Finkelstein et al., 1975; Abe and Kimura, 1996).

DL-propargylglycine (PAG) irreversibly inhibits CSE, and to a lesser extent, CBS. Soluble in saline or organic solvents, it has been used *in vivo* at concentrations between 25-100 mg/kg to reduce inflammation in models of pancreatitis and oedema (Bhatia et al., 2005b) and endotoxaemia (Collin et al., 2005).

1.5.3 H_2S interactions *in vivo*

It is thought that most H_2S signalling occurs via protein sulfhydration. This is where cysteine residues in proteins, including receptors, are modified to persulfide groups, thereby inducing a conformational change of the protein (Mustafa et al., 2009). At present, no specific endogenous receptor has been identified for H_2S. Based on the actions of NO and CO *in vivo*, It follows that H_2S should bind to proteins as easily and non-selectively as its fellow neurotransmitters, due to its physicochemical properties. H_2S is reported to activate several cation channels: K_{ATP} (Zhao et al., 2001), L-type calcium channels (Sun et al., 2008), BK_{Ca} (Telezhkin et al., 2010), and the TRPA1 receptor (Streng et al., 2008).

The ability of H_2S to activate the TRPA1 channel was first outlined by Streng and colleagues in the urothelium in the bladder (Streng et al., 2008). Since then, the relationship between H_2S and TRPA1 has become clearer. The TRPA1 activator allicin (Macpherson et al., 2005) is reported to be an H_2S donor (Benavides et al., 2007). TRPA1 has also recently been suggested to be the mediator of both the pro-nociceptive (Andersson et al., 2012) and vasodilatory (Pozsgai et al., 2012) actions of H_2S, however these are very preliminary studies, with some evidence gained from studies using extremely high concentrations of sulfide salts. Therefore it is not certain whether these effects are truly H_2S-induced, rather than off-target effects of high dose/concentrations.

Endogenous mediators can modify the actions of H_2S. Testosterone (Bucci et al., 2009) and NO (Zhao and Wang, 2002) can both increase activity of H_2S-producing enzymes. Insulin has been suggested as an endogenous inhibitor of liver CBS (Ratnam et al., 2002) and may also have an inhibitory role on CSE (Wang, 2003).

As is the case with many promising novel targets, the purported physiological roles of H_2S have been numerous. However the best-supported roles in health and disease are for H_2S in pain, the vasculature and inflammation.

1.5.4 H_2S actions in pain

The role of H_2S in pain is contentious, with reports of it being both anti- (Distrutti et al., 2006; Cunha and Verri, 2007) and pro-nociceptive (Kawabata et al., 2007; Matsunami et al., 2008; Maeda et al., 2009). The gasotransmitter's electrophilic nature and ability to activate a number of ion channels, which are important in sensory perception including pain, means that it could play a key role in certain pain states. Andersson and colleagues recently suggested that TRPA1 mediates the pro-nociceptive activity of H_2S (via NaSH), using TRPA1 KO mice to show that the TRP channel is key in the ability of H_2S to depolarise somatic pain-sensing neurons (Andersson et al., 2012).

1.5.5 H_2S actions in vasculature

In the vasculature, H_2S is predominantly considered to be vasorelaxant and pro-angiogenic. The angiogenic actions of H_2S have been shown both *in vitro* (Cai et al., 2007) and *in vivo* (Papapetropoulos et al., 2009), and is suggested to be mediated by the effects of the gasotransmitter on vascular endothelial growth factor (VEGF). The vasorelaxant effects of H_2S are perhaps more relevant to this thesis, given the important role of the vasculature, both peripheral and visceral, in thermoregulation.

The actions of H_2S on K_{ATP} channels is considered to be the basis of its purported vasoactive abilities (Zhao et al., 2001). However, H_2S has also been shown to activate other ion channels (the IK_{Ca} and SK_{Ca} channels) by S-sulfhydration (Mustafa et al., 2011). In terms of other channels, some groups have shown that BK_{Ca} is involved in H_2S signalling in carotid artery and mesenteric vessels (Telezhkin et al., 2010; Jackson-Weaver et al., 2011) however other have been unable to affect H_2S-induced vasodilation with BK_{Ca} blockade in aortic rings (Zhao et al., 2001). The voltage gated K^+ channel is also reported to be activated by H_2S to cause vasorelaxation, as an inhibitor of the K_v7 channel blocks vasorelaxation (Martelli et al., 2013).

As previously mentioned, H_2S has a role in hypertension; GYY4137 decreases blood pressure in L-NAME induced hypertensive rodents and spontaneously hypertensive rats (Li et al., 2008b). Additionally, i.v. administration of NaSH reduced the mean arterial blood pressure of anaesthetised mice (Ali et al., 2006). Finally, and most importantly, CSE KO mice are hypertensive, a phenotype that is reversed on administration of NaSH (Yang et al., 2008).

1.5.6 H_2S actions in inflammation

H_2S is known as an irritant compound; initial signs of H_2S toxicity include eye inflammation (Lambert et al., 2006), and early reports of H_2S poisoning included lung inflammation. The inflammatory role of H_2S is not restricted to its irritant nature; H_2S has also been implicated in inflammatory states such as experimental colitis, and sepsis. Sepsis, and subsequent septic shock, is characterised by total body inflammation after an infection – usually bacterial although sometimes due to other microbes (Astiz and Rackow, 1998). Severe vascular dysfunction can occur after sepsis, due to hypotension and hypoperfusion (Astiz and Rackow, 1998). Li and colleagues have shown the involvement of H_2S in lipopolysaccharide-induced endotoxic shock (Li et al., 2005), whereby exogenous H_2S in the form of GYY4137 is protective. This finding is in contrast to studies by others investigating H_2S in animal models of sepsis, demonstrating that H_2S salts and donors are pro-inflammatory (Hui et al., 2003; Collin et al., 2005; Zhang, 2006). Hui and colleagues showed increased arterial H_2S in rats with septic and endotoxic shock (Hui et al., 2003), whilst other groups showed that blocking endogenous H_2S production was beneficial in treating organ damage subsequent to septic/endotoxic shock (Collin et al., 2005; Zhang, 2006).

H_2S has a role in oedema formation. Pulmonary oedema is characteristic of H_2S poisoning. In animal models of oedema formation; exogenous H_2S via sodium salts NaSH and Na_2S suppresses oedema formation in carrageenan-injected hindpaws via K_{ATP} and regulates leukocyte adhesion at the endothelium (Zanardo et al., 2006) – however these studies may have been limited by use of the relatively non-selective antagonist BCA, which blocks PLP-dependent enzymes including CBS and CSE. Bhatia et al., in contrast, showed that endogenous H_2S production has a protective role here: PAG dose dependently decreases inflammation in carrageenan treated paws (Bhatia et al., 2005a).

In terms of other inflammatory conditions, there are higher levels of H_2S in the synovial fluid of joints of patients with rheumatoid arthritis and also an increase in H_2S in joints of those with other forms of arthritis (Whiteman et al., 2010a). Further, Li and colleagues recently showed that exogenous H_2S via the slow-release donor GYY4137 is anti-inflammatory in a CFA-induced model of joint inflammation (Li et al., 2013), this effect being dependent on the timing of GYY4137 administration. Therefore, H_2S is a complex mediator of joint inflammation.

Perhaps most pertinent to this thesis is the proposed role of H_2S in neurogenic inflammation. Intraperitoneal injection of NaSH into naïve mice resulted in a significant increase in plasma SP and resultant lung inflammation that was dependent on the NK1 receptor (not NK2 or CGRP dependent) in a model of sepsis-induced lung injury (Zhang et al., 2007b). In the isolated guinea pig airway, NaSH administration resulted in release of SP and CGRP from sensory nerve terminals, and led to airway constriction through capsaicin and NKR1/NKR2-transient receptor potential vanilloid 1 (TRPV1)-dependent pathways (Trevisani et al., 2005; Ang et al., 2010). In a similar vein, NaSH caused the release of inflammatory neuropeptides, mediated by TRPV1 in the rat bladder and detrusor muscle leading to smooth muscle contraction (Patacchini et al., 2004; Patacchini et al., 2005). More recently, treatment of isolate rat tracheae or the pinna with NaSH was shown to release CGRP, mediated by TRPA1; this effect was inhibited with the TRPA1 antagonist HC030031 (Pozsgai et al., 2012).

1.5.7 H_2S actions in metabolism and thermoregulation

H_2S can suspend animation in rodents (Blackstone et al., 2005; Volpato et al., 2008; Aslami et al., 2010; Seitz et al., 2012), but not other, larger mammalian species (Li et al., 2008a). This suggests that the processes involved are pertinent to smaller animals and dependent on mechanisms occurring in small mammals and not larger species. The suspended animation does not occur via the same mechanism as general anaesthesia (Li et al., 2012). In studies by Roth and colleagues, mice were exposed to 80ppm inhaled H_2S. This lowered the oxygen consumption and carbon dioxide output and lasted for over 6 hours – during this time the metabolic rate also reduced by approximately 90%. Interestingly in terms of this thesis, this drop in metabolic rate was accompanied by a reduction in core body temperature to approximately 2°C above room temperature (Blackstone et al., 2005). The suggested mechanism for this

response is via inhibition of mitochondrial cytochrome c oxidase and the subsequent reduction in respiration rate (Nicholls et al., 2013). Mitochondrial cytochrome c oxidase is part of the electron transport chain; therefore inhibition by H_2S results in a slower metabolic rate and alteration of the mitochondrial redox state (Mancardi et al., 2009). This leads to decreased ATP production. This is characteristic of general hypometabolic states, which can also be induced by reduction in O_2 availability or CO administration (Padilla and Roth, 2001; Nystul and Roth, 2004), and is the basis of the toxicity of H_2S at higher doses.

The ability of H_2S to induce hypometabolic states and effectively suspend animation has proven an interesting target for protecting organs from damage during transport for organ transplantation and for preventing the damage caused during multiple organ failure (Aslami et al., 2010). However results from studies vary, and animation cannot be suspended in all mammalian species. Whilst the mechanisms most likely do involve cytochrome c oxidase inhibition, there is a fine balance between toxic and beneficial side effects and the targets of H_2S are diverse with roles in many physiological and pathophysiological processes. Therefore it is important to fully understand the mechanisms of this phenomenon before applying it for therapeutic advantage.

1.6 Summary

TRP channels play a wide role in physiology and pathophysiology. TRPV1 and TRPA1 are particularly interesting members of this superfamily as their roles in pain and inflammation make them exciting targets for novel pharmaceutical development. However, development of TRPV1 antagonists revealed an unexpected on-target side effect of hyperthermia. This revelation led researchers to find that TRPV1 is a tonically active ion channel that is key in maintaining a normal body temperature. TRPV1 and TRPA1 can be functionally expressed non-neuronally, which was not expected when TRPV1 antagonists for pain and inflammation were being developed. Whilst the involvement of TRPV1 in thermoregulation is becoming evident, it is not clear whether TRPA1 is also involved in core body temperature control. TRPA1 is also activated by H_2S, a foul-smelling gas that has recently been found to be exogenously produced. This gasotransmitter has a wide range of physiological roles, including roles in the vasculature and a suggested key role in metabolism. Studies in mice show that H_2S may induce a hypometabolic state, consistent with

hibernation. Therefore it may be possible that hypothermia via the TRPA1 agonist H_2S can mitigate TRPV1 antagonist-mediated hyperthermia.

1.7 Aims

The aims of this PhD project were to investigate TRPV1 antagonist-induced hyperthermia, particularly the involvement of the related TRPA1 channel, and its purported agonist H_2S. To do this, we aim to:

Investigate the effects of several TRPV1 and TRPA1 antagonists on pain and thermoregulation, to determine if TRPA1 antagonists affect core body temperature to the same extent as TRPV1 antagonists;

Investigate the vascular responses of TRPV1 and TRPA1 channels in the periphery; in particular, the capacities of TRPV1 antagonists to inhibit capsaicin-induced vascular responses and TRPA1 antagonists to inhibit mustard oil – induced vascular responses will be investigated.

Investigate the interplay between TRPA1 and TRPV1 in antagonist-induced hyperthermia with the use of coadministration studies and KO mice.

Determine if there is a role for H_2S in TRPV1 antagonist – induced changes in core body temperature. In particular, the effects of both fast- and slow-release H_2S donors on TRPV1 antagonist-induced core body temperature changes will be studied. The effects of H_2S on the peripheral vasculature will also be determined, in blood flow and plasma extravasation studies.

Chapter 2 Materials and Methods

2.1 Animals

All experiments were carried out according to the United Kingdom Home Office Animals (Scientific Procedures) Act (1986) and, more recently, the EU Directive 86/609/EEC. Experiments described were carried out with male and female CD1 mice (26-40g; Charles River, UK), age-matched male and female TRPV1 WT and KO (>8 weeks old, 26-40g) or age-matched male TRPA1 WT and KO mice (>8 weeks old, 35-40g).

All mice were housed under controlled conditions (12 hours light: dark cycle - lights on at 0700; 21±2°C; 40-50% humidity) with free access to food and water.

2.1.1 Generation of TRPV1 WT and KO mice

TRPV1 KO mice were gifted from Merck Sharp and Dohme (Harlow, UK) and bred in-house. Mice were bred on a C57BL6/129SVJ background and the TRPV1 channel was knocked out by replacing the exon encoding a portion of the fifth and the entire sixth transmembrane domain (i.e. the pore-forming loop) with a neomycin gene (Caterina et al., 2000).

TRPV1 WT and KO mice used in these studies were from an internally maintained colony (Keeble et al., 2005). In order to confirm the genotype of the mice, an ear biopsy (2 mm) was obtained from each mouse at 3 weeks of age using 2mm stainless steel ear punches (VWR equipment, UK). The genomic DNA was extracted using a commercially available REDEXtract – N – AMP Tissue PCR kit (Sigma-Aldrich). DNA was amplified by PCR using the primers detailed in Table 2.1. The PCR reaction mixture was made up as illustrated in Table 2.2. A thermal cycler (PTC-225 Peltier Thermal Cycler, MJ Research, USA) was used to denature the genomic DNA and activate the *Taq* polymerase for 14.5 minutes at 95°C, then 35 cycles of denaturation at 95°C for 30 seconds; annealing at 60°C for 60 seconds; and elongation at 72°C for 60 seconds (with a final elongation for 60 seconds) were used to amplify the gene of interest.

Primer	Sequence
TRPV1 forward	5’ CGA GGA TGG GAA GAA TAA CTC ACT G 3’
TRPV1 reverse	5’ GGA TGA TGA AGA CAG CCT TGA AGT C 3’
Neomycin forward	5’ TTT TGT CAA GAC CGA CCT GTC C 3’
Neomycin reverse	5’ CCC TCA GAA GAA CTC GTC AAG AAG 3’
TRPA1 WT forward	5’-TCC TGC AAG GGT GAT TGC GTT GTC TA-3’
TRPA1 WT reverse	5’-TCA TCT GGG CAA CAA TGT CAC CTG CT-3’
TRPA1 KO forward	5’-CCT CGA ATC GTG GAT CCA CTA GTT CTA GAT-3’
TRPA1 KO reverse	5’-GAG CAT TAC TTA CTA GCA TCC TGC CGT GCC-3’

Table 2.1 Primers used in TRPV1 and TRPA1 genotyping experiments. The primers detailed in the table above were used in PCR experiments to amplify the genes of interest, along with their sequences.

Reaction mix component	Volume/reaction (µl)
REDEXtract – N – AMP PCR Reaction Mix	10
TRPV1 Forward primer (5 pmol/µl)	2
TRPV1 Reverse primer (5 mol/µl)	2
Neomycin Forward primer (5 pmol/µl)	2
Neomycin Reverse primer (5 pmol/µl)	2
Extracted genomic DNA	5

Table 2.2 PCR reaction mix for genotyping TRPV1 mice. Each component of the reaction mix was added to the reaction in the volumes shown, and run through the thermocycler to amplify the correct gene of interest.

The amplified products were visualised via gel electrophoresis. 15µl of amplification products and 5µl DNA ladder (Hyperladder II; Bioline, UK) were run at 90V for 20 minutes on an agarose gel (1.8% w/v; Sigma-Aldrich) in 1% tris-borate-EDTA buffer (Sigma-Aldrich). The primers for TRPV1 WT mice were expected to amplify a product of approximately 188 base pairs (bp) and those for the neomycin cassette were anticipated to amplify a product of approximately 700bp. Ethidium bromide (3.9 µl/50 ml of 1% TBE + agarose) was added to enable visualisation of the products under a UV camera (Syngene, G-Box) as in Figure 2.1.

2.1.2 Genotyping TRPA1 wild type and knockout mice

TRPA1 WT and KO mice were provided by Professor Susan Brain (King's College London, UK). TRPA1 KO mice were originally generated in a similar way to the TRPV1 KO mice by replacing exons encoding the 5th and 6th transmembrane domain including the pore-forming loop with a cassette containing an internal ribosome entry sire (IRES) with a human placental alkaline phosphatase gene (PLAP) and a polyadenylation sequence as previously described (Kwan et al., 2006). Male chimaeric mice were generated, and mated with C57BI/6J or B6129PF2/J mice to produce heterozygote animals which were subsequently interbred (Kwan et al., 2006) to generate the TRPA1 mice used in these studies.

The genotyping of the TRPA1 mice was carried out in a similar way to that detailed in section 2.1.1. Genomic DNA from ear punches or tail snips was extracted using the REDExtract-N-AMPTM Tissue PCR kit and PCR was using the primers detailed in Table 2.1 (Eurofins Scientific, Europe). The PCR reaction mixture was constituted as shown in Table 2.2. The thermal cycler was used to denature the DNA and activate the *Taq* polymerase for 2 minutes at 94°C. Subsequently, 34 cycles of 94°C for 30 seconds, 64°C for 30 seconds, 68°C for 30 seconds were used to amplify the gene of interest. The amplified products were analysed by gel electrophoresis in the same way as detailed in section 2.1.1 (Figure 2.2). WT bands were expected at 310bp and TRPA1 KO bands at 200bp. Both bands were expected in heterozygous mice as a consequence of the generation protocol.

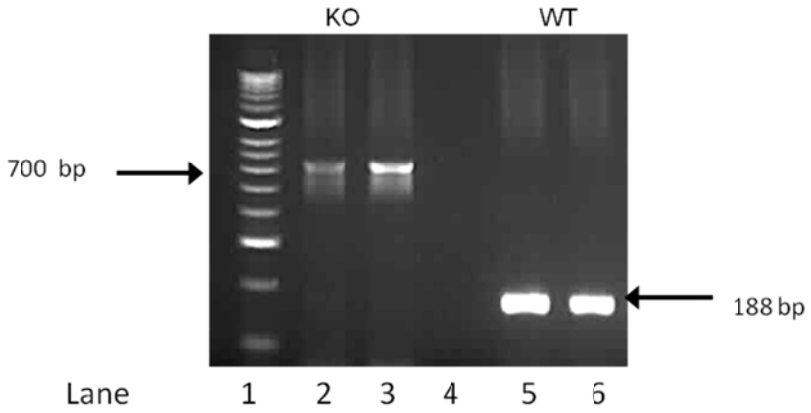

Figure 2.1 Gel electrophoresis image demonstrating TRPV1 WT (188bp) and KO (neomycin, 700bp) genomic DNA. WT mouse genomic DNA was loaded in lanes 5 and 6, and KO mouse genomic DNA loaded in lanes 2&3. Lane 1 contained the DNA ladder and lane 4 was left unloaded.

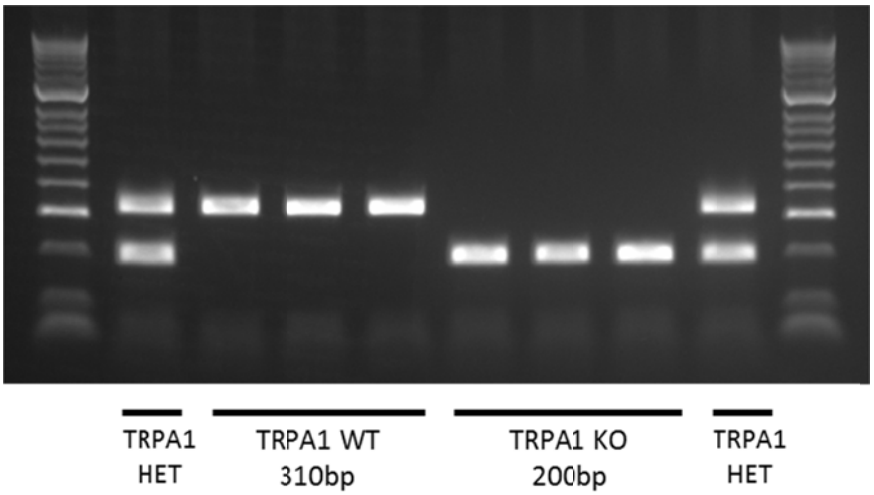

Figure 2.2 Gel electrophoresis image demonstrating TRPA1 WT (310bp) and KO (200bp) genomic DNA. WT, heterozygous (HET) and KO genomic DNA was loaded as indicated.

2.2 Preparation and administration of experimental compounds

Table 2.3 shows the compounds investigated in the following studies. Compounds were prepared on the day of use. Where compounds required a DMSO vehicle, stock solutions in DMSO were prepared on receipt of the solid form and frozen at -20C, ready for dilution on day of use.

Drugs were administered intraperitoneally (i.p.) using 25G needles whilst intradermal (i.d.) and intravenous (i.v.) injections were administered using 27G needles. Intramuscular (i.m.) injections were given via 30G insulin syringes (Micro-Fine Insulin syringes; 0.3 ml; BD Medical. Franklin Lakes, NJ).

Orally administered compounds were administered via bulb-tipped oral gavage needles.

Compound	Molecular weight	Study	Used as	Dose/ concentration	Route of administration	Vehicle	Volume administered	Source
JNJ17203212	419.32	All studies	TRPV1 antagonist	30 mg/kg	i.p.	10% DMSO	10 ml/kg	Tocris Bioscience. Abingdon, UK
SB366791	287.75		TRPV1 antagonist	5 mg/kg	i.p.	10% DMSO	10 ml/kg	Mountford Lab. KCL, UK
TCS5861528	369.42		TRPA1 antagonist	10 mg/kg	p.o.	10% DMSO	5 ml/kg	Tocris Bioscience. Abingdon, UK
HC030031	355.39		TRPA1 antagonist	100 mg/kg	p.o.	10% DMSO	5 ml/kg	Tocris Bioscience. Abingdon, UK
GYY4137	376.47	Telemetry	Slow release H_2S donor	50 mg/kg	i.p.	Saline	10 ml/kg	Wood Lab. University of Exeter, UK
dGYY4137	311.38		GYY4137 without H_2S	50 mg/kg	I.p.	Saline	10 ml/kg	Wood Lab. University of Exeter, UK
NaSH	56.063		Fast release H_2S donor	5.6 mg/kg	i.p.	Saline	10 ml/kg	Sigma-Aldrich. Dorset, UK
D,L-Propargylglycine	113.11		CSE inhibitor	11 mg/kg	i.p.	Saline	10 ml/kg	Sigma-Aldrich. Dorset, UK
Buprenorphine	467.64		Analgesic	10 µg/kg	i.m.	Saline	100 µl	Alstoe Ltd, animal health, York, UK
Isoflurane	184.5		Anaesthetic (recovery)	3-5%	inhaled	5% O_2	As required	Animalcare Ltd, York UK.
Tyrode's Solution	N/A	Skin assay	Physiological solution	N/A	i.d.	N/A	50 µl	Prepared in laboratory
Substance P	1,347.63		Neuropeptide	300 pMol/50 µl	i.d.	Tyrode's Solution	50 µl	Sigma-Aldrich. Dorset, UK
CGRP	3789.4		Neuropeptide	10 pMol/50 µl	i.d.	Tyrodes Solution	50 µl	ANASPEC. Cambridge, UK.

Compound	Molecular weight	Study	Used as	Dose/ concentration	Route of administration	Vehicle	Volume administered	Source
L-Cysteine	121.16	Skin assay	H_2S precursor	5 nmol-5 µmol/50 µl	i.d.	Tyrodes Solution	50 µl	Sigma-Aldrich. Dorset, UK
GYY4137	376.47		Slow release H_2S donor	5 nmol-5 µmol/50 µl	i.d.	Tyrodes Solution	50 µl	Wood Lab. University of Exeter, UK
NaSH	56.063		Fast release H_2S donor	5 nmol-5 µmol/50 µl	i.d.	Tyrodes Solution	50 µl	Sigma-Aldrich. Dorset, UK
Capsaicin	305.41	FLPI	TRPV1 agonist	Ear: 200 µg Knee: 10 nmol	Topical Topical	100% Ethanol 100% Ethanol	20 µl 10 µl	Sigma-Aldrich. Dorset, UK
Mustard Oil	99.15		TRPA1 agonist	Ear: 0.3 mg Knee: 0.3 mg	Topical Topical	Paraffin oil 100% Ethanol	20 µl 10 µl	Sigma-Aldrich. Dorset, UK
GYY4137	376.47		Slow release H_2S donor	100 µM-1 M	Topical	50% ethanol	Ear: 20 µl Knee: 10 µl	Wood Lab. University of Exeter, UK
NaSH	56.063		Fast release H_2S donor	100 µM-1 M	Topical	50% ethanol	Ear: 20 µl Knee: 10 µl	Sigma-Aldrich. Dorset, UK
Ketamine	237.72		Co-administered as non-recovery anaesthetic	75 mg/kg	i.p.	Saline	10 ml/kg	Vetoquinol Ltd. Buckingham, UK
Medetomidine	200.28			1 mg/kg	i.p.	Saline	10 ml/kg	Orion Pharma Ltd. Berkshire, UK
Saline	N/A	All studies	For hydration/as a vehicle	As required				Baxter Healthcare Ltd. Thetford, UK

Table 2.3 Compounds used in *in vivo* experiments. Includes dose/concentration, route of administration, vehicle and volume administered.

2.3 Measuring mechanical and thermal nociceptive thresholds

Two methods of testing nociceptive thresholds were utilised: the Hargreaves method of thermal nociceptive threshold testing and an automated Von Frey test – the dynamic plantar aesthesiometer (Ugo Basile). The Hargreaves method was used as measure of thermal pain thresholds, and the Von Frey to measure mechanical pain thresholds. Both techniques have been used to determine whether antagonists increase basal nociceptive thresholds, thereby demonstrating analgesic efficacy. The treatment of all animals used in naïve pain threshold studies was randomised and blinded until analysis of results.

2.3.1 TRPV1 and TRPA1 antagonists in thermal nociceptive threshold testing

Hind paw thermal nociceptive thresholds were determined using the Hargreaves method before, and then at set intervals after the administration of TRPV1 and TRPA1 antagonists. Timescales varied between compounds.

Mice were placed in a Perspex behavioural box in separate chambers (Figure 2.3) and allowed to acclimatise for thirty minutes before readings were taken. Readings were obtained by applying a constant automated heat source (Ugo Basile, Italy; 50 Watts, 10 volts) to the plantar surface of the paw until paw withdrawal. The paw withdrawal latency (PWL) was measured by the apparatus as seconds, and a cut-off time of 22 seconds was used to avoid tissue damage to the area where the heat source was applied. Three measurements per paw (a total of 6 per mouse per time point) were recorded over thirty minutes, and the mean of all six values per animal were recorded as the thermal nociceptive threshold for each mouse. A maximum of 30 minutes was taken to measure thresholds at each time interval.

2.3.2 TRPV1 and TRPA1 antagonists in mechanical nociceptive threshold testing

Hind paw mechanical nociceptive thresholds were determined using a dynamic plantar aesthesiometer (Ugo Basile, Italy), an automated version of a Von Frey hair filament, according to the same schedule outlined in section 2.3.1.

Mice were placed in a Perspex behavioural box with a wire mesh floor (Figure 2.4) to facilitate the contact between the filament and the mouse's hind paw. The mice were allowed to acclimatise for thirty minutes

in their chambers before readings were obtained. Measurements were obtained using a straight metal Von Frey filament (0.5mm diameter), which exerted a ramped upward force (increasing by 1g every 0.1 second) after making contact with the plantar surface of the hind paw until the paw was withdrawn. Results were expressed as paw withdrawal thresholds (g), i.e. the maximum force withstood. Three measurements per paw were recorded at each time point (giving a total of six measurements per mouse), and the mean of all six values per animal were recorded as the mechanical nociceptive threshold for each mouse. A maximum of 30 minutes was taken to measure thresholds at each time interval.

Figure 2.3 Experimental set up for thermal nociceptive threshold testing. The Hargreaves apparatus was used to determine thermal nociceptive thresholds of mice before and after administration of TRPV1 and TRPA1 antagonists.

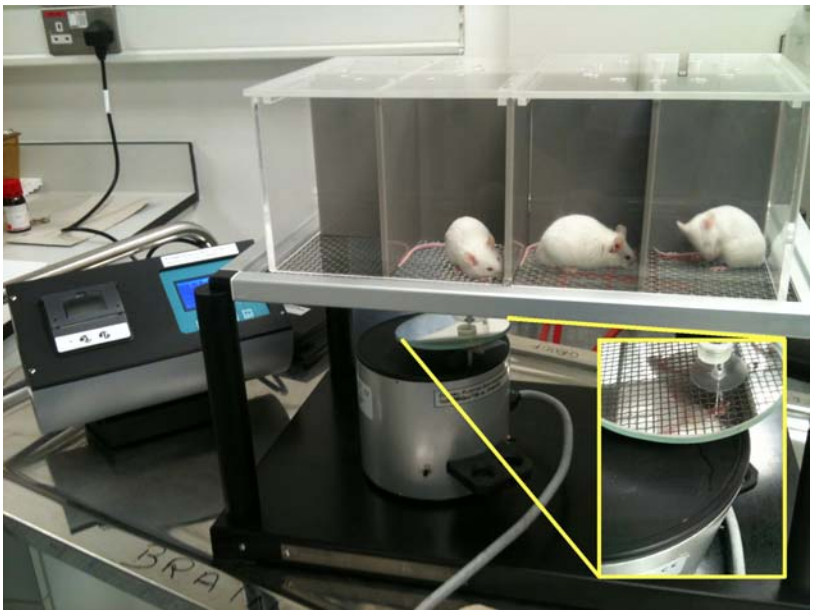

Figure 2.4 Experimental set up for mechanical nociceptive threshold testing. The dynamic plantar aesthesiometer was used to measure mechanical nociceptive thresholds of CD1 mice before and after administration of TRPV1 and TRPA1 antagonists. Inset shows close up of mirror used to focus filament on hind paw.

2.4 Measuring changes in core body temperature using radiotelemetry

Radiotelemetry devices were used to determine the effect of all compounds of interest on the core body temperature of conscious, ambulatory male mice for 24 hours post drug administration, compared to a baseline period of an hour prior to administration. The telemetry device (DSI, St Paul, MN, USA) enabled the simultaneous measurement of locomotor activity and core body temperature.

2.4.1 Implantation of telemetry probes.

Mice (30-35g) were prepared for implantation of temperature telemetry probes under aseptic conditions. Mice received pre-operative analgesia (buprenorphine; 10µg/kg Vetagesic, Alstoe Ltd, Animal Health. York, UK) and then implanted with radiotelemetry devices (TA10TA-F20; DSI, St Paul, MN, USA) under isoflurane (3-5% isoflurane (Animalcare Ltd. York, UK); 3-5% O2) in the abdominal cavity for body temperature recording. After disinfecting the area with iodine, a sterile drape was applied, in line with aseptic procedure. A midline incision was made in the skin and the abdominal wall. The probe was implanted before suturing the abdominal wall and skin (Vicryl 4.0, Johnson and Johnson, UK). Mice were singly-housed in clean cages and allowed to recover from anaesthesia in front of a heat lamp. A recovery period of 7-10 days was allowed before telemetry recording commenced.

2.4.2 Recording core body temperature of conscious ambulatory mice.

Mouse cages were positioned on telemetry receiver plates (RPC-1; Data Sciences), and radio signals from the implanted transmitter were monitored with a fully automated data acquisition system (Dataquest ART; DSI, St Paul, MN, USA). Baseline measurements were taken for one hour from 1100 before either p.o. or i.p. administration of compounds and vehicles. For co-administration/pre-treatment studies (for example in section 5.3.3), the first compound was administered 30 minutes before the main compound administration, to allow for adequate circulation. The Dataquest acquisition software received temperature and activity data for 120 seconds every ten minutes, resulting in six measurements per hour.

2.5 Measuring peripheral blood flow using speckle contrast imaging

A speckle contrast blood flow imager (moorFLPI; Moor Instruments, Devon, UK) was used to image real-time changes in flux, indicative of blood flow, in the pinna and the exposed synovial membrane of the knee joint in response to various compounds. The exposed synovial membrane was investigated as previous studies have shown a vasoconstriction response to capsaicin in this tissue (Cambridge and Brain, 1993; Keeble and Brain, 2006).

The moorFLPI apparatus uses the Doppler effect (Figure 2.5) by applying a laser beam to the area of interest. When the beam reaches vessels in the region of interest, passing erythrocytes scatter the beam of light. The built-in photodetector receives the scattered photons to produce an image. As flow increases, erythrocytes cause an increase in interference with the scattered laser, causing a variation in intensity. All flux intensity figures obtained by the FLPI are an average of the readings from the region of interest. The varying intensity pattern is known as a speckle pattern (Boas and Dunn, 2010).

2.5.1 Measuring blood flow in the ear in response to various agonists

Mice were anaesthetised using 75 mg/kg ketamine (Vetoquinol Ltd, Buckingham, UK) and 1 mg/kg medetomidine (Orion Pharma Ltd, Berkshire, UK), coadministered in saline, fifteen minutes before baseline blood flow of a defined region of interest on each ear was taken. The pinna of the ear has been well characterised as a model of neurogenic inflammation. After a baseline period of 5-10 minutes (until stable), 10 µl of the agonist/donor of interest was applied to each side of one ear and its vehicle was applied to each side of the other ear. In this way, each mouse was its own control. The blood flow changes were measured for 30 minutes after application of agonist.

The knee joints of the same animal were dissected following ear blood flow measurements: the skin overlying the joint was removed, and the patellar tendon dissected. This exposed the synovial membrane to enable direct application of 10 µl of compound of interest to one synovial membrane, and vehicle to the opposite membrane. Again, each mouse acted as its own control. The changes in blood flow were measured for 20 minutes after application.

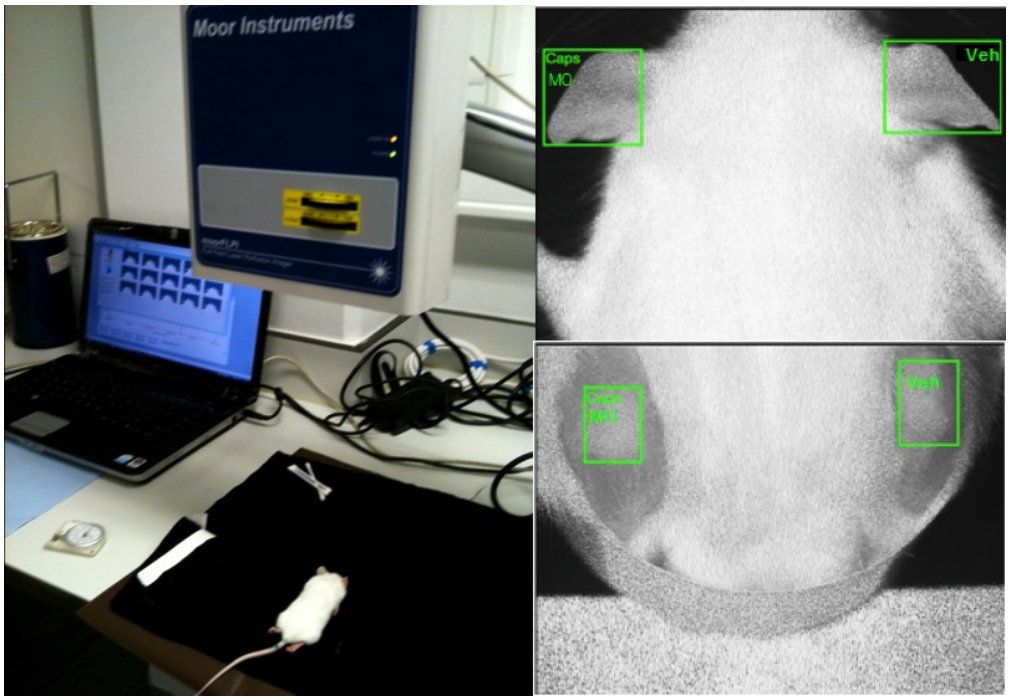

Figure 2.5 FLPI set up to investigate the effects of topical agonists on microvasculature regions on interest. Right panels show typical region of interest set up for ear and knee data collection. Caps = Capsaicin, MO= Mustard Oil, Veh= Vehicle application sites.

2.5.2 The effect of antagonists on agonist-induced changes in blood flow

In order to establish the effects of the selected antagonists on capsaicin- and mustard oil - induced changes in blood flow, animals were treated with antagonists one or two hours prior to imaging according to the time course of action as determined by nociception experiments. Mice were anaesthetised fifteen minutes before baseline measurements were taken. Capsaicin or mustard oil was applied to the ear and exposed synovial membrane as in section 2.5.1, and blood flow was recorded for 20-30 minutes after application. The blood flow in the ear and the knee of the same mouse was monitored, and for antagonist studies the order of ear and knee was alternated in order to control for differences in time after treatment.

2.6 Measurement of dorsal skin plasma extravasation

2.6.1 Dorsal skin injections and collection of samples

Intradermal injections were made in the dorsal skin of mice to determine the effects of H_2S donors alone and in conjunction with inflammatory neuropeptides on plasma extravasation and vasodilation in the dorsal skin cutaneous microvasculature. Age matched male and female CD1 mice (20-25 g) were anaesthetised using 75 mg/kg ketamine (Vetoquinol Ltd, Buckingham, UK) and 1mg/kg medetomidine (Orion Pharma Ltd, Berkshire, UK), co-administered in saline. Dorsal fur was removed to facilitate i.d. injection of compounds and collection of skin samples at the end of the procedure. Mice were kept on a heated mat for the duration of the experiment to maintain core body temperature.

An i.v. injection of Evans blue dye was administered (5 µl/g body weight) and the dye was allowed to circulate for 20 minutes before i.d. injection of 50 µl compounds into the dorsal skin. After injection, sites were marked out as indicated in Figure 2.6. The injection sites were randomised between mice in order to account for variations in skin thickness across the dorsal region.

Thirty minutes after i.d. injection, a blood sample (0.5-1.0 ml) was collected by cardiac puncture, using a 25 G needle and 1 ml syringe washed through with heparin (500 I.U/ml heparin sodium, LEO Pharma, UK) to prevent coagulation. Samples were centrifuged at 2500 RPM for 20 minutes to enable collection of plasma containing Evans blue dye. After cardiac puncture, mice were sacrificed and all dorsal skin injection sites were excised, weighed and dimensions were measured using callipers (Mitutoyo, Hampshire, UK).

2.6.2 Evans Blue extraction and quantification

Skin sites were collected in 500 µl formamide in Eppendorff tubes and placed in a water bath at 65°C overnight in order to extract the Evans blue content of each sample. To determine the Evans blue content of the extracted sample, 100 µl of Evans blue standard (0-6 µg/ml in formamide) were pipetted in triplicate in a 96 well plate. 100 µl of each sample was added in triplicate, and the plate was read at 620 nm in the plate reader. For normalisation of all samples, the plasma concentration of Evans blue was determined, against an Evans blue standard curve constituted in saline.

Figure 2.6 Demarcation of i.d. injection sites on a female CD1 mouse injected with Evans Blue dye. Marks were made at four points around each injection 'blister' with a different coloured pen to show the limits, enabling clean excision of each site without colour contamination from the pen.

2.7 *In vitro* methods

2.7.1 Tissue collection

Liver, brain and whole skin samples were collected under sterile conditions from TRPV1 WT and KO mice (n=6) in order to determine relative levels of the H_2S-producing enzymes CBS and CSE in qRT-qPCR and protein expression studies. Nuclease-free collection vessels were used to store half of each organ in RNAlater (Applied Biosystems®, Life Technologies Ltd, Paisley, UK) at 4°C for at least 24 hours and then at -20°C for mRNA analysis. RNAlater contains various RNases that preserve the integrity of the samples. The other half was snap frozen in liquid nitrogen and stored at -80°C for protein analysis.

2.7.2 Measurement of gene expression using Real Time Polymerase Chain Reaction

The quantitative reverse-transcription polymerase chain reaction (qRT-PCR) was used to determine relative CBS and CSE gene expression in brain, liver and skin samples. The PCR enables the amplification and therefore detection and identification of the genes of interest.

2.7.2.1 Isolation and purification of total RNA

Total RNA was extracted from the samples detailed in section 2.7.1. Whole tissue samples were homogenised: tissues were transferred into 2.0 ml round-bottomed microcentrifuge tubes with a 5mm stainless steel bead and 1ml of Qiazol reagent. The tissues were disrupted in a Tissue Lyser II® (2-5min, 30Hz) which used the 'bead-milling' method for homogenisation, ensuring sterility whilst homogenising. Phase separation was initiated by the subsequent addition of 200µl chloroform and centrifugation (12,000g, 15 minutes, 4°C).

The Qiagen Microarray RNA extraction kit (Qiagen, UK), was used to extract total RNA according to manufacturer's instructions. In brief, the kit used a QIAzol lysis reagent, to induce phase separation; the tissue homogenate was centrifuged in a solution containing water-saturated phenol and chloroform. This separated the homogenate into an upper aqueous phase, containing nucleic acids such as RNA; and an organic lower phase containing proteins and other debris (Chomczynski and Sacchi, 1987).

The Qiagen kit provided silicon-based spin columns, enabling the purification and extraction of RNA using 70% ethanol (in RNA/DNA free water) and wash buffers RW1 and RPE. RW1 and RPE are phosphate buffers that enable the nucleic acids to bind to the silica membrane whilst washing off excess ethanol. The samples were loaded onto the spin column before being centrifuged and washed a number of times. After centrifugation in the spin columns, the RNA (30–50 µl) was eluted in nucleotide-free H_2O and stored at –80 °C until reverse transcribed.

2.7.2.2 Reverse Transcription

Prior to reverse transcription, the extracted RNA concentration of each elution was determined using the Nanodrop 1000 spectrophotometer (THERMOscientific, UK*)*; absorbance was measured at 230nm. Any contamination by ethanol or guanidine was ascertained by measuring purity $A_{260/280}$ values. A ratio of ~2.0 was accepted as "pure" for RNA.

In order to perform RT-qPCR, a commercially available kit (High Capacity RNA-to-cDNA Kit; Applied Biosystems, Life Technologies Ltd, Paisley, UK) was used to reverse transcribe total RNA (500 ng–1 µg) to complementary DNA (cDNA). This kit allows the reverse transcription of up to 2 µg RNA in a 20µl reaction volume. To prepare the reaction mix, up to 9 µl total RNA was included. This was diluted to the appropriate concentration using nuclease free H_2O as required. 10 µl of 20x RT buffer and 1 µl of 20 x Enzyme mix was added to complete the reaction mix. A negative control that omitted the active enzyme was also included. Samples were reverse transcribed in accordance to the manufacturer's guidelines using a thermal cycler (DNA Engine Tetrad 2 Peltier Thermal Cycler): at 37°C for 60 minutes, 95 °C for 5 minutes, and held at 4°C for a minimum of 5 minutes. Generated cDNA was subsequently stored at -20°C until used in RT-qPCR.

Target Gene	Primer Sequence (5'-3')	Accession number	Product length (base pairs)
CBS	F: CACGAGCAGATCCAATCACGA R: TGCCACGAAGTTTAGCAGGT	NM_144855.3	138
CSE	F: ACCTCAATAGTCGGCTTCGTT R: TGAGAGGGTAGCCCAGGATAAA	NM_145953.2	199
HPRT	F: TCC TCC TCA GAC CGC TTT T R: CCT GGT TCA TCA TCG CTA ATC	NM_013556.2	90
PLA_2	F: TGG ATA TAA ACC ATC TCC ACC A R: GGG AAG GGA TAC CTA TGT TCA GA	NC_000070.5	77

Table 2.4 Sequence of PCR primers used in this project with corresponding GenBank accession numbers for all target genes. CBS: Cystathionine Beta Synthase; CSE: Cystathionine Gamma Lyase; HPRT: Hypoxanthine Phosphoribosyltransferase; PLA2: Phospholipases A2. F: Forward, R: Reverse. HPRT and PLA2 were used as housekeeping genes i.e. positive controls.

Component	Volume (µl)
SYBRGreen Mastermix (Sensimix No-ROX Kit; Bioline, London, UK)	5
forward primer (10µM) (Sigma-Aldrich)	0.5
reverse primer (10µM) (Sigma-Aldrich)	0.5
Nuclease-free H2O (Sigma-Aldrich)	2
cDNA	2

Table 2.5 Relative components of the final RT-qPCR mastermix to amplify the genes of interest, the reaction mix was made up as above. A negative control that omitted the active enzyme was also included. Samples were reverse transcribed in accordance to the manufacturer's guidelines using a thermal cycler (DNA Engine Tetrad 2 Peltier Thermal Cycler): at 37°C for 60 minutes, 95 °C for 5 minutes, and held at 4°C for a minimum of 5 minutes. Generated cDNA was subsequently stored at -20°C until used in RT-qPCR.

2.7.2.3 Quantitative RT-PCR

The cDNA generated was amplified using Real time PCR. A Sybergreen based PCR mix was used, together with primers for the specific genes of interest (Table 2.4). The 10 µl (total volume) reaction mixture was made up of the components illustrated in Table 2.5. Samples were then loaded into 100 well gene discs (Qiagen) using a robot (CAS1200, Corbett Robotics). The loaded genes were amplified using a real-time PCR thermal cycler (Rotor-Gene 6000, Qiagen) under the following conditions: hold 95°C; 40 cycles of 10s at 57°C and 15s at 72°C; 5s, melt at 68-90°C. Melt curves for each reaction were examined to exclude primer-dimer formation and ensure that only one product was amplified.

The Rotorgene 6000 series software was used to analyse raw data and target gene expression was expressed as copies/µl. In order to compare gene expression between samples, expression values were normalised to the reference housekeeping genes hypoxanthine guanine phosphoribosyl transferase (HPRT) and phospholipase A2 (PLA2) – which are expressed at a constant level in all tissues. Normalisation factors for each sample were obtained using the GeNorm v1.2 software (Vandesompele et al., 2002). This software used the geometric mean of the selected housekeeping genes to generate a normalisation factor. Thus, qRT-PCR results were presented as mean ± S.E.M. of copies/µl of each gene.

2.7.3 Protein Quantification

2.7.3.1 Sample preparation

Samples collected in section 2.7.1 for protein analysis were removed from -80°C storage and kept on ice until needed. Tissue was put in 300 µl of homogenising buffer (RIPA buffer: 150 mM NaCl, 1.0% IGEPAL® CA-630, 0.5% sodium deoxycholate, 0.1% sodium dodecyl sulphate (SDS) and 50 mM Tris, pH 8.0. Sigma-Aldrich) containing Protease inhibitor cocktail (Sigma-Aldrich) and homogenised in the TissueLyser II, where the frequency and duration was variable dependent on when the tissue was evenly dispersed.

2.7.3.2 Determination of protein concentration

The Lowry copper-based protein assay (Lowry et al., 1951) was used to determine protein concentrations of each sample. This assay is based on the Biuret test to detect peptide bonds. In the presence of proteins (regardless of composition), cupric ions form coloured complexes in alkaline solutions. The conventional Lowry protein assay method was employed (Lowry et al., 1951) using a protocol and reagents supplied by BioRAD (Reagent A + Reagent B kit (Bio-Rad, UK).

In brief, 5 µl of BSA standard (0.1-2 mg/ml, bovine serum albumin (BSA); Sigma-Aldrich) or sample (diluted 1:50 for liver and brain, and 1:10 for skin to fall within the range of standard concentrations) were loaded in triplicate into a standard 96-well plate. 25 µl of BioRad reagent A and then 200 µl of BioRad reagent B were added to each well and the plate was agitated briefly and incubated at room temperature for 15 min. The colour intensity was analysed by a microtiter plate reader (SpectraMAX 190, used with SOFTmaxPRO software, version 3.13, Molecular Devices Corporation, California, USA) at an absorbance frequency of 750 nm. Background absorption was removed by comparing all values to 0 mg/ml BSA and a standard curve was plotted using the known concentrations of BSA standards. The unknown sample concentrations were extrapolated from the equation generated.

2.7.3.3 Sodium-Dodecyl Sulphate - Polyacrylamide Gel Electrophoresis (SDS-PAGE)

Protein samples (20-50 µg) were added to Laemmli sample buffer (50 mM Tris-HCl pH 6.8, 2% SDS, 10% glycerol, 1% β-mercaptoethanol, 0.02% bromophenol blue) in a 1:10 sample buffer/loading volume ratio prior to being denatured at 95°C for 5 minutes and cooled at room temperature, ready for SDS-PAGE.

Acrylamide gels were made on the day of use by poured between two glass plates separated with a 1mm spacer (Biorad, UK), and were comprised of a lower 'resolving' gel and upper 'stacking' gel. **Table 2.6** shows the recipes used for each gel. Once set, samples and protein ladder marker (8 µl; Rainbow marker, GE healthcare, UK) were loaded into wells for separation by electrophoresis.

The gels were loaded into an electrophoresis tank (BioRad Mini-Protein III; BioRad, USA) containing running buffer (10 % Tris-glycine buffer (BioRad, USA), 0.5 % of 20 % SDS pH 7.2 (National Diagnostics), double-distilled H_2O), and run at 170V for 30-45 mins, or until the dye front reached the end of the gel.

Gel	Component	Volume (per gel)
Resolving gel (10 % polyacrylamide)	ddH_2O	3.75 ml
	0.5 M Tris-HCl (pH8.8)	2.25 ml
	30 % acrylamide	3 ml
	10 % Ammonium persulfate (APS)	45 µl
	100 % Tetramethylethylenediamine (TEMED)	15 µl
Stacking gel (5 % polyacrylamide)	ddH_2O	1.75 ml
	Tris-HCl (pH6.8)	750 µl
	30 % acrylamide	500 µl
	10 % APS	25 µl
	100 % TEMED	10 µl

Table 2.6 Components of Resolving and Stacking gels for SDS-PAGE. Protein samples (20-50 µg) were added to Laemmli sample buffer (50 mM Tris-HCl pH 6.8, 2% SDS, 10% glycerol, 1% β-mercaptoethanol, 0.02% bromophenol blue) in a 1:10 sample buffer/loading volume ratio prior to being denatured at 95°C for 5 minutes and cooled at room temperature, ready for SDS-PAGE. Acrylamide gels were made on the day of use by poured between two glass plates separated with a 1mm spacer (Biorad, UK), and were comprised of a lower 'resolving' gel and upper 'stacking' gel – recipes as given in the table.

2.7.3.4 Western Blotting

A semi-dry protocol was used to transfer proteins to polyvinylidene fluoride (PVDF) membranes (Millipore, UK), ready for immunoblotting. The polyacrylamide gel was removed from the casing and allowed to equilibrate in transfer buffer (10 % Tris-Glycine buffers (BioRad, USA), 15 % Methanol (Fisher scientific, UK), double-distilled H_2O). Filter paper (General purpose protein blotting membrane, pore size 0.45µm, binding capacity 80-100 µg/cm^2; BioRad, USA) was also saturated in the transfer buffer and PVDF membranes (Millipore, UK) were activated by brief immersion in methanol (5 seconds). When activated, the PVDF membrane was saturated in transfer buffer.

The prepared filter paper was placed on the semi-dry electrophoretic transfer cell (BioRad, USA), followed by the PVDF membrane. The gels were placed on top of the membrane and an additional filter paper was placed on top. The proteins were transferred onto the PVDF membrane running at 20 V for 2 hours using the transfer cell. Transfer was confirmed using Ponceau S stain (Sigma-Aldrich).

As soon as proteins were transferred, membranes were blocked in 5% milk solution (5% w/v non-fat milk powder, 0.1 % Tween-20, PBS) for 1 hour at room temperature. The membranes were subsequently washed in PBS 0.1 % Tween-20 (1 x 15 min, 3 x 5 min) and incubated with primary antibody at 4°C overnight. Antibodies used are shown in Table 2.7. The primary antibody was washed from the membrane as above and a horseradish peroxidise-linked secondary antibody (diluted in 3 % non fat dry milk in PBS) was incubated at room temperature for 1 hour.

Antibody	Target	Weight of target (kDa)	Host Species	Species Reactivity	Dilution	Supplier
Primary	CBS	36.7	Mouse (monoclonal)	Human/ mouse	1:1000	Abnova (H00000875-M01)
Primary	CSE	70.1	Mouse (monoclonal)	Human/ mouse	1:1000	Abnova (H00001491-M01)
Primary	GAPDH	37-40	Mouse (monoclonal)	Human/ mouse	1:5000	Applied Biosystems (AM4300)
Secondary	Mouse IgG (horseradish peroxidase conjugated)	Goat (polyclonal)		Mouse	1:5000	Millipore (AP124P)

Table 2.7 Antibodies used in Western blotting experiments. CBS- cystathionine beta synthase; CSE- cystathionine gamma lyase; GAPDH - Glyceraldehyde 3-phosphate dehydrogenase. Antibodies were diluted in 5% BSA supplemented with sodium azide. After protein transfer, the washed membranes containing protein were incubated with primary antibody at 4°C overnight. The primary antibody was washed from the membrane as above and a horseradish peroxidise-linked secondary antibody (diluted in 3 % non fat dry milk in PBS) was incubated at room temperature for 1 hour.

2.8 Statistical analysis

All *in vivo* results were expressed as mean ± S.E.M. unless otherwise stated. As a result of normalisation, detailed in section 2.7.2.3, qRT-PCR results were presented as mean ± S.E.M. of copies/µl of each gene. In protein experiments using semi-quantitative western blots, results were presented as mean ± S.E.M. of the target protein/reference protein ratio in arbitrary densitometry units.

Statistical analyses were performed using either Student's t-tests or two-way ANOVA (analysis of variance) or repeated measures ANOVA, followed by Bonferroni *post hoc* tests, as indicated. Results were expressed as significant when $P < 0.05$.

Chapter 3 Characterisation of TRPV1 and TRPA1 antagonists in Pain and Thermoregulation

3.1 Introduction

TRPV1 antagonists of various structures have proven efficacy in tests of nociceptive thresholds and inflammatory models – both *in vivo* and *in vitro* – but many have the unwanted side effect of inducing hyperthermia (Gavva et al., 2007a; Honore et al., 2009). Whilst the underlying mechanisms behind the roles of TRPV1 in pain and inflammation are generally well understood and extensively reviewed (Alawi and Keeble, 2010; Brederson et al., 2013), the mechanisms of TRPV1 antagonist-induced hyperthermia are not. When administered to TRPV1 KO mice, TRPV1 antagonists did not cause hyperthermia – evidence that hyperthermia is an on-target effect (Gavva et al., 2008). This suggests that TRPV1 is tonically active *in vivo*, to maintain a low deep body temperature: blocking TRPV1 would therefore remove the regulatory 'brake' on core body temperature, resulting in an increase (Romanovsky et al., 2009). Core body temperature homeostasis is controlled by the central nervous system. However, the hyperthermic effects of TRPV1 antagonism are not centrally mediated, as administration of peripherally restricted antagonists still results in hyperthermia (Tamayo et al., 2008). However, some TRPV1 antagonists do not cause hyperthermia (Wang et al., 2002), indicating that mechanisms at the molecular level are important in determining whether or not an antagonist will be hyperthermic. Garami and colleagues undertook analysis of the ability of several different antagonists to block the different modes of activation of TRPV1 (heat, protons and capsaicin) and suggested that blocking the proton mode of activation resulted in hyperthermia (Garami et al., 2010).

TRPA1 is also involved in nociception and TRPA1 antagonists have shown efficacy in nociceptive testing (McNamara et al., 2007) and inflammatory conditions (Fernandes et al., 2011). Preliminary studies using TRPA1 antagonists show that they do not have an effect on core body temperature under baseline conditions (Ding et al., 2008; Chen et al., 2011), however studies have been limited to newly-developed TRPA1 antagonists. To this end, the effects of TRPA1 antagonism are not as well investigated, and the potential of this channel is still yet to be fully realised.

As discussed in section 1.1, TRPA1 and TRPV1 are very closely related members of the TRP superfamily of receptor proteins. They have the ability to form functional heteromers (Fischer et al., 2014) and are often co-expressed on neuronal cells (Story et al., 2003). This interaction presents another interesting avenue for novel analgesic treatments.

In this chapter, the effects of several TRPV1 and TRPA1 antagonists on nociceptive thresholds and core body temperature were investigated.

3.2 Hypothesis and Aims

The aims of this chapter are to investigate the effects of TRPV1 antagonists SB366791 and JNJ17203212 and TRPA1 antagonists HC030031 and TCS5861528 on pain thresholds and core body temperature of naïve mice.

The effects of these antagonists on naïve mechanical and thermal nociceptive thresholds will be investigated. We hypothesise that TRPV1 antagonists will increase thermal nociceptive thresholds whilst TRPA1 antagonists will increase mechanical nociceptive thresholds.

Using analgesic doses of the TRPV1 and TRPA1 antagonists, the effects of these compounds on core body temperature and activity will be characterised. We hypothesise that whilst TRPV1 antagonists will increase core body temperature of naïve mice, TRPA1 antagonists will have no effect on core body temperature, suggesting it is not tonically active in the control of deep body temperature. In terms of locomotor activity, TRPV1 and TRPA1 antagonists will not have a significant effect on naïve mice.

3.3 Results

3.3.1 The effects of TRPV1 antagonists on nociceptive thresholds

In these studies, the efficacy of the TRPV1 antagonists, SB366791 and JNJ17203212, in blocking thermal and mechanical nociception was investigated using blinded, randomised experiments. The mechanical and thermal nociceptive thresholds of naïve male CD1 mice were measured before and after the administration of the compounds. Mechanical thresholds, i.e. paw withdrawal threshold (PWT, g) were tested using an automated Von Frey system and thermal thresholds i.e. paw withdrawal latency (PWL, sec) using the Hargreaves' method. Thresholds for SB366791 were tested at two and four hours after treatment (Figure 3.1). Time points were determined by extrapolating from previous experiments. For JNJ17203212, thresholds were taken at one, two and three hours post-administration (Figure 3.2).

During mechanical threshold testing, no significant difference in PWT was seen between drug- and vehicle-treated groups for both SB366791 and JNJ17203212. In thermal threshold testing, SB366791-treated mice demonstrated an increased PWL at four hours post-administration compared to vehicle (mean PWL vehicle: 9.325 ± 0.622 seconds vs SB366791: 12.946 ± 0.638 seconds. $P<0.05$, n=9-10). Similarly, JNJ17203212-treated mice demonstrated a significantly increased PWL compared to vehicle at three hours (mean PWL vehicle: 10.986 ± 0.193 seconds vs JNJ17203212: 15.108 ± 1.433 seconds. $P<0.01$, n=6).

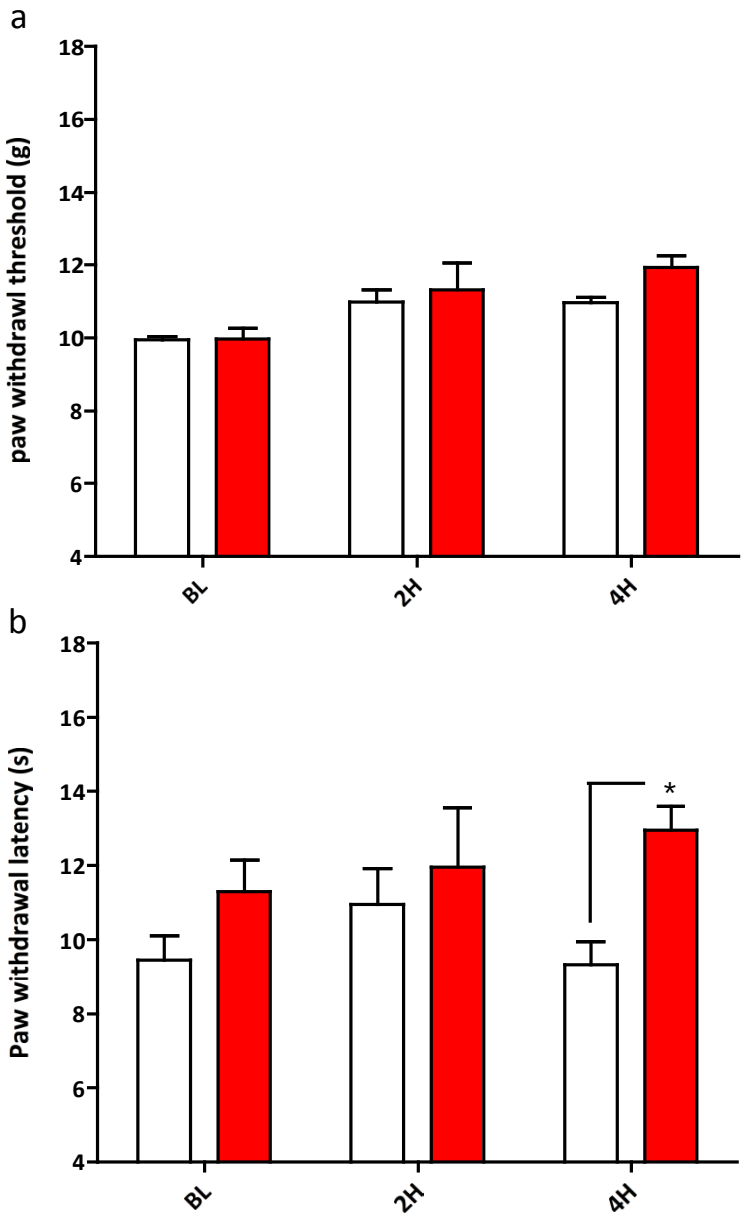

Figure 3.1 The effects of 5 mg kg^{-1} SB366791 i.p. (■) vs vehicle ( ) on a) paw withdrawal thresholds (PWT) in the dynamic plantar aesthesiometer test of mechanical nociception, and b) paw withdrawal latency (PWL) in the Hargreaves test of thermal nociception in male CD1 mice (n=9-10).

Measurements were taken before (baseline, BL) and two (2H) and four (4H) hours after drug administration.

*P<0.05 with respect to vehicle control, repeated measures ANOVA and Bonferroni *post hoc* test.

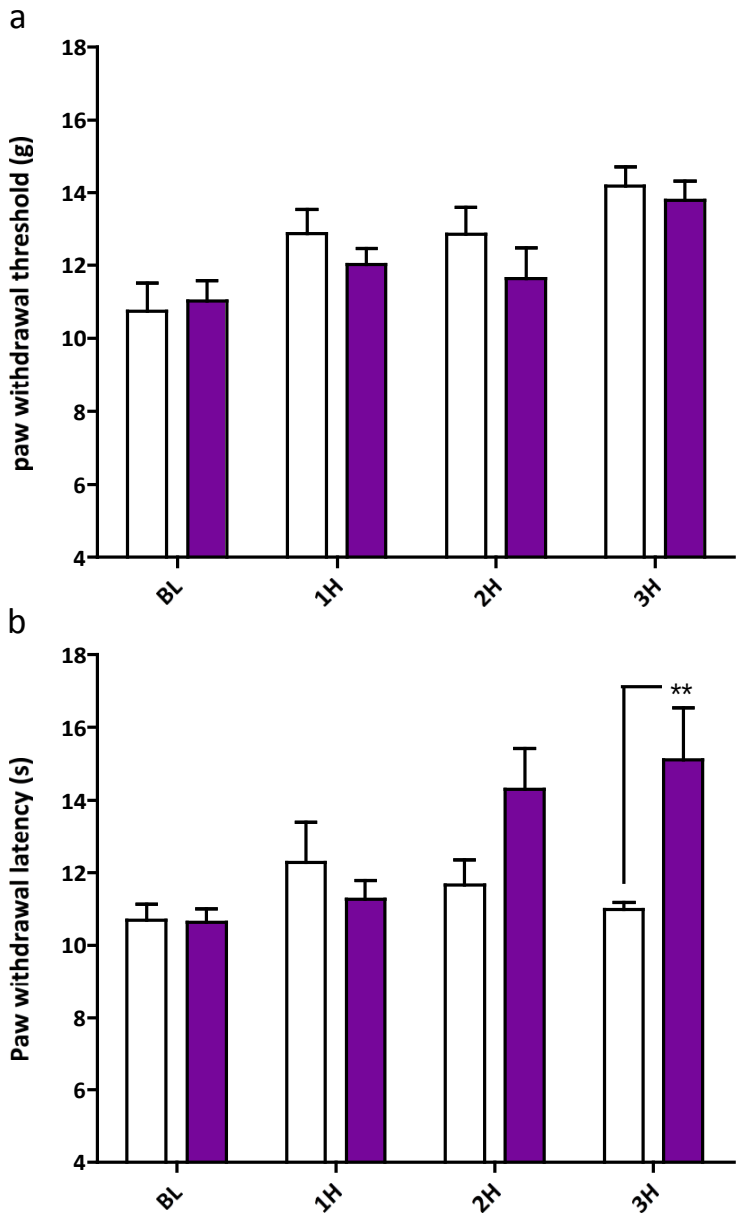

Figure 3.2 The effects of 30 mg/kg JNJ17203212 (■)vs vehicle ( ) on a) paw withdrawal thresholds (PWT) in the dynamic plantar aesthesiometer test of mechanical nociception, and b) paw withdrawal latency (PWL) in the Hargreaves test of thermal nociception in male CD1 mice (n=6).

Measurements were taken before (baseline, BL) and one (1H) two (2H) and three (3H) hours after drug administration.

**P<0.01 with respect to vehicle, repeated measures ANOVA and Bonferroni *post hoc* test.

3.3.2 The effects of TRPA1 antagonists on nociceptive thresholds.

The mechanical and thermal nociceptive thresholds of naïve male CD1 mice were tested before and after the administration of the TRPA1 antagonists HC030031 (Figure 3.3) and TCS5861528 (Figure 3.4) in blinded, randomised experiments. Mechanical thresholds were tested using an automated Von Frey system and the thermal thresholds using the Hargreaves' method. Thresholds were measured at one and two hours (Figure 3.1) after oral administration of each compound as outlined in section 2.3.

No difference was demonstrated between drug- and vehicle-treated groups in both mechanical and thermal threshold testing for both antagonists. HC030031-treated mice demonstrated a significant increase from baseline in the paw withdrawal threshold one hour post-gavage ($P<0.05$). HC030031- and vehicle-treated mice also showed an increase in paw withdrawal latency one and two hours after treatment, compared to baseline ($P<0.05$).

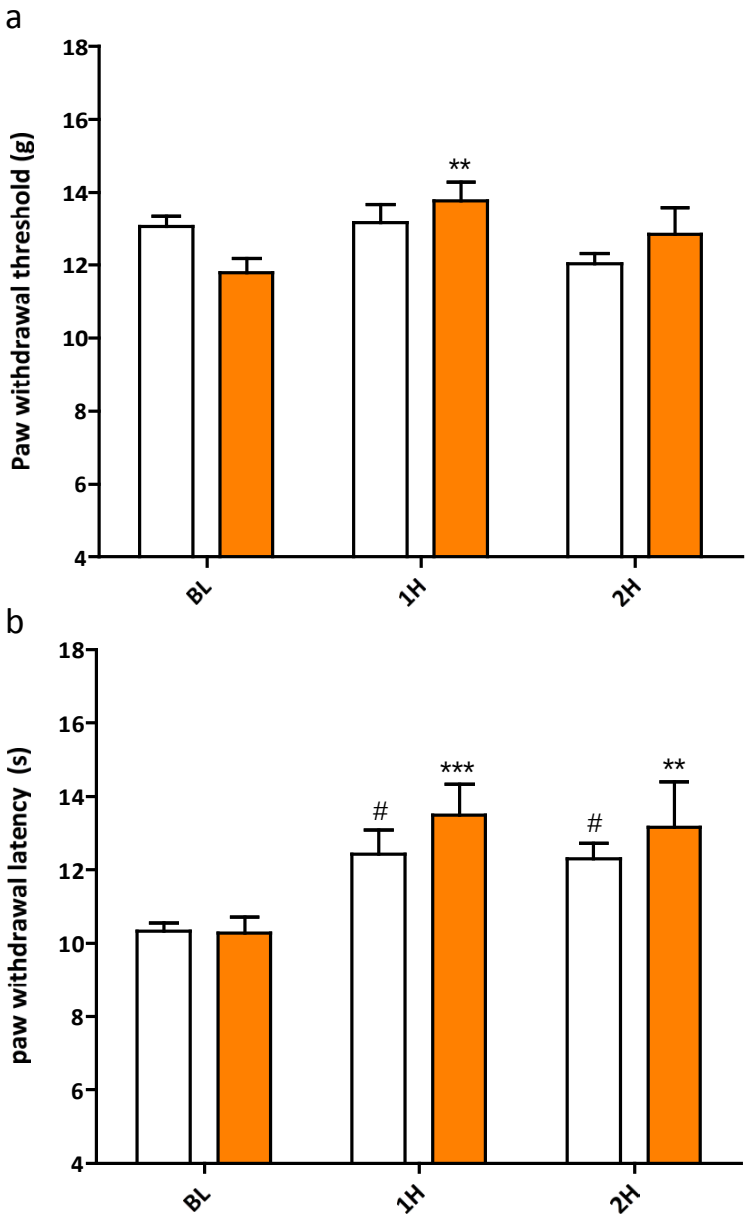

Figure 3.3 The effects of 100 mg/kg HC030031 (■)vs vehicle ( ) on a) paw withdrawal thresholds (PWT) in the dynamic plantar aesthesiometer test of mechanical nociception, and b) paw withdrawal latency (PWL) in the Hargreaves test of thermal nociception in male CD1 mice (n=6).

Measurements were taken before (baseline, BL) and one (1H) and two (2H) hours after drug administration.

**P<0.01 ***P<0.005 with respect to naïve baseline measurements of HC030031-treated mice.

#P<0.05 with respect to naïve baseline measurements of vehicle-treated mice.

Statistics: repeated measures ANOVA and Bonferroni *post hoc* test.

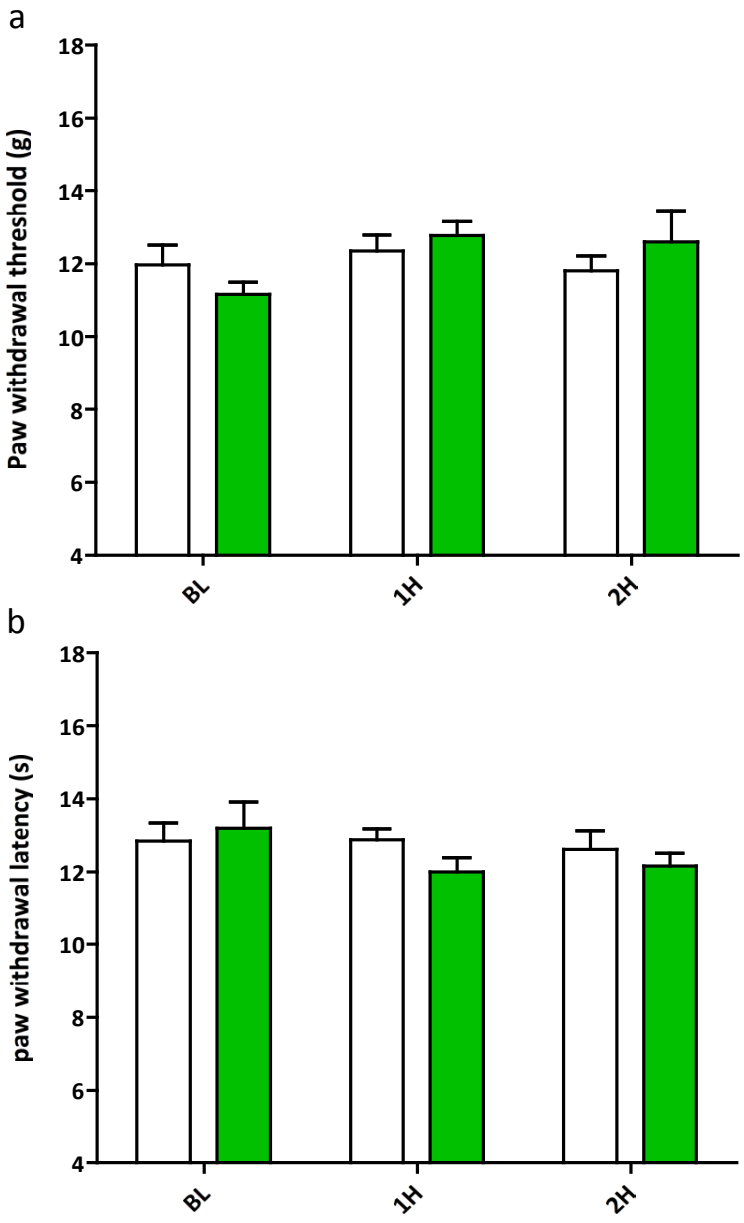

Figure 3.4 The effects of 10 mg/kg TCS5861528 (■) vs vehicle ( ) on a) paw withdrawal thresholds (PWT) in the dynamic plantar aesthesiometer test of mechanical nociception, and b) paw withdrawal latency (PWL) in the Hargreaves test of thermal nociception in male CD1 mice (n=6).

Measurements were taken before (baseline, BL) and one (1H) and two (2H) hours after drug administration.

3.3.3 The effects of TRPV1 antagonists on core body temperature of conscious mice

The effect of administration of SB366791 and JNJ17203212 on the core body temperature and activity of naïve male CD1 mice was investigated using radiotelemetry. These results show that blocking TRPV1 at pharmacologically active doses (as ascertained via nociceptive threshold testing in section 3.3.1) has different effects on core body temperature, depending on the compound.

The core body temperature and activity levels of naive male CD1 mice are shown in Figure 3.5. The mean core body temperature during the light cycle usually rests between 36-36.5°C. During the dark cycle, there is a significant increase in body temperature of mice, corresponding with an increase in activity levels and consistent with expected nocturnal behaviour.

Administration of 5 mg/kg SB366791 (Figure 3.6) resulted in no significant change in body temperature compared to vehicle-treated mice (n=5). There was also no significant difference between the activities of mice in each treatment group.

Administration of 30 mg/kg JNJ17203212 (Figure 3.7) resulted in a significant increase in body temperature (n=5, +1.32±0.21°C, $P<0.01$ at 2 hours post treatment). There is a trend toward increased activity 1 hour post-injection in JNJ17203212-treated mice vs. vehicle; however this is not significant.

Administration of 30 mg/kg JNJ17203212 to TRPV1 WT and KO mice (Figure 3.8) confirmed that the hyperthermia induced by JNJ17203212 was TRPV1-mediated: there was a significant difference between JNJ17203212-treated WT and KO mice at one and two hours post i.p. administration (n=4, Δ1.47°C $P<0.01$ at 1 hour, Δ1.36° C $P<0.05$ at 2 hours post treatment).

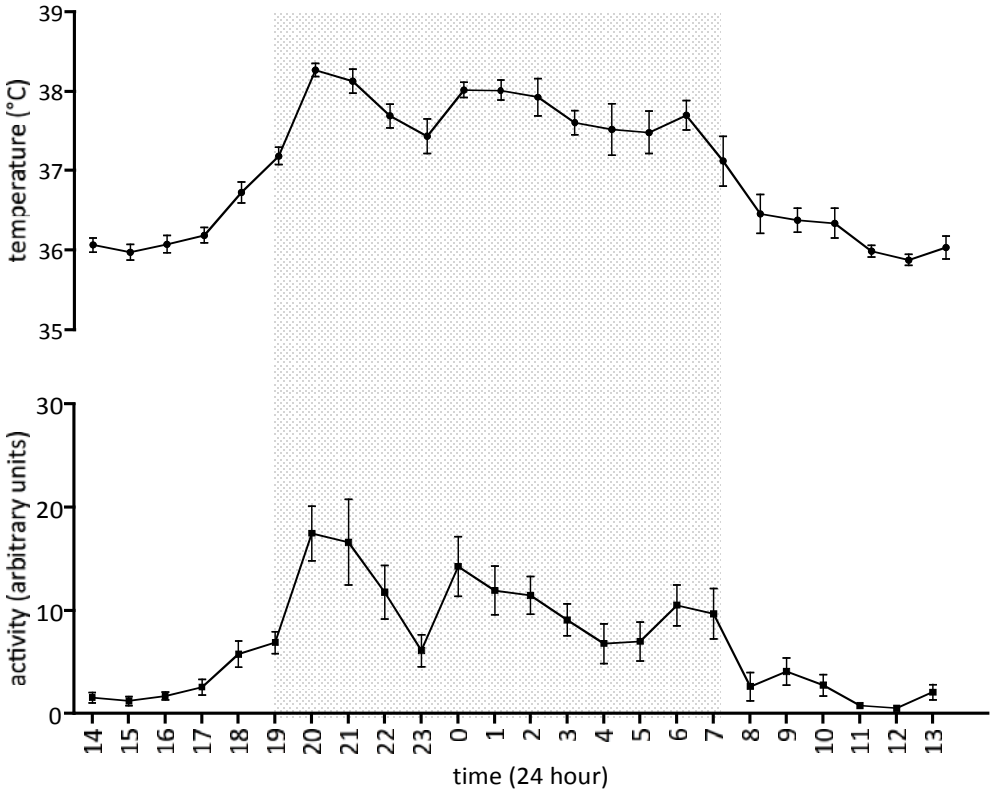

Figure 3.5 The core body temperature (top) and activity levels (bottom) of naïve, telemetered, male CD1 mice over 24 hours. Mice underwent telemetry probe implantation and recovered for a week before their core body temperature was monitored for 24 hours. The mice were left uninterrupted during that period. Shaded areas indicate dark cycle; activity increases during dark cycle lead to corresponding increases in core body temperature. n=8.

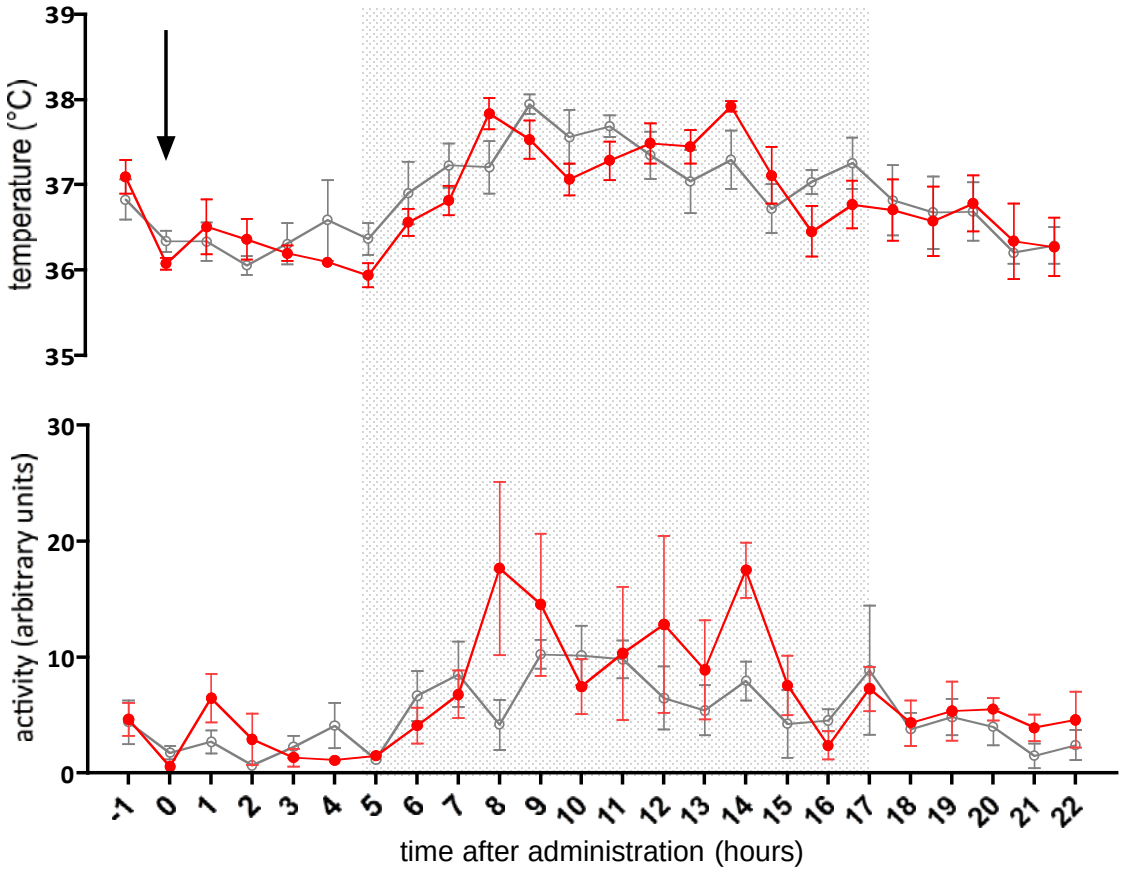

Figure 3.6 The effects of 5 mg/kg SB366791 i.p. (■) and vehicle (10 µl/g) (■) on (top) core body temperature and (bottom) activity levels of male CD1 mice. After one hour of baseline measurement, mice were administered compound and the core body temperature was measured for the rest of the day and overnight. n=5. No significant difference between treatment groups (repeated measures ANOVA and Bonferroni *post hoc* test). Shaded area indicates dark cycle.

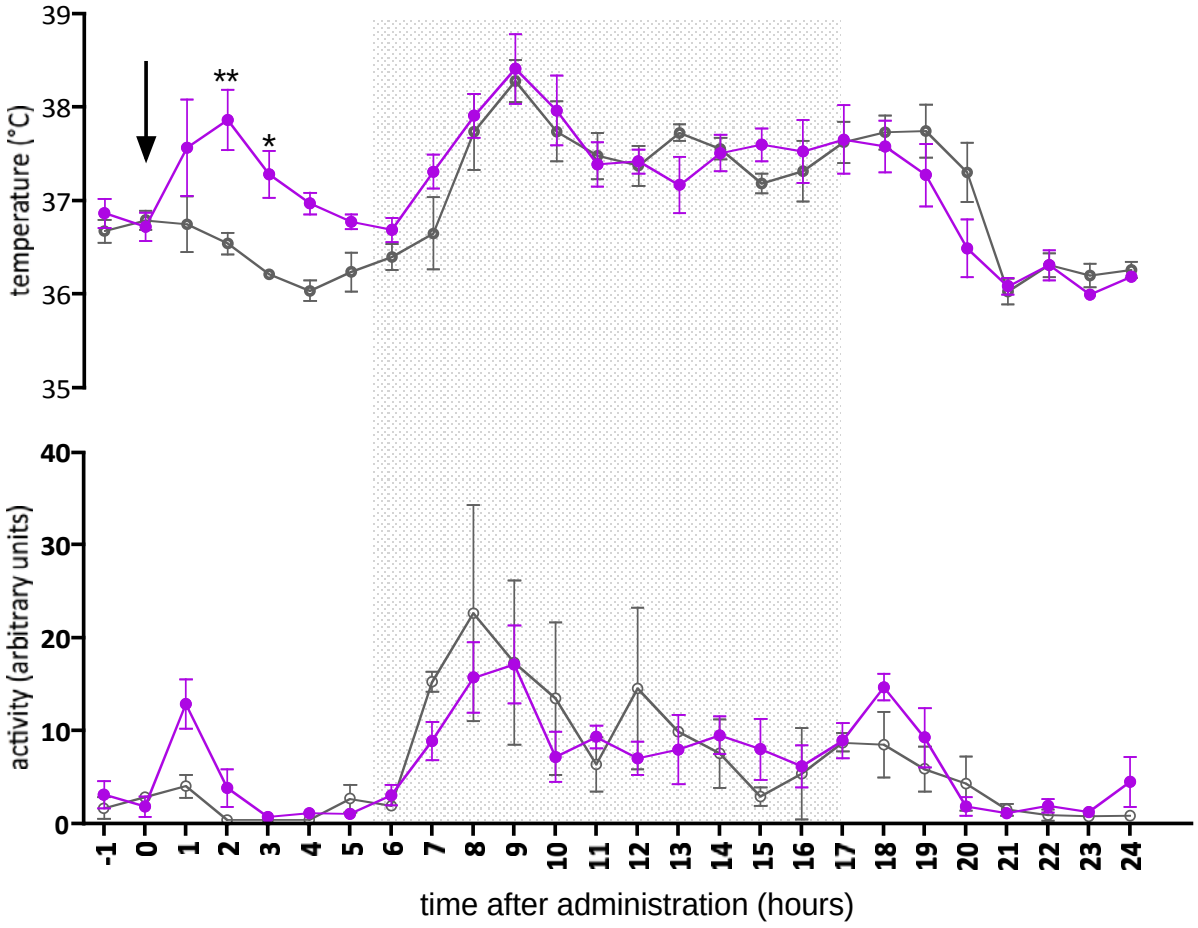

Figure 3.7 The effects of 30 mg/kg JNJ17203212 i.p. (■) and vehicle (10 µl/g) (■) on (top) core body temperature and (bottom) activity levels of male CD1 mice. n=5. Shaded area indicates dark cycle. After one hour of baseline measurement, mice were administered compound and the core body temperature was measured for 24 hours. *=P<0.05, **=P<0.01, as determined by repeated measures ANOVA and Bonferroni *post hoc* test to compare all treatment groups

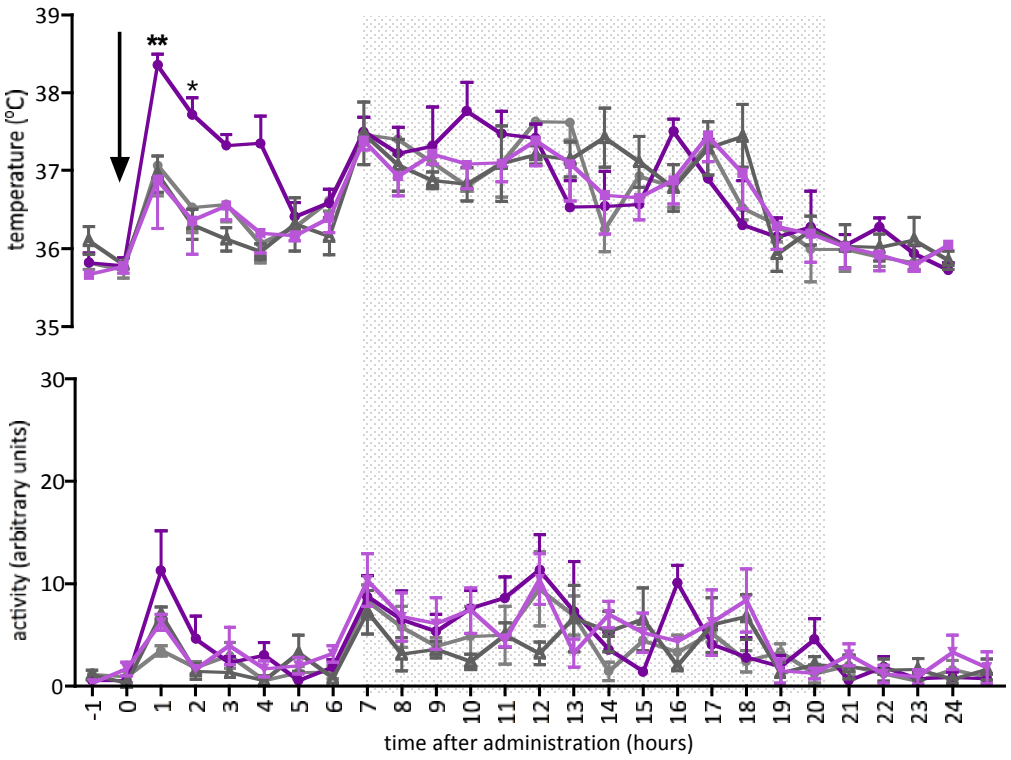

Figure 3.8 Hyperthermic effects of JNJ17203212 are TRPV1-dependent. After one hour of baseline measurement, 30 mg/kg JNJ17203212 or vehicle (10 µl/g) was administered i.p to TRPV1 WT and KO mice (n=5) and the core body temperature (top) and activity (bottom) were measured for 24 hours.

(•) TRPV1 WT mice treated with JNJ17203212

(■) JNJ17203212-treated TRPV1 KO mice

(○) vehicle-treated TRPV1 WT mice

(Δ) Vehicle treated TRPV1 KO mice.

*P<0.05, **P<0.01 with respect to vehicle-treated WT mice - repeated measures ANOVA and Bonferroni *post hoc* test.

3.3.4 The effects of TRPA1 antagonists on core body temperature

The effects of orally administered TRPA1 antagonists HC030031 (Figure 3.9) and TCS5861528 (Figure 3.10) on core body temperature and activity of male CD1 mice were investigated using radiotelemetry.

After one hour of baseline measurement, mice were administered either 100 mg/kg HC030031 or 10 mg/kg TCS5861528 via oral gavage (n=5), and core body temperature and activity measurements were taken over 22 hours. Administration of 100 mg/kg HC030031 had no effect on core body temperature or activity levels of the mice- no significant difference was found between antagonist- and vehicle- treated mice. Animals administered 10 mg/kg TCS5861528 did not have significantly different core body temperature or activity levels compared to their vehicle-treated counterparts.

Thus, these two TRPA1 antagonists administered orally do not change core body temperature or activity of male CD1 mice.

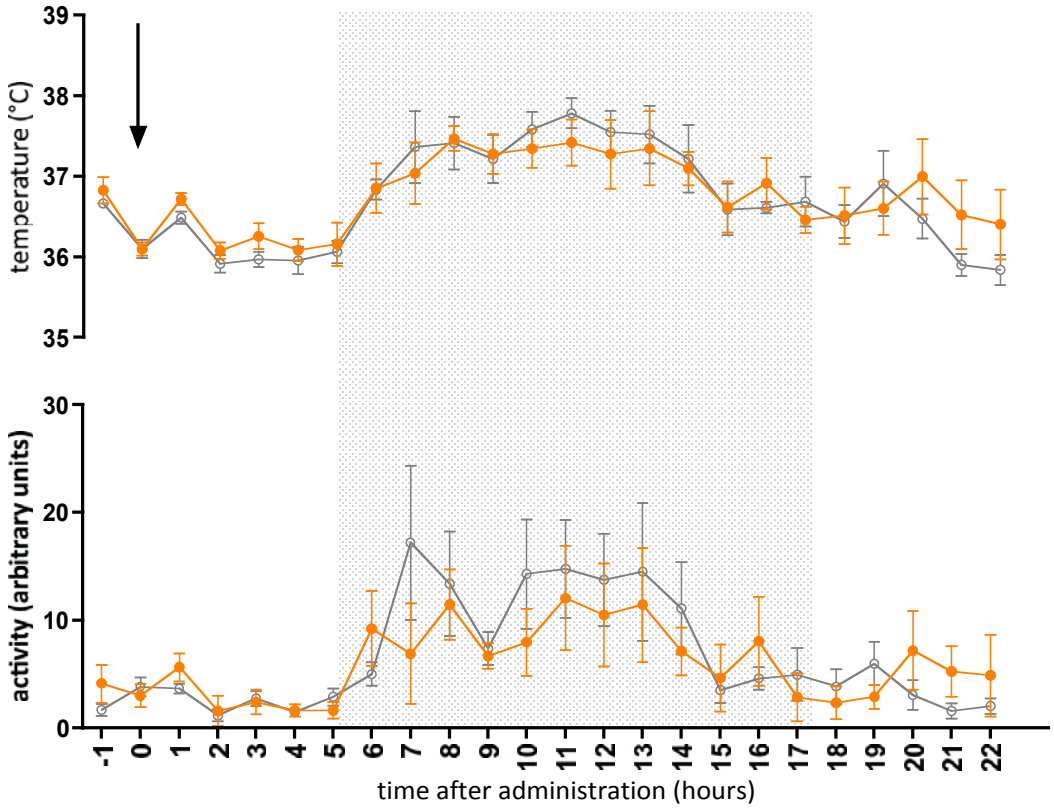

Figure 3.9 The effects of 100 mg/kg HC030031 p.o. (■) and vehicle (■) on (top) core body temperature and (bottom) activity levels of male CD1 mice. After one hour of baseline measurement, mice were administered compound and the core body temperature was measured for the rest of the day and overnight. n=5. No significant difference between treatment groups (repeated measures ANOVA and Bonferroni *post hoc* test). Shaded area indicates dark cycle.

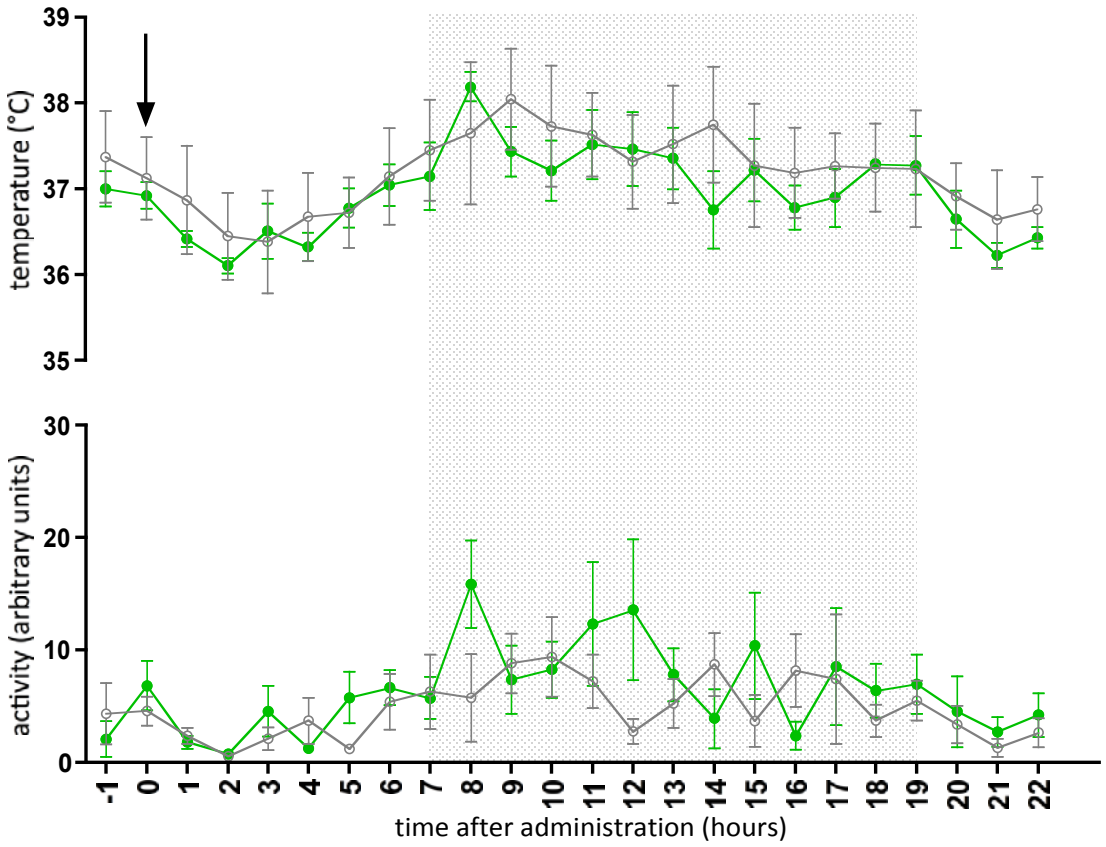

Figure 3.10 The effects of 10 mg/kg TCS5861528 p.o. (■) and vehicle (■) on (top) core body temperature and (bottom) activity levels of male CD1 mice. After one hour of baseline measurement, mice were administered compound and the core body temperature was measured for the rest of the day and overnight. n=5. No significant difference between treatment groups (repeated measures ANOVA and Bonferroni *post hoc* test). Shaded area indicates dark cycle.

3.4 Discussion

3.4.1 Key findings

- TRPV1 antagonism significantly increases thermal, not mechanical nociceptive thresholds
- TRPA1 antagonism can significantly and transiently increase mechanical, not thermal nociceptive thresholds
- TRPV1 antagonism has varied effects on core body temperature, depending on the antagonist used
- TRPV1 antagonist-induced hyperthermia is mediated by TRPV1
- TRPA1 antagonism has no effect on core body temperature

3.4.2 The effect of TRPV1 antagonists on pain

TRPV1 has long been highlighted as an important target in the development of novel analgesics. Its location on primary sensory neurons, role as an integrator of noxious stimuli, and involvement in neurogenic inflammation, causes it to be an attractive target for the treatment of various inflammatory conditions including pruritus (Fernandes et al., 2013) and painful conditions such as rheumatoid arthritis (Fernandes et al., 2011). The aims of this chapter were to investigate the effect of TRPV1 antagonists SB366791 and JNJ17203212 and TRPA1 antagonists HC030031 and TCS5861528 on pain thresholds and core body temperature of naïve mice.

In the present study, different TRPV1 antagonists had different effects on pain thresholds and core body temperature. Nociceptive thresholds were used to study the role of TRPV1 in acute pain, rather than investigating the channel in chronic, hyperalgesic pain. SB366791 (5 mg/kg) was not able to significantly increase mechanical pain thresholds, but did significantly increase thermal nociceptive thresholds 4 hours after treatment. JNJ17203212 (30 mg/kg) was similarly unable to significantly increase mechanical nociceptive thresholds, but did significantly increase thermal nociceptive thresholds 3 hours after intraperitoneal administration.

3.4.3 The effect of TRPA1 antagonists on pain

The two TRPA1 antagonists used in these studies had similar effects on nociceptive thresholds. Whilst TCS5861528 (10 mg/kg, 2% DMSO) had no significant effect on core body temperature, activity, or mechanical or thermal pain thresholds, HC030031 (100 mg/kg, 10% DMSO) had some effect on nociceptive thresholds. HC030031 significantly increased mechanical nociceptive thresholds at one hour but not two hours after treatment. There was no significant difference in thermal nociceptive thresholds between treatment groups however there was an increase in thermal thresholds for both groups after treatment, which was stable over time. It has been documented that systemically administered DMSO can raise nociceptive thresholds (Colucci et al., 2008), albeit at much higher doses than were used in this study. Nevertheless, it is conceivable that, together with repeated exposure to painful thermal stimuli, this could contribute to desensitisation of the footpads to painful stimuli and subsequently increase nociceptive thresholds (Le Bars et al., 2001).

The ability of HC030031, a TRPA1 antagonist, to increase mechanical nociceptive thresholds correlates well with studies of other TRPA1 inhibitors (Petrus et al., 2007), and highlights the emerging role of TRPA1 in pain conditions with a mechanical element – particularly in models of arthritis (Fernandes et al., 2011; 2012; Garrison and Stucky, 2014). HC030031 has been shown to attenuate inflammatory- and neuropathy-induced mechanical hypersensitivity, using CFA- and formalin-induced pain models (Eid et al., 2008).

3.4.4 The effect of TRPV1 antagonists on core body temperature

Unlike SB366791, JNJ17203212 caused a pronounced hyperthermic response when administered to CD1 mice, which was sustained over a period of 3 hours post injection. This was expected from previous studies investigating the pharmacological effects of JNJ17203212 (Swanson et al., 2005). The hyperthermia was mediated by TRPV1, as TRPV1 KO mice did not display a hyperthermic phenotype. Neither compound affected the activity rate of the mice therefore blockade of TRPV1 and subsequent increase in core body temperature could not be attributed to hyperkinesia, a phenotype exhibited by TRPV1 KO mice as seen by Garami and colleagues (Garami et al., 2010).

As JNJ17203212 did not affect the rate of activity, activity is unlikely to be a contributing factor to the hyperthermia seen here. However, it is also important to note that the activity measurement made by the

telemetry equipment used in these studies was rudimentary, and to entirely exclude activity as a contributing factor to JNJ17203212-induced hyperthermia, more sensitive activity measurements, such as those using an activity wheel are required, coupled with respirometry measurements to determine whether increase in oxygen consumption is seen with TRPV1 antagonism.

In accordance with the findings of Garami and colleagues, which investigated the ability of different TRPV1 antagonists to block different modes of activation of TRPV1, JNJ17203212 inhibits proton activation of TRPV1 whilst SB366791 does not (Garami et al., 2010). In fact, SB366791 has an IC_{50} of >4000nM for the proton activation mode of TRPV1 (Garami et al., 2010) whereas a close analogue of JNJ17203212 (a structurally similar compound investigated in development of JNJ17203212 that was not continued due to lack of bioavailability) did inhibit low pH – activation of TRPV1 in a dose-dependent manner (Swanson et al., 2005). The ability of JNJ17203212 itself to block the pH mode of TRPV1 activation has not been investigated. SB366791 has previously been used at lower concentrations than those used in this thesis, in hyperalgesia studies, to show the importance of TRPV1 in TNFα –induced hyperalgesia (Russell et al., 2009; Fernandes et al., 2011).

3.4.5 The effect of TRPA1 antagonists on core body temperature

Neither TRPA1 antagonist had an effect on the core body temperature of male CD1 mice when administered orally. It has been reported that these compounds do have an effect on core body temperature when administered intraperitoneally (personal communication, Bevan lab) however our studies used the oral administration route due to the hydrophobic nature of the compounds, to ensure correct dosage. Previous studies have shown that other TRPA1 antagonists do not alter core body temperature (Chen et al., 2011), or that changes in body temperature elicited by purported TRPA1 agonists are not mediated by TRPA1 (Ding et al., 2008). Whilst it may follow that some other so-called 'thermo TRP' channels, i.e. TRP channels with a role in thermosensation, have key roles in thermoregulation, it seems that this unlikely to be the case for TRPA1.

3.4.6 Conclusions

The aims of this chapter were to investigate the effects of TRPV1 antagonists SB366791 and JNJ17203212 and TRPA1 antagonists HC030031 and TCS5861528 on pain thresholds and core body temperature of

naïve mice. We hypothesised that TRPV1 antagonists would increase thermal nociceptive thresholds whilst TRPA1 antagonists would increase mechanical nociceptive thresholds.

We also hypothesised that whilst TRPV1 antagonists would increase core body temperature of naïve mice, TRPA1 antagonists would have no effect on core body temperature. This chapter has provided evidence to support these hypotheses.

The studies in this chapter support the evidence that TRPV1 is tonically active in the control of body temperature, as blockade of the channel causes hyperthermia. JNJ172903212 (30 mg/kg) and SB366791 (5 mg/kg) increased thermal but not mechanical pain thresholds of naïve CD1 mice. Whilst systemic treatment with SB366791 did not affect core body temperature of CD1 mice compared to vehicle-treated control, JNJ17203212 administration resulted in an increase in core body temperature lasting two hours before returning to a normal temperature with respect to vehicle-treated mice. Conversely, TRPA1 is not tonically active in the control of body temperature, as blocking the channel in naïve mice had no effect on core body temperature. HC030031 (100 mg/kg) was able to increase mechanical pain thresholds whilst TCS5861528 had no effect on any pain thresholds in naïve CD1 mice.

These findings support the literature findings that TRPV1 is tonically active, as antagonism of the channel would not otherwise result in changes in core body temperature. In the next chapter, the effects of these antagonists on the vasculature will be explored, to determine whether their ability to cause hyperthermia is related to their action in the vasculature, an important thermoregulatory bed.

Chapter 4 Characterisation of the roles of TRPV1 and TRPA1 in blood flow

4.1 Introduction

Although TRPV1 and TRPA1 were initially discovered on primary sensory neurons, expression has more recently been discovered on other tissues throughout the body (Fernandes et al., 2012). This expression is functional, and may be a cause of the unexpected side effects of TRPV1 antagonists in clinical trials.

The roles of TRPA1 and TRPV1 in the vasculature have recently been the focus of a great deal of investigation. Capsaicin has long been known to be vasoactive, and this effect has been attributed to activation of TRPV1 on sensory neurons and subsequent release of inflammatory neuropeptides. This local neurogenic inflammation includes vascular changes in the smooth muscle layer (Brain and Grant, 2004). More recently, expression of TRPV1 has been shown on vascular smooth muscle cells, where activation causes influx of calcium ions and, in turn, constriction in certain tissues: isolated arteriolar smooth muscle cells (Czikora et al., 2012), skeletal muscle (Kark et al., 2008), and the synovial membrane (Keeble and Brain, 2006). Therefore, the role of TRPV1 in the vasculature is a complex one, which seems to be cell expression dependent. TRPA1 has also been investigated in the vasculature, as activation of this channel also releases vasoactive mediators (Earley et al., 2009). Some of the vascular responses to H_2S have been attributed to its ability to activate TRPA1 (Streng et al., 2008; Pozsgai et al., 2012). It is not yet known if activation of TRPA1 has differing effects in different microvascular beds, like TRPV1.

The vasculature is an instrumental part of thermoregulation in humans and other mammals (Morrison and Nakamura, 2011). Modulation of the vasculature in the skin allows cooling or restriction of heat loss depending on the situation. Vascular TRPV1 has been implicated in antagonist-mediated hyperthermia; Steiner and colleagues showed that tail skin vasoconstriction is involved in this hyperthermia in rats (Steiner et al., 2007). In this chapter, the effects of the TRPV1 agonist capsaicin, and the TRPA1 agonist mustard oil, on two different microvascular beds were investigated using Laser Doppler flow imaging. The ability of several TRPV1 and TRPA1 antagonists to block vascular responses elicited by these compounds was also investigated.

4.2 Hypothesis and Aims

The aims of this chapter are to establish the effects of capsaicin and mustard oil on two microvascular beds, the pinna and the exposed synovial membrane of the knee. This will distinguish between neuronal and non-neuronal channel activation – whilst non-neuronal TRPV1 has been well-characterised, non-neuronal TRPA1 is less so (Fernandes et al., 2012). Subsequently, the ability of TRPV1 antagonists, SB366791 and JNJ17203212, to inhibit capsaicin responses and TRPA1 antagonists, HC030031 and TCS5861528, to inhibit mustard oil responses will be investigated.

The effects of capsaicin and mustard oil on naïve blood flow will be investigated. We hypothesise that capsaicin will increase flux in the ear via activation of TRPV1 and release of inflammatory neuropeptides including CGRP; and decrease flux in the knee via activation of TRPV1 directly on smooth muscle cells allowing Ca^{2+} directly into the cell; whilst mustard oil will increase flux in both beds via inflammatory neuropeptides.

Using doses of the TRPV1 and TRPA1 antagonists determined in chapter 3, the effects of these compounds on agonist induced vascular responses will be investigated. We hypothesise that the effects will follow those seen in chapter 3, that is, JNJ17203212 will be able to block capsaicin responses in both beds, whilst SB366791 will not, and that both HC030031 and TCS5861528 will be able to block mustard oil induced blood flow changes.

4.3 Results

4.3.1 Characterisation of the effects of capsaicin on blood flow in the ear and exposed synovial membrane

The moorFLPI laser Doppler perfusion imaging system was used to determine the effect of the TRPV1 agonist capsaicin on blood flow in two distinct microcirculatory beds – the ear and the exposed synovial membrane. Topical application of capsaicin to one ear/synovial membrane was compared to topical application of the vehicle on the contralateral side.

Application of capsaicin to the ipsilateral ear (10 mg/ml, 10µl each side of ear) resulted in a significant increase in flux (maximum flux 116.5 ± 10.9%, $P<0.005$ vs vehicle), indicative of an increase in blood flow (Figure 4.1) compared to vehicle control (100% ethanol, 10µl each side of the ear). Peak flux was seen approximately 15 minutes post application. Conversely, application of capsaicin to the exposed synovial membrane (10 nmol, 10 µl) resulted in a significant decrease in flux (lowest flux at 10 minutes post-application: 40.1 ± 5.1%, $P<0.05$ vs vehicle), indicative of a decrease in blood flow (Figure 4.1) compared to vehicle control (100% ethanol, 10 µl).

4.3.2 Characterisation of the effects of mustard oil on blood flow in the ear and exposed synovial membrane

The laser Doppler perfusion imaging system was used to determine the effects of the TRPA1 agonist, mustard oil, on blood flow in the same two vascular beds as in section 4.3.1 – the ear and exposed synovial membrane. Topical application of mustard oil to one ear/synovial membrane was compared to the contralateral ear/synovial membrane, which was treated topically with vehicle.

Application of mustard oil to the ear (6%, 10 µl each side) resulted in a significant increase in flux (maximum flux 165.3 ± 11.0%, $P<0.001$ vs vehicle), indicative of an increase in blood flow (Figure 4.2) compared to vehicle control (100% paraffin oil, 10 µl each side). Similarly (Figure 4.2), application of mustard oil to the exposed synovial membrane (1%, 10 µl) resulted in a significant increase in flux (maximum flux 125.0 ± 4.0%, $P<0.05$ vs vehicle) compared to vehicle control (100% ethanol, 10 µl).

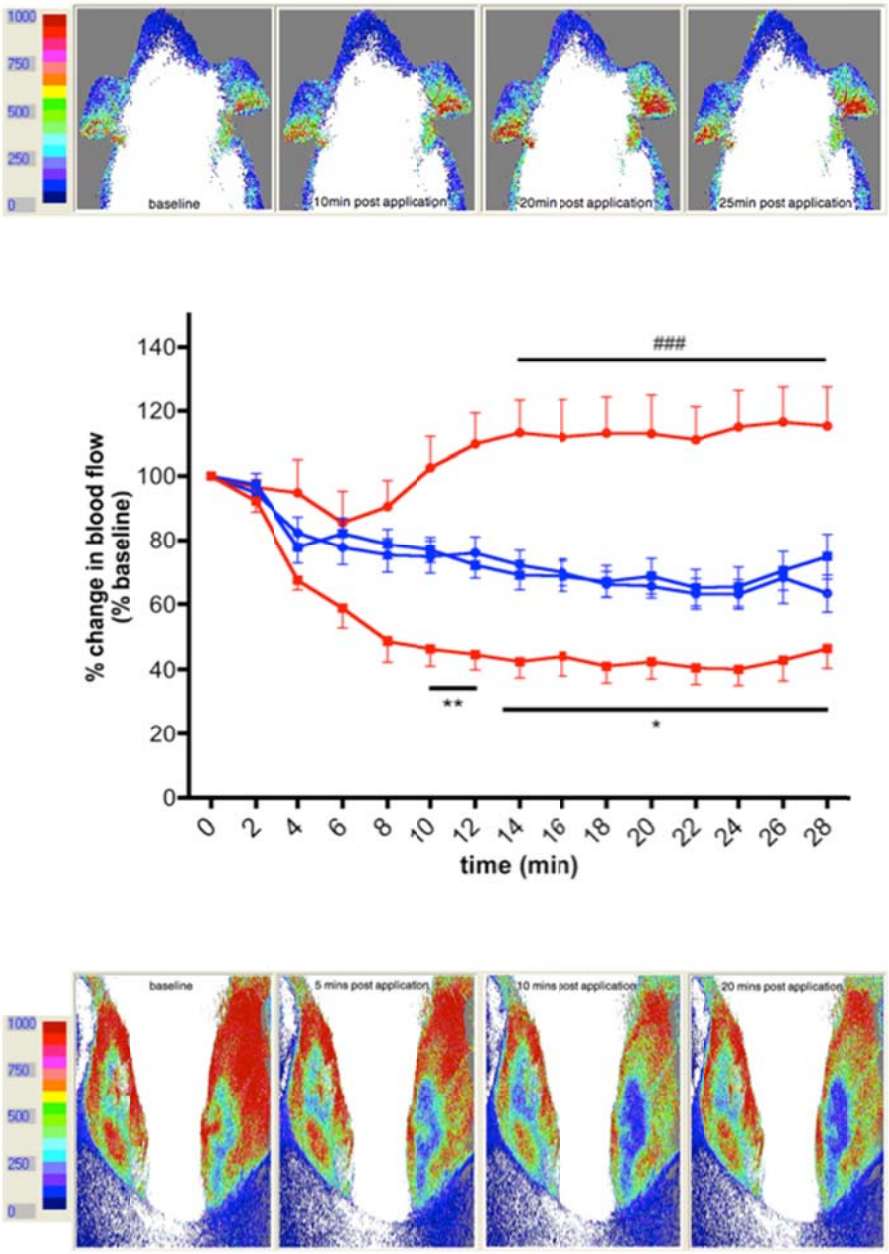

Figure 4.1 Characterisation of the effects of capsaicin on the ear and exposed synovium of anaesthetised male CD1 mice. (n=7-8). *Top panel:* typical images from the MoorFLPI data acquisition software shows that application of capsaicin (10mg/ml; right ear) leads to an increase in flow (increased redness) compared to vehicle (left ear). *Middle panel:* average percentage change in flux from baseline. Capsaicin applied to the ear (●) results in a 20% increase in flux, a significant difference ($P<0.005$) from ethanol vehicle applied to the ear (●). Conversely, capsaicin applied to the exposed synovial membrane (■) results in a 60% decrease in flux, a significant difference ($P<0.01$) from ethanol vehicle applied to the contralateral membrane (■). *Bottom panel:* typical images show that application of capsaicin (10nmol in 10µl) to the exposed synovial membrane (right knee) results in a decrease in flow (increased blueness) compared to vehicle (left knee). Statistics: RM ANOVA and *post hoc* Bonferroni test.

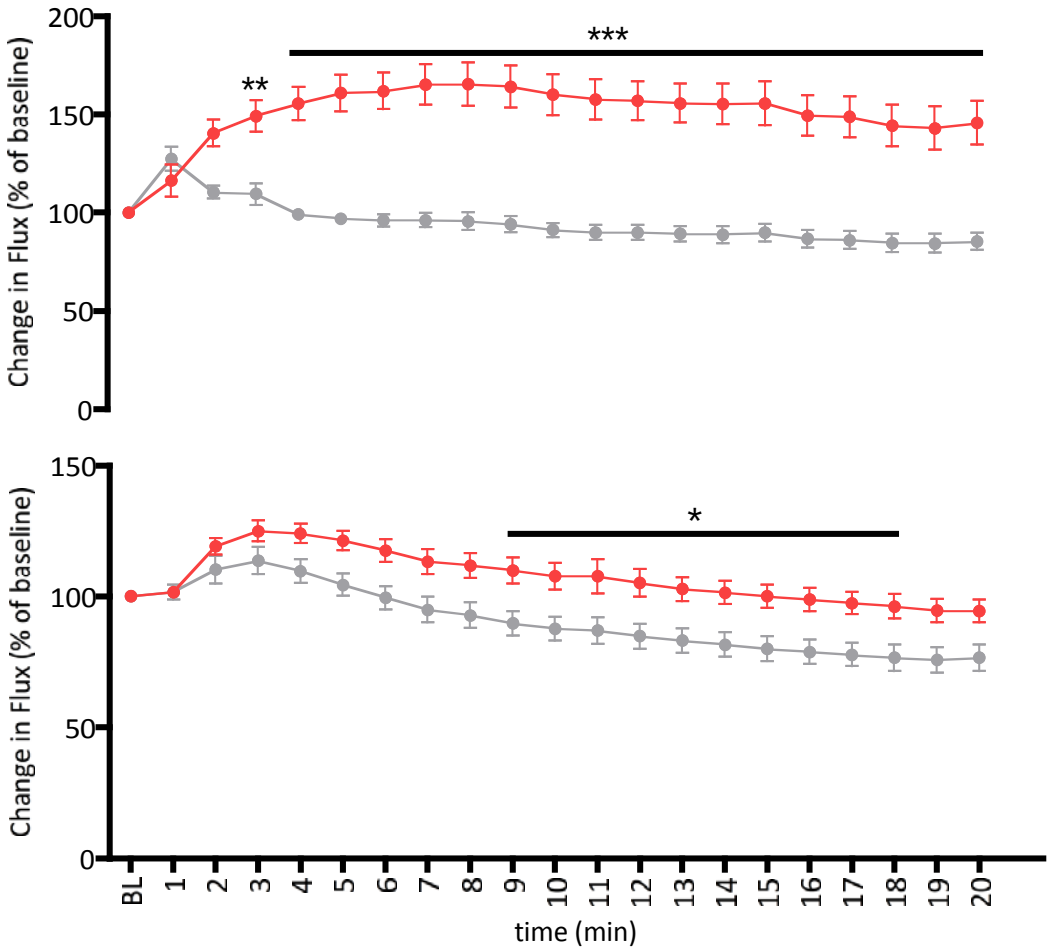

Figure 4.2 Application of mustard oil to (top) the ear and (bottom) the exposed synovial membrane of anaesthetised male CD1 mice. Application of 6% mustard oil (•) to the ear results in a significantly increased flux compared to paraffin oil vehicle (•) (n=13, P<0.005). Similarly, application of 1% mustard oil (•) to the exposed synovial membrane results in a significantly increased flux compared to ethanol vehicle (•) (n=10, P<0.05). The increase in flux in response to mustard oil in the ear was considerably larger (50%) than that displayed in the knee (25%).

Statistics: RMANOVA and Bonferroni *post hoc* test.

4.3.3 The effects of TRPV1 antagonists on capsaicin-induced blood flow changes in the ear and exposed synovial membrane

Having characterised the standard blood flow changes elicited by topical application of capsaicin to the ear and exposed synovial membrane (section 4.3.1), the ability of the TRPV1 antagonists, SB366791 and JNJ17203212, to block the responses was investigated.

Male CD1 mice were injected with 5 mg/kg SB366791 or vehicle i.p. Two hours following injection, mice were anaesthetised using urethane and placed on their front to enable baseline ear blood flow measurements. Following a ten-minute baseline measurement period, capsaicin (10 mg/ml, 10 µl each side) was applied to one ear and vehicle (100% ethanol, 10 µl each side) to the other. Blood flow was monitored for thirty minutes after application of capsaicin or vehicle. The capsaicin-treated ear of vehicle-control mice displayed an increase in flux consistent with a significant increase in blood flow compared with the contralateral vehicle-treated ear (maximum flux 116.5 ± 10.9% vs 69.9±4.2%, respectively; $P<0.05$). Mice treated with 5 mg/kg SB366791 displayed the same significant increase in blood flow when treated with capsaicin vs vehicle (maximum flux 106.0±5.6% vs 76.2 ± 6.1% respectively, $P<0.05$), showing that SB366791 is not able to block capsaicin-mediated changes in blood flow in the ear (Figure 4.3).

The knee joints of the same male CD1 mice were dissected to expose the synovial membrane, enabling direct topical application of capsaicin or vehicle to the membrane itself. The mice were placed on their back to enable clear measurement of baseline blood flow. Following a ten-minute baseline measurement period, capsaicin (10 nmol, 10 µl) was applied to one knee joint and vehicle (100% ethanol, 10 µl) to the other. Blood flow was monitored for thirty minutes after application of capsaicin. Capsaicin applied to the exposed synovial membrane caused a significant decrease in flux, consistent with a decrease in blood flow compared to the contralateral, vehicle-treated knee (lowest flux 40.9 ± 3.9% vs 67.8 ± 4.5% respectively; $P<0.05$). Mice treated with 5 mg/kg SB366791 displayed the same significant decrease in blood flow when treated with capsaicin vs vehicle-treated contralateral ear (lowest flux 50.6 ± 6.1% vs 70.3 ± 8.7% respectively, $P<0.05$), showing that SB366791 is not able to block capsaicin-medicated changes in blood flow in the exposed synovial membrane.

To investigate the effects of 30 mg/kg JNJ17203212 i.p. on blood flow, male CD1 mice were anaesthetised one hour after treatment with JNJ17203212 using 75 mg/kg ketamine and 1 mg/kg medetomidine administered in saline and kept on a heated mat to ensure stable core body temperature. Following a 10-minute baseline recording of ear blood flow, capsaicin (10 mg/ml, 10 µl each side) was applied to one ear and vehicle (100% ethanol, 10 µl each side) to the contralateral side. Blood flow was monitored for thirty minutes after application of capsaicin. The capsaicin-treated ear of vehicle-treated mice displayed an increase in flux consistent with a significant increase in blood flow compared with the contralateral vehicle-treated ear (maximum flux 204.0 ± 13.4 vs 67.4 ± 9.6%, respectively; $P<0.005$). Mice treated with JNJ17203212 displayed no significant increase in blood flow in the ear in response to capsaicin compared with vehicle control (maximum flux 90.5 ± 16.4% vs 65.2 ± 7.9%, respectively), showing that JNJ17203212 attenuates capsaicin-mediated increases in blood flow in the ear.

To investigate the ability of JNJ17203212 to block capsaicin-induced blood flow changes in the exposed synovial membrane, the knee joint of the same male mouse was dissected to expose the membrane and baseline blood flow was measured. After ten minutes of baseline recording, capsaicin (10 nmol, 10 µl) was applied to one knee joint and vehicle (100 % ethanol, 10 µl) to the other. The capsaicin-treated knee of vehicle-treated mice displayed a decrease in flux consistent with a significant decrease in blood flow compared to the contralateral, vehicle-treated synovial membrane (lowest flux 41.7 ± 3.9% vs 69.5 ± 4.0%, respectively; $P<0.05$). Mice treated with JNJ17203212 displayed a decrease in blood flow consistent with expected capsaicin responses, however the magnitude of the decrease was significantly reduced ($P<0.005$). Thus, JNJ17203212 reduced capsaicin-induced decrease in blood flow in the synovial membrane.

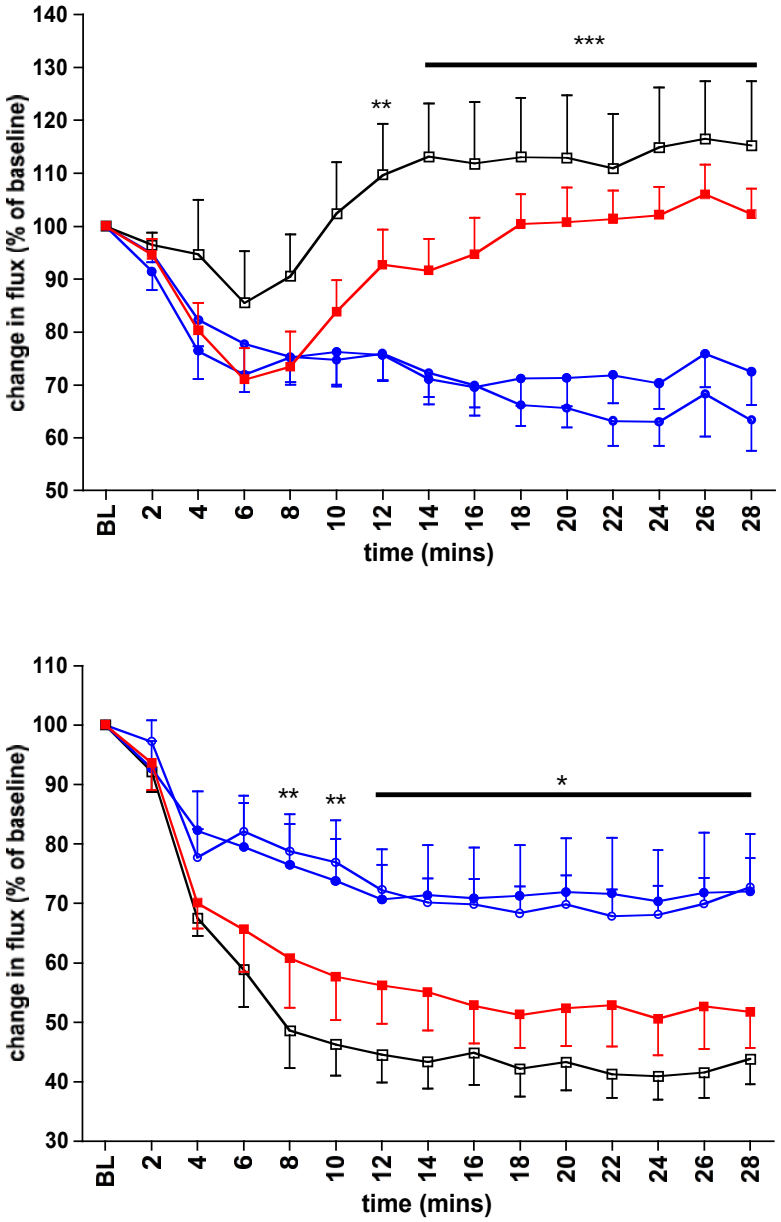

. Figure 4.3 SB366791 (5 mg/kg) does not inhibit capsaicin-induced increases in flux in the ear, or capsaicin-induced decreases in flux in the exposed synovial membrane of anaesthetised male CD1 mice (n=7) O=vehicle-treated mouse, vehicle on region of interest;•=SB366791-treated mouse, vehicle on region of interest; ■= SB366791-treated mice, capsaicin on region of interest; □= vehicle-treated mice, capsaicin on region of interest. Statistics: RMANOVA followed by Bonferroni *post hoc* test

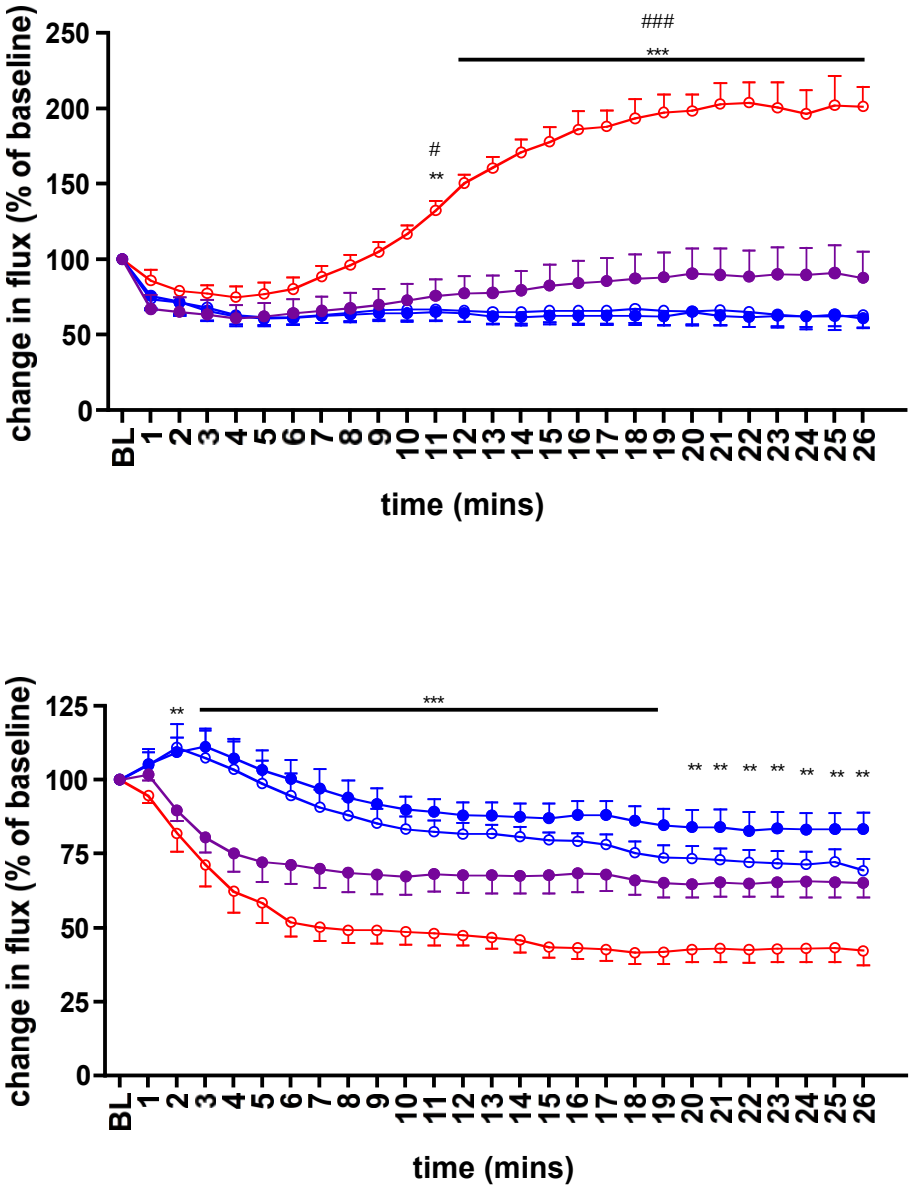

Figure 4.4 The TRPV1 antagonist JNJ17203212 (30 mg/kg) significantly inhibited capsaicin-induced changes in blood flow in the ear and exposed synovial membrane of anaesthetised male CD1 mice (n=8). ○=vehicle, vehicle; ○= vehicle, capsaicin;●= JNJ17203212, vehicle; ●=JNJ17203212, capsaicin.

Statistics: RMANOVA and Bonferroni *post hoc* test.

4.3.4 The effects of TRPA1 antagonists on mustard oil-induced changes in blood flow in the ear and exposed synovial membrane.

Having characterised the standard blood flow changes elicited by topical application of mustard oil to the ear and exposed synovial membrane (section 4.3.2), the ability of the TRPA1 antagonists HC030031 and TCS5861528 to block the responses was investigated.

Male CD1 mice were treated with 100 mg/kg HC030031 by oral gavage. One hour following injection, mice were anaesthetised using 75 mg/kg ketamine and 1 mg/kg medetomidine administered in saline and kept on a heated mat to ensure stable core body temperature. Following a ten-minute baseline measurement period, mustard oil (6%, 10 µl each side of the ear) was applied to one ear and vehicle (100 % paraffin oil, 10 µl each side of the ear) to the other. Blood flow was monitored for thirty minutes after application of mustard oil (Figure 4.5). The mustard oil-treated ear of vehicle-treated mice displayed an increase in flux consistent with a significant increase in blood flow compared with the contralateral vehicle-treated ear. Mice treated with 100 mg/kg HC030031 displayed a slight attenuation of mustard oil induced blood flow changes in comparison with vehicle-treated mice (Figure 4.5).

As in section 4.3.3, the knee joints of the same male CD1 mice were dissected to expose the synovial membrane, enabling direct topical application of mustard oil or vehicle to the membrane itself. Mice were placed on their back to enable clear visualisation of the exposed synovial membrane and measurement of baseline blood flow. Following a ten-minute baseline measurement period, mustard oil (1 %, 10 µl) was applied to one knee joint and vehicle (100 % ethanol, volume) to the other. Blood flow was monitored for thirty minutes after application of mustard oil (Figure 4.5). Knees treated with mustard oil underwent an increase in flux - consistent with an increase in blood flow - compared to the contralateral, vehicle-treated knee. Mice treated with 100 mg/kg HC030031 displayed the same significant increase in blood flow when treated with mustard oil vs vehicle, showing that HC030031 was not able to block mustard oil-mediated changes in blood flow in the exposed synovial membrane.

Hence, whilst 100 mg/kg HC030031 p.o. does not antagonise mustard oil-induced changes in blood flow in the knee, it can partially reduce mustard oil-induced increases in blood flow in the ear.

In order to investigate the effects of 10 mg/kg TCS5861528 p.o. on blood flow, male CD1 mice were anaesthetised one hour after oral treatment with TCS5861528 using 75 mg/kg ketamine and 1 mg/kg medetomidine administered in saline and kept on a heated mat to ensure stable core body temperature. Following a 10-minute baseline recording of ear blood flow, mustard oil (6 %, 10 µl each side of the ear) was applied to one ear and vehicle (100 % paraffin oil, 10 µl each side of the ear) to the contralateral side. Blood flow was monitored for thirty minutes after application of agonist (Figure 4.6). The mustard oil-treated ear of vehicle-treated mice displayed an increase in flux consistent with a significant increase in blood flow compared with the contralateral vehicle-treated ear. Mice treated with TCS5861528 displayed a characteristic increase in blood flow in the ear in response to mustard oil compared with vehicle control, showing that 10 mg/kg TCS5861528 p.o. cannot block mustard oil-mediated increases in blood flow in the ear.

The knee joint of the same male mouse was dissected to expose the synovial membrane and baseline blood flow was measured. After ten minutes of baseline recording, mustard oil (1 %, 10 µl) was applied to one knee joint and vehicle (100 % ethanol, 10 µl) to the other. The mustard oil-treated knee of vehicle-treated mice displayed an increased flux consistent with a significant increase in blood flow compared to the contralateral, vehicle-treated synovial membrane. TCS5861528-treated mice showed the same increase in flux (Figure 4.6), indicating that 10 mg/kg TCS5861528 p.o. does not affect mustard oil-induced changes in blood flow in the synovial membrane.

Thus, 10 mg/kg TCS5861528 p.o. has no effect on mustard oil-induced changes in blood flow in the ear and the exposed synovial membrane.

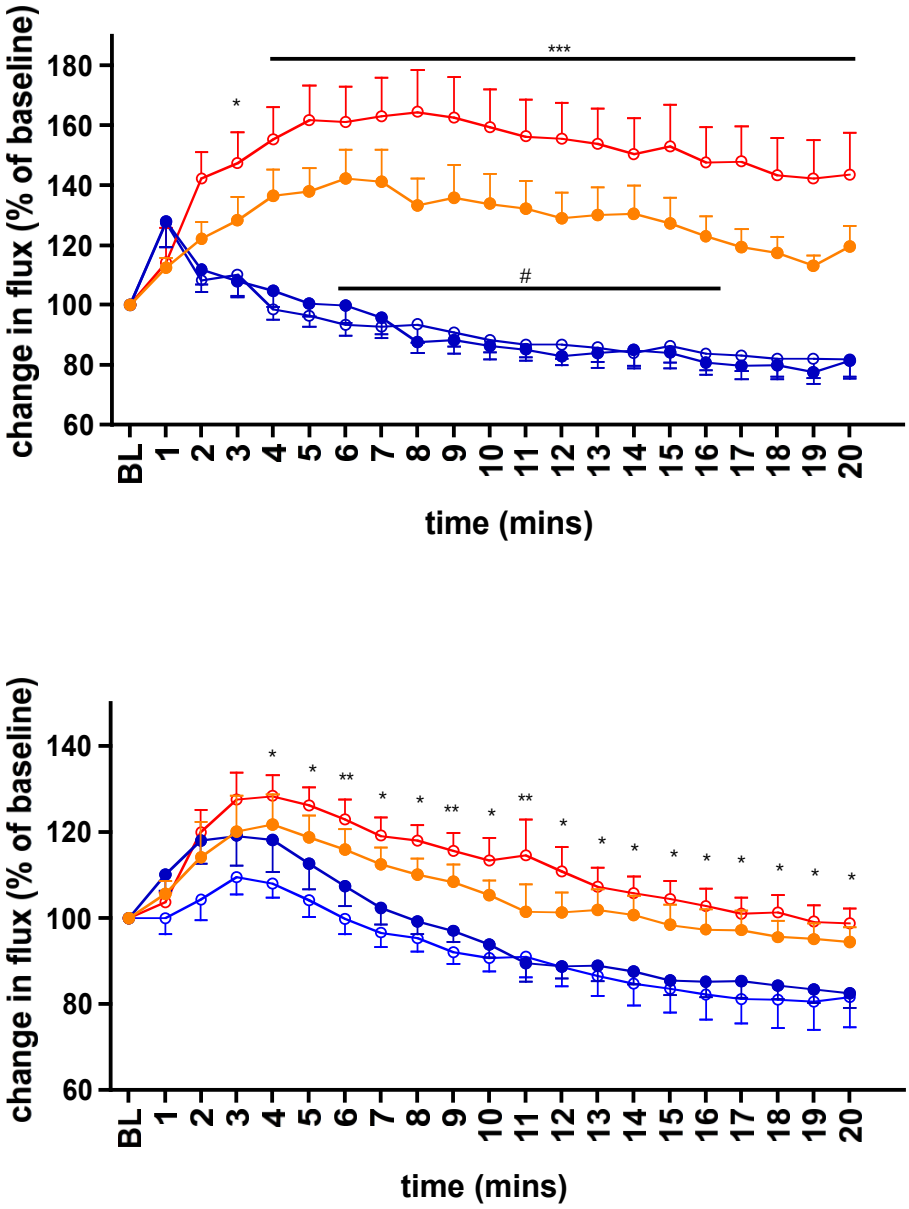

Figure 4.5 The effect of 100 mg/kg HC030031 on mustard oil-induced changes in blood flow in the ear and exposed synovial membrane. Male CD1 mice (n=6) were anaesthetised (ketamine/medetomidine). After a ten-minute baseline period, mustard oil was applied to (top) one ear and vehicle (paraffin oil) applied to the contralateral ear. In the bottom panel, mustard oil was applied to one exposed synovial membrane and vehicle (ethanol) applied to the contralateral joint. ○=vehicle, vehicle; ○= vehicle, capsaicin;●= HC030031, vehicle; ●=HC030031, capsaicin. Statistical tests: RMANOVA and Bonferroni *post hoc* test.

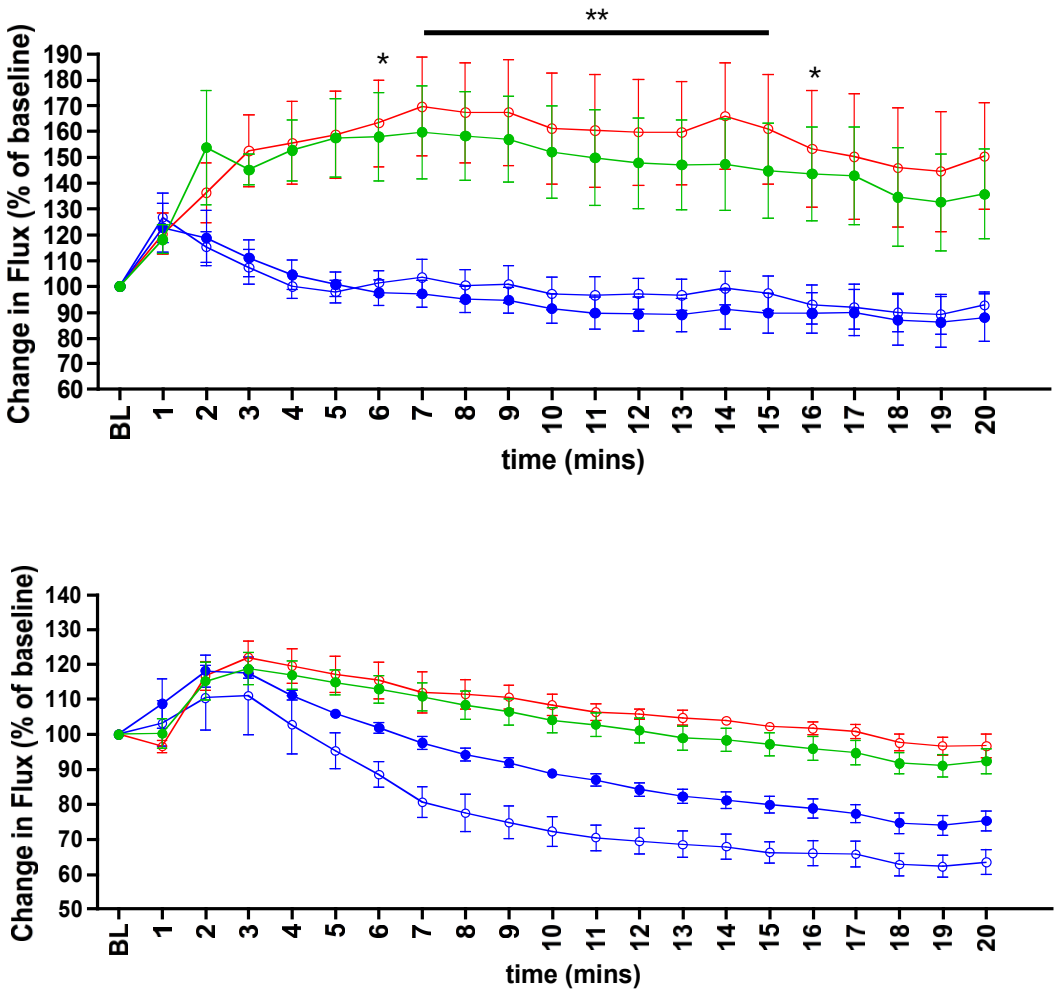

Figure 4.6 The effect of 10 mg/kg TCS5861528 p.o. on mustard oil-induced changes in blood flow in the ear and exposed synovial membrane. Male CD1 mice (n=7) were anaesthetised (ketamine/medetomidine) 45 minutes after treatment with TCS5861528. After a ten-minute baseline period, mustard oil was applied to (top) one ear and vehicle (paraffin oil) applied to the contralateral ear. In the bottom panel, mustard oil was applied to one exposed synovial membrane and vehicle (ethanol) applied to the contralateral joint. ○=vehicle, vehicle; ○= vehicle, capsaicin;●= TCS5861528, vehicle; ●=TCS5861528, capsaicin. Statistical tests: RMANOVA and Bonferroni *post hoc* test.

4.4 Discussion

4.4.1 Key findings

- Capsaicin increases blood flow in the pinna and decreases blood flow in the exposed synovial membrane
- Mustard oil increases blood flow in both the pinna and the exposed synovial membrane
- Different TRPV1 antagonists have different effects on capsaicin-induced blood flow changes in the pinna and exposed synovial membrane.
- TRPA1 antagonists have no significant effect on mustard oil-induced blood flow changes in the pinna and exposed synovial membrane

These studies investigated the effects of TRP antagonists on blood flow, with the aim of correlating these effects with the ability to induce changes in body temperature. The ability of TRPV1 and TRPA1 antagonists to inhibit capsaicin- and mustard oil-induced vascular changes was determined. Capsaicin was used in two different microvascular beds to determine the ability of the different antagonists to block neuronal and non-neuronal TRPV1 channels. Mustard oil was also investigated to determine the effects of activation of TRPA1 in the same microvascular beds.

4.4.2 The effect of capsaicin on the vasculature in different tissues

Capsaicin, the archetypal TRPV1 agonist, has contrasting effects in the microvascular beds investigated in these studies. In the pinna, a well-characterised model of neuronal TRPV1 (Grant et al., 2002; Starr et al., 2008) , topical capsaicin results in an increase in flux – synonymous with vasodilation –peaking at approximately 15 minutes post-application. This response has been characterised previously, and is caused by activation of neuronal TRPV1, which leads to release of the inflammatory neuropeptides, Substance P and CGRP (Grant et al., 2002). It is dependent on TRPV1 as vasodilation is not seen in TRPV1 KO mice (Starr et al., 2008). This dilation together with release of inflammatory peptides is typical of neurogenic inflammation, a key marker of neuronal TRPV1 activation (Jancsó et al., 1967). Conversely, capsaicin applied to the exposed synovial membrane of the knee caused a rapid and profound (10 minutes to peak) reduction in flow, which is consistent with vasoconstriction. Activation of TRPV1 in vascular tissues has previously been shown to result in vasoconstriction (Keeble and Brain, 2006; Kark et al., 2008;

Czikora et al., 2012; Toth et al., 2014). This is not the typical response seen with neuronal TRPV1 activation i.e. a dilatory response to release of inflammatory neuropeptides. The mechanisms for this 'non-neuronal' response have not been defined, however the likely causes are either activation of TRPV1 directly located on smooth muscles, facilitating calcium entry into the cell (Kark et al., 2008) or release of the vasoconstrictor Neuropeptide Y (Keeble and Brain, 2006). The findings of the present study, together with the evidence from previous experiments show that there are two distinct types of TRPV1 channel, with opposing functions, expressed in or adjacent to the vasculature.

The two responses had different dynamics. Whilst the increase in flow in the pinna was gradual, reaching the maximum flow by 15 ± 2 minutes, the decrease in flow in the knee had a rapid onset and reached lowest flux by 12 minutes, likely due to direct application to the membrane, thus, no need to penetrate the skin cuticle, as in the pinna.

4.4.3 The ability of TRPV1 antagonists to block capsaicin-induced blood flow responses

The ability of SB366791 and JNJ17203212 to inhibit capsaicin-induced blood flow responses was investigated, in order to determine whether non-neuronal or neuronal TRPV1 was involved in the hyperthermia seen in Chapter 3. To this end, the same systemically administered doses of these compounds were used. Mice were pre-treated with antagonists one hour before topical application of capsaicin, which fell within the timescale of onset to JNJ17203212-induced hyperthermia.

10 mg/kg SB366791 had no significant effect on capsaicin-induced vascular responses in both the pinna and exposed synovial membrane, however the response was reduced compared to capsaicin-treated ears of vehicle-pretreated mice. A higher dose was not used in these studies due to complications with the solubility of SB366791 at higher doses. Garami and colleagues have shown that whilst SB366791 has very low potency to block the proton and heat mode of activation of TRPV1, the IC_{50} for blockade of activation by 500 nM capsaicin was 547 ± 231 nM. In comparison with other widely used TRPV1 antagonists, such as the hyperthermia-inducing AMG9810 (Gavva et al., 2005), this is 10 times less potent (Garami et al., 2010). The reduced potency for inhibition of capsaicin-activation of TRPV1 may explain why SB366791 is unable to block vascular changes induced by topical application of capsaicin.

30 mg/kg JNJ17203212 significantly inhibited capsaicin-induced vascular responses in both the pinna and exposed synovial membrane. In the pinna, JNJ17203212 reduced capsaicin-induced vasodilation from. In the exposed synovial membrane, JNJ17203212 also significantly inhibited vasoconstriction, with a statistically significant difference at 20 minutes after topical application of capsaicin. Our laboratory investigations have found that euthermic (i.e. no effect on temperature) antagonists have no effect on the 'non-neuronal' capsaicin-induced vasoconstriction in the exposed synovial membrane. However, JNJ17203212 is unique amongst the hyperthermic antagonists investigated in our laboratory (including AMG9810) in its ability to attenuate capsaicin-induced vasoconstriction in this tissue. Whilst the development of a model of neuronal and non-neuronal TRPV1 activation in the same mouse, described in this chapter, has the potential to help shed light on the involvement of these two subsets of TRPV1 in hyperthermia, we will not be able to utilise it to its full potential until the exact mechanisms of the non-neuronal activation are elucidated. Moreover, it will be important to consider whether the 'non-neuronal' TRPV1 activation described in the exposed synovial membrane is demonstrative of all 'non-neuronal' vascular TRPV1 activation. Indeed, it will be worth considering if this is in fact a 'non-neuronal' response rather than simply the effects of an alternative neuropeptide or removal of vasodilation.

4.4.4 The effect of mustard oil on the vasculature in different body tissues

Mustard oil caused an increase in flux, indicative of an increase in blood flow, in both microvascular beds investigated in the present study. In the pinna, this is consistent with previous findings that mustard oil-induced vasodilation is neuropeptide-dependent (Banvolgyi et al., 2004; Grant et al., 2005). Mustard oil applied to the exposed synovial membrane also results in vasodilation. In previous studies, TRPA1 was shown to be involved in cerebral artery dilation, and this dilation was endothelium-dependent (Earley et al., 2009). In this study, Mustard oil-induced vasodilation was not mediated by nitric oxide or prostanoids, rather by calcium-activated potassium channels on endothelial cells and inwardly rectifying potassium channels on arterial myocytes (Earley et al., 2009). The role of TRPA1 in the vasculature has not been as thoroughly studied as TRPV1, with the focus being on vessels involved in the nervous system (Earley et al., 2009; Nassini et al., 2012).

4.4.5 The ability of TRPA1 antagonists to block mustard oil-induced blood flow responses

The ability of TCS5861528 and HC030031 to inhibit mustard oil-induced blood flow responses was investigated. The same systemically administered doses of these compounds as those in studies in chapter 3 were used. Mice were pre-treated with antagonists one hour before topical application of capsaicin, which fell in the timescale of onset to HC030031-induced increase in mechanical nociceptive thresholds.

100 mg/kg HC030031 did not significantly inhibit mustard oil-induced vasodilation in the pinna and exposed synovial membrane. This contrasts with other studies, showing that TRPA1-mediated vasodilation can be inhibited by HC030031. This, however, is likely due to the studies in this chapter being carried out *in vivo* whilst the other studies performed *in vitro* assays (Earley et al., 2009; Kunkler et al., 2011).

10 mg/kg TCS5861528 also did not significantly inhibit mustard oil-induced vasodilation in the pinna and exposed synovial membrane. This, together with the results from chapter 3 showing that TCS5861528 is unable to increase nociceptive thresholds, suggests that 10 mg/kg TCS5861528 is not active in mice used in these studies. We have not increased the dose of TCS5861528 used due to solubility problems with the compound. Wei and colleagues have shown efficacy of TCS5861528 in a diabetes model. A chronic dosing schedule of 30 mg/kg TCS5861528 twice a day attenuated mechanical hypersensitivity in diabetic rats (Jancsó-Gábor et al., 1970a; 1970b; Long et al., 1990; Olivier et al., 2003; Wei et al., 2009). However TCS5861528 has not been used in vascular studies previously.

4.4.6 Conclusions

In this chapter, we attempted to determine if the doses of antagonist used in body temperature studies inhibit TRPV1 and TRPA1 agonist-induced vascular changes in the murine pinna or exposed synovial membrane. We have found that the TRPV1 antagonist JNJ17203212 could block the agonist-induced responses, showing that dose used in Chapter 3 are also pharmacologically active in these vascular tissues. Whilst it is well - established that control of skin blood flow may play role in TRPV1 antagonist-induced hyperthermia, we have not been able to establish a firm correlation.

Chapter 5 Investigation of the role of TRPA1 in TRPV1 antagonist-induced hyperthermia

5.1 Introduction

Whilst TRPV1 antagonism is associated with hyperthermia, knocking out the TRPV1 receptor in mice does not affect core body temperature (Caterina et al., 2000; Garami et al., 2011). Some have found that whilst thermosensation is impaired (Tóth et al., 2010; Chen et al., 2011), normal thermoregulation is intact under baseline conditions. This suggests that there is an underlying mechanism to compensate for the loss of this 'thermostat', ensuring the ability to regulate core body temperature.

TRPV1 is co-expressed with TRPA1 in many tissues (for review, see Fernandes et al., 2012); and the two channels have been shown to be able to form functional heteromers (Fischer et al., 2014), with roles particularly in nociception (Akopian, 2011). If compensation is indeed accounting for the normal core body temperature of TRPV1 KO mice, TRPA1 is a good candidate for this due to close structural, functional and location.

Whilst TRPA1 has been defined as a sensor of cold temperatures (Story et al., 2003; Bandell et al., 2004; Kwan et al., 2006), unlike TRPV1 it has not been implicated in the control of body temperature. Recently Aubdool and colleagues discovered that its role as a cold sensor is critical in the vascular response to cold and it plays an active role in preventing tissue damage by cold (Aubdool et al., 2014). This shows that whilst there is not yet a basal thermoregulatory function of TRPA1 (i.e. that it is tonically active to control temperature, like TRPV1 purportedly is), TRPA1's role in the vasculature contributes to thermoregulation in cold temperatures (Aubdool et al., 2014).

This chapter investigated the role of TRPA1 in TRPV1 antagonist-induced hyperthermia, and also if TRPA1 has a compensatory role in TRPV1 KO mice.

5.2 Hypothesis and Aims

The aims of this chapter are to investigate the role of TRPA1 in TRPV1 antagonist-induced hyperthermia, specifically the hyperthermia induced by JNJ17203212. The core body temperature of TRPV1 knockout mice is not significantly different from that of wild type mice, therefore we hypothesise that TRPA1 is, at least in part, compensating for the loss of the TRPV1 receptor.

The effects of the TRPA1 antagonist HC030031 on the core body temperature of TRPV1 knock out mice will be investigated. As this will cause TRPA1 function to be inhibited, we expect to see a hyperthermic response if the receptor is compensating for the knock out of TRPV1.

The effects of JNJ17203212 on the core body temperature of TRPA1 knock out mice will be investigated, in order to determine if TRPV1 antagonism can cause hyperthermia without the presence of the TRPA1 channel. We hypothesise that involvement of TRPA1 in the hyperthermic response would render JNJ17203212 euthermic in TRPA1 knock out mice.

The effects of pre-treatment with HC030031 on JNJ17203212-treated naïve CD1 mice will also be investigated, in order to determine if antagonising both receptors concomitantly will remove JNJ17203212-induced hyperthermia.

5.3 Results

5.3.1 Basal core body temperature of TRPV1 WT and KO mice

The core body temperature of telemetered naïve male CD1 mice follows a diurnal pattern, with a core body temperature of 36.08±0.04°C in daylight hours and 37.47±0.07°C in the night cycle. Figure 5.1 shows the body temperature and activity levels of naïve male TRPV1 WT and KO mice over 24 hours. There is no significant difference in the activity and core body temperature between genotypes (repeated measures ANOVA).

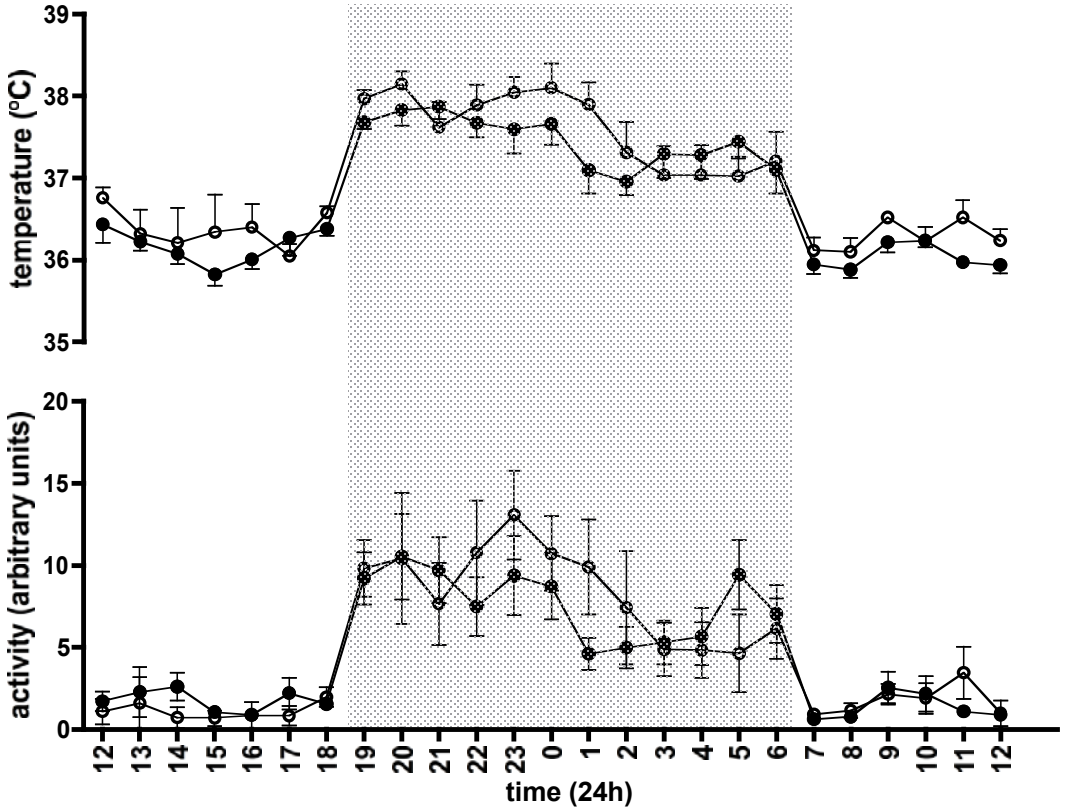

Figure 5.1 The core body temperature (top) and activity (bottom) of telemetered naive male (n=6) TRPV1 WT (closed circles) and KO mice (open circles). After implanting a temperature telemetry probe intraperitoneally, mice were left to recover for a week before being placed on receivers to monitor their temperature continuously over 24 hours. Data are shown as mean ± SEM. There is no significant difference between genotypes for both body temperature and activity levels (repeated measures ANOVA). Shaded area indicates the dark cycle.

5.3.2 The effect of a TRPA1 antagonist on the core body temperature of TRPV1 WT and KO mice

Telemetered male TRPV1 WT and KO mice (n=6) were administered 100 mg/kg HC030031 or vehicle (0.1% DMSO in saline, dosing volume of 5 ml/kg) via oral gavage after a one-hour baseline recording, and monitored for 24 hours (Figure 5.2) as outlined in section 2.4. Previously, we reported no effect of HC030031 on body temperature in WT mice and CD1 mice (see Figure 3.9). In this study, again no significant difference was demonstrated between WT mice treated with vehicle and those treated with HC030031. However, KO mice treated with HC030031 had a hypothermic body temperature that was significantly lower than that of KO mice treated with vehicle from one to two hours after treatment ($P<0.001$ with respect to vehicle-treated KO mice, repeated measures ANOVA) before returning to normal body temperature.

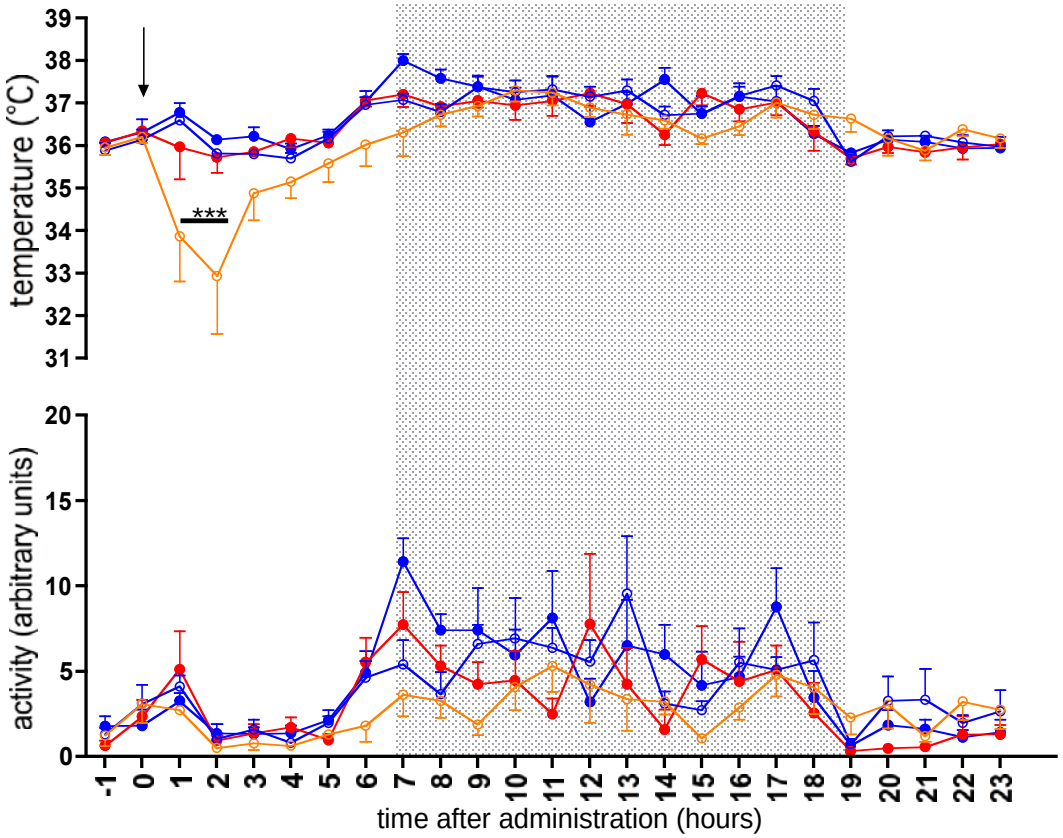

Figure 5.2 Administration of 100 mg/kg HC030031 in telemetered male TRPV1 WT and KO mice (n=6) after a one-hour baseline period. Mice lacking the TRPV1 receptor have a significantly decreased body temperature in response to this compound (P<0.001, peak at 2 hours post treatment, 32.94 ± 1.36) compared to WT animals. Shaded area indicates the dark cycle.

Key: •= vehicle treated WT; o=vehicle treated KO; •=HC030031-treated WT; o= HC030031-treated KO.

***P<0.001, by RM ANOVA and *post hoc* Bonferroni test.

5.3.3 The effect of treatment with HC030031 on JNJ17203212-induced hyperthermia

Telemetered naïve male CD1 mice were administered either 100 mg/kg HC030031 or vehicle (0.1% DMSO in saline, dosing volume of 5 ml/kg) by oral gavage after a one-hour baseline recording (Figure 5.3). After 30 minutes, mice were administered 30 mg/kg JNJ17203212 via i.p. injection and temperature and activity were monitored for an acute period of 3 hours.

Animals treated with the vehicle+JNJ17203212 combination displayed an increase in body temperature in line with studies of naïve JNJ17203212 treatment, where a similar effect was observed (refer to previous figure). Mice pre-treated with HC030031 displayed an immediate increase in body temperature; subsequent treatment with JNJ17203212 increased the core body temperature further (Figure 5.3). Mice treated with HC030031+vehicle displayed an unexpected response – the core body temperature after the first injection, i.e. HC030031 was not altered; however, subsequent administration of vehicle resulted in a significant drop in core body temperature, lasting one hour (Figure 5.3).

5.3.4 The effect of JNJ17203212 on the core body temperature of TRPA1 WT and KO mice

Telemetered male TRPA1 WT and KO mice (n=4) were treated with 30 mg/kg JNJ17203212 via intraperitoneal injection after a one-hour baseline recording, and monitored for 24 hours (Figure 5.4) as outlined in section 2.4. There was no significant difference between the core body temperature and activity of TRPA1 WT and KO mice at baseline, and no difference between vehicle-treated WT and KO mice after administration. Both vehicle- and JNJ17203212-treated mice exhibited a hyperthermic profile, however there was no significant difference in this response between vehicle and JNJ17203212 mice. TRPA1 KO mice treated with JNJ17203212 had an increased hyperthermic response.

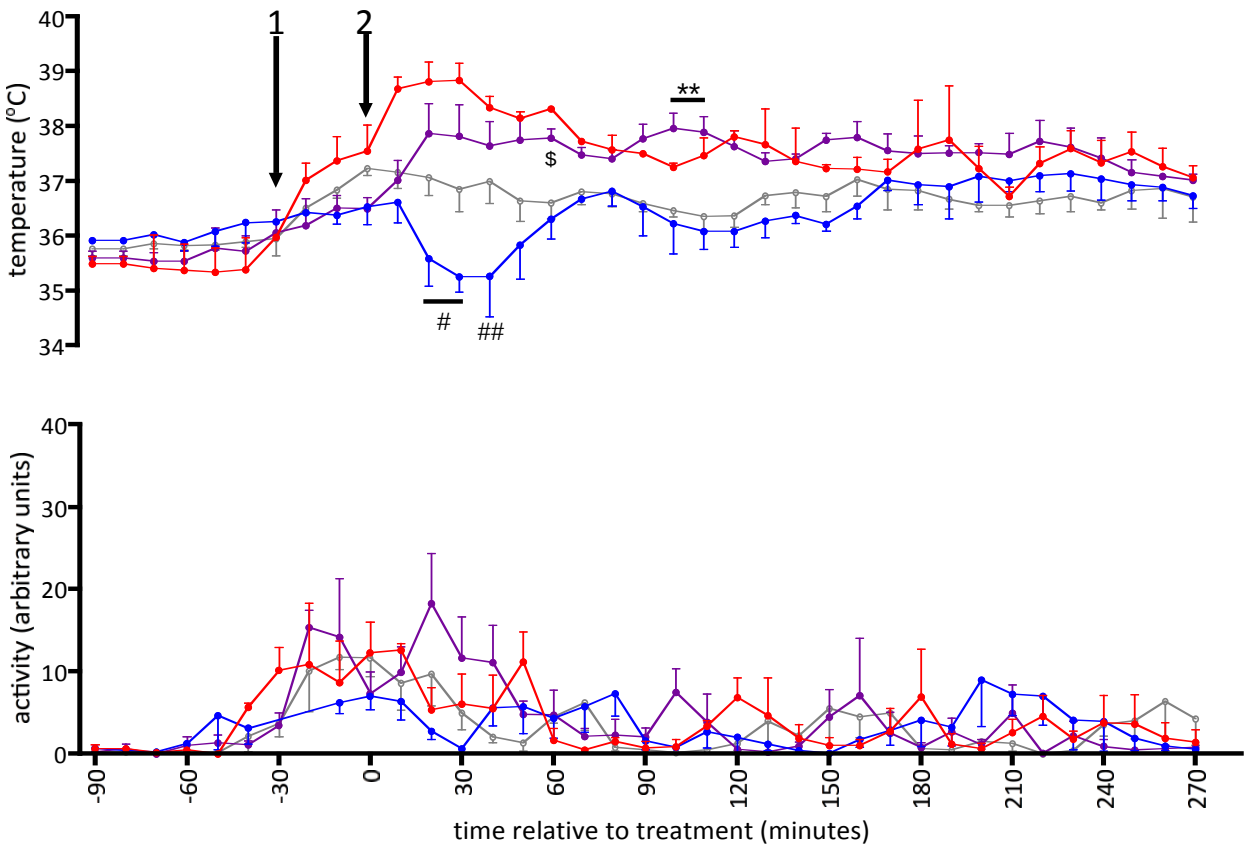

Figure 5.3 The effect of oral administration of the TRPA1 antagonist HC030031 (1) 30 minutes before administration of JNJ17203212 (2) on core body temperature. Male CD1 mice (n=3-4) were treated with 100mg/kg HC030031 or vehicle 30 minutes before administration of 30mg/kg JNJ17203212 or vehicle via i.p. injection.

Key: ● - Vehicle + Vehicle; ● - Vehicle + JNJ17203212; ● - HC030031 + Vehicle; ● - HC030031 + JNJ17203212.

**- P<0.01; $ - P<0.05; #P<0.05; ##P<0.01 with respect to Vehicle + Vehicle treated mice (●).

Statistics: RM ANOVA followed by *post hoc* Bonferroni test.

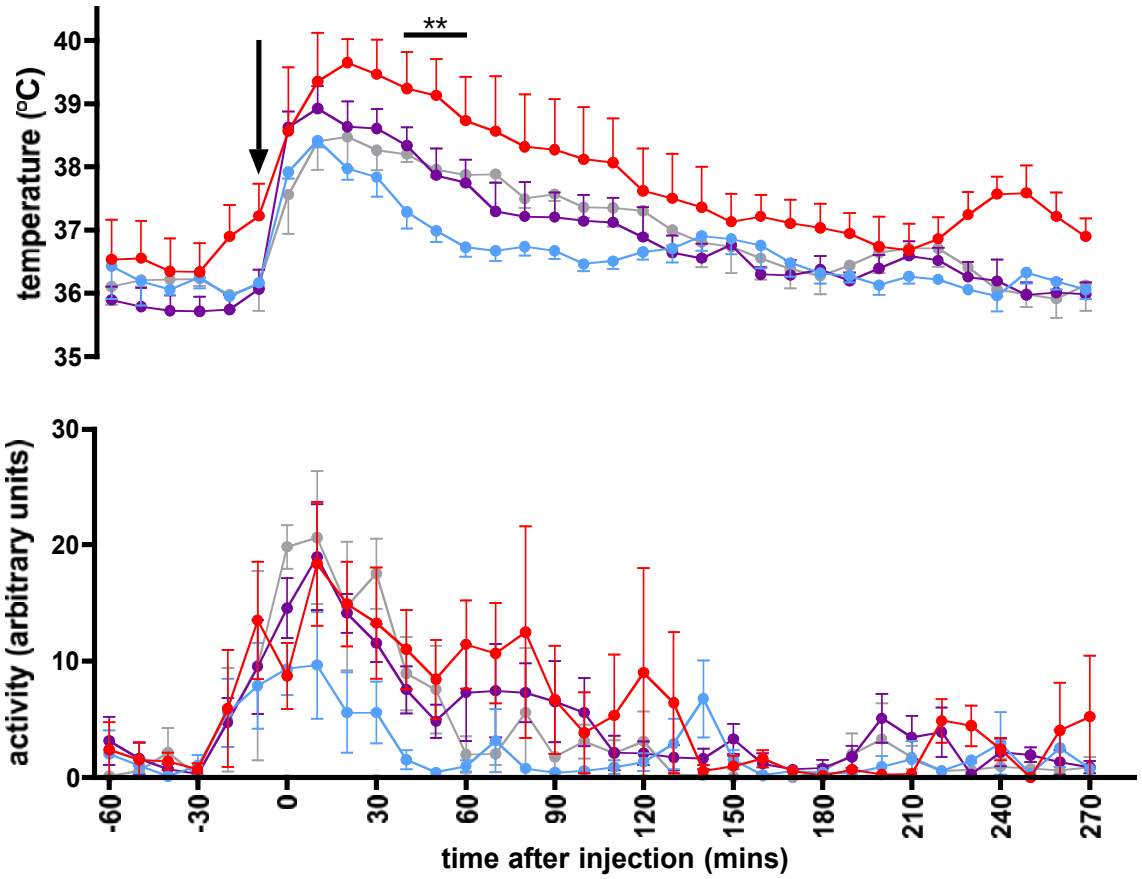

Figure 5.4 The core body temperature (top) and activity (bottom) of TRPA1 WT and KO mice (n=4) after i.p. injection (arrow) of 30 mg/kg JNJ17203212 or vehicle. **(P<0.01, n=4).

Key: = WT vehicle, = WT JNJ17203212, = KO vehicle, = KO JNJ17203212. **P<0.01 vs KO vehicle.

Statistical test: RM ANOVA and *post hoc* Bonferroni test.

5.4 Discussion

5.4.1 Key findings

- Whilst HC030031 had no effect on naïve animals, administration in TRPV1 knockout mice resulted in a significant decrease in core body temperature.
- Pre-treatment with HC030031 had no significant effect on the hyperthermia induced by JNJ17203212.
- Treatment with JNJ17203212 resulted in significant hyperthermia in TRPA1 knockout but not wild type mice, compared to vehicle treatment.

In this chapter, the role of TRPA1 in JNJ17203212-induced hyperthermia was investigated. TRPV1 and TRPA1 knock out mice and the TRPA1 antagonist HC030031 were used in functional *in vivo* studies to determine if a thermoregulatory relationship between the two receptors exists.

5.4.2 Absence of TRPV1 has no effect on core body temperature.

The basal core body temperature of male TRPV1 KO mice was the same as that of their WT littermates. This is in accordance with previous studies showing that whilst TRPV1 antagonism can result in hyperthermia, mice without the TRPV1 receptor have a normal core body temperature profile (Garami et al., 2011) and TRPV1 KO mice can regulate core body temperature when thermally challenged (Szelenyi et al., 2004). In contrast, rats that have been desensitised with capsaicin lose their ability to thermoregulate (Jancsó-Gábor et al., 1970a; 1970b) and Toth and colleagues showed that siRNA knockdown of TRPV1 in mice affects their thermoregulatory abilities (Tóth et al., 2010). Therefore, although a role for TRPV1 in thermoregulation is emerging, it is not clear: different models show different effects.

5.4.3 TRPA1 antagonism results in hypothermia in the absence of TRPV1.

In section 3.3.4, it was shown that HC030031 had no effect on the core body temperature of naïve CD1 mice. Whilst HC030031 also had no effect on the core body temperature of TRPV1 WT mice, administration of the compound to TRPV1 KO mice resulted in a profound, significant decrease in core body temperature. We originally hypothesised that if TRPA1 were involved in compensating for

thermoregulation in TRPV1 knockout mice, a hyperthermic profile would be observed. Instead, the opposite occurred, with a significant decrease in core body temperature seen after TRPA1 inhibition in TRPV1 knockout mice. This is interesting because in studies of the ability of TRPA1 antagonists to disrupt core body temperature, all studies have shown evidence to support the findings in chapter 3 of this thesis – i.e. that TRPA1 antagonists do not affect body temperature (Eid et al., 2008; Wei et al., 2009; Chen et al., 2011).

The reason for the hypothermia is not known. Whilst it has been reported that the vehicle, DMSO can cause hypothermia (over a range of doses) in rodents (Altland et al., 1966; Ashwood-Smith, 1967), the reduction in core body temperature was not seen in vehicle treated mice. It has not been documented that HC030031 can cause hypothermia, therefore this study presents the first evidence that oral treatment with HC030031 can cause changes in core body temperature.

Further investigating the role of TRPA1 in TRPV1 antagonist-mediated hyperthermia, we blocked TRPA1 channels using HC030031 before treating the mice with JNJ17203212. Pre-treating JNJ17203212-treated CD1 mice with HC030031 did not alter their core body temperature. However, pre-treating vehicle control mice with HC030031 resulted in a drop in core body temperature, similar to that seen in TRPV1 KO mice treated with this TRPA1 antagonist.

Stress can also cause a change in core body temperature in mammals, however this is usually associated with a spike in temperature consistent with an increase in locomotion (Long et al., 1990; Olivier et al., 2003). In fact, stress can become a learned behaviour simply in response to handling (Eikelboom, 1986). The mice used in telemetry studies were singly housed for a week, to facilitate recovery and prevent injury to stitches protecting surgical incisions (as male mice have a tendency to fight). One undesirable effect of being singly housed is that the mice may become stressed or ‘anxious’. In addition, due to the poor solubility of HC030031, this compound was administered by oral gavage in the entire series of experiments conducted in this thesis. Naïve mice subjected to oral gavage of vehicle (in this study, 0.1% DMSO) did not exhibit any changes in core body temperature (Section 3.3.4 of this thesis), which is consistent with the literature (Eid et al., 2008). There is no evidence in the literature for a stress response to cause a drop in temperature to the same extent seen in this chapter. Additionally, if hypothermia was

due to stress of oral gavage, the vehicle-treated animals should have also had this response. It may be that the temperature response to TRPA1 antagonism varies between strains, as differences between strains can account for difference in metabolism and other factors pertinent to these studies (Leon, 2005).

These results did not agree with the hypothesis that TRPA1 directly compensates for the loss of TRPV1, using both pharmacological and genetic modification tools.

5.4.4 The effect of JNJ17203212 on the core body temperature of TRPA1 KO mice

Intraperitoneal injection of 30 mg/kg JNJ17203212 in TRPA1 KO mice resulted in a hyperthermic response. TRPA1 WT mice treated with JNJ17203212 did not show a hyperthermic response when compared to vehicle. Observations made during the studies suggested that the cohorts of TRPA1 WT and KO mice used in these studies were hyperkinetic, and displayed 'stressed' behaviours. This reflects studies by Bodkin and colleagues, which showed that TRPA1 KO mice were hyperactive (Bodkin et al., 2014). These could have confounded the results of the experiment.

5.4.5 Conclusions

This chapter investigated the relationship between TRPA1 and TRPV1 in antagonist-induced hyperthermia. The core body temperature of TRPV1 KO mice is normal, compared to their WT littermates. Whilst the hypothesis that TRPA1 is directly compensating for loss of TRPV1 in KO mice was not proven, this does not mean that there is no role for TRPA1. This chapter provided novel evidence that treatment of TRPV1 KO mice with HC030031 resulted in acute hypothermia. The mechanism for this is not understood. The hyperthermia induced by the TRPV1 antagonist JNJ17203212 in naïve CD1 mice is not antagonised by HC030031. Treatment with HC030031 resulted in hypothermia when TRPV1 was deleted but not in TRPV1 wild type mice. The mechanism of TRPA1 antagonist (HC030031)-induced hypothermia is not well understood and merits further study, as TRPA1 research indicates this channel's efficacy in a multitude of inflammatory conditions (Nilius et al., 2012).

Finally, JNJ17203212 was hyperthermic in TRPA1 KO mice. These data together show that, whilst TRPA1 is not key in JNJ17203212-induced hyperthermia, its effects on thermoregulation are far more complex than expected.

Chapter 6 The effect of H_2S on TRPV1 antagonist-induced hyperthermia

6.1 Introduction

The experiments presented thus far in this thesis have investigated a role for TRPA1 in temperature control, particularly with respect to TRPV1 antagonism. It has been shown that TRPA1 knock out/inhibition has no effect on baseline body temperature. This, however, is no indication that TRPA1 activation doesn't alter core body temperature itself. This chapter, therefore, investigates the effects of the putative TRPA1 agonist H_2S on thermoregulation.

H_2S is a foul smelling gas with physiological activity. Several enzymes involved in the metabolism of sulphur- containing amino acids can produce it endogenously, and the predominant H_2S-producing enzymes in mammals are Cystathionine Beta Synthase (CBS) and Cystathionine Gamma Lyase (CSE). H_2S can be donated by sulphur salts, such as NaSH or Na_2S, which are fast releasing donors; or GYY4137 (Li et al., 2008b), which releases H_2S more slowly.

The physiological roles of H_2S are wide ranging and have only recently been elucidated. H_2S is purported to cause vasodilation (Zhao and Wang, 2002), inflammation (Bhatia et al., 2005b), and affect nociception (Distrutti et al., 2006). H_2S is reported to activate several cation channels: K_{ATP} (Zhao and Wang, 2002), L-type calcium channels (Sun et al., 2008), BK_{Ca} (Telezhkin et al., 2010), and, most relevant to this thesis, the TRPA1 receptor (Streng et al., 2008).

H_2S can suspend animation in some mammalian species (Blackstone et al., 2005; Volpato et al., 2008; Aslami et al., 2010; Seitz et al., 2012), but not others (Li et al., 2008a). This is not the same mechanism as general anaesthesia (Li et al., 2012). In studies by Roth and colleagues, mice were exposed to 80 ppm inhaled H_2S. This lowered their oxygen consumption and carbon dioxide output and lasted for over 6 hours – during this time their metabolic rate also reduced by approximately 90%. Crucially for this chapter, this drop in metabolic rate was accompanied by a reduction in core body temperature to approximately 2°C above room temperature (Blackstone et al., 2005). The suggested mechanism for this response is via inhibition of Cytochrome c oxidase and subsequent reduction in respiration rate (Nicholls et al., 2013).

The action of H_2S on TRPA1 is currently being investigated, and its role in the vasculature has been emphasised with studies showing that the vasodilatory ability of H_2S donors is TRPA1-dependent (Pozsgai et al., 2012). Following on from the investigation of the role of TRPA1 in TRPV1 antagonist- induced hyperthermia in the previous chapter, this chapter will investigate whether H_2S has an effect on core body temperature. Further, the question of whether endogenous H_2S production could compensate for TRPV1 loss in TRPV1 KO mice is investigated.

6.2 Hypothesis and Aims

The aims of this chapter are to investigate if H_2S has a role in TRPV1 antagonist – induced hyperthermia or a compensatory role in TRPV1 KO mice. We hypothesise that H_2S, which activates TRPA1 amongst other channels, compensates for the loss of TRPV1 in KO mice via TRPA1.

The links between H_2S and TRPV1 antagonist-induced hyperthermia will be investigated. Both protein and RNA studies will be used to determine if the H_2S producing enzymes CSH and CBS are upregulated in the skin of TRPV1 KO mice. If H_2S has a compensatory role in TRPV1 KO mice, we expect to see upregulation of one or both of these enzymes increasing H_2S production endogenously, in turn causing vasodilation which facilitates heat loss, resulting in a normal body temperature.

Functional studies will be conducted, to determine the effects of H_2S donation *in vivo*. The effects of H_2S donors on core body temperature and blood flow will be determined, in naïve mice. Subsequently, the effects of administration with an H_2S donor on mice treated with JNJ17203212 will be investigated to determine if H_2S can attenuate TRPV1 antagonist-induced hyperthermia. It is hypothesised that application of H_2S donors in blood flow studies will result in vasodilation. The vasodilatory activity of H_2S donors may inhibit TRPV1 antagonist-induced hyperthermia via heat loss facilitated by vasodilation.

6.3 Results

6.3.1 Investigation of H_2S producing enzymes in TRPV1 WT and KO mice

In order to determine any interplay of H_2S and TRPV1 in skin (a major thermoregulatory organ), the RNA and protein levels of CBS and CSE were determined in the dorsal skin, liver and whole brain of male TRPV1 WT and KO littermates. The liver was chosen as a positive control for both enzymes, and the whole brain to determine differences, if any, in CBS expression in TRPV1 WT and KO mice.

The highest expression of RNA of both enzymes was in the liver tissues (Figure 6.1). For CBS there was ten times more CBS RNA expression found in liver than in the brain and relatively negligible expression of this H_2S producing enzyme in the dorsal skin. There was relatively little expression of CSE RNA in brain and dorsal skin tissues compared to liver, and no difference was seen between genotypes.

The levels of CBS and CSE protein expression were investigated in the same tissues of TRPV1 WT and KO mice (n=6). Statistical analysis as outlined in section 2.7.3 showed that there was no significant difference in expression of CSE protein between TRPV1 WT and KO mice, albeit a trend towards an increase in expression was seen in KO mice (Figure 6.2). In terms of CBS expression, there was very little CBS protein expressed in the whole brain with no significant difference between genotypes. However in both the liver and dorsal skin, there was a significant increase in CBS protein expression in KO mice compared to WT ($P<0.01$ and $P<0.05$, respectively).

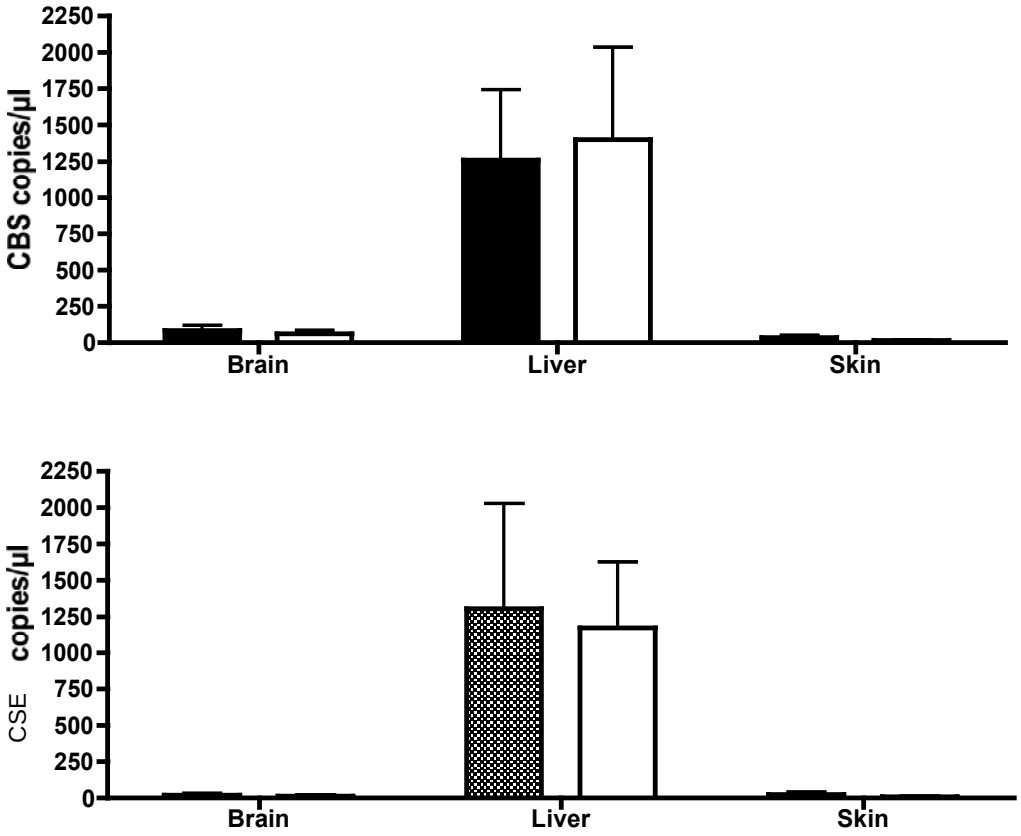

Figure 6.1 RNA expression analysis of Cystathionine Beta Synthase (CBS) and Cystathionine Gamma Lyase (CSE) by qRT-PCR in naive TRPV1 WT and KO mice. Results are mean ± s.e.m. n= 5-6. CBS and CSE were analysed in skin, liver and brain samples. Results were tested by unpaired Student's t test.

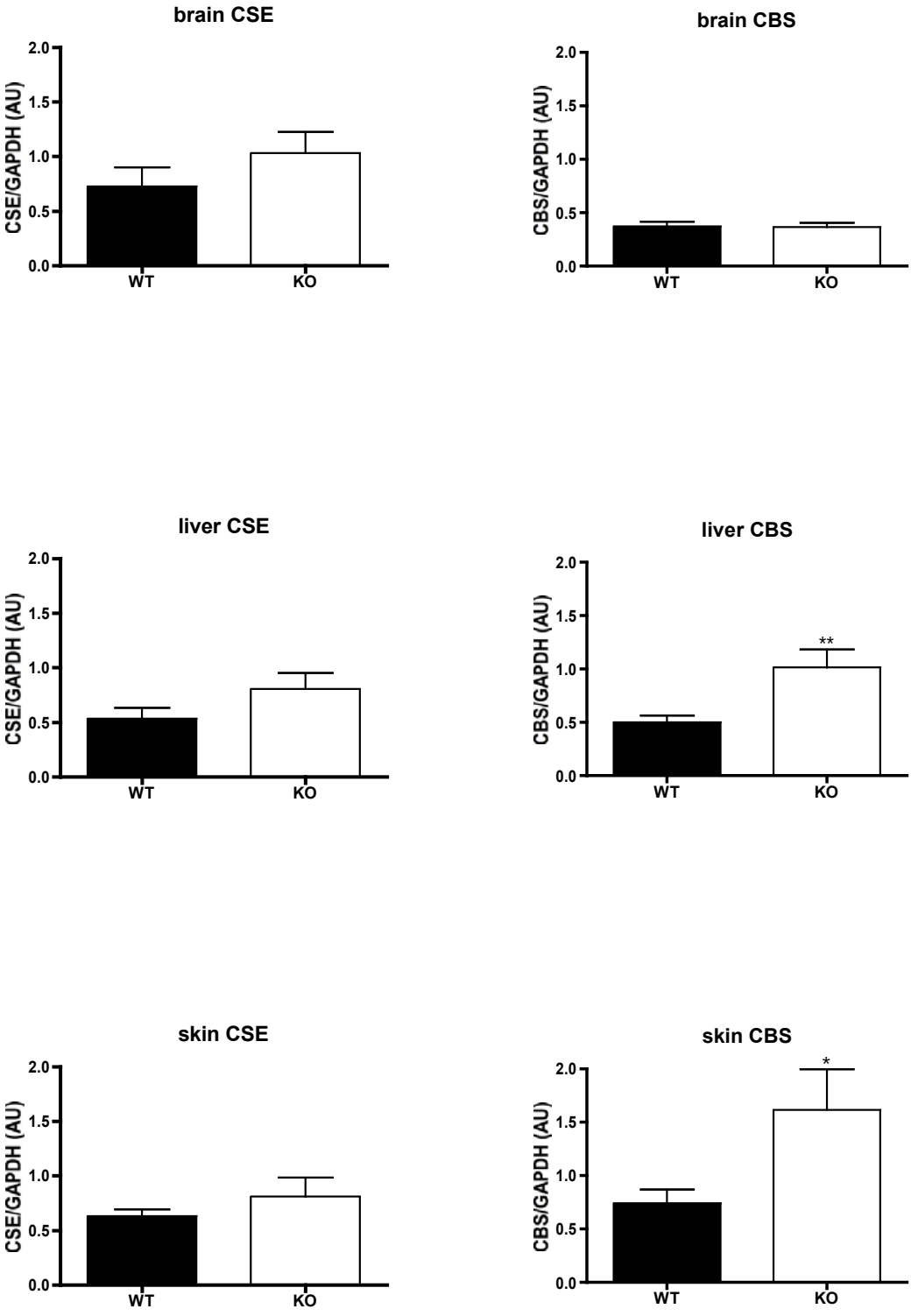

Figure 6.2 Protein expression analysis of Cystathionine Beta Synthase (CBS) and Cystathionine Gamma Lyase (CSE) by Western blot in naive TRPV1 WT and KO mice. Results are mean ± s.e.m. n= 5-6 CBS and CSE were analysed in skin, liver and brain samples and normalised to loading control (GAPDH), expressed as arbitrary densitometry units. *p<0.05, **p<0.01 TRPV1 WT vs. TRPV1 KO mice, as determined by unpaired Student's t test.

6.3.2 The effect of manipulating H_2S levels on core body temperature of naïve CD1 mice

The effects of the H_2S generating compounds NaSH (Figure 6.3) and GYY4137 (Figure 6.4), and the CSE inhibitor D,L-propargylglycine (PAG, Figure 6.5) on the core body temperature and activity of male CD1 mice were investigated using radiotelemetry. PAG was used rather than aminooxyacetic acid or another CBS inhibitor due to the poor selectivity profile of CBS inhibitors. Mice were carefully observed during PAG administration for toxic effects.

After one hour of baseline measurement, mice were administered 5.6mg/kg NaSH, 50 mg/kg GYY4137 or 11mg/kg PAG via intraperitoneal injection (n=5), and core body temperature and activity measurements were taken over 22 hours. Administration of 5.6mg/kg NaSH (Figure 6.3) had no effect on core body temperature or activity levels of the mice. No significant difference was found between antagonist- and vehicle- treated mice. Animals administered 50 mg/kg GYY4137 (Figure 6.4) did not have significantly different core body temperature or activity levels compared to their vehicle-treated counterparts.

Animals administered 11 mg/kg PAG did not have significantly different core body temperature or activity levels compared to their vehicle-treated counterparts (Figure 6.5). However, PAG-treated mice displayed a transient reduction in body temperature of approximately 0.5°C compared to vehicle at two hours post-injection. There was a normal diurnal variation in temperature and activity levels.

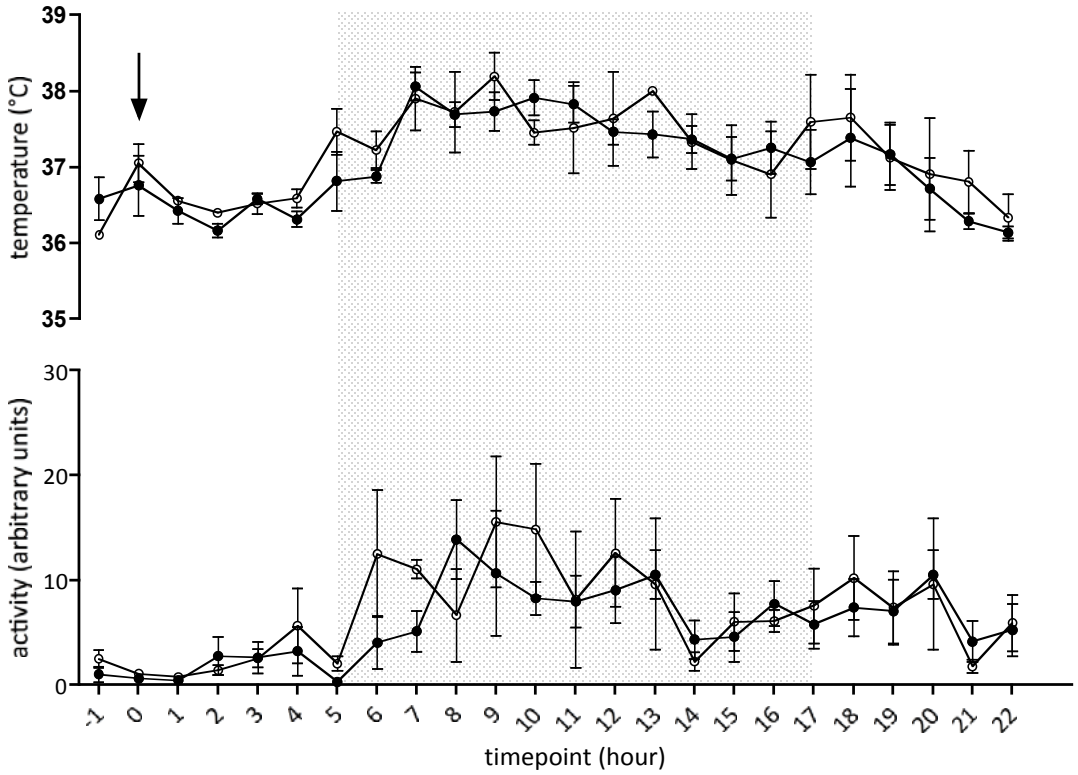

Figure 6.3 Administration of 5.6 mg/kg NaSH i.p. (•) in telemetered male CD1 mice (n=4). Mice were treated after a one-hour baseline period. There was no significant difference between the body temperature of mice treated with 5.6 mg/kg NaSH or vehicle (saline, **o**) and a normal diurnal variation in temperature and activity was seen. Shaded area indicates dark cycle.

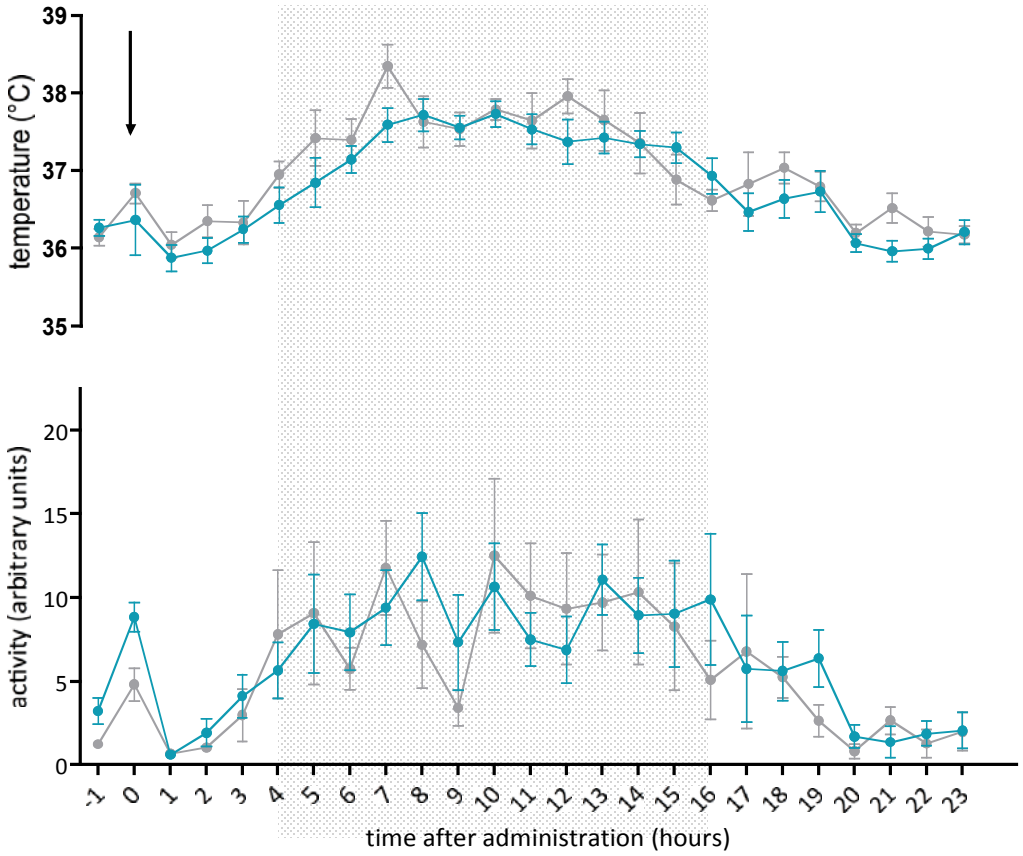

Figure 6.4 Administration of 50 mg/kg GYY4137 in telemetered male CD1 mice (n=7). Mice were administered GYY4137 intraperitoneally after a one hour baseline period. There was no significant difference between the body temperature of mice treated with GYY4137 (•) compared to vehicle (saline, •). There was a normal diurnal variation in temperature and activity levels. Shaded area indicated dark cycle.

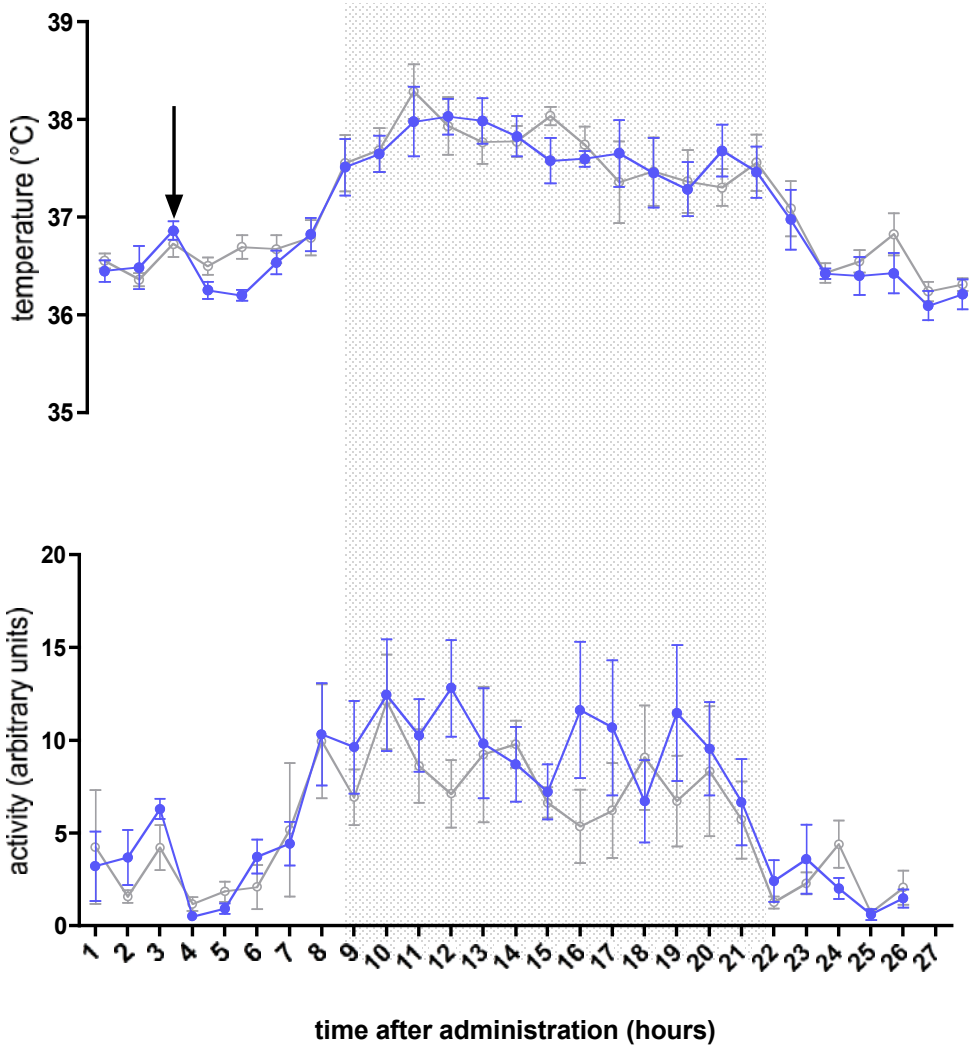

Figure 6.5 The effect of i.p. administration of 11 mg/kg D,L-propargylglycine (PAG) in telemetered male CD1 mice (n=7). After a one hour baseline period, mice were injected with vehicle or saline. There was no significant difference between the body temperature of mice treated with PAG (•) or vehicle (saline, •). Shaded area indicates dark cycle.

6.3.3 The effects of H_2S donors on blood flow

In order to investigate the effects of H_2S donors on blood flow, naïve male CD1 mice were anaesthetised using 75 mg/kg ketamine and 1 mg/kg medetomidine administered in saline and kept on a heated mat to ensure stable core body temperature. The knee joint of the mouse was dissected to expose the synovial membrane and baseline blood flow was measured. After ten minutes of baseline recording, NaSH (100 µM or 300 µM; 10 µl) or GYY4137 (30 µM, 100 µM or 300 µM; 10 µl) was applied to one knee joint and vehicle (50% ethanol, 10µl) to the other. Due to its potent ability to cause vasodilation via donation of NO, Sodium Nitroprusside (SNP) was also applied to the exposed synovial membrane of a separate cohort of mice as a positive control (100 nM, 10 µM or 100 µM; 10 µl).

Application of 100 µM SNP (Figure 6.6a) resulted in an increased flux consistent with a significant increase in blood flow compared to the contralateral, vehicle-treated synovial membrane (maximum SNP response 154.474 ± 8.901% vs max veh response 113.77 ± 6.347%; $P<0.05$). Lower concentrations of SNP did not significantly alter flux compared to vehicle treated knees (Figure 6.6a).

Application of both 100 µM and 300 µM NaSH to the exposed synovial membrane (Figure 6.6b) did not have a significant effect on flux and therefore blood flow compared to vehicle.

The response to 100 µM GYY4137 to the exposed synovial membrane (Figure 6.6c) was not significantly different from vehicle, however 300 µM GYY4137 resulted in a significant decrease in flux compared to baseline ($P<0.05$).

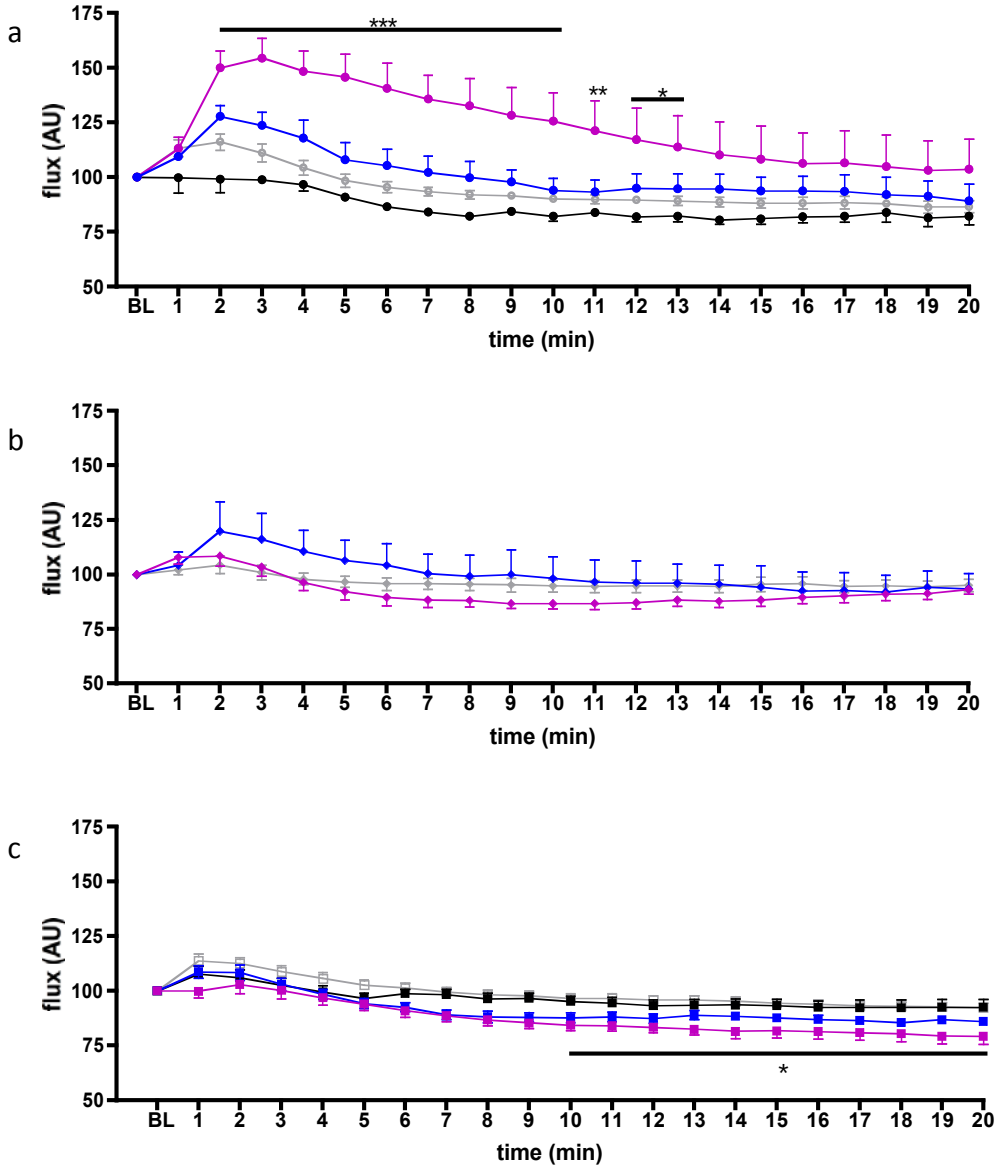

Figure 6.6 Application of (a) Sodium Nitroprusside, (b) Sodium Hydrosulfide, and (c) GYY4137, to the exposed synovial membrane of anaesthetised male CD1 mice (n=7) had variable effects on blood flow in the area. Whilst application of SNP resulted in an increase in blood flow (indicative of vasodilation), there was no effect of the sulfide donor or salt. *P<0.05, **P<0.01, ***P<0.005 with respect to vehicle (as deemed by RMANOVA and Bonferroni *post hoc* test.

○ = vehicle ● = 100 nM Sodium Nitroprusside (SNP) ● = 10 µM SNP ● = 100 µM SNP

◆ = vehicle ◆ = 100 µM NaSH ◆ =300 µM NaSH

□= vehicle ■ = 30 µM GYY4137, ■ =100 µM GYY4137 ■ =300 µM GYY4137

6.3.4 The effect of H_2S on plasma extravasation

The effects of the same H_2S donors and the H_2S precursor L-cysteine on a different microvascular bed were investigated via measurement of dorsal skin plasma extravasation (section 2.6). Both male and female mice were used in these studies (n=6). Mice were anaesthetised using 75 mg/kg ketamine and 1mg/kg medetomidine administered in saline, and once reflexes were absent, injected with Evans Blue dye (EB) intravenously. Thirty minutes after EB administration, SP, vehicle or SP and co-injection solution (Figure 6.8, see x axis) were administered i.d. and then 8mm diameter circles of skin at injection sites were excised after 30 minutes. The volume of each site and the amount of EB in each tissue sample was calculated as detailed in sections 2.6.1 and 2.6.2, respectively. Before testing responses to co-injection with Substance P, an inflammatory mediator known to cause plasma extravasation, each compound was tested alone. NaSH, GYY4137, Substance P and CGRP injection sites had significantly higher volumes than uninjected sites, but L-cysteine did not result in a significantly increase volume (Figure 6.7). SP co-injected with CGRP or 100 mM NaSH resulted in a significantly increased amount of EB per mg tissue in the injection site ($P<0.01$). The volume graph (Figure 6.8, bottom panel) shows that the volume of each site was variable and this did not correlate with actual amount of EB present in the tissue (Figure 6.8, top panel). The volume measurement showed the gross size of the tissue (it is expected that plasma extravasation increases tissue swelling), whereas EB binds albumin and therefore is a measure of albumin content of the tissue.

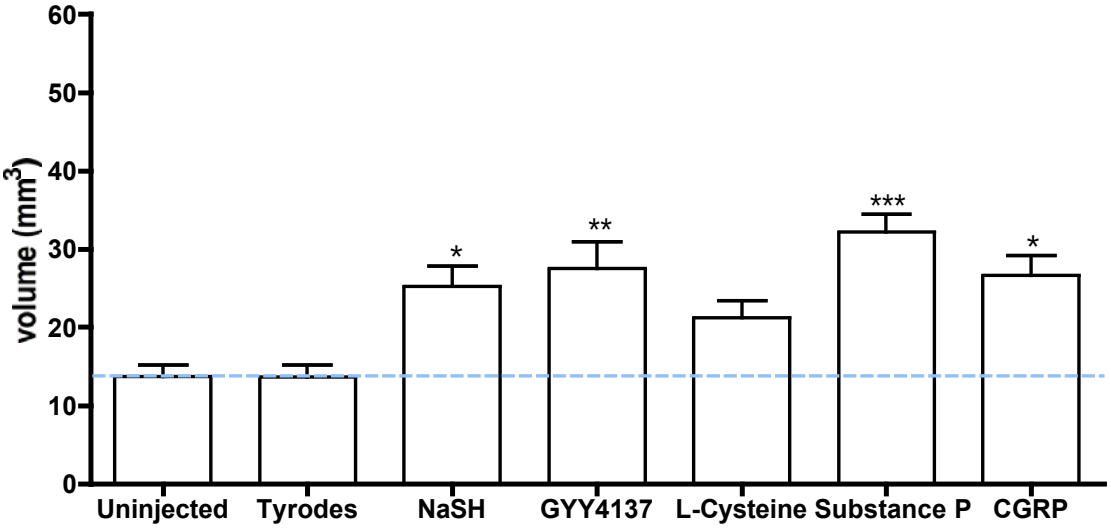

Figure 6.7 The effects of H_2S on plasma extravasation in the dorsal skin of male and female CD1 mice (n=6). 30 minutes after i.v. injection of Evans Blue dye (EB), compounds (see x axis) were administered i.d. and excised after 30 minutes. EB dye accumulation is not shown here as i.v. injection in this study were insufficient. Volume of each injection site 90 minutes after injection (mm^3) is shown.

*P<0.05, **P<0.01 ***P<0.001 with respect to uninjected dorsal skin sites, by one way ANOVA.

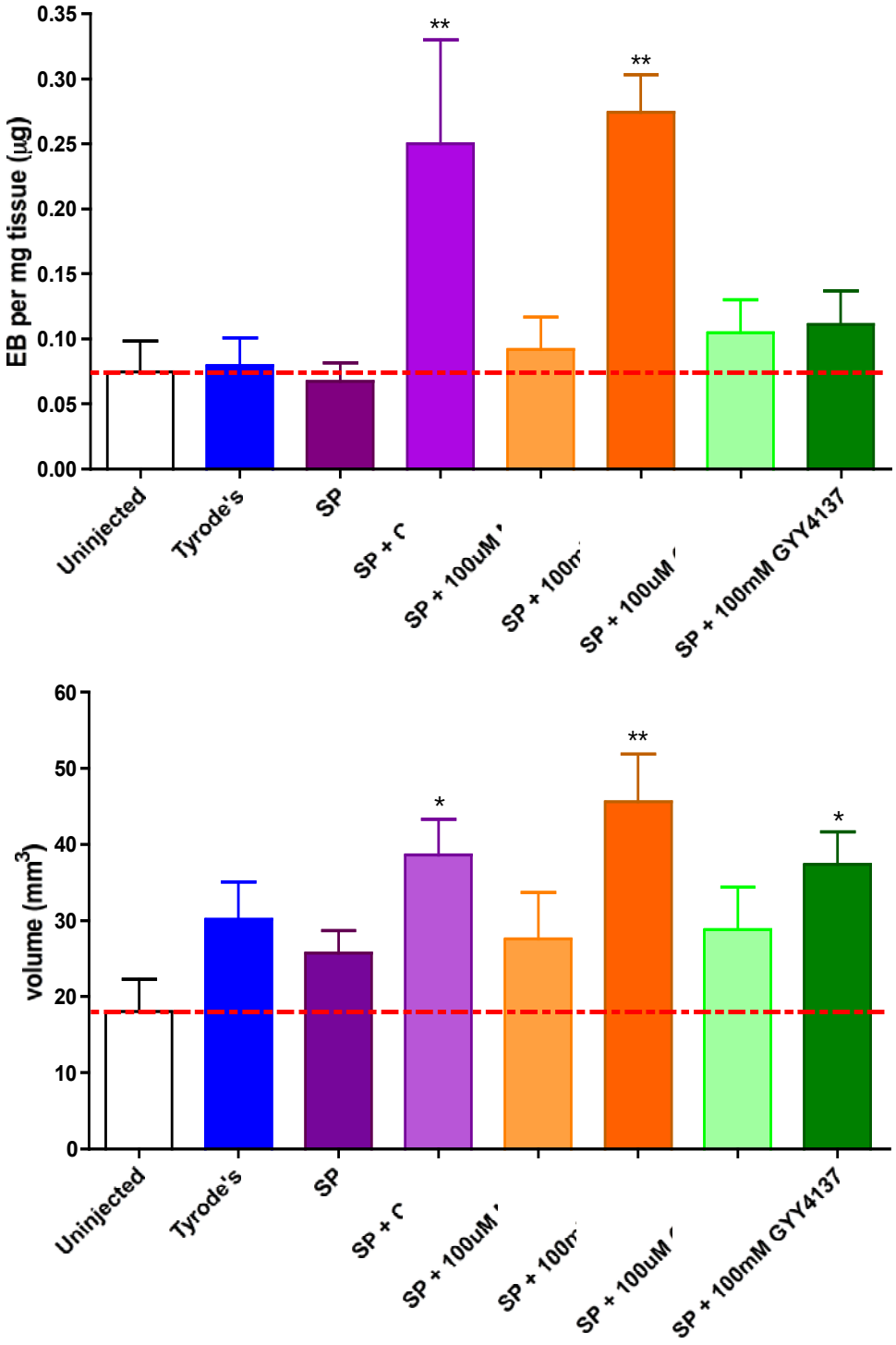

Figure 6.8 The effect of NaSH and GYY4137 on Substance P (SP)-mediated plasma extravasation in the dorsal skin of male and female CD1 mice (n=6).

Top: amount of Evans Blue dye per mg of tissue (mg) for each injection site; Bottom: volume of each injection site 90 minutes after injection (mm^3). *P<0.05, **P<0.01 with respect to uninjected dorsal skin sites. (as tested by ANOVA and Bonferroni *post hoc* test).

6.3.5 The effect of TRPV1 deletion on H_2S - induced plasma extravasation

Figure 6.8 showed that administering NaSH with SP has a similar effect to CGRP administered with SP on the amount of EB accumulated in the dorsal skin. In order to determine the role, if any, of TRPV1 in this plasma extravasation, 100 mM NaSH and 100 mM GYY4137 were used in conjunction with SP in TRPV1 WT and KO mice (Figure 6.9).

The volume of each injection site was calculated (Figure 6.9, bottom panel); all treatments had a significantly higher volume than vehicle –treated and uninjected sites. Measurements of Evans blue accumulation, however, show that only KO mice treated with NaSH and both genotypes treated with L-Cysteine accumulated a significantly higher amount of EB than the uninjected sites (Figure 6.9, top panel).

The volume and EB accumulation in the injection site of substance P (SP) and CGRP coadministration was not significantly different between genotypes. In contrast, co-administration of SP+GYY4137 resulted in a significant difference between KO and WT skin volumes ($P<0.05$, Figure 6.9 bottom panel).

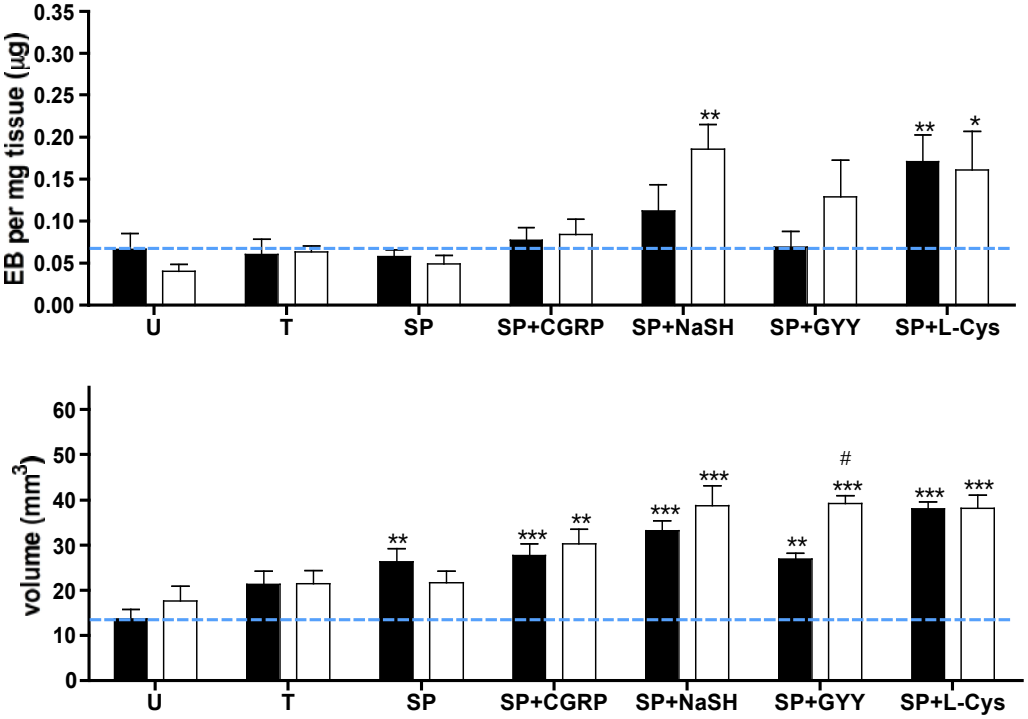

Figure 6.9 The effect of TRPV1 deletion on i.d. Substance P and H_2S donor coadministration in the dorsal skin of female mice (n=6). TRPV1 wild type (black bars); TRPV1 knock out (white bars).

Top: EB per mg of tissue was measured; bottom: volume of each injection site (mm^3).

Treatments: U=Uninjected; T=Tyrodes; SP=Substance P; SP+CGRP= Substance P and CGRP; SP+NaSH= Substance P and 100 mM Sodium Hydrosulfide; SP+GYY= Substance P + 100 mM GYY4137; SP+L-CYS= Substance P and 100 mM L-cysteine.

*P<0.05, **P<0.01, ***P<0.005 with respect to uninjected site of respective genotype

#P<0.05 with respect to WT, as determined by ANOVA.

6.3.6 The effects of blocking endogenous H_2S production on L-cysteine donor – induced plasma extravasation

TRPV1 WT female mice were pre-treated with the CSE inhibitor PAG an hour before i.d. injections with Substance P, CGRP and L-cysteine (Figure 6.10).

PAG had no significant effect on the amount of EB in each injection site. PAG significantly reduced the volume of sites injected with SP+CGRP. All other excised sites of PAG-pre-treated mice had a decreased volume compared to vehicle.

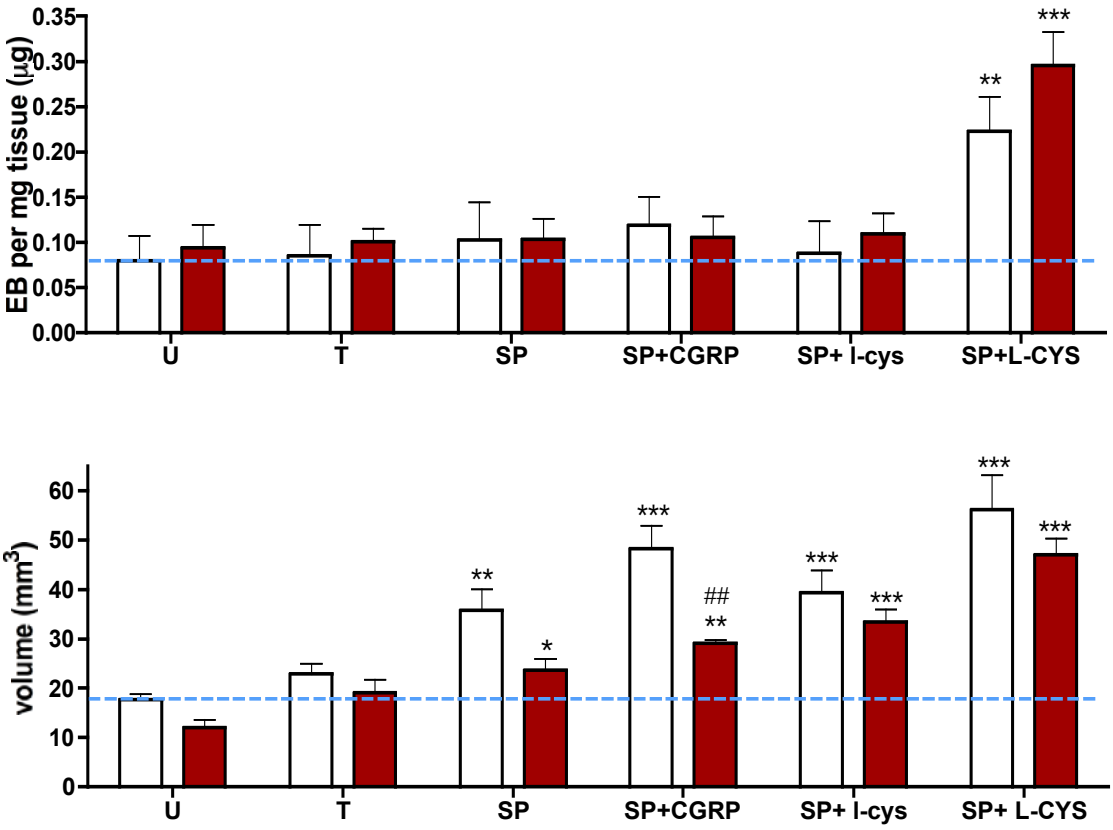

Figure 6.10 The effects of D,L-Propargylglycine (PAG) on i.d. Substance P and H_2S donor L-cysteine coadministration in the dorsal skin of female TRPV1 wild type mice (n=4). PAG (red bar); saline vehicle (white bar). Top: EB per mg of tissue was measured; bottom: volume of each injection site (mm^3).

Treatments: U=Uninjected; T=Tyrodes; SP=Substance P; SP+CGRP= Substance P and CGRP; SP+l-cys= Substance P and 100µM L-cysteine; SP+L-CYS= Substance P and 100 mM L-cysteine.

*P<0.05, **P<0.01, ***P<0.005 with respect to uninjected site of respective genotype as determined by ANOVA

6.3.7 The effect of GYY4137 on JNJ17203212-induced hyperthermia

The effect of H_2S on JNJ17203212-induced hyperthermia was investigated using the slow-release donor GYY4137. As seen in Figure 6.4, GYY4137 administered alone to naïve mice has no effect on core body temperature, when compared to vehicle-treated mice.

Male CD1 mice were implanted with temperature telemetry probes and recovered for one week. After a baseline recording of one hour, 50 mg/kg GYY4137 was administered intraperitoneally. Thirty minutes later, 30 mg/kg JNJ17203212 was administered intraperitoneally and the mice monitored for a further six hours.

After the first injection of 50 mg/kg GYY4137 or vehicle, there was a small increase in body temperature, consistent with a stress response. The second injection, of 30 mg/kg JNJ17203212 resulted in a further increase in body temperature, significantly different from vehicle treated mice. JNJ17203212 treated mice that were pre-treated with GYY4137 had a significantly delayed and reduced hyperthermic response (37.33 ± 0.56°C vs. 38.47 ± 0.23°C).

To determine whether the reduction in hyperthermia was due to H_2S release by GYY4137, mice were pre-treated with a decomposed analogue of GYY4137 without the H_2S-releasing moiety – dGYY4137 – before treatment with JNJ17203212 (Figure 6.12). Mice pre-treated with dGYY4137 displayed a similar reduced, delayed hyperthermia as those pre-treated with GYY4137 (n=4). There was no significant difference between dGYY4137 and GYY4137 pre-treated mice.

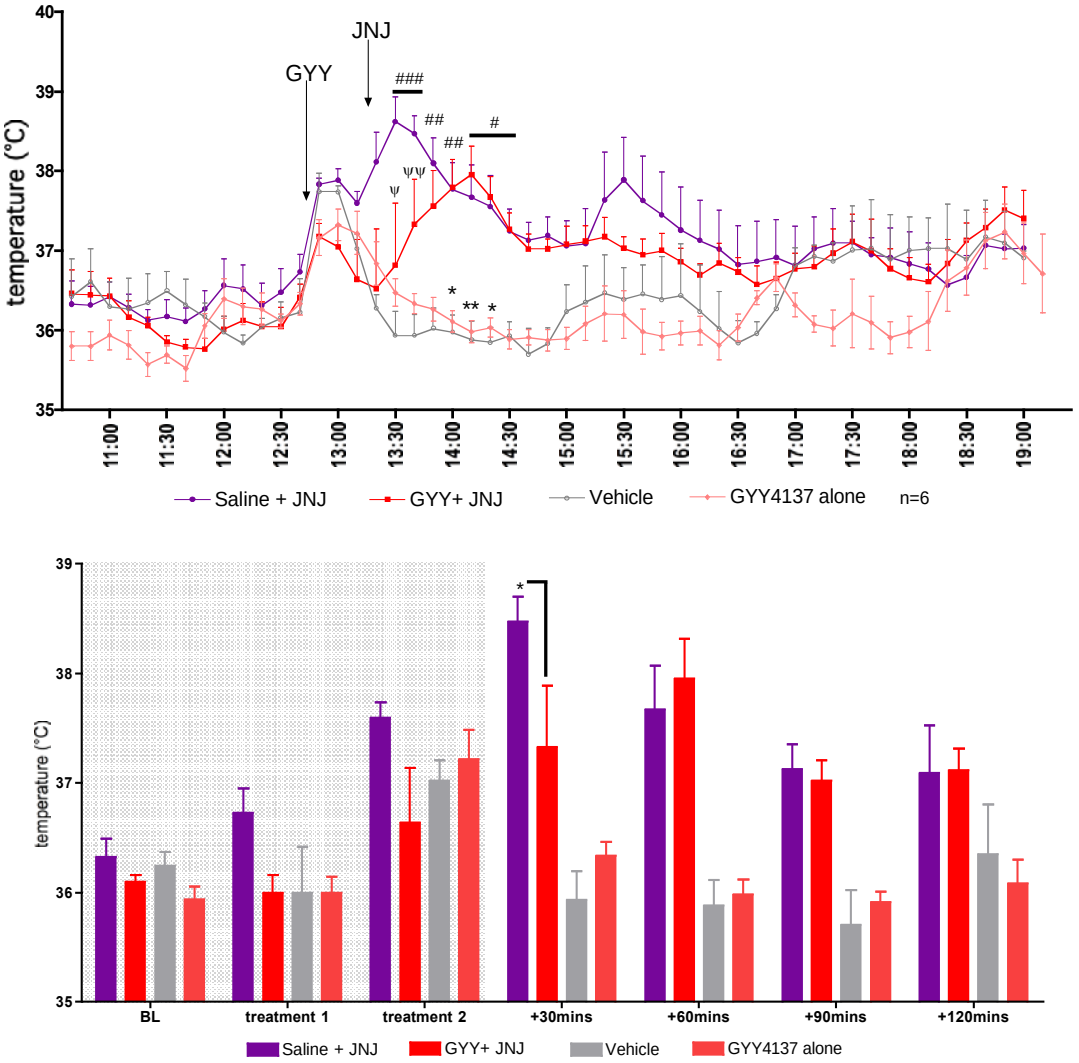

Figure 6.11 Top: the effect of pre-treatment with GYY4137 on JNJ17203212-mediated hyperthermia in male CD1 mice (n=6) over an acute period of seven hours post treatment. Telemetered mice were treated with 50 mg/kg GYY4137 or saline vehicle after a one-hour baseline recording. Thirty minutes later, mice were treated with 30 mg/kg JNJ17203212 or vehicle. Bottom: means at specific timepoints in treatment schedule (BL=Baseline, +*n* minutes = time after treatment 2). Shaded area is time before JNJ17203212 treatment.

*P<0.05, **P<0.01 vehicle vs GYY4137+JNJ17203212

#P<0.05, ##P<0.01 ###P<0.001 vehicle vs Saline+JNJ17203212

ΨP<0.05, ΨΨP<0.01 GYY4137+JNJ17203212 vs Saline+JNJ17203212

Tests: RM ANOVA followed by Bonferroni *post hoc* test.

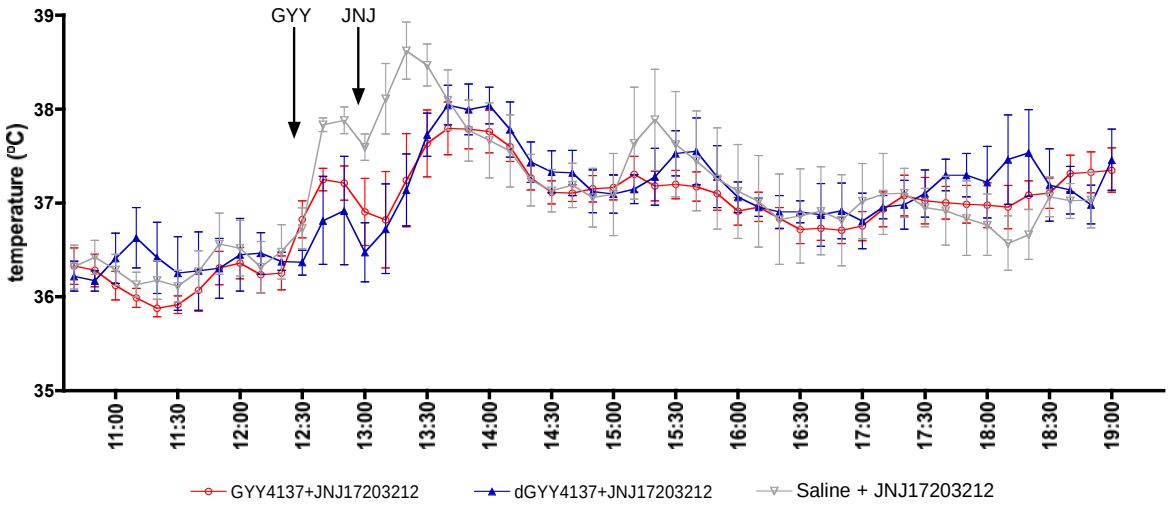

Figure 6.12 Pre-treatment with 50 mg/kg decomposed GYY4137 (dGYY4137) reduces JNJ17203212-induced hyperthermia in male CD1 mice (n=4). dGYY4137, i.e. GYY4137 with a reduced ability to release H_2S, reduced JNJ17203212-induced hyperthermia to a similar extent as GYY4137.

GYY = administration of 50 mg/kg GYY4137; JNJ= administration of 30 mg/kg JNJ17203212.

6.4 Discussion

6.4.1 Key findings

- Whilst expression of CSE protein did not differ between TRPV1 WT and KO mice, the expression of CBS protein was significantly higher in the liver and skin of KO mice
- Modifying levels of H_2S *in vivo* had no effect on the core body temperature of naïve CD1 mice
- H_2S generating compounds had a reduced effect on blood flow in the synovial membrane compared to a NO donor
- High doses of H_2S generating compounds and an H_2S precursor increased plasma extravasation in the skin of naïve CD1 mice to a greater extent than CGRP
- Administration of GYY4137 in TRPV1 KO mice resulted in significantly increased plasma extravasation than WT mice
- JNJ17203212 treated mice that were pre-treated with GYY4137 had a delayed and reduced hyperthermic response. This response was also seen with dGYY4137.

In this chapter the role of H_2S in JNJ17203212-induced hyperthermia was investigated. Protein biochemistry and PCR studies were conducted to determine levels of endogenous H_2S producing enzymes in TRPV1 WT and KO mice. Temperature telemetry experiments were conducted to determine the effect of H_2S donors and D,L-Propargylglycine (PAG) on the core body temperature of naïve CD1 mice. The effects of H_2S donors were investigated in studies of blood flow using the FLPI apparatus and studies of plasma extravasation using skin assay in CD1 mice. The effects of H_2S donors on plasma extravasation were also determined using TRPV1 WT and KO mice. Finally the effects of GYY4137 on JNJ17203212-induced hyperthermia were investigated using temperature telemetry experiments.

6.4.2 Investigation of H_2S producing enzymes in TRPV1 WT and KO mice

Expression of RNA and protein of the H_2S producing enzymes CBS and CSE was investigated in the skin of TRPV1 WT and KO mice. This was to determine whether knocking out TRPV1 would result in increased expression of these enzymes and subsequent upregulation of H_2S production to compensate for loss of

TRPV1. No significant difference in expression of H_2S producing enzyme mRNA levels was seen between genotypes. Further, the levels of CBS and CSE RNA expressed in these tissues was very low in brain and skin, with fewer than 100 copies/µl. Protein biochemistry studies of enzyme levels were expressed as a ratio of GAPDH expression, rather than actin or tubulin. This is due to our observations that cytoskeletal protein expression is significantly different between TRPV1 WT and KO mice (unpublished observations, Keeble lab), therefore actin expression would differ between genotype. Studies of CSE levels confirmed that there was no significant difference in expression between genotypes. In contrast, levels of CBS protein were significantly higher in the skin and liver of TRPV1 KO mice than WT. Xu and colleagues have shown that TRPV1 (and P2X3) is co-localised with CBS in neuronal tissues (Xu et al., 2009). CBS has many physiological roles (Wang, 2002), however colocalisation suggests that an interplay between these two proteins is feasible (Xu et al., 2009). In this thesis, tissue levels were determined using whole tissue homogenates as a crude measure; therefore particularly high levels of expression of each enzyme were not expected, particularly in RNA studies. For further, more detailed analysis the tissues can be examined in immunohistochemical imaging studies (as has been shown by Telezhkin et al., 2010; Qu et al., 2013 and others) – this will also have the added benefit of determining localisation of expression.

6.4.3 The effects of H_2S donors on blood flow and plasma extravasation

In the present studies both fast- and slow-release H_2S donors were used in the exposed synovial membrane. This was to determine the activity of H_2S in a tissue bed known to functionally express non-neuronal TRPV1. GYY4137 and NaSH had little effects on blood flow in the knee synovial membrane, particularly when compared with the activity of SNP, the NO donor, which is a potent vasodilator. Conversely, in studies of plasma extravasation, these compounds used in conjunction with Substance P increased plasma extravasation to a comparable extent as Substance P with CGRP (another potent vasodilator). Previous studies have shown the vasodilatory potential of H_2S. From the first study characterising the effects of GYY4137, it has been noted that *in vitro* assays show fair vasodilatory potential of GYY4137, however *in vivo* experiments have largely been limited to its effects in pathophysiology, or on artificially evoked tone (Li et al., 2008b; Chitnis et al., 2013). NaSH, on the other hand, is the most commonly used simple sulfide salt, to investigate the vasodilatory effects of exogenous H_2S. Studies have shown that the response to 'exogenous H_2S' is due to activation of various ion channels (Hosoki et al., 1997; Zhao and Wang, 2002; Cheng et al., 2004; Tang et al., 2005; Sun et al., 2008; Pozsgai

et al., 2012). In their studies, White and colleagues showed that the vasodilatory response to NaSH could not be repeated more than once in the same vessel, since it was mediated by the release of neurotransmitters in a similar way to capsaicin (White et al., 2013).

Further studies use the skin assay technique in TRPV1 WT and KO mice to show the effects of these potential vasodilators on plasma extravasation. Substance P is an inflammatory neuropeptide, which, when released, results in plasma extravasation (Harrison and Geppetti, 2001). It is often co-released with CGRP, a potent vasodilator (Brain et al., 1985), thereby enhancing plasma extravasation at the injury site. We used this experimental model to determine the effects of H_2S as a vasodilator in a model of inflammation. We measured plasma extravasation as both volume of each site and also Evans Blue dye (EB) accumulation –the latter being a measure of albumin accumulation. At high doses (100 mM), both donors significantly increased the volume of injection sites with respect to the uninjected site, and to a similar extent as CGRP. In the EB accumulation study, only 100 mM GYY4137 or NaSH had the potential to increase plasma extravasation to a similar extent to CGRP. When the TRPV1 channel was knocked out, there was a greater EB accumulation in response to 100 mM NaSH compared to WT mice. More importantly, considering the H_2S-producing enzyme studies at the beginning of this chapter, there was no significant difference between the ability of L-Cysteine to cause EB accumulation in KO and WT mice. L-cysteine was used in this study as a precursor for H_2S. When comparing the volumes of injected sites in TRPV1 WT and KO mice, only 100 mM GYY4137 resulted in difference between treatment groups, with KO injection sites having a larger volume than WT. EB accumulation does not correlate with the volume of each injection site. Evans Blue accumulation is not the only method of measuring plasma extravasation – it is possible to determine extravasation using radioactivity accumulation studies with I^{125} (Grant et al., 2005), which measures albumin levels. Using the mathematical equation for volume calculations alone has been shown to be effective as a rudimentary measure of plasma extravasation in studies by other groups (Kodji et al., 2013). However, we show here that this is not indicative of extravasation of albumin. As radiolabelled studies have been shown to be a finer measure of plasma extravasation than EB accumulation, further studies with radiolabelled album may be able to determine the true effects of these H_2S modulators in a more reliable manner.

Finally, studies to investigate the effect of the CSE inhibitor PAG on L-Cysteine-induced plasma extravasation were conducted. In terms of EB accumulation, only mice injected with L-Cysteine had a significantly elevated EB accumulation compared to baseline. This was surprising; the control of Substance P + CGRP showed no increase compared to baseline, at least in terms of EB accumulation. On the other hand, injection of Substance P + CGRP produced the anticipated increase in volume in vehicle pre-treated mice, as did Substance P + L Cysteine at both 100 mM and 100 µM concentrations. PAG pre-treated mice had a significantly reduced volume of Substance P + CGRP injection site, with respect to vehicle pre-treated mice (see Figure 6.10). L-cysteine injection sites were not significantly different between treatment groups, however PAG pre-treated mice showed a trend towards a lower volume. PAG is of course a non-specific compound, as its effects on CSE can have an impact on a variety of cellular processes including the transsulfuration pathway (Griffith, 1987) and glutathione synthesis (Lertratanangkoon et al., 1999) and not simply H_2S production.

6.4.4 The effect of manipulating H_2S levels on core body temperature

H_2S donors had no effect on the core body temperature of naïve CD1 mice, compared to vehicle treated mice. The fast release donor NaSH (5.6 mg/kg) and slow release donor GYY4137 (50 mg/kg) were used in doses seen to be pharmacologically active in vascular studies (Li et al., 2008b). The rationale behind this was to use a relevant dose rather than determine a dose response relationship. Both donors did not significantly affect core body temperature compared to vehicle-treated animals, however there was a trend towards a slightly lowered core body temperature in GYY4137-treated naïve mice.

Inhaled H_2S is known to cause suspended animation, which includes a drop in core body temperature (Blackstone et al., 2005; Volpato et al., 2008). Previously, the effects of H_2S donors on core body temperature have only been indirectly studied by Aslami and colleagues, who showed that infusion of NaSH (36 µmol/kg/h) in intubated rats caused a dose dependent reduction in core body temperature (Aslami et al., 2010). Our group has continued to investigate the effects of H_2S donors on core body temperature and have evidence that GYY4137 and NaS, when administered i.c.v. via an implanted cannula, cause a profound drop in core body temperature. Peripheral administration, as in these studies, showed no effect on core body temperature (Wilson et al., 2014). These studies, together with the studies

in this chapter suggest that H_2S donors can have an effect on core body temperature, but this effect is centrally mediated.

However, administration of the CSE inhibitor, PAG (11 mg/kg), resulted in a drop in core body temperature of approximately 0.5°C. Statistical testing showed that this was not a significant difference. As PAG is an inhibitor of CSE (Stipanuk and Beck, 1982), its effects are not limited to inhibition of H_2S synthesis (Wang, 2002). As it has been noted that PAG can be nephrotoxic, as the D-enantiomer can produce a nephrotoxic metabolite (Konno et al., 2000), all mice were closely monitored and did not show any signs of decline in health. The results in this chapter together with more recent research from our group show that whilst providing exogenous H_2S causes a decrease in core body temperature, so does blocking endogenous H_2S production.

6.4.5 The effect of GYY4137 on JNJ17203212-induced hyperthermia

In the study of the effect of GYY4137 on TRPV1 antagonist-induced hyperthermia, the donor was administered 30 minutes before i.p. injection of JNJ17203212 in CD1 mice. Whilst administration of GYY4137 alone in naïve CD1 mice had no effect on core body temperature at the dose used, administration before JNJ17203212 resulted in a significant reduction in core body temperature with respect to saline pre-treated mice also treated with JNJ17203212. The duration of this reduction was short – by 60 minutes after treatment with JNJ17203212 there was no significant difference between the two groups. Thus, there was a rightward shift of the hyperthermic response when mice were administered GYY4137. This was, however, also seen with the decomposed GYY4137 – a version of GYY4137 that is no longer able to release H_2S, or releases a negligible amount. This suggests that either H_2S is not the cause of attenuation of TRPV1 antagonist-induced hyperthermia, or that the dGYY4137 did, in fact, release some H_2S.

H_2S has recently been characterised as a TRPA1 agonist, with proposed roles in vasodilation (Zhao and Wang, 2002; Pozsgai et al., 2012), inflammation (Bhatia et al., 2005b), and nociception (Distrutti et al., 2006; Andersson et al., 2012). The ability of H_2S to induce hypothermia has been suggested to be as a result of its ability to inhibit cytochrome c oxidase (Nicholls and Kim, 1981, 1982). However, the studies in this chapter highlight other targets of H_2S may yet play a role. The ability of TRPA1 to mediate

temperature dysfunction, and the studies subsequent to experiments shown in this thesis, makes it a candidate for this role. It has been shown by Eberhardt and colleagues that TRPA1 and H_2S producing enzymes are colocalised (Eberhardt et al., 2014), so the interplay between H_2S and TRPA1 is plausible.

6.4.6 Conclusions

This chapter investigated the relationship between TRPV1 and H_2S. Levels of CBS protein were higher in TRPV1 KO mice compared to WT, whilst CSE protein was similar between genotypes. H_2S donors had no vasodilatory effect in the exposed synovial membrane of the knee, however application of high concentrations GYY4137 resulted in a decrease in blood flow. In studies of plasma extravasation, high doses of both NaSH and GYY4137 potentiated plasma extravasation when coadministered with Substance P, in a similar manner to CGRP. Finally, whilst systemic administration of H_2S donors did not affect the core body temperature of naïve CD1 mice, when administered with the TRPV1 antagonist JNJ17203212, GYY4137 caused a reduction in antagonist-mediated hyperthermia, which was transient. This effect was also seen with dGYY4137, which means it may not have been due to H_2S release.

We have shown that whilst H_2S does not alter body temperature under basal conditions, it can reduce the effects of TRPV1 antagonist induced hyperthermia. These studies have not presented TRPA1 as the target for this. However, further experiments in our lab have shown that TRPA1 is critical for this effect as TRPA1 KO mice do not get H_2S-induced hypothermia (Wilson et al, 2014). This is reinforced by evidence in the literature that TRPA1 is important for the vasodilatory effects of H_2S (Zhao and Wang, 2002; Pozsgai et al., 2012; Eberhardt et al., 2014) with vasodilation being an important component of thermoregulation (Romanovsky et al., 2009). We have not proven that H_2S compensates for loss of TRPV1 to normalise body temperature, and the ability of H_2S to decrease TRPV1 antagonist-induced hyperthermia was not proven, as dGYY4137 produced the same response as GYY4137. This could however be because the dGYY4137 still releases more H_2S than anticipated. We have shown that H_2S-producing enzymes are upregulated in the skin of TRPV1 KO mice, a major thermoregulatory organ. Further, increases in plasma extravasation can be seen in TRPV1 KO mice in response to L-cysteine. Whilst H_2S has been shown to be vasodilatory via the release of inflammatory neuropeptides (Pozsgai et al., 2012), our studies show that minimal effects occur in the exposed synovial membrane – which may suggest that H_2S has no role on non neuronal TRPA1.

These studies have investigated the actions of two H_2S generating compounds in vascular models and core body temperature, with an interest in interplay with TRPV1. Whilst H_2S donors had very little effects on naïve animals, their effects are significant when used in non-naïve animals.

Chapter 7 General Discussion

7.1 Summary of Results

The studies in this thesis investigated TRPV1 antagonist-induced hyperthermia, a response that set back the development of TRPV1 antagonists as therapeutic compounds for the treatment of pain and inflammatory conditions. The mechanisms of this hyperthermic response have not been determined, however several hypotheses have been proposed. These include the theory that blockade of different modes of activation of TRPV1 affect whether a compound is hyperthermic – the proton mode of activation appears to be particularly important for the hyperthermic effect. Although the exact mechanism of hyperthermia has not been elucidated, it has brought the constitutive role of TRPV1 in the control of core body temperature to the fore. In the present studies, the TRPV1 antagonist JNJ17203212 but not SB366791 was hyperthermic, correlating with previous findings that JNJ17203212 is able to inhibit the proton mode of TRPV1 activation whilst SB366791 is not (Swanson et al., 2005; Garami et al., 2010). TRPA1 antagonism does not affect core body temperature whilst TRPV1 antagonism has varied effects, depending on the antagonist used. Hyperthermia was mediated by TRPV1 as it was abolished in TRPV1 KO mice. Whilst the TRPA1 antagonist, HC030031, had no effect on naïve animals, administration in TRPV1 KO mice resulted in a significant decrease in core body temperature. Similarly, pre-treating vehicle control mice with HC30031 resulted in a drop in core body temperature.

TRPV1 KO mice have a normal core body temperature under ambient temperature conditions, which suggests that a compensatory mechanism is in place to maintain the core body temperature in the absence of TRPV1. These studies showed that TRPA1 does not directly compensate for the loss of TRPV1 in KO mice – i.e. TRPA1 antagonism did not restore a hyperthermic profile in TRPV1 KO mice.

The effects of exogenous H_2S on TRPV1 antagonist-induced hyperthermia were determined; this is the first time that it has been shown that both GYY4137 and dGYY4137 temporarily attenuate JNJ17203212-induced hyperthermia. The effect of H_2S donors in TRPV1 KO mice was not investigated during this thesis and to our knowledge have not been investigated by other groups, instead favouring the investigation of H_2S in TRPA1 KO mice due to H_2S being an activator of TRPA1.

This thesis also shows that whilst exogenous H_2S does not cause vasodilation in the exposed synovial membrane of naïve CD1 mice to the same extent as NO, it does potentiate SP-evoked plasma extravasation in the skin assay: whilst H_2S donors had very little effects on naïve animals, their effects are significant when used in non-naïve animals.

7.2 The hyperthermic TRPV1 antagonist JNJ17203212 inhibits changes in flow in the microvasculature

JNJ17203212 is a hyperthermic TRPV1 antagonist that inhibits both neuronal and non-neuronal TRPV1 in our model of microvascular blood flow. Conversely, SB366791 – a euthermic TRPV1 antagonist does not inhibit capsaicin responses in both beds. The vasculature is a key organ in thermoregulation; the peripheral regions are important for both retention of heat in cold environments by vasoconstriction, and vasodilation to dissipate excess heat. In rodents, the majority of vascular heat loss occurs from the tail, due the fact that it has no fur and because of a high density of arteriovenous anastomoses. In rats, about 25% of basic metabolic heat is dissipated in the tail skin, therefore its importance in thermoregulation is clear (Young and Dawson, 1982). Vascular changes preceding and during TRPV1 antagonist-induced hyperthermia have previously been characterised. In mice treated with the hyperthermic TRPV1 antagonist, AMG0347, tail skin vasoconstriction preceded the measured increase in core body temperature (Steiner et al., 2007). This suggests that the vasculature plays an important role in TRPV1 antagonist-induced hyperthermia. JNJ17203212 was the only compound that caused hyperthermia in these studies, and the only compound able to inhibit capsaicin-induced blood flow changes in the synovial membrane – our model of 'non-neuronal' TRPV1. It may be that the ability of this compound to block 'non-neuronal' TRPV1 plays a role in hyperthermia, however other hyperthermic TRPV1 antagonists, such as AMG9810, are not able to inhibit capsaicin responses in this model in our lab.

TRPV1 antagonists are only hyperthermic in conscious mice; TRPV1-mediated hyperthermia has not been shown in anaesthetised mice. This suggests that locomotion may be necessary for the hyperthermic response. It may be that stress is a component of the heightened hyperthermic responses. As previously discussed, stress can cause a change in core body temperature in mammals, however this is usually associated with a spike in temperature consistent with an increase in locomotion (Long et al., 1990; Olivier

et al., 2003). In fact, stress can become a learned behaviour simply in response to handling ((Eikelboom, 1986). TRPV1 knock out mice are reported to be hyperkinetic (Garami et al., 2011), another proposed hypothesis for the increase in core body temperature of KO mice. The authors proposed that peripheral TRPV1 tonically suppresses general locomotor activity, however the contribution of hyperkinesis to the non-hyperthermic profile of TRPV1 KO has not been defined. This thesis has not shown an effect of TRPV1 antagonism on activity levels of mice, but the methods of activity measurement were crude. Further investigation using appropriate apparatus will elucidate the role, if any, of activity in TRPV1 antagonist-induced hyperthermia.

7.3 TRPA1 in thermoregulation

Whilst TRPV1 plays a key role in maintaining normal body temperatures (Gavva et al., 2007b), this thesis shows that TRPA1 likely does not, as the TRPA1 antagonists used do not affect baseline core body temperature of naïve mice. Studies from other groups show that TRPA1 KO mice have a normal temperature profile (Story et al., 2003), and other TRPA1 antagonists do not affect core body temperature (Chen et al., 2011). We have shown that TRPA1 is not involved in thermoregulation to the same extent as TRPV1, i.e. it is not tonically active. This correlates with previous studies from other groups that show that TRPA1 antagonists do not affect core body temperature (Eid et al., 2008; Chen et al., 2011). However, the effect of TRPA1 antagonism in this thesis is intriguing. Treatment with HC030031 in co-administration studies of the role of TRPA1 in TRPV1 antagonist-induced hyperthermia, and treatment of TRPV1 KO mice with HC030031 resulted in a significant drop in core body temperature. These findings were surprising as the literature suggests that TRPA1 antagonists do not affect core body temperature. In contrast, blockade of the thermoTRP channel TRPM8 has been shown to reduce core body temperature (de Oliveira et al., 2014). Constitutive activity of the TRPA1 channel has not previously been shown, supporting our observations that blocking the channel had an effect only in non-naïve animals. Observations during these experiments showed that both TRPA1 WT and KO mice were hyperkinetic. This has not been shown before and could be due to the litter; it has previously been shown that only KO mice from the same TRPA1 colony were hyperactive, as determined by voluntary wheel running in their home cages (Bodkin et al., 2014).

7.4 H_2S and TRPV1

Whilst expression of CSE protein did not differ between TRPV1 WT and KO mice, the expression of CBS protein was significantly higher in the liver and skin of KO mice. Expression of CBS is generally considered to be restricted to the central nervous system, with minimal expression outside of this locale (Hosoki et al., 1997; Meier et al., 2001). It has previously been shown that CBS expression can be upregulated in pathophysiological states in various non-neuronal tissues (Nieman et al., 2004; Miao et al., 2012) and CBS has been found in vascularised tissue such as mouse retina (Markand et al., 2013). CBS has been found co-localised with both TRPV1 (Xu et al., 2009) and TRPA1 (Eberhardt et al., 2014) It may be that CBS is upregulated to compensate for TRPV1 loss however there remains a great deal of work to confirm this.

Similarly to the actions of TRPA1 antagonists investigated in this thesis, the effects of exogenous H_2S differed in naïve mice and experimental models. Whilst H_2S donors had no effect on core body temperature in naïve CD1 mice, coadministration of GYY4137 with JNJ17203212 reduced JNJ17203212-induced hyperthermia. However, treatment of mice with dGYY4137 resulted in the same response, suggesting that this effect may not be due to H_2S release. In fact, these studies did not determine the ability of our stock of GYY4137 to release H_2S. The effects of H_2S on core body temperature have been investigated by other groups, alongside its role in metabolism (Blackstone et al., 2005; Volpato et al., 2008; Aslami et al., 2010). H_2S has the ability to reduce metabolic rate, which is accompanied by a reduction in core body temperature. The majority of accounts attribute these effects of H_2S to inhibition of cytochrome c oxidase (Nicholls et al., 2013). Our group has continued to study the temperature effects of H_2S using NaSH and GYY4137. Whilst, similarly to the studies in this thesis, administration of H_2S generating compounds in the periphery does not affect core body temperature; i.c.v. administration causes a significant decrease in core body temperature (Wilson et al., 2014). This effect was removed in TRPA1 KO mice. This suggests that H_2S acts via centrally located TRPA1 to induce hypothermia. However, this does not explain the hypothermic effects demonstrated in my experiments, as both GYY4137 and dGYY4137 were administered systemically and caused a decrease in temperature.

In a similar vein, whilst H_2S donors applied topically to the synovial membrane of the knee had minimal vasodilatory effects, and injection of these compounds alone had no significant effect on plasma extravasation; co-injection with Substance P resulted in significantly increased plasma extravasation

compared to vehicle treatment, and a comparable amount with respect to SP co-injection with CGRP, a potent vasodilator (Brain et al., 1985). In TRPV1 KO mice, GYY4137 co-injected with SP resulted in significantly increased plasma extravasation (by volume) compared to WT mice, and NaSH co-injected with SP resulted in significantly increased plasma extravasation by EB measurement compared to WT mice. Studies have shown the involvement of H_2S, both endogenous and exogenous, in oedema formation, however this is of course complex and the two studies reach contradictory conclusions. Whilst Zanardo and colleagues showed that exogenous H_2S suppressed oedema formation by carrageenan, via a mechanism mimicked by a K_{ATP} agonist, Bhatia et al., showed that endogenous H_2S via treatment with exogenous L-cysteine encouraged oedema formation in carrageenan induced hindpaw inflammation (Bhatia et al., 2005a). As suggested by Whiteman and WInyard, this is most likely due to differing protocols being observed in each laboratory (Whiteman and Winyard, 2011). Our studies contribute to the findings that H_2S causes oedema rather than suppressing it. The mechanisms behind this were not elucidated. Bhatia and colleagues suggested that the pro-inflammatory effects were facilitated by increased biosynthesis of H_2S via CSE activity (Bhatia et al., 2005a). Our results suggest the same; C57/BL6J mice pre-treated with PAG had a trend towards decreased oedema as measured by volume of each site. The involvement of H_2S in plasma extravasation remains to be defined. However it seems that in studies co-injecting NaSH, GYY4137 and L-Cysteine with SP, these H_2S donors and precursor acted very similarly to CGRP as injection site volume was increased to a similar degree. This highlights the vasodilator activity of H_2S in models of inflammation.

7.5 Study limitations and further work

In order to progress the work presented in this thesis, the limitations of the studies should be discussed.

Chapter 3 outlined the effects of TRPV1 and TRPA1 antagonists in thermal and mechanical pain studies and their effects on baseline core body temperature of naïve male CD1 mice. The pain thresholds of the mice were determined using the automated von Frey apparatus (dynamic plantar aesthesiometer) and thermal thresholds were elucidated using an automated Hargreaves apparatus. The automatic measurements gathered were used to determine the effects of antagonists over time. As the observations of the ability to increase pain thresholds was conducted in the same mouse (i.e. the same mouse was tested once in the morning for baseline and then twice - or three times in the case of JNJ17203212 – further for thresholds after drug treatment, the effects of time should be factored in to the

measurements. A vehicle control was used to correct for this however it should be taken into consideration. Another observation from Chapter 3 was that the TRPA1 antagonist TCS5861528 did not increase naïve pain thresholds nor did it affect the core body temperature of naïve mice. Studies by other groups have shown that TCS5861528 is effective in animal models of pain, however it has been studied in hyperalgesia models such as diabetic mice or its ability to block agonist-induced pain rather than its effects on baseline nociceptive thresholds (Wang et al., 2008; Wei et al., 2009; 2010a; 2010b; Chen et al., 2011; Wei et al., 2012). This suggests that perhaps measuring nociceptive thresholds in pain models rather than baseline thresholds of naïve mice will be more appropriate for the investigation of TRPA1. HC030031 also had no effect on the core body temperature of naïve mice – however in studies in chapter 5 it was able to modify body temperature. It may be, therefore, that TRPA1 is important in pathophysiological states rather than maintaining baseline states.

As previously discussed, chapter 4 investigated the roles of TRPA1 and TRPV1 in blood flow- using the laser Doppler speckle imager. The effects of mustard oil, and therefore TRPA1 were consistent in the ear and exposed synovial membrane, i.e. a vasodilatory response was observed in both beds. The effect of capsaicin via TRPV1 differed, however, with vasodilation in the ear and vasoconstriction in the exposed synovial membrane – the latter response widely accepted as mediated by non-neuronal TRPV1. However, the mechanisms behind this have not been fully elucidated, and it is not known whether it is indeed independent of sensory nerves. To confirm any involvement of neuronal TRPV1 and/or sensory nerves (e.g. if the vasoconstriction is simply loss of vasodilation by inflammatory neuropeptides), denervation of the sensory nerves using either capsaicin or RTX would allow us to investigate a non-neuronal mechanism for the vasoconstriction in the synovial membrane. Immunohistochemical studies could also be utilised to determine the location of TRPV1 expression.

Chapter 5 investigated the interaction between TRPV1 and TRPA1 in thermoregulation. This was determined using co-administration studies and treatment of KO mice with antagonists. The co-administration studies revealed a significant hypothermic response to administration of HC030031 that was not shown in naïve studies in chapter 3. As previously discussed, this may have been confounded by a stress element as the mice were handled more frequently than those in naïve studies. Removal of the stressful stimulus can be used to determine if the stress of handling 'unmasked' the hypothermic effects

of HC030031. The simplest method of removing the handling stress would be to use a cannula, implanted at the same time as the telemetry probe. This would enable far less stressful administration of compounds to further examine the effects of the two classes of antagonist in concert.

Chapter 5 also showed that inhibition of TRPA1 in TRPV1 KO mice does not 'reinstate' a hyperthermic profile. As previously discussed, the effects of exogenous H_2S were not investigated in TRPV1 KO mice, therefore future experiments treating TRPV1 KO mice with NaSH and GYY4137 should be conducted to determine whether H_2S really is compensating for the loss of TRPV1.

Finally, chapter 6 investigated the involvement of H_2S in the TRPV1 antagonist-induced hyperthermia, or indeed if increased endogenous production of H_2S compensated for the loss of TRPV1 in temperature control of TRPV1 KO mice. The major limitations in this study were the pharmacological tools used to determine the involvement of H_2S. The selectivity of PAG, the CSE inhibitor has been disputed. PAG inhibits CSE by irreversibly binding to the PLP binding site. Many other enzymes have PLP binding sites, such as L-alanine transaminase (Whiteman et al., 2011). The role of endogenous H_2S production in TRPV1 antagonist induced hyperthermia could be better-elucidated using CSE KO mice, which were not available at the time of the experiment.

7.6 Final conclusions

The TRPV1 antagonists studied in this thesis increased core body temperature of naïve mice whilst TRPA1 antagonists had no effect on core body temperature of naïve mice. A model of neuronal and 'non-neuronal' TRPV1 activation in the vasculature of a single mouse was characterised; JNJ17203212 was the only antagonist able to block capsaicin-induced vascular changes. The TRPA1 agonist mustard oil caused vasodilation in two vascular beds, which was insurmountable by the selected TRPA1 antagonists. TRPA1 does not directly compensate for TRPV1 loss in TRPV1 KO mice, however blockade of TRPA1 in TRPV1 KO mice results in a significant decrease in core body temperature – mimicked by mice co-administered a TRPV1 and a TRPA1 antagonist. We have shown however that H_2S acts as a vasodilator in the skin, however this is unlikely to play a role in TRPV1 antagonist-induced hyperthermia, as administration of both GYY4137 and dGYY4137 result in attenuation of the hyperthermic profile.

References

Abe, K., and Kimura, H. (1996). The possible role of hydrogen sulfide as an endogenous neuromodulator. The Journal of Neuroscience *16*: 1066–1071.

Akiba, Y., Kato, S., Katsube, K.-I., Nakamura, M., Takeuchi, K., Ishii, H., et al. (2004). Transient receptor potential vanilloid subfamily 1 expressed in pancreatic islet β cells modulates insulin secretion in rats. Biochemical and Biophysical Research Communications *321*: 219–225.

Akopian, A.N. (2011). Regulation of Nociceptive Transmission at the Periphery Via TRPA1-TRPV1 Interactions. Current Pharmaceutical Biotechnology *12*: 89–94.

Akopian, A.N., Ruparel, N.B., Jeske, N.A., and Hargreaves, K.M. (2007). Transient receptor potential TRPA1 channel desensitization in sensory neurons is agonist dependent and regulated by TRPV1-directed internalization. The Journal of Physiology *583*: 175–193.

Akopian, A.N., Ruparel, N.B., Patwardhan, A., and Hargreaves, K.M. (2008). Cannabinoids desensitize capsaicin and mustard oil responses in sensory neurons via TRPA1 activation. Journal of Neuroscience *28*: 1064–1075.

Alawi, K., and Keeble, J. (2010). The paradoxical role of the transient receptor potential vanilloid 1 receptor in inflammation. Pharmacology and Therapeutics *125*: 181–195.

Ali, M.Y., Ping, C.Y., Mok, Y.-Y., Ling, L., Whiteman, M., Bhatia, M., et al. (2006). Regulation of vascular nitric oxide in vitroand in vivo; a new role for endogenous hydrogen sulphide? British Journal of Pharmacology *149*: 625–634.

Almeida, M.C., Steiner, A.A., Branco, L.G.S., and Romanovsky, A.A. (2006). Cold-seeking behavior as a thermoregulatory strategy in systemic inflammation. European Journal of Neuroscience *23*: 3359–3367.

Altland, P.D., Highman, B., and Parker, M. (1966). Induction of Hypothermia by Dimethyl Sulfoxide in Rats Exposed to Gold. Proceedings of the Society for Experimental Biology and Medicine *123*: 853–859.

Anand, U., Otto, W., Facer, P., Zebda, N., Selmer, I., Gunthorpe, M.J., et al. (2008). TRPA1 receptor localisation in the human peripheral nervous system and functional studies in cultured human and rat sensory neurons. Neuroscience Letters *438*: 221–227.

Andersson, D.A., Gentry, C., and Bevan, S. (2012). TRPA1 Has a Key Role in the Somatic Pro-Nociceptive Actions of Hydrogen Sulfide. PLoS ONE *7*: e46917.

Andersson, D.A., Gentry, C., Moss, S., and Bevan, S. (2009). Clioquinol and pyrithione activate TRPA1 by increasing intracellular Zn^{2+}. Proceedings of the National Academy of Science USA *106*: 8374–8379.

Andre, E., Gatti, R., Trevisani, M., Preti, D., Baraldi, P.G., Patacchini, R., et al. (2009). Transient receptor potential ankyrin receptor 1 is a novel target for pro-tussive agents. British Journal of Pharmacology *158*: 1621–1628.

Andrè, E., Campi, B., Materazzi, S., Trevisani, M., Amadesi, S., Massi, D., et al. (2008). Cigarette smoke-induced neurogenic inflammation is mediated by alpha,beta-unsaturated aldehydes and the TRPA1 receptor in rodents. Journal of Clinical Investigations. *118*: 2574–2582.

Ang, S.-F., Moochhala, S.M., and Bhatia, M. (2010). Hydrogen sulfide promotes transient receptor potential vanilloid 1-mediated neurogenic inflammation in polymicrobial sepsis*. Critical Care Medicine *38*: 619–628.

Ashwood-Smith, M.J. (1967). Radioprotective and Cryoprotective Properties of Dimethyl Sulfoxide in Cellular Systems. Annals of the New York Academy of Sciences *141*: 45–62.

Aslami, H., Heinen, A., Roelofs, J.J.T.H., Zuurbier, C.J., and Juffermans, N.P. (2010). Suspended animation

inducer hydrogen sulfide is protective in an in vivo model of ventilator-induced lung injury. Intensive Care Medicine *36*: 1946–1952.

Astiz, M.E., and Rackow, E.C. (1998). Septic shock. The Lancet *351*: 1501–1505.

Atoyan, R., Shander, D., and Botchkareva, N.V. (2009). Non-neuronal expression of transient receptor potential type A1 (TRPA1) in human skin. Journal of Investigative Dermatology *129*: 2312–2315.

Aubdool, A.A., Graepel, R., Kodji, X., and Alawi, K.M. (2014). TRPA1 is essential for the vascular response to environmental cold exposure : Nature Communications. 5: 5732

Babes, A., Fischer, M.J.M., Filipovic, M., Engel, M.A., Flonta, M.-L., and Reeh, P.W. (2013). The anti-diabetic drug glibenclamide is an agonist of the transient receptor potential Ankyrin 1 (TRPA1) ion channel. European Journal of Pharmacology *704*: 15–22.

Bandell, M., Story, G.M., Hwang, S.W., Viswanath, V., Eid, S.R., Petrus, M.J., et al. (2004). Noxious Cold Ion Channel TRPA1 Is Activated by Pungent Compounds and Bradykinin. Neuron *41*: 849–857.

Banerjee, R., and Zou, C.-G. (2005). Redox regulation and reaction mechanism of human cystathionine-β-synthase: a PLP-dependent hemesensor protein. Archives of Biochemistry and Biophysics. *433*: 144–156.

Banvolgyi, A., Palinkas, L., Berki, T., Clark, N., Grant, A.D., Helyes, Z., et al. (2005). Evidence for a novel protective role of the vanilloid TRPV1 receptor in a cutaneous contact allergic dermatitis model. Journal of Neuroimmunology. *169*: 86–96.

Banvolgyi, A., Pozsgai, G., Brain, S.D., Helyes, Z.S., Szolcsanyi, J., Ghosh, M., et al. (2004). Mustard oil induces a transient receptor potential vanilloid 1 receptor-independent neurogenic inflammation and a non-neurogenic cellular inflammatory component in mice. Neuroscience *125*: 449–459.

Bautista, D.M., Jordt, S.E., Nikai, T., Tsuruda, P.R., Read, A.J., Poblete, J., et al. (2006). TRPA1 mediates the inflammatory actions of environmental irritants and proalgesic agents. Cell *124*: 1269–1282.

Bautista, D.M., Movahed, P., Hinman, A., Axelsson, H.E., Sterner, O., Hogestatt, E.D., et al. (2005). Pungent products from garlic activate the sensory ion channel TRPA1. Proceedings of the National Academy of Science USA *102*: 12248–12252.

Beauchamp, R.O., Bus, J.S., Popp, J.A., Boreiko, C.J., Andjelkovich, D.A., and Leber, P. (1984). A Critical Review of the Literature on Hydrogen Sulfide Toxicity. Critical Reviews in Toxicology *13*: 25–97.

Benavides, G.A., Squadrito, G.L., Mills, R.W., Patel, H.D., Isbell, T.S., Patel, R.P., et al. (2007). Hydrogen sulfide mediates the vasoactivity of garlic. Proceedings of the National Academy of Science USA *104*: 17977–17982.

Bertolini, A., Ferrari, A., Ottani, A., Guerzoni, S., Tacchi, R., and Leone, S. (2006). Paracetamol: new vistas of an old drug. CNS Drug Reviews *12*: 250–275.

Berne and Levy (2010) Physiology, 6th Updated Edition. Koeppen BM, Stanton BA. Mosby Elsevier, p116.

Bessac, B.F., Sivula, M., Hehn, von, C.A., Escalera, J., Cohn, L., and Jordt, S.-E. (2008). TRPA1 is a major oxidant sensor in murine airway sensory neurons. Journal of Clinical Investigation. *118*: 1899–1910.

Bevan, S., Hothi, S., Hughes, G., James, I.F., Rang, H.P., Shah, K., et al. (1992). Capsazepine: a competitive antagonist of the sensory neurone excitant capsaicin. British Journal of Pharmacology *107*: 544–552.

Bhatia, M., Sidhapuriwala, J., Moochhala, S.M., and Moore, P.K. (2005a). Hydrogen sulphide is a mediator of carrageenan-induced hindpaw oedema in the rat. British Journal of Pharmacology *145*: 141–144.

Bhatia, M., Wong, F.L., Di Fu, Lau, H.Y., Moochhala, S.M., and Moore, P.K. (2005b). Role of hydrogen sulfide in acute pancreatitis and associated lung injury. The FASEB Journal. 19(6):623-5.

Birder, L.A., Nakamura, Y., Kiss, S., Nealen, M.L., Barrick, S., Kanai, A.J., et al. (2002). Altered urinary bladder function in mice lacking the vanilloid receptor TRPV1. Nature Neuroscience. *5*: 856–860.

Blackstone, E., Morrison, M., and Roth, M.B. (2005). H_2S Induces a Suspended Animation-Like State in Mice. Science *308*: 518–518.

Boas, D.A., and Dunn, A.K. (2010). Laser speckle contrast imaging in biomedical optics. Journal of Biomedical Optics. *15*: 011109.

Bodkin, J.V., Thakore, P., Aubdool, A.A., Liang, L., Fernandes, E.S., Nandi, M., et al. (2014). Investigating the potential role of TRPA1 in locomotion and cardiovascular control during hypertension. Pharmacology Research and Perspectives *2*: e00052.

Boss, O., Samec, S., Dulloo, A., Seydoux, J., Muzzin, P., and Giacobino, J.P. (1997a). Tissue-dependent upregulation of rat uncoupling protein-2 expression in response to fasting or cold. FEBS Letters. *412*: 111–114.

Boss, O., Samec, S., Paoloni-Giacobino, A., Rossier, C., Dulloo, A., Seydoux, J., et al. (1997b). Uncoupling protein-3: a new member of the mitochondrial carrier family with tissue-specific expression. FEBS Letters. *408*: 39–42.

Boulant, J.A. (2000). Role of the Preoptic-Anterior Hypothalamus in Thermoregulation and Fever. Clinical Infectious Diseases *31*: S157–161.

Brain, S.D., and Grant, A.D. (2004). Vascular Actions of Calcitonin Gene-Related Peptide and Adrenomedullin. Physiological Reviews *84*: 903–934.

Brain, S.D., Williams, T.J., Tippins, J.R., Morris, H.R., and MacIntyre, I. (1985). Calcitonin gene-related peptide is a potent vasodilator. Nature *313*: 54–56.

Braunstein, A.E., Goryachenkova, E.V., and Lac, N.D. (1969). Reactions catalysed by serine sulfhydrase from chicken liver. Biochimica et Biophysica Acta. *171*: 366–368.

Brederson, J.-D., Kym, P.R., and Szallasi, A. (2013). Targeting TRP channels for pain relief. European Journal of Pharmacology. *716*: 61–76.

Brierley, S.M., Hughes, P.A., Page, A.J., Kwan, K.Y., Martin, C.M., O'Donnell, T.A., et al. (2009). The ion channel TRPA1 is required for normal mechanosensation and is modulated by algesic stimuli. Gastroenterology *137*: 2084–2095.e3.

Bucci, M., Mirone, V., Di Lorenzo, A., Vellecco, V., Roviezzo, F., Brancaleone, V., et al. (2009). Hydrogen Sulphide Is Involved in Testosterone Vascular Effect. European Urology *56*: 378–384.

Bulling, D., Kelly, D., and Bond, S. (2001). Adjuvant-induced joint inflammation causes very rapid transcription of β-preprotachykinin and α-CGRP genes in innervating sensory ganglia. Journal of Neurochemistry 77(2):372-382

Cai, W.-J., Wang, M.-J., Moore, P.K., Jin, H.-M., Yao, T., and Zhu, Y.-C. (2007). The novel proangiogenic effect of hydrogen sulfide is dependent on Akt phosphorylation. Cardiovascular Research *76*: 29–40.

Cambridge, H., and Brain, S.D. (1993). The effect of intra-articular capsaicin on passive synovial anaphylaxis and blood flow in the rat knee joint. Brain Research *618*: 238–245.

Cao, T., Pinter, E., Al-Rashed, S., Gerard, N., Hoult, J.R., and Brain, S.D. (2000). Neurokinin-1 Receptor Agonists Are Involved in Mediating Neutrophil Accumulation in the Inflamed, But Not Normal, Cutaneous Microvasculature: An In Vivo Study Using Neurokinin-1 Receptor Knockout Mice. The Journal of Immunology *164*: 5424–5429.

Caterina, M.J., Leffler, A., Malmberg, A.B., Martin, W.J., Trafton, J., Petersen-Zeitz, K.R., et al. (2000). Impaired nociception and pain sensation in mice lacking the capsaicin receptor. Science *288*: 306–313.

Caterina, M.J., Schumacher, M.A., Tominaga, M., Rosen, T.A., Levine, J.D., and Julius, D. (1997). The capsaicin receptor: a heat-activated ion channel in the pain pathway. Nature *389*: 816–824.

Cavanaugh, D.J., Chesler, A.T., Jackson, A.C., Sigal, Y.M., Yamanaka, H., Grant, R., et al. (2011). Trpv1 reporter mice reveal highly restricted brain distribution and functional expression in arteriolar smooth muscle cells. Journal of Neuroscience *31*: 5067–5077.

Chattopadhyay, M., Kodela, R., Nath, N., Dastagirzada, Y.M., Velazquez-Martinez, C.A., Boring, D., et al. (2012). Hydrogen sulfide-releasing NSAIDs inhibit the growth of human cancer cells: A general property and evidence of a tissue type-independent effect. Biochemical Pharmacology. *83*: 715–722.

Chen, J., Joshi, S.K., DiDomenico, S., Perner, R.J., Mikusa, J.P., Gauvin, D.M., et al. (2011). Selective blockade of TRPA1 channel attenuates pathological pain without altering noxious cold sensation or body temperature regulation. Pain *152*: 1165–1172.

Cheng, Y., Ndisang, J.F., Tang, G., Cao, K., and Wang, R. (2004). Hydrogen sulfide-induced relaxation of resistance mesenteric artery beds of rats. AJP: Heart and Circulatory Physiology *287*: H2316–H2323.

Chitnis, M.K., Njie-Mbye, Y.F., Opere, C.A., Wood, M.E., Whiteman, M., and Ohia, S.E. (2013). Pharmacological actions of the slow release hydrogen sulfide donor GYY4137 on phenylephrine-induced tone in isolated bovine ciliary artery. Experimental Eye Research *116*: 350–354.

Chomczynski, P., and Sacchi, N. (1987). Single-step method of RNA isolation by acid guanidinium thiocyanate-phenol-chloroform extraction. Analytical Biochemistry *162*: 156–159.

Chotani, M.A., Flavahan, S., Mitra, S., Daunt, D., and Flavahan, N.A. (2000). Silent α_2C-adrenergic receptors enable cold-induced vasoconstriction in cutaneous arteries. AJP: Heart and Circulatory Physiology *278*: H1075–H1083.

Chu, C.J., Huang, S.M., De Petrocellis, L., Bisogno, T., Ewing, S.A., Miller, J.D., et al. (2003). N-oleoyldopamine, a novel endogenous capsaicin-like lipid that produces hyperalgesia. Journal of Biological Chemistry. 278: 13633–13639.

Chuang, H.H., Prescott, E.D., Kong, H., Shields, S., Jordt, S.E., Basbaum, A.I., et al. (2001). Bradykinin and nerve growth factor release the capsaicin receptor from PtdIns(4,5)P2-mediated inhibition. Nature *411*: 957–962.

Clapham, D.E. (2003). TRP channels as cellular sensors. Nature *426*: 517–524.

Clapham, D.E. (2015). Structural biology: Pain-sensing TRPA1 channel resolved. Nature *520*: 439–441.

Collin, M., Anuar, F.B.M., Murch, O., Bhatia, M., Moore, P.K., and Thiemermann, C. (2005). Inhibition of endogenous hydrogen sulfide formation reduces the organ injury caused by endotoxemia. British Journal of Pharmacology *146*: 498–505.

Colucci, M., Maione, F., Bonito, M., Piscopo, A., Digiannuario, A., and Pieretti, S. (2008). New insights of dimethyl sulphoxide effects (DMSO) on experimental in vivo models of nociception and inflammation. Pharmacological Research *57*: 419–425.

Cosens, D.J., and Manning, A. (1969). Abnormal electroretinogram from a Drosophila mutant. Nature *224*: 285–287.

Costa, S.K.P., Yshii, L.M., Poston, R.N., Muscará, M.N., and Brain, S.D. (2006). Pivotal role of endogenous tachykinins and the NK1 receptor in mediating leukocyte accumulation, in the absence of oedema formation, in response to TNFalpha in the cutaneous microvasculature. Journal of Neuroimmunology. *171*: 99–109.

Cunha, T.M., and Verri, W.A., Jr. (2007). Hydrogen sulfide, is it a promise analgesic drug or another inflammatory pain mediator? Pain *130*: 300–302.

Cvetkov, T.L., Huynh, K.W., Cohen, M.R., and Moiseenkova-Bell, V.Y. (2011). Molecular Architecture and Subunit Organization of TRPA1 Ion Channel Revealed by Electron Microscopy. Journal of Biological Chemistry *286*: 38168–38176.

Czikora, A., Lizanecz, E., Bakó, P., Rutkai, I., Ruzsnavszky, F., Magyar, J., et al. (2012). Structure-activity relationships of vanilloid receptor agonists for arteriolar TRPV1. British Journal of Pharmacology *165*: 1801–1812.

da Costa, D.S.M., Meotti, F.C., Andrade, E.L., Leal, P.C., Motta, E.M., and Calixto, J.B. (2010). The involvement of the transient receptor potential A1 (TRPA1) in the maintenance of mechanical and cold hyperalgesia in persistent inflammation. Pain 148(3):431-7.

Dai, Y., Moriyama, T., Higashi, T., Togashi, K., Kobayashi, K., Yamanaka, H., et al. (2004). Proteinase-Activated Receptor 2-Mediated Potentiation of Transient Receptor Potential Vanilloid Subfamily 1 Activity Reveals a Mechanism for Proteinase-Induced Inflammatory Pain. The Journal of Neuroscience *24*: 4293–4299.

Dai, Y., Wang, S., Tominaga, M., Yamamoto, S., Fukuoka, T., Higashi, T., et al. (2007). Sensitization of TRPA1 by PAR2 contributes to the sensation of inflammatory pain. Journal of Clinical Investigation. *117*: 1979–1987.

de Oliveira, C., Garami, A., Lehto, S.G., Pakai, E., Tekus, V., Pohoczky, K., et al. (2014). Transient Receptor Potential Channel Ankyrin-1 Is Not a Cold Sensor for Autonomic Thermoregulation in Rodents. The Journal of Neuroscience. 34(13):4445– 4452

Ding, Z., Gomez, T., Werkheiser, J.L., Cowan, A., and Rawls, S.M. (2008). Icilin induces a hyperthermia in rats that is dependent on nitric oxide production and NMDA receptor activation. European Journal of Pharmacology *578*: 201–208.

Diogenes, A., Akopian, A.N., and Hargreaves, K.M. (2007). NGF up-regulates TRPA1: implications for orofacial pain. Journal of Dental Research. *86*: 550–555.

Distrutti, E., Sediari, L., Mencarelli, A., Renga, B., Orlandi, S., Antonelli, E., et al. (2006). Evidence That Hydrogen Sulfide Exerts Antinociceptive Effects in the Gastrointestinal Tract by Activating K_{ATP} Channels. The Journal of Pharmacology and Experimental Therapeutics *316*: 325–335.

Doihara, H., Nozawa, K., Kawabata-Shoda, E., Kojima, R., yokoyama, T., and ito, H. (2009). Molecular cloning and characterization of dog TRPA1 and AITC stimulate the gastrointestinal motility through TRPA1 in conscious dogs. European Journal of Pharmacology *617*: 124–129.

Earley, S., Gonzales, A.L., and Crnich, R. (2009). Endothelium-Dependent Cerebral Artery Dilation Mediated by TRPA1 and Ca^{2+}-Activated K^+ Channels. Circ. Res. *104*: 987–994.

Eberhardt, M., Dux, M., Namer, B., Miljkovic, J., Cordasic, N., Will, C., et al. (2014). H2S and NO cooperatively regulate vascular tone by activating a neuroendocrine HNO–TRPA1–CGRP signalling pathway. Nature Communications *5*: 4381.

Edvinsson, L., Fredholm, B.B., Hamel, E., Jansen, I., and Verrecchia, C. (1985). Perivascular peptides relax cerebral arteries concomitant with stimulation of cyclic adenosine monophosphate accumulation or release of an endothelium-derived relaxing factor in the cat. Neuroscience Letters *58*: 213–217.

Edvinsson, L., Gulbenkian, S., Barroso, C.P., Cunha e Sá, M., Polak, J.M., Mortensen, A., et al. (1998). Innervation of the human middle meningeal artery: immunohistochemistry, ultrastructure, and role of endothelium for vasomotility. Peptides *19*: 1213–1225.

Eid, S.R., Crown, E.D., Moore, E.L., Liang, H.A., Choong, K.-C., Dima, S., et al. (2008). HC-030031, a TRPA1 selective antagonist, attenuates inflammatory- and neuropathy-induced mechanical hypersensitivity. Molecular Pain *4*: 48.

Eikelboom, R. (1986). Learned anticipatory rise in body temperature due to handling. Physiology and

Behavior. *37*: 649–653.

Enokido, Y., Suzuki, E., Iwasawa, K., Namekata, K., Okazawa, H., and Kimura, H. (2005). Cystathionine β-synthase, a key enzyme for homocysteine metabolism, is preferentially expressed in the radial glia/astrocyte lineage of developing mouse CNS. FASEB Journal 9(13):1854-6.

Erickson, P.F., Maxwell, I.H., Su, L.-J., Baumann, M., and Glode, L.M. (1990). Sequence of cDNA for rat cystathionine gamma lyase and comparison of deduced amino acid sequence with related Escherichia coli enzymes. Biochemical Journal *269*: 335–340.

Fernandes, E.S., Fernandes, M.A., and Keeble, J.E. (2012). The functions of TRPA1 and TRPV1: moving away from sensory nerves. British Journal of Pharmacology *166*: 510–521.

Fernandes, E.S., Russell, F.A., Spina, D., McDougall, J.J., Graepel, R., Gentry, C., et al. (2011). A distinct role for transient receptor potential ankyrin 1, in addition to transient receptor potential vanilloid 1, in tumor necrosis factor alpha-induced inflammatory hyperalgesia and Freund's complete adjuvant-induced monarthritis. Arthritis & Rheumatism *63*: 819–829.

Fernandes, E.S., Vong, C.T., Quek, S., Cheong, J., Awal, S., Gentry, C., et al. (2013). Superoxide generation and leukocyte accumulation: key elements in the mediation of leukotriene B4-induced itch by transient receptor potential ankyrin 1 and transient receptor potential vanilloid 1. The FASEB Journal *27*: 1664–1673.

Finkelstein, J.D., Kyle, W.E., Martin, J.L., and Pick, A.M. (1975). Activation of cystathionine synthase by adenosylmethionine and adenosylethionine. Biochemical and Biophysical Research Communications *66*: 81–87.

Fischer, M.J.M., Balasuriya, D., Jeggle, P., Goetze, T.A., McNaughton, P.A., Reeh, P.W., et al. (2014). Direct evidence for functional TRPV1/TRPA1 heteromers. European Journal of Physiology 466(12):2229-41.

Fleury, C., Neverova, M., Collins, S., Raimbault, S., Champigny, O., Levi-Meyrueis, C., et al. (1997). Uncoupling protein-2: a novel gene linked to obesity and hyperinsulinemia. Nature Genetics. *15*: 269–272.

Freedman, R.R., Sabharwal, S.C., Moten, M., and Migaly, P. (1992). Local temperature modulates alpha 1- and alpha 2-adrenergic vasoconstriction in men. AJP - Heart and Circulatory Physiology *263*: H1197–H1200.

Furne, J., Springfield, J., Koenig, T., DeMaster, E., and Levitt, M.D. (2001). Oxidation of hydrogen sulfide and methanethiol to thiosulfate by rat tissues: a specialized function of the colonic mucosa. Biochemical Pharmacology *62*: 255–259.

Garami, A., Pakai, E., Oliveira, D.L., Steiner, A.A., Wanner, S.P., Almeida, M.C., et al. (2011). Thermoregulatory Phenotype of the Trpv1 Knockout Mouse: Thermoeffector Dysbalance with Hyperkinesis. Journal of Neuroscience *31*: 1721–1733.

Garami, A., Shimansky, Y.P., Pakai, E., Oliveira, D.L., Gavva, N.R., and Romanovsky, A.A. (2010). Contributions of Different Modes of TRPV1 Activation to TRPV1 Antagonist-Induced Hyperthermia. Journal of Neuroscience *30*: 1435–1440.

Garrison, S.R., and Stucky, C.L. (2014). Contribution of Transient Receptor Potential Ankyrin 1 to Chronic Pain in Aged Mice With Complete Freund's Adjuvant-Induced Arthritis. Arthritis & Rheumatology *66*: 2380–2390.

Gavva, N.R., Bannon, A.W., Hovland, D.N.J., Lehto, S.G., Klionsky, L., Surapaneni, S., et al. (2007a). Repeated administration of vanilloid receptor TRPV1 antagonists attenuates hyperthermia elicited by TRPV1 blockade. Journal of Pharmacology and Experimental Therapeutics *323*: 128–137.

Gavva, N.R., Bannon, A.W., Surapaneni, S., Hovland, D.N.J., Lehto, S.G., Gore, A., et al. (2007b). The vanilloid receptor TRPV1 is tonically activated in vivo and involved in body temperature regulation. Journal of Neuroscience *27*: 3366–3374.

Gavva, N.R., Tamir, R., Qu, Y., Klionsky, L., Zhang, T.J., Immke, D., et al. (2005). AMG 9810 [(E)-3-(4-t-butylphenyl)-N-(2, 3-dihydrobenzo [b][1, 4] dioxin-6-yl) acrylamide], a novel vanilloid receptor 1 (TRPV1) antagonist with antihyperalgesic properties. The Journal of Pharmacology and Experimental Therapeutics 313:474–484.

Gavva, N.R., Treanor, J.J., Garami, A., Fang, L., Surapaneni, S., Akrami, A., et al. (2008). Pharmacological blockade of the vanilloid receptor TRPV1 elicits marked hyperthermia in humans. Pain *136*: 202–210.

Golech, S.A., McCarron, R.M., Chen, Y., Bembry, J., Lenz, F., Mechoulam, R., et al. (2004). Human brain endothelium: coexpression and function of vanilloid and endocannabinoid receptors. Molecular Brain Research *132*: 87–92.

Golozoubova, V., Hohtola, E., Matthias, A., Jacobsson, A., Cannon, B., and Nedergaard, J. (2001). Only UCP1 can mediate adaptive nonshivering thermogenesis in the cold. FASEB Journal. *15*: 2048–2050.

Grant, A.D., Gerard, N.P., and Brain, S.D. (2002). Evidence of a role for NK1 and CGRP receptors in mediating neurogenic vasodilatation in the mouse ear. British Journal of Pharmacology. *135*: 356–362.

Grant, A.D., Pintér, E., Salmon, A.-M.L., and Brain, S.D. (2005). An examination of neurogenic mechanisms involved in mustard oil-induced inflammation in the mouse. European Journal of Pharmacology *507*: 273–280.

Griffith, O.W. (1987). Mammalian sulfur amino acid metabolism: An overview. (Methods in Enzymology), pp 366–376.

Gu, Q., and Lin, R.-L. (2010). Heavy metals zinc, cadmium, and copper stimulate pulmonary sensory neurons via direct activation of TRPA1. Journal of Applied Physiology. *108*: 891–897.

Gunthorpe, M.J., Rami, H.K., Jerman, J.C., Smart, D., Gill, C.H., Soffin, E.M., et al. (2004). Identification and characterisation of SB-366791, a potent and selective vanilloid receptor (VR1/TRPV1) antagonist. Neuropharmacology *46*: 133–149.

Hamamoto, T., Takumida, M., Hirakawa, K., Takeno, S., and Tatsukawa, T. (2008). Localization of transient receptor potential channel vanilloid subfamilies in the mouse larynx. Acta Otolaryngologica *128*: 685–693.

Harrison, S., and Geppetti, P. (2001). Substance P. The International Journal of Biochemistry and Cell Biology *33*: 555–576.

Hay, D.L., Conner, A.C., Howitt, S.G., Smith, D.M., and Poyner, D.R. (2004). The Pharmacology of Adrenomedullin Receptors and Their Relationship to CGRP Receptors. Journal of Molecular Neuroscience *22*: 105–114.

Hayes, P., Meadows, H.J., Gunthorpe, M.J., Harries, M.H., Duckworth, M.D., Cairns, W., et al. (2000). Cloning and functional expression of a human orthologue of rat vanilloid receptor-1. Pain *88*: 205–215.

Henderson, R. (2013). Structural biology: Ion channel seen by electron microscopy. Nature *504*: 93–94.

Hinman, A., Chuang, H.-H., Bautista, D.M., and Julius, D. (2006). TRP channel activation by reversible covalent modification. Proceedings of the National Academy of Sciences of the USA. *103*: 19564–19568.

Holzer, P. (1998). Neurogenic vasodilatation and plasma leakage in the skin. General Pharmacology *30*: 5–11.

Honda, M., Suzuki, M., Nakayama, K., and Ishikawa, T. (2007). Role of α_2C-adrenoceptors in the reduction of skin blood flow induced by local cooling in mice. British Journal of Pharmacology *152*: 91–100.

Honore, P., Chandran, P., Hernandez, G., Gauvin, D.M., Mikusa, J.P., Zhong, C., et al. (2009). Repeated dosing of ABT-102, a potent and selective TRPV1 antagonist, enhances TRPV1-mediated analgesic activity in rodents, but attenuates antagonist-induced hyperthermia. Pain *142*: 27–35.

Hosoki, R., Matsuki, N., and Kimura, H. (1997). The Possible Role of Hydrogen Sulfide as an Endogenous Smooth Muscle Relaxant in Synergy with Nitric Oxide. Biochemical and Biophysical Research Communications *237*: 527–531.

Hu, H., Bandell, M., Petrus, M.J., Zhu, M.X., and Patapoutian, A. (2009). Zinc activates damage-sensing TRPA1 ion channels. Nature Chemical Biology *5*: 183–190.

Huang SM1, Bisogno T, Trevisani M, Al-Hayani A, De Petrocellis L, Fezza F, Tognetto M, Petros TJ, Krey JF, Chu CJ, Miller JD, Davies SN, Geppetti P, Walker JM, Di Marzo V (2002). An endogenous capsaicin-like substance with high potency at recombinant and native vanilloid VR1 receptors. Proceedings of the National Academy of Sciences of the USA *99*(12):8400-5.

Hui, Y., Du, J., Tang, C., Bin, G., and Jiang, H. (2003). Changes in arterial hydrogen sulfide (H2S) content during septic shock and endotoxin shock in rats. Journal of Infection *47*: 155–160.

Hwang SW1, Cho H, Kwak J, Lee SY, Kang CJ, Jung J, Cho S, Min KH, Suh YG, Kim D, Oh U (2000). Direct activation of capsaicin receptors by products of lipoxygenases: endogenous capsaicin-like substances. Proceedings of the National Academy of Sciences of the USA. 97(11):6155-60.

Inoue, K., Koizumi, S., Fuziwara, S., Denda, S., Inoui, K., and denda, M. (2002). Functional Vanilloid Receptors in Cultured Normal Human Epidermal Keratinocytes. Biochemical and Biophysical Research Communications *291*: 124–129.

Iwasaki, A., Inoue, K., and Hukuda, S. (1995). Distribution of neuropeptide-containing nerve fibers in the synovium and adjacent bone of the rat knee joint. Clinical Experimental Rheumatology *13*: 173–178.

Jackson-Weaver, O., Paredes, D.A., Bosc, L.V.G., Walker, B.R., and Kanagy, N.L. (2011). Intermittent Hypoxia in Rats Increases Myogenic Tone Through Loss of Hydrogen Sulfide Activation of Large-Conductance Ca^{2+}-Activated Potassium Channels. Circulation Research. *108*: 1439–1447.

Jancsó, N., Jancso-Gabor, A., and Szolcsanyi, J. (1967). Direct evidence for neurogenic inflammation and its prevention by denervation and by pretreatment with capsaicin. British Journal of Pharmacology and Chemotherapy *31*: 138–151.

Jancsó-Gábor, A., Szolcsanyi, J., and Jancsó, N. (1970a). Irreversible impairment of thermoregulation induced by capsaicin and similar pungent substances in rats and guinea-pigs. Journal of Physiology (London) *206*: 495–507.

Jancsó-Gábor, A., Szolcsányi, J., and Jancsó, N. (1970b). Stimulation and desensitization of the hypothalamic heat-sensitive structures by capsaicin in rats. Journal of Physiology *208*: 449–459.

Jaquemar, D., Schenker, T., and Trueb, B. (1999). An ankyrin-like protein with transmembrane domains is specifically lost after oncogenic transformation of human fibroblasts. Journal of Biological Chemistry *274*: 7325–7333.

Ji, R.-R., Samad, T.A., Jin, S.-X., Schmoll, R., and Woolf, C.J. (2002). p38 MAPK Activation by NGF in Primary Sensory Neurons after Inflammation Increases TRPV1 Levels and Maintains Heat Hyperalgesia. Neuron *36*: 57–68.

Jordt, S.E., Bautista, D.M., Chuang, H.H., McKemy, D.D., Zygmunt, P.M., Hogestatt, E.D., et al. (2004). Mustard oils and cannabinoids excite sensory nerve fibres through the TRP channel ANKTM1. Nature *427*: 260–265.

Juaneda, C., Dumont, Y., and Quirion, R. (2000). The molecular pharmacology of CGRP and related peptide receptor subtypes. Trends in Pharmacological Sciences *21*: 432–438.

Julien, C., Marcouiller, F., Bretteville, A., Khoury, El, N.B., Baillargeon, J., Hebert, S., et al. (2012). Dimethyl Sulfoxide Induces Both Direct and Indirect Tau Hyperphosphorylation. PLOS ONE *7*: e40020.

Kanai, Y., Nakazato, E., Fujiuchi, A., Hara, T., and Imai, A. (2005). Involvement of an increased spinal TRPV1

sensitization through its up-regulation in mechanical allodynia of CCI rats. Neuropharmacology *49*: 977–984.

Karashima, Y., Damann, N., Prenen, J., Talavera, K., Segal, A., Voets, T., et al. (2007). Bimodal action of menthol on the transient receptor potential channel TRPA1. Journal of Neuroscience *27*: 9874–9884.

Karashima, Y., Prenen, J., Meseguer, V., Owsianik, G., Voets, T., and Nilius, B. (2008). Modulation of the transient receptor potential channel TRPA1 by phosphatidylinositol 4,5-biphosphate manipulators. European Journal of Physiology *457*: 77–89.

Karashima, Y., Talavera, K., Everaerts, W., Janssens, A., Kwan, K.Y., Vennekens, R., et al. (2009). TRPA1 acts as a cold sensor in vitro and in vivo. Proceedings of the National Academy of Sciences of the USA. *106*: 1273–1278.

Kark, T., Bagi, Z., Lizanecz, E., Pasztor, E.T., Erdei, N., Czikora, A., et al. (2008). Tissue-specific regulation of microvascular diameter: opposite functional roles of neuronal and smooth muscle located vanilloid receptor-1. Molecular Pharmacology *73*: 1405–1412.

Kawabata, A., Ishiki, T., Nagasawa, K., Yoshida, S., Maeda, Y., Takahashi, T., et al. (2007). Hydrogen sulfide as a novel nociceptive messenger. Pain *132*: 74–81.

Keeble, J., Russell, F., Curtis, B., Starr, A., Pinter, E., and Brain, S.D. (2005). Involvement of transient receptor potential vanilloid 1 in the vascular and hyperalgesic components of joint inflammation. Arthritis and Rheumatism *52*: 3248–3256.

Keeble, J.E., and Brain, S.D. (2006). Capsaicin-induced vasoconstriction in the mouse knee joint: a study using TRPV1 knockout mice. Neuroscience Letters. *401*: 55–58.

Kery, V., Poneleit, L., and Kraus, J.P. (1998). Trypsin Cleavage of Human Cystathionine β-Synthase into an Evolutionarily Conserved Active Core: Structural and Functional Consequences. Archives of Biochemistry and Biophysics *355*: 222–232.

Kochukov, M.Y. (2006). Thermosensitive TRP ion channels mediate cytosolic calcium response in human synoviocytes. AJP: Cell Physiology *291*: C424–C432.

Kodji, X., Thakore, P., Aubdool, A.A., van Baardewijk, J., Fernandes, M.A., Keeble, J.E., et al. (2013). Use of a mathematical formula in association with the Evans Blue dye technique to quantify oedema formation in skin. Proceedings of the British Pharmacological Society *11*: 119P.

Koltzenburg, M., and McMahon, S.B. (1986). Plasma extravasation in the rat urinary bladder following mechanical, electrical and chemical stimuli: evidence for a new population of chemosensitive primary sensory afferents. Neuroscience Letters. *72*: 352–356.

Konno, R., Ikeda, M., Yamaguchi, K., Ueda, Y., and Niwa, A. (2000). Nephrotoxicity of D -propargylglycine in mice. Archives of Toxicology *74*: 473–479.

Koplas, P.A., Rosenberg, R.L., and Oxford, G.S. (1997). The Role of Calcium in the Desensitization of Capsaicin Responses in Rat Dorsal Root Ganglion Neurons. The Journal of Neuroscience *17*: 3525–3537.

Kozak, L.P., and Harper, M.E. (2000). Mitochondrial uncoupling proteins in energy expenditure. Annual Review of Nutrition. *20*: 339–363.

Kunkler, P.E., Ballard, C.J., Oxford, G.S., and Hurley, J.H. (2011). TRPA1 receptors mediate environmental irritant-induced meningeal vasodilatation. Pain *152*: 38–44.

Kwan, K.Y., Allchorne, A.J., Vollrath, M.A., Christensen, A.P., Zhang, D.-S., Woolf, C.J., et al. (2006). TRPA1 Contributes to Cold, Mechanical, and Chemical Nociception but Is Not Essential for Hair-Cell Transduction. Neuron *50*: 277–289.

Kwan, K.Y., Glazer, J.M., Corey, D.P., Rice, F.L., and Stucky, C.L. (2009). TRPA1 modulates

mechanotransduction in cutaneous sensory neurons. Journal of Neuroscience *29*: 4808–4819.

Lagoutte, E., Mimoun, S., Andriamihaja, M., Chaumontet, C., Blachier, F., and Bouillaud, F. (2010). Oxidation of hydrogen sulfide remains a priority in mammalian cells and causes reverse electron transfer in colonocytes. Biochimica et Biophysica Acta *1797*: 1500–1511.

Lambert, T.W., Goodwin, V.M., Stefani, D., and Strosher, L. (2006). Hydrogen sulfide (H2S) and sour gas effects on the eye. A historical perspective. Science of the Total Environment *367*: 1–22.

Latorre, R., Zaelzer, C., and Brauchi, S. (2009). Structure-functional intimacies of transient receptor potential channels. Quarterly Reviews of Biophysics *42*: 201–246.

Lazzeri, M., Vannucchi, M.G., Zardo, C., Spinelli, M., Beneforti, P., Turini, D., et al. (2004). Immunohistochemical evidence of vanilloid receptor 1 in normal human urinary bladder. European Urology *46*: 792–798.

Le Bars, D., Gozariu, M., and Cadden, S.W. (2001). Animal Models of Nociception. Pharmacological Reviews *53*: 597–652.

Lembeck, F., and Holzer, P. (1979). Substance P as neurogenic mediator of antidromic vasodilation and neurogenic plasma extravasation. Naunyn-Schmiedeberg's Archives of Pharmacology *310*: 175–183.

Leon, L.R. (2005). The use of gene knockout mice in thermoregulation studies. Journal of Thermal Biology *30*: 273–288.

Lertratanangkoon, K., Scimeca, J.M., and Wei, J.-N. (1999). Inhibition of Glutathione Synthesis with Propargylglycine Enhances N-Acetylmethionine Protection and Methylation in Bromobenzene-Treated Syrian Hamsters. The Journal of Nutrition 129: 649–656.

Li, J., Zhang, G., Cai, S., and Redington, A.N. (2008). Effect of inhaled hydrogen sulfide on metabolic responses in anesthetized, paralyzed, and mechanically ventilated piglets. Pediatric Critical Care Medicine *9*: 110–112.

Li, L., Bhatia, M., Zhu, Y.Z., Zhu, Y.-C., Ramnath, R.D., Wang, Z.J., et al. (2005). Hydrogen sulfide is a novel mediator of lipopolysaccharide-induced inflammation in the mouse. The FASEB Journal *19*: 1196–1198.

Li, L., Fox, B., Keeble, J., Salto-Tellez, M., Winyard, P.G., Wood, M.E., et al. (2013). The complex effects of the slow-releasing hydrogen sulfide donor GYY4137 in a model of acute joint inflammation and in human cartilage cells. Journal of Cellular and Molecular Medicine *17*: 365–376.

Li, L., Salto-Tellez, M., Tan, C.-H., Whiteman, M., and Moore, P.K. (2009). GYY4137, a novel hydrogen sulfide-releasing molecule, protects against endotoxic shock in the rat. Free Radical Biology & Medicine *47*: 103–113.

Li, L., Whiteman, M., Guan, Y.Y., Neo, K.L., Cheng, Y., Lee, S.W., et al. (2008). Characterization of a Novel, Water-Soluble Hydrogen Sulfide-Releasing Molecule (GYY4137): New Insights Into the Biology of Hydrogen Sulfide. Circulation *117*: 2351–2360.

Li, R.Q., McKinstry, A.R., Moore, J.T., Caltagarone, B.M., Eckenhoff, M.F., Eckenhoff, R.G., et al. (2012). Is Hydrogen Sulfide-Induced Suspended Animation General Anesthesia? Journal of Pharmacology and Experimental Therapeutics *341*: 735–742.

Linley, J.E., Rose, K., Ooi, L., and Gamper, N. (2010). Understanding inflammatory pain: ion channels contributing to acute and chronic nociception. European Journal of Physiology *459*: 657–669.

Long, N.C., Vander, A.J., and Kluger, M.J. (1990). Stress-induced rise of body temperature in rats is the same in warm and cool environments. Physiology & Behavior *47*: 773–775.

Lowell, B.B., and Spiegelman, B.M. (2000). Towards a molecular understanding of adaptive thermogenesis. Nature *404*: 652–660.

Lowry, O.H., Rosebrough, N.J., Farr, A.L., and Randall, R.J. (1951). PROTEIN MEASUREMENT WITH THE FOLIN PHENOL REAGENT. Journal of Biological Chemistry *193*: 265–275.

Lutaif, N.A., Rocha, E.M., Veloso, L.A., Bento, L.M., and Gontijo, J.A.R. (2008). Renal contribution to thermolability in rats: role of renal nerves. Nephrology Dialysis Transplantation *23*: 3798–3805.

Macpherson, L.J., Dubin, A.E., Evans, M.J., Marr, F., Schultz, P.G., Cravatt, B.F., et al. (2007). Noxious compounds activate TRPA1 ion channels through covalent modification of cysteines. Nature *445*: 541–545.

Macpherson, L.J., Geierstanger, B.H., Viswanath, V., Bandell, M., Eid, S.R., Hwang, S., et al. (2005). The pungency of garlic: activation of TRPA1 and TRPV1 in response to allicin. Current Biology *15*: 929–934.

Macpherson, L.J., Hwang, S.W., Miyamoto, T., Dubin, A.E., Patapoutian, A., and Story, G.M. (2006). More than cool: promiscuous relationships of menthol and other sensory compounds. Molelcular and Cellular Neuroscience *32*: 335–343.

Maeda, Y., Aoki, Y., Sekiguchi, F., Matsunami, M., Takahashi, T., Nishikawa, H., et al. (2009). Hyperalgesia induced by spinal and peripheral hydrogen sulfide: Evidence for involvement of Cav3.2 T-type calcium channels. Pain *142*: 127–132.

Mancardi, D., Penna, C., Merlino, A., Del Soldato, P., Wink, D.A., and Pagliaro, P. (2009). Physiological and pharmacological features of the novel gasotransmitter: Hydrogen sulfide. Biochimica et Biophysica Acta - Bioenergetics *1787*: 864–872.

Markand, S., Tawfik, A., Ha, Y., Gnana-Prakasam, J., Sonne, S., Ganapathy, V., et al. (2013). Cystathionine Beta Synthase Expression in Mouse Retina. Current Eye Research *38*: 597–604.

Martelli, A., Testai, L., Breschi, M.C., Lawson, K., McKay, N.G., Miceli, F., et al. (2013). Vasorelaxation by hydrogen sulphide involves activation of Kv7 potassium channels. Pharmacological Research *70*: 27–34.

Mathai, J.C., Missner, A., Kugler, P., Saparov, S.M., Zeidel, M.L., Lee, J.K., et al. (2009). No facilitator required for membrane transport of hydrogen sulfide. Proceedings of the National Academy of Sciences of the USA *106*: 16633–16638.

Matsunami, M., Tarui, T., Mitani, K., Nagasawa, K., Fukushima, O., Okubo, K., et al. (2008). Luminal hydrogen sulfide plays a pronociceptive role in mouse colon. Neurogastroenterology *58*: 751–761.

McGaraughty, S.P., Chu, K.L., Perner, R.J., DiDomenico, S., Kort, M.E., and Kym, P.R. (2010). TRPA1 modulation of spontaneous and mechanically evoked firing of spinal neurons in uninjured, osteoarthritic, and inflamed rats. Molecular Pain *6*:14

McLatchie, L.M., Fraser, N.J., Main, M.J., Wise, A., Brown, J., Thompson, N., et al. (1998). RAMPs regulate the transport and ligand specificity of the calcitonin-receptor-like receptor. Nature *393*: 333–339.

McNamara, C.R., Mandel-Brehm, J., Bautista, D.M., Siemens, J., Deranian, K.L., Zhao, M., et al. (2007). TRPA1 mediates formalin-induced pain. Proceedings of the National Academy of Sciences of the USA *104*: 13525–13530.

Meier, M., Janosik, M., Kery, V., Kraus, J.P., and Burkhard, P. (2001). Structure of human cystathionine beta-synthase: a unique pyridoxal 5'-phosphate-dependent heme protein. The EMBO Journal *20*: 3910–3916.

Mergler, S., Valtink, M., Coulson-Thomas, V.J., Lindemann, D., Reinach, P.S., Engelmann, K., et al. (2010). TRPV channels mediate temperature-sensing in human corneal endothelial cells. Experimental Eye Research *90*: 758–770.

Miao, X., Meng, X., Wu, G., Ju, Z., Zhang, H.-H., Hu, S., et al. (2012). Upregulation of cystathionine-β-synthetase expression contributes to inflammatory pain in rat temporomandibular joint. Molecular Pain *10*: 791–896.

Moilanen, L.J., Hamalainen, M., Lehtimaki, L., Nieminen, R.M., and Moilanen, E. (2015). Urate Crystal Induced Inflammation and Joint Pain Are Reduced in Transient Receptor Potential Ankyrin 1 Deficient Mice – Potential Role for Transient Receptor Potential Ankyrin 1 in Gout. PLoS ONE *10*: e0117770.

Moiseenkova-Bell, V.Y., Stanciu, L.A., Serysheva, I.I., Tobe, B.J., and Wensel, T.G. (2008). Structure of TRPV1 channel revealed by electron cryomicroscopy. Proceedings of the National Academy of Sciences of the USA *105*: 7451–7455.

Morrison, S.F., and Nakamura, K. (2011). Central neural pathways for thermoregulation. Frontiers in Bioscience *16*: 74–104.

Mustafa, A.K., Gadalla, M.M., Sen, N., Kim, S., Mu, W., Gazi, S.K., et al. (2009). H_2S Signals Through Protein S-Sulfhydration. Science Signalling *2*: ra72.

Mustafa, A.K., Sikka, G., Gazi, S.K., Steppan, J., Jung, S.M., Bhunia, A.K., et al. (2011). Hydrogen Sulfide as Endothelium-Derived Hyperpolarizing Factor Sulfhydrates Potassium Channels. Circulation Research *109*: 1259–1268.

Nagata, K., Duggan, A., Kumar, G., and garcia-Anoveros, J. (2005). Nociceptor and Hair Cell Transducer Properties of TRPA1, a Channel for Pain and Hearing. Journal of Neuroscience *25*: 4052–4061.

Nassini, R., Materazzi, S., Vriens, J., Prenen, J., Benemei, S., De Siena, G., et al. (2012). The 'headache tree' via umbellulone and TRPA1 activates the trigeminovascular system. Brain *135*: 376–390.

Nedergaard, J., Bengtsson, T., and Cannon, B. (2007). Unexpected evidence for active brown adipose tissue in adult humans. AJP- Endocrinology and Metabolism. *293*: E444–52.

Nicholls, P., Marshall, D.C., Cooper, C.E., and Wilson, M.T. (2013). Sulfide inhibition of and metabolism by cytochrome c oxidase. Biochemical Society Transactions *41*: 1312–1316.

Nieman, K.M., Rowling, M.J., Garrow, T.A., and Schalinske, K.L. (2004). Modulation of Methyl Group Metabolism by Streptozotocin-induced Diabetes and All-trans-retinoic Acid. The Journal of Biological Chemistry *279*: 45708–45712.

Nilius, B., and Voets, T. (2004). Diversity of TRP channel activation. Novartis Foundation Symposium. *258*: 140–9– discussion 149–59– 263–6.

Nilius, B., Appendino, G., and Owsianik, G. (2012). The transient receptor potential channel TRPA1: from gene to pathophysiology. European Journal of Physiology *464*: 425–458.

Nozawa, K., Kawabata-Shoda, E., Doihara, H., Kojima, R., Okada, H., Mochizuki, S., et al. (2009). TRPA1 regulates gastrointestinal motility through serotonin release from enterochromaffin cells. Proceedings of the National Academy of Sciences of the USA *106*: 3408–3413.

Numazaki, M., Tominaga, T., Takeuchi, K., Murayama, N., Toyooka, H., and Tominaga, M. (2003). Structural determinant of TRPV1 desensitization interacts with calmodulin. Proceedings of the National Academy of Sciences of the USA *100*: 8002–8006.

Nystul, T.G., and Roth, M.B. (2004). Carbon monoxide-induced suspended animation protects against hypoxic damage in Caenorhabditis elegans. Proceedings of the National Academy of Sciences of the USA *101*: 9133–9136.

Ohnuki, K., Haramizu, S., Oki, K., Watanabe, T., Yazawa, S., and Fushiki, T. (2001). Administration of capsiate, a non-pungent capsaicin analog, promotes energy metabolism and suppresses body fat accumulation in mice. Bioscience, Biotechnology, and Biochemistry. *65*: 2735–2740.

Olivier, B., Zethof, T., Pattij, T., van Boogaert, M., van Ooerschot Ruud, Leahy, C., et al. (2003). Stress-induced hyperthermia and anxiety: pharmacological validation. European Journal of Pharmacology *463*: 117–132.

Padilla, P.A., and Roth, M.B. (2001). Oxygen deprivation causes suspended animation in the zebrafish embryo. Proceedings of the National Academy of Sciences of the USA *98*: 7331–7335.

Papapetropoulos, A., Pyriochou, A., Altaany, Z., Yang, G., Marazioti, A., Zhou, Z., et al. (2009). Hydrogen sulfide is an endogenous stimulator of angiogenesis. Proceedings of the National Academy of Sciences of the USA *106*: 21972–21977.

Papapetropoulos, A., Whiteman, M., and Cirino, G. (2015). Pharmacological tools for hydrogen sulphide research: a brief, introductory guide for beginners. British Journal of Pharmacology *172*: 1633–1637.

Patacchini, R., Santicioli, P., Giuliani, S., and Maggi, C.A. (2004). Hydrogen sulfide (H2S) stimulates capsaicin-sensitive primary afferent neurons in the rat urinary bladder. British Journal of Pharmacology *142*: 31–34.

Patacchini, R., Santicioli, P., Giuliani, S., and Maggi, C.A. (2005). Pharmacological investigation of hydrogen sulfide (H_2S) contractile activity in rat detrusor muscle. European Journal of Pharmacology *509*: 171–177.

Pedersen, S.F., Owsianik, G., and Nilius, B. (2005). TRP channels: an overview. Cell Calcium *38*: 233–252.

Peier AM, Moqrich A, Hergarden AC, Reeve AJ, Andersson DA, Story GM, Earley TJ, Dragoni I, McIntyre P, Bevan S, Patapoutian A. (2002). A TRP channel that senses cold stimuli and menthol. Cell 108(5):705-15.

Petrus, M., Peier, A.M., Bandell, M., Hwang, S., Huynh, T., Olney, N., et al. (2007). A role of TRPA1 in mechanical hyperalgesia is revealed by pharmacological inhibition. Molecular Pain *3*: 40.

Pozsgai, G., Hajna, Z., Bagoly, T., Boros, M., Kemény, Á., Materazzi, S., et al. (2012). The role of transient receptor potential ankyrin 1 (TRPA1) receptor activation in hydrogen-sulphide-induced CGRP-release and vasodilation. European Journal of Pharmacology *689*: 56–64.

Qu, R., Tao, J., Wang, Y., Zhou, Y., Wu, G., Xiao, Y., et al. (2013). Neonatal colonic inflammation sensitizes voltage-gated Na+ channels via upregulation of cystathionine β-synthetase expression in rat primary sensory neurons. AJP- Gastrointestinal Liver Physiology *304*: G743–G772.

Ratnam, S., Maclean, K.N., Jacobs, R.L., Brosnan, M.E., Kraus, J.P., and Brosnan, J.T. (2002). Hormonal Regulation of Cystathionine beta -Synthase Expression in Liver. Journal of Biological Chemistry *277*: 42912–42918.

Rawls, S.M., Gomez, T., Ding, Z., and Raffa, R.B. (2007). Differential behavioral effect of the TRPM8/TRPA1 channel agonist icilin (AG-3-5). European Journal of Pharmacology *575*: 103–104.

Robert, K., Vialard, F., Thiery, E., Toyama, K., Sinet, P.M., Janel, N., et al. (2003). Expression of the Cystathionine Beta Synthase (CBS) Gene During Mouse Development and Immunolocalization in Adult Brain. Journal of Histochemistry & Cytochemistry *51*: 363–371.

Romanovsky, A.A., Almeida, M.C., Garami, A., Steiner, A.A., Norman, M.H., Morrison, S.F., et al. (2009). The Transient Receptor Potential Vanilloid-1 Channel in Thermoregulation: A Thermosensor It Is Not. Pharmacological Reviews *61*: 228–261.

Rosenbaum, T., Gordon-Shaag, A., Munari, M., and Gordon, S.E. (2003). Ca2+/Calmodulin Modulates TRPV1 Activation by Capsaicin. The Journal of General Physiology *123*: 53–62.

Ruparel, N.B., Patwardhan, A.M., Akopian, A.N., and Hargreaves, K.M. (2008). Homologous and heterologous desensitization of capsaicin and mustard oil responses utilize different cellular pathways in nociceptors. Pain *135*: 271–279.

Ruparel, N.B., Patwardhan, A.M., Akopian, A.N., and Hargreaves, K.M. (2011). Desensitization of Transient Receptor Potential Ankyrin 1 (TRPA1) by the TRP Vanilloid 1-Selective Cannabinoid Arachidonoyl-2 Chloroethanolamine. Molecular Pharmacology *80*: 117–123.

Russell, F.A., Fernandes, E.S., Courade, J.-P., Keeble, J.E., and Brain, S.D. (2009). Tumour necrosis factor α

mediates transient receptor potential vanilloid 1-dependent bilateral thermal hyperalgesia with distinct peripheral roles of interleukin-1β, protein kinase C and cyclooxygenase-2 signalling. Pain *142*: 264–274.

Sanz-Salvador, L., Andres-Borderia, A., Ferrer-Montiel, A., and Planells-Cases, R. (2012). Agonist- and Ca2+-dependent Desensitization of TRPV1 Channel Targets the Receptor to Lysosomes for Degradation. Journal of Biological Chemistry *287*: 19462–19471.

Saunders, C.I., Kunde, D.A., Crawford, A., and Geraghty, D.P. (2007). Expression of transient receptor potential vanilloid 1 (TRPV1) and 2 (TRPV2) in human peripheral blood. Molecular Immunology *44*: 1429–1435.

Savidge, J., Davis, C., Shah, K., Colley, S., Phillips, E., Ranasinghe, S., et al. (2002). Cloning and functional characterization of the guinea pig vanilloid receptor 1. Neuropharmacology *43*: 450–456.

Sawada, Y., Hosokawa, H., Hori, A., Matsumura, K., and Kobayashi, S. (2007). Cold sensitivity of recombinant TRPA1 channels. Brain Research *1160*: 39–46.

Searcy, D.G., and Lee, S.H. (1998). Sulfur reduction by human erythrocytes. Journal of Experimental Zoology *282*: 310–322.

Seitz, D.H., Fröba, J.S., Niesler, U., Palmer, A., Veltkamp, H.A., Braumüller, S.T., et al. (2012). Inhaled Hydrogen Sulfide Induces Suspended Animation, But Does Not Alter the Inflammatory Response After Blunt Chest Trauma. Shock *37*: 197–204.

Seki, N., Shirasaki, H., Kikuchi, M., Sakamoto, T., Watanabe, N., and Himi, T. (2006). Expression and localization of TRPV1 in human nasal mucosa. Rhinology *44*: 128–134.

Sexton, A., McDonald, M., Cayla, C., Thiemermann, C., and Ahluwalia, A. (2007). 12-Lipoxygenase-derived eicosanoids protect against myocardial ischemia/reperfusion injury via activation of neuronal TRPV1. FASEB Journal. *21*: 2695–2703.

Silva, C.R., Oliveira, S.M., Rossato, M.F., Dalmolin, G.D., Guerra, G.P., da Silveira Prudente, A., et al. (2011). The involvement of TRPA1 channel activation in the inflammatory response evoked by topical application of cinnamaldehyde to mice. Life Sciences *88*: 1077–1087.

Simons, C.T., Carstens, M.I., and Carstens, E. (2003). Oral irritation by mustard oil: self-desensitization and cross-desensitization with capsaicin. Chemical Senses *28*: 459–465.

Smith, R.P., and Abbanat, R.A. (1966). Protective effect of oxidized glutathione in acute sulfide poisoning. Toxicology and Applied Pharmacology *9*: 209–217.

Starr, A., Graepel, R., Keeble, J., Schmidhuber, S., Clark, N., Grant, A., et al. (2008). A reactive oxygen species-mediated component in neurogenic vasodilatation. Cardiovascular Research *78*: 139–147.

Steiner, A.A., Turek, V.F., Almeida, M.C., Burmeister, J.J., Oliveira, D.L., Roberts, J.L., et al. (2007). Nonthermal activation of transient receptor potential vanilloid-1 channels in abdominal viscera tonically inhibits autonomic cold-defense effectors. Journal of Neuroscience *27*: 7459–7468.

Stipanuk, M.H., and Beck, P.W. (1982). Characterization of the enzymic capacity for cysteine desulphydration in liver and kidney of the rat. Biochemical Journal *206*: 267–277.

Story, G.M., Peier, A.M., Reeve, A.J., Eid, S.R., Mosbacher, J., Hricik, T.R., et al. (2003). ANKTM1, a TRP-like channel expressed in nociceptive neurons, is activated by cold temperatures. Cell *112*: 819–829.

Streng, T., Axelsson, H.E., Hedlund, P., Andersson, D.A., Jordt, S.-E., Bevan, S., et al. (2008). Distribution and Function of the Hydrogen Sulfide–Sensitive TRPA1 Ion Channel in Rat Urinary Bladder. European Urology *53*: 391–400.

Sugiura, T., Tominaga, M., Katsuya, H., and Mizumura, K. (2002). Bradykinin Lowers the Threshold Temperature for Heat Activation of Vanilloid Receptor 1. Journal of Neurophysiology *88*: 544–548.

Sun, Y.G., Cao, Y.X., Wang, W.W., Ma, S.F., Yao, T., and Zhu, Y.C. (2008). Hydrogen sulphide is an inhibitor of L-type calcium channels and mechanical contraction in rat cardiomyocytes. Cardiovascular Research *79*: 632–641.

Swanson, D.M., Dubin, A.E., Shah, C., Nasser, N., Chang, L., Dax, S.L., et al. (2005). Identification and Biological Evaluation of 4-(3-Trifluoromethylpyridin-2-yl)piperazine-1-carboxylic Acid (5-Trifluoromethylpyridin-2-yl)amide, a High Affinity TRPV1 (VR1) Vanilloid Receptor Antagonist. Journal of Medicinal Chemistry *48*: 1857–1872.

Szelenyi, Z., Hummel, Z., Szolcsanyi, J., and Davis, J.B. (2004). Daily body temperature rhythm and heat tolerance in TRPV1 knockout and capsaicin pretreated mice. European Journal of Neuroscience *19*: 1421–1424.

Szolcsanyi, J., and Jancso-Gabor, A. (1975). Sensory effects of capsaicin congeners I. Relationship between chemical structure and pain-producing potency of pungent agents. Arzneimittelforschung *25*: 1877–1881.

Tamayo, N., Liao, H., Stec, M.M., Wang, X., Chakrabarti, P., Retz, D., et al. (2008). Design and Synthesis of Peripherally Restricted Transient Receptor Potential Vanilloid 1 (TRPV1) Antagonists. Journal of Medicinal Chemistry *51*: 2744–2757.

Tang, G., Wu, L., Liang, W., and Wang, R. (2005). Direct Stimulation of KATP Channels by Exogenous and Endogenous Hydrogen Sulfide in Vascular Smooth Muscle Cells. Molecular Pharmacology *68*: 1757–1764.

Telezhkin, V., Brazier, S.P., Cayzac, S.H., Wilkinson, W.J., Riccardi, D., and Kemp, P.J. (2010). Mechanism of inhibition by hydrogen sulfide of native and recombinant BKCa channels. Respiratory Physiology & Neurobiology *172*: 169–178.

Toth, A., Czikora, A., Pasztor, E.T., Dienes, B., Bai, P., Csernoch, L., et al. (2014). Vanilloid Receptor-1 (TRPV1) Expression and Function in the Vasculature of the Rat. Journal of Histochemistry & Cytochemistry *62*: 129–144.

Tóth, D.M., Szőke, É., Bölcskei, K., Kvell, K., Bender, B., Bősze, Z., et al. (2010). Nociception, neurogenic inflammation and thermoregulation in TRPV1 knockdown transgenic mice. Cell and Molecular Life Sciences *68*: 2589–2601.

Trevisan, G., Hoffmeister, C., Rossato, M.F., Oliveira, S.M., Silva, M.A., Ineu, R.P., et al. (2013). Transient Receptor Potential Ankyrin 1 Receptor Stimulation by Hydrogen Peroxide Is Critical to Trigger Pain During Monosodium Urate-Induced Inflammation in Rodents. Arthritis & Rheumatism *65*: 2984–2995.

Trevisani, M., Patacchini, R., Nicoletti, P., Gatti, R., Gazzieri, D., Lissi, N., et al. (2005). Hydrogen sulfide causes vanilloid receptor 1-mediated neurogenic inflammation in the airways. British Journal of Pharmacology *145*: 1123–1131.

Trevisani, M., Siemens, J., Materazzi, S., Bautista, D.M., Nassini, R., Campi, B., et al. (2007). 4-Hydroxynonenal, an endogenous aldehyde, causes pain and neurogenic inflammation through activation of the irritant receptor TRPA1. Proceedings of the National Academy of Sciences of the USA *104*: 13519–13524.

Tsutsumi, M., Denda, S., ikeyama, K., goto, M., and denda, M. (2010). Exposure to Low Temperature Induces Elevation of Intracellular Calcium in Cultured Human Keratinocytes. Journal of Investigative Dermatology *130*: 1945–1948.

van Abeelen, A.F.M., de Krom, M., Hendriks, J., Grobbee, D.E., Adan, R.A.H., and van der Schouw, Y.T. (2008). Variations in the uncoupling protein-3 gene are associated with specific obesity phenotypes. European Journal of Endocrinology *158*: 669–676.

Vandesompele, J., De Preter, K., Pattyn, F., Poppe, B., Van Roy, N., De Paepe, A., et al. (2002). Accurate normalization of real-time quantitative RT-PCR data by geometric averaging of multiple internal control genes. Genome Biology *3*: research0034.1–0034.11.

Varga, A., Németh, J., Szabó, Á., McDougall, J.J., Zhang, C., Elekes, K., et al. (2005). Effects of the novel TRPV1 receptor antagonist SB366791 in vitro and in vivo in the rat. Neuroscience letters *385*: 137–142.

Volpato, G.P., Searles, R., Yu, B., Scherrer-Crosbie, M., Bloch, K.D., Ichinose, F., et al. (2008). Inhaled Hydrogen Sulfide: A Rapidly Reversible Inhibitor of Cardiac and Metabolic Function in the Mouse. Anesthesiology *108*: 659–668.

Wang, Q., Wang, X.L., Liu, H.R., Rose, P., and Zhu, Y.Z. (2010). Protective effects of cysteine analogues on acute myocardial ischemia: novel modulators of endogenous H_2S production. Antioxidants & Redox Signaling *12*: 1155–1165.

Wang, R. (2002). Two's company, three's a crowd: can H_2S be the third endogenous gaseous transmitter? FASEB Journal *16*: 1792–1798.

Wang, R. (2003). The Gasotransmitter Role of Hydrogen Sulfide. Antioxidants & Redox Signaling *5*: 493–501.

Wang, R. (2012). Physiological Implications of Hydrogen Sulfide: A Whiff Exploration That Blossomed. Physiological Reviews *92*: 791–896.

Wang, S., Dai, Y., Fukuoka, T., Yamanaka, H., Kobayashi, K., Obata, K., et al. (2007). Phospholipase C and protein kinase A mediate bradykinin sensitization of TRPA1: a molecular mechanism of inflammatory pain. Brain *131*: 1241–1251.

Wang, Y., Szabo, T., Welter, J.D., Toth, A., Tran, R., Lee, J., et al. (2002). High Affinity Antagonists of the Vanilloid Receptor. Molecular Pharmacology *62*: 947–956.

Wang, Y.Y., Chang, R.B., Waters, H.N., McKemy, D.D., and Liman, E.R. (2008). The Nociceptor Ion Channel TRPA1 Is Potentiated and Inactivated by Permeating Calcium Ions. Journal of Biological Chemistry *283*: 32691–32703.

Watanabe, M., Osada, J., Aratani, Y., Kluckman, K., Reddick, R., Malinow, M.R., et al. (1995). Mice deficient in cystathionine beta-synthase: animal models for mild and severe homocyst(e)inemia. Proceedings of the National Academy of Sciences of the USA *92*: 1585–1589.

Wei, H., Chapman, H., Saarnilehto, M., Kuokkanen, K., Koivisto, A., and Pertovaara, A. (2010a). Roles of cutaneous versus spinal TRPA1 channels in mechanical hypersensitivity in the diabetic or mustard oil-treated non-diabetic rat. Neuropharmacology *58*: 578–584.

Wei, H., Hamalainen, M., Saamilehto, M., Koivisto, A., and Pertovaara, A. (2009). Attenuation of Mechanical Hypersensitivity by an Antagonist of the TRPA1 Ion Channel in Diabetic Animals. Anesthesiology 147–154.

Wei, H., Karimaa, M., Korjamo, T., Koivisto, A., and Pertovaara, A. (2012). Transient Receptor Potential Ankyrin 1 Ion Channel Contributes to Guarding Pain and Mechanical Hypersensitivity in a Rat Model of Postoperative Pain. Anesthesiology *117*: 137–148.

Wei, H., Koivisto, A., and Pertovaara, A. (2010b). Spinal TRPA1 ion channels contribute to cutaneous neurogenic inflammation in the rat. Neuroscience Letters *479*: 253–256.

Weisiger, R.A., Pinkus, L.M., and Jakoby, W.B. (1980). Thiol S-methyltransferase: suggested role in detoxication of intestinal hydrogen sulfide. Biochemical Pharmacology *29*: 2885–2887.

White, B.J.O., Smith, P.A., and Dunn, W.R. (2013). Hydrogen sulphide-mediated vasodilatation involves the release of neurotransmitters from sensory nerves in pressurized mesenteric small arteries isolated from rats. British Journal of Pharmacology *168*: 785–793.

Whiteman, M., and Winyard, P.G. (2011). Hydrogen sulfide and inflammation: the good, the bad, the ugly and the promising. Expert Review of Clinical Pharmacology *4*: 13–32.

Whiteman, M., Haigh, R., Tarr, J.M., Gooding, K.M., Shore, A.C., and Winyard, P.G. (2010a). Detection of hydrogen sulfide in plasma and knee-joint synovial fluid from rheumatoid arthritis patients: relation to clinical and laboratory measures of inflammation. Annals of the New York Academy of Sciences *1203*: 146–150.

Whiteman, M., Le Trionnaire, S., Chopra, M., Fox, B., and Whatmore, J. (2011). Emerging role of hydrogen sulfide in health and disease: critical appraisal of biomarkers and pharmacological tools. Clinical Sciences *121*: 459–488.

Whiteman, M., Li, L., Rose, P., Tan, C.-H., Parkinson, D.B., and Moore, P.K. (2010b). The Effect of Hydrogen Sulfide Donors on Lipopolysaccharide-Induced Formation of Inflammatory Mediators in Macrophages. Antioxidants and Redox Signaling *12*: 1147–1154.

Wilson, H.V., Riahi, R., Solymar, M., Pakai, E., Tekus, V., Pinter, E., et al. (2014). Involvement of the transient receptor potential ankyrin 1 (TRPA1) channel in the thermoregulatory effects of hydrogen sulfide. Pharmacology 2014 OB012.

Woolf, C.J., Safieh-Garabedian, B., Ma, Q.-P., Crilly, P., and Winter, J. (1994). Nerve growth factor contributes to the generation of inflammatory sensory hypersensitivity. Neuroscience *62*: 327–331.

Xu, G.-Y., Winston, J.H., Shenoy, M., Zhou, S., Chen, J.D., and Pasricha, P.J. (2009). The endogenous hydrogen sulfide producing enzyme cystathionine-β synthase contributes to visceral hypersensitivity in a rat model of irritable bowel syndrome. Molecular Pain *5*: 44.

Yang, D., Luo, Z., Ma, S., Wong, W.T., Ma, L., Zhong, J., et al. (2010). Activation of TRPV1 by Dietary Capsaicin Improves Endothelium-Dependent Vasorelaxation and Prevents Hypertension. Cell Metabolism *12*: 130–141.

Yang, G., Wu, L., Jiang, B., Yang, W., Qi, J., Cao, K., et al. (2008). H2S as a Physiologic Vasorelaxant: Hypertension in Mice with Deletion of Cystathionine γ-Lyase. Science *322*: 587–590.

Yang, X.-R., Lin, M.-J., McIntosh, L.S., and Sham, J.S.K. (2006). Functional expression of transient receptor potential melastatin- and vanilloid-related channels in pulmonary arterial and aortic smooth muscle. Am. J. Physiol. Lung Cell Mol. Physiol. *290*: L1267–76.

Young, A.A., and Dawson, N.J. (1982). Evidence for on-off control of heat dissipation from the tail of the rat. Canadian Journal of Physiology and Pharmacology *60*: 392–398.

Zanardo, R.C.O., Brancaleone, V., Distrutti, E., Fiorucci, S., Cirino, G., and Wallace, J.L. (2006). Hydrogen sulfide is an endogenous modulator of leukocyte-mediated inflammation. FASEB Journal. *20*: 2118–2120.

Zhang, F., Yang, H., Wang, Z., Mergler, S., Liu, H., Kawakita, T., et al. (2007a). Transient receptor potential vanilloid 1 activation induces inflammatory cytokine release in corneal epithelium through MAPK signaling. Journal of Cellular Physiology *213*: 730–739.

Zhang, H. (2006). Role of hydrogen sulfide in cecal ligation and puncture-induced sepsis in the mouse. AJP: Lung Cellular and Molecular Physiology *290*: L1193–L1201.

Zhang, H., Hegde, A., Ng, S.W., Adhikari, S., Moochhala, S.M., and BHATIA, M. (2007b). Hydrogen Sulfide Up-Regulates Substance P in Polymicrobial Sepsis-Associated Lung Injury. The Journal of Immunology *179*: 4153–4160.

Zhang, L.L., Liu, D.Y., Ma, L.Q., Luo, Z.D., Cao, T.B., Zhong, J., et al. (2007c). Activation of transient receptor potential vanilloid type-1 channel prevents adipogenesis and obesity. Circulation Research *100*: 1063–1070.

Zhao, W., Zhang, J., Lu, Y., and Wang, R. (2001). The vasorelaxant effect of H_2S as a novel endogenous gaseous KATP channel opener. The EMBO Journal *20*: 6008–6016.

Zhao, W., and Wang, R. (2002). H2S-induced vasorelaxation and underlying cellular and molecular

mechanisms. AJP: Heart and Circulatory Physiology *283*: H474–H480.

Zygmunt, P.M., Petersson, J., Andersson, D.A., Chuang, H.-H., Sorgard, M., Di Marzo, V., et al. (1999). Vanilloid receptors on sensory nerves mediate the vasodilator action of anandamide. Nature *400*: 452–457.